

TRAINING COURSE SERIES

No. 87

Educational Hypothetical Severe Accident Nuclear Power Plant Simulator

Theory and User Manual with Exercises

EDUCATIONAL HYPOTHETICAL
SEVERE ACCIDENT
NUCLEAR POWER PLANT SIMULATOR

The following States are Members of the International Atomic Energy Agency:

| | | |
|-------------------------------------|-------------------------------------|--|
| AFGHANISTAN | GEORGIA | PAKISTAN |
| ALBANIA | GERMANY | PALAU |
| ALGERIA | GHANA | PANAMA |
| ANGOLA | GREECE | PAPUA NEW GUINEA |
| ANTIGUA AND BARBUDA | GRENADA | PARAGUAY |
| ARGENTINA | GUATEMALA | PERU |
| ARMENIA | GUINEA | PHILIPPINES |
| AUSTRALIA | GUYANA | POLAND |
| AUSTRIA | HAITI | PORTUGAL |
| AZERBAIJAN | HOLY SEE | QATAR |
| BAHAMAS, THE | HONDURAS | REPUBLIC OF MOLDOVA |
| BAHRAIN | HUNGARY | ROMANIA |
| BANGLADESH | ICELAND | RUSSIAN FEDERATION |
| BARBADOS | INDIA | RWANDA |
| BELARUS | INDONESIA | SAINT KITTS AND NEVIS |
| BELGIUM | IRAN, ISLAMIC REPUBLIC OF | SAINT LUCIA |
| BELIZE | IRAQ | SAINT VINCENT AND THE GRENADINES |
| BENIN | IRELAND | SAMOA |
| BOLIVIA, PLURINATIONAL STATE OF | ISRAEL | SAN MARINO |
| BOSNIA AND HERZEGOVINA | ITALY | SAUDI ARABIA |
| BOTSWANA | JAMAICA | SENEGAL |
| BRAZIL | JAPAN | SERBIA |
| BRUNEI DARUSSALAM | JORDAN | SEYCHELLES |
| BULGARIA | KAZAKHSTAN | SIERRA LEONE |
| BURKINA FASO | KENYA | SINGAPORE |
| BURUNDI | KOREA, REPUBLIC OF | SLOVAKIA |
| CABO VERDE | KUWAIT | SLOVENIA |
| CAMBODIA | KYRGYZSTAN | SOMALIA |
| CAMEROON | LAO PEOPLE'S DEMOCRATIC REPUBLIC | SOUTH AFRICA |
| CANADA | LATVIA | SPAIN |
| CENTRAL AFRICAN REPUBLIC | LEBANON | SRI LANKA |
| CHAD | LESOTHO | SUDAN |
| CHILE | LIBERIA | SWEDEN |
| CHINA | LIBYA | SWITZERLAND |
| COLOMBIA | LIECHTENSTEIN | SYRIAN ARAB REPUBLIC |
| COMOROS | LITHUANIA | TAJIKISTAN |
| CONGO | LUXEMBOURG | THAILAND |
| COOK ISLANDS | MADAGASCAR | TOGO |
| COSTA RICA | MALAWI | TONGA |
| CÔTE D'IVOIRE | MALAYSIA | TRINIDAD AND TOBAGO |
| CROATIA | MALI | TUNISIA |
| CUBA | MALTA | TÜRKİYE |
| CYPRUS | MARSHALL ISLANDS | TURKMENISTAN |
| CZECH REPUBLIC | MAURITANIA | UGANDA |
| DEMOCRATIC REPUBLIC OF THE CONGO | MAURITIUS | UKRAINE |
| DENMARK | MEXICO | UNITED ARAB EMIRATES |
| DJIBOUTI | MONACO | UNITED KINGDOM OF GREAT BRITAIN AND NORTHERN IRELAND |
| DOMINICA | MONGOLIA | UNITED REPUBLIC OF TANZANIA |
| DOMINICAN REPUBLIC | MONTENEGRO | UNITED STATES OF AMERICA |
| ECUADOR | MOROCCO | URUGUAY |
| EGYPT | MOZAMBIQUE | UZBEKISTAN |
| EL SALVADOR | MYANMAR | VANUATU |
| ERITREA | NAMIBIA | VENEZUELA, BOLIVARIAN REPUBLIC OF |
| ESTONIA | NEPAL | VIET NAM |
| ESWATINI | NETHERLANDS, KINGDOM OF THE | YEMEN |
| ETHIOPIA | NEW ZEALAND | ZAMBIA |
| FIJI | NICARAGUA | ZIMBABWE |
| FINLAND | NIGER | |
| FRANCE | NIGERIA | |
| GABON | NORTH MACEDONIA | |
| GAMBIA, THE | NORWAY | |
| | OMAN | |

The Agency's Statute was approved on 23 October 1956 by the Conference on the Statute of the IAEA held at United Nations Headquarters, New York; it entered into force on 29 July 1957. The Headquarters of the Agency are situated in Vienna. Its principal objective is "to accelerate and enlarge the contribution of atomic energy to peace, health and prosperity throughout the world".

TRAINING COURSE SERIES No. 87

EDUCATIONAL HYPOTHETICAL
SEVERE ACCIDENT
NUCLEAR POWER PLANT SIMULATOR
THEORY AND USER MANUAL WITH EXERCISES

INTERNATIONAL ATOMIC ENERGY AGENCY
VIENNA, 2025

COPYRIGHT NOTICE

All IAEA scientific and technical publications are protected by the terms of the Universal Copyright Convention as adopted in 1952 (Geneva) and as revised in 1971 (Paris). The copyright has since been extended by the World Intellectual Property Organization (Geneva) to include electronic and virtual intellectual property. Permission may be required to use whole or parts of texts contained in IAEA publications in printed or electronic form. Please see www.iaea.org/publications/rights-and-permissions for more details. Enquiries may be addressed to:

Publishing Section
International Atomic Energy Agency
Vienna International Centre
PO Box 100
1400 Vienna, Austria
tel.: +43 1 2600 22529 or 22530
email: sales.publications@iaea.org
www.iaea.org/publications

For further information on this publication, please contact:

Nuclear Power Technology Development Section
International Atomic Energy Agency
Vienna International Centre
PO Box 100
1400 Vienna, Austria
Email: Official.Mail@iaea.org

EDUCATIONAL HYPOTHETICAL SEVERE ACCIDENT NUCLEAR POWER PLANT SIMULATOR:
THEORY AND USER MANUAL WITH EXERCISES

IAEA, VIENNA, 2025
IAEA-TCS-87
ISSN 1018-5518

© IAEA, 2025

Printed by the IAEA in Austria
May 2025
<https://doi.org/10.61092/iaea.h7tv-0uiq>

FOREWORD

The IAEA provides a wide range of resources for education and training in nuclear related fields, including a variety of workshops; educational and training courses; fellowship programmes and schools; e-learning modules and basic principle nuclear power plant simulators; and various publications, including the those in the IAEA's Training Course Series. This knowledge is shared to encourage and support nuclear related learning across and between IAEA Member States.

A hands-on approach to learning is vital to efficient and thorough nuclear education. The IAEA supports such learning with its suite of basic principle and part-task nuclear power plant simulators. These are particularly effective for understanding nuclear power plant designs and for analysing specific physical and operational phenomena. Additionally, the training material provided supports users from Member States in successfully interacting with the simulators and in broadening their knowledge on the simulators themselves as well as the scientific theory behind nuclear power plant operation in normal and transient conditions. Training carried out using online simulators is highly cost effective and can help Member States with limited resources enhance their nuclear education programmes.

This publication provides a comprehensive overview of the severe accident simulator, covering both theoretical concepts and practical applications, along with a set of relevant exercises.

The IAEA officers responsible for this publication were T. Jevremovic and A. Miassoedov of the Division of Nuclear Power.

EDITORIAL NOTE

This publication has been prepared from the original material as submitted by the contributors and has not been edited by the editorial staff of the IAEA. The views expressed remain the responsibility of the contributors and do not necessarily reflect those of the IAEA or the governments of its Member States.

Guidance and recommendations provided here in relation to identified good practices represent expert opinion but are not made on the basis of a consensus of all Member States.

Neither the IAEA nor its Member States assume any responsibility for consequences which may arise from the use of this publication. This publication does not address questions of responsibility, legal or otherwise, for acts or omissions on the part of any person.

The use of particular designations of countries or territories does not imply any judgement by the publisher, the IAEA, as to the legal status of such countries or territories, of their authorities and institutions or of the delimitation of their boundaries.

The mention of names of specific companies or products (whether or not indicated as registered) does not imply any intention to infringe proprietary rights, nor should it be construed as an endorsement or recommendation on the part of the IAEA.

The authors are responsible for having obtained the necessary permission for the IAEA to reproduce, translate or use material from sources already protected by copyrights.

The IAEA has no responsibility for the persistence or accuracy of URLs for external or third party Internet web sites referred to in this publication and does not guarantee that any content on such web sites is, or will remain, accurate or appropriate.

CONTENTS

| | | |
|------|--|-----|
| 1. | INTRODUCTION..... | 1 |
| 1.1. | BACKGROUND..... | 1 |
| 1.2. | OBJECTIVE..... | 1 |
| 1.3. | SCOPE | 2 |
| 1.4. | STRUCTURE..... | 2 |
| 2. | THEORY MANUAL | 3 |
| 2.1. | SEVERE ACCIDENT MODEL..... | 3 |
| 2.2. | NUCLEAR POWER PLANT MODELS FOR NORMAL OPERATION..... | 59 |
| 3. | USER MANUAL | 79 |
| 3.1. | GENERAL INSTRUCTIONS..... | 79 |
| 3.2. | REFERENCE NUCLEAR POWER PLANT DESCRIPTION | 88 |
| 3.3. | MAIN FEATURES OF THE SIMULATOR..... | 110 |
| | REFERENCES..... | 135 |
| | ANNEX I..... | 137 |
| | ANNEX II | 139 |
| | ABBREVIATIONS | 203 |
| | NOMENCLATURE FOR SEVERE ACCIDENT MODEL | 205 |
| | CONTRIBUTORS TO DRAFTING AND REVIEW | 207 |

1. INTRODUCTION

1.1. BACKGROUND

The China Nuclear Power Operation Technology Corporation, Ltd. (CNPO) supplied the International Atomic Energy Agency (IAEA) with the Educational Hypothetical Severe Accident Simulator (ESAS) for educational and training purposes related to severe accidents in nuclear power plants (NPPs).

Severe accidents in NPPs are rare but potentially catastrophic events where multiple safety barriers fail, resulting in a significant core degradation. These accidents typically involve the loss of core cooling and the risk of core meltdown, potentially followed by the release of radioactive gases and particles if containment systems fail. They can be triggered by various events such as loss of coolant accidents (LOCA) combined with safety injection system failure, station blackout (SBO) from external power loss, or other combination of failures. The inability to remove decay heat from the reactor core can exacerbate these accidents, leading to fuel overheating, fuel rod cladding failure, and the potential for release of radioactive fission products.

In the event of a severe accident, the fuel in the reactor core may undergo partial or complete melting due to extreme temperatures. If not contained, the molten core has the potential to breach the reactor pressure vessel (RPV) and reach the containment structure, risking the release of radioactive materials into the environment and posing significant health and environmental hazards. To prevent and mitigate such accidents, NPPs are equipped with multiple layers of safety systems and features. These include redundant cooling systems, emergency core cooling systems, and passive safety systems that leverage natural forces like gravity and convection to cool the core. In the event of a severe accident, engineered safety systems and operator interventions are implemented to minimize core damage and control the release of radioactive materials, with the objective to mitigate its consequences and limit offsite protective actions in their location, duration and necessity.

Mitigating severe accidents is of utmost significance with continuous advancements in nuclear safety regulations and protocols shaped by lessons learned from historic incidents like Chernobyl and Fukushima Daiichi NPP. Advanced reactor designs and passive safety systems have been developed to enhance the inherent safety of NPPs and reduce the likelihood of severe accidents.

1.2. OBJECTIVE

The IAEA offers several educational basic principle NPP simulators to its Member States for the use on personal computers. These simulators aim to advance the understanding in the fundamentals of a NPP, their operational characteristics and highlight the diversity in reactor concepts. With the simulators come a range of additional materials, such as user and theory manuals. These simulators are intended to enhance understanding of NPP fundamentals, operational characteristics, and the variety of reactor concepts. Accompanying these

simulators are additional resources, including user and theory manuals. This publication is intended to contribute to the progress of nuclear education and training by explaining the theory behind ESAS, guiding users on simulator utilization, and offering a set of relevant exercises.

The use of the ESAS simulator is limited to providing general response characteristics of reactor systems and is not intended for plant-specific applications such as design, safety assessments, licensing, or operator training.

The information on how to obtain the IAEA NPP simulators can be found on the IAEA webpage:

<https://www.iaea.org/topics/nuclear-power-reactors/nuclear-reactor-simulators-for-education-and-training>

1.3. SCOPE

The scope of this publication is to offer guidance on installing, utilizing, and understanding the ESAS. It encompasses explanations of the modelling methodology for severe accidents in pressurized water reactor (PWR) type NPPs, as utilized in the ESAS. Additionally, it covers the setup, initialization, startup procedures, and key features of the ESAS, along with a general overview of the reference NPP. The simulator is based on a generic advanced PWR with both active and passive safety systems, allowing users to simulate various scenarios in normal and malfunctioning conditions. Its primary focus is on simulating severe accident scenarios, with numerous exercises provided to illustrate ESAS usage.

1.4. STRUCTURE

This publication consists of two main sections: the theory manual, the user manual, and an annex with detailed descriptions of relevant exercises. The theory manual describes the models utilized for severe accident simulation as well as those for simulating normal operating conditions. The user manual is further into four sections detailing the simulator's installation, startup, and initialization. Lastly, the annex with exercises covers descriptions of operational scenarios spanning normal operation, malfunctions, transient conditions, design basis accidents, and severe accidents.

2. THEORY MANUAL

The Theory Manual offers an in-depth explanation of the physics models that form the foundation for ESAS, a description of the reference NPP, and the key features of the simulator.

2.1. SEVERE ACCIDENT MODEL

Simulating severe accidents in NPPs necessitates extensive computational models that can replicate the development of events and the response of the reactor system under extreme and off-normal conditions. This section offers explanations of the fundamental elements incorporated in the severe accident model utilized in ESAS.

2.1.1. Primary thermal hydraulics model

This section describes nodalization of the primary system, and the description of the thermodynamics and hydraulics models of the primary reactor system.

2.1.1.1. *Primary system nodalization*

The nodalization of the primary system of a reference PWR plant is illustrated in Fig. 1. The individual nodes are indicated by the numbers assigned to various parts of the system. For modelling purposes, the coolant circulation system is divided into broken and unbroken loops. A broken loop contains primary system breaks and is treated separately. For SBO scenario, the broken loop may be defined as a loop containing the pressurizer (PZR), which is connected to its hot leg, since this is the only asymmetrical condition. In this model, loop 1 is either a broken loop or an unbroken loop. Loops 2 and 3 are always unbroken loops.

The nodalization scheme for the primary circuit's water inventory is illustrated in Fig. 2. For each of the regions, the nodes with a water inventory are considered separately: cold legs, intermediate legs, and downcomer nodes in the broken and/or unbroken loops. The downcomer water inventory (labelled DC in Fig. 2, see also Table 1) includes the water in the downcomer regions, the lower head as well as in the initial horizontal part of the cold legs from the RPV to the reactor coolant pumps. One water pool may combine several control volumes for the simulation of gas transport. This approach is adopted as the code mainly focuses on the prediction of thermal hydraulics conditions and the transport of fission products after the core is uncovered. Therefore, compared with the water transport, more detailed gas transport processes are required.

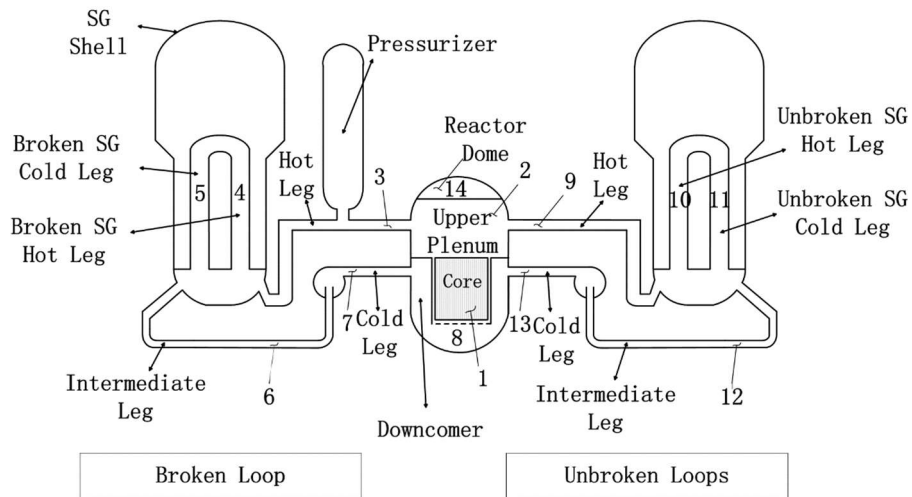


FIG. 1. Nodalization of the PWR primary system (courtesy of CNPO).

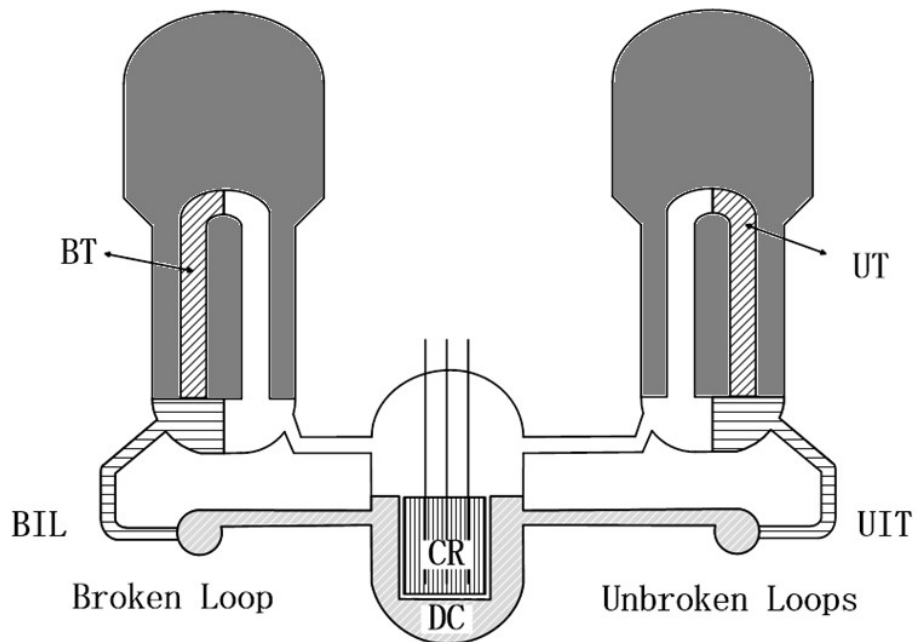


FIG. 2. Nodalization of the primary system water inventory (refer to Table 2) (courtesy of CNPO).

TABLE 1. EXPLANATION OF LABELS USED IN FIG. 2

| Label | Definition | Shading |
|-------|-------------------------------------|---------|
| CR | Core | |
| DC | Downcomer | ▨ |
| UIT | Unbroken loop intermediate tubes | ≡ |
| UT | Unbroken loop steam generator tubes | ▨ |
| BIL | Broken loop intermediate leg | ≡ |
| BT | Broken loop steam generator tubes | ▨ |
| - | Hot leg and upper plenum | □ |

Water that is neither in the cold side of the primary coolant loops nor in the downcomer is treated as if it were within the water pool of the reactor core. Thus, only after the water level drops below the height of the hot leg nozzle, the water mass in the reactor core water pool will be equivalent to the water mass in the actual reactor core. The mass of water in other nodes (for example, the hot leg) is algebraically computed according to the total water mass of the reactor core water pool. Each node is characterised by its gas temperature, hydrogen mass fraction and up to 4 (thermal) structure temperatures. The nodalization of the reactor core is distinctly separate from that of the primary circuit loops. The reactor core is modelled as a traditional quasi-steady state. This entails that steam and hydrogen released from the core to the primary circuit nodes are treated as if they had entered the core control volume at a certain point.

2.1.1.2. Thermodynamics model of a primary system

In the primary system model, the liquid and gas phases are usually considered separately. However, there are conditions in which the phases are treated together as a homogeneous mixture of both gas and liquid. This is implemented when the void fraction in the system is smaller than under two phase separation conditions, when the main coolant pumps are in operation and/or when the system is in the initial stage of a large break accident. As a result, the mixture behaves as a single substance and the flow rate will then be treated using a homogeneous two-phase model. When the two phases are mixed, the void fraction in the primary system is assumed to be a constant, thus adopting the overall average void fraction. The void fraction in the coolant exiting through the break of the primary system is also set to this value. By adjusting the flow rate of the water between the nodes of the primary system one can ensure the correct mass balance of water corresponding to the given void fraction. Energy exchange between nodes is computed in order to maintain a constant temperature in the water pool. When the flow rate through one of the main coolant pumps is insufficient to create a homogeneous flow, or when the inventory of the coolant drops sufficiently to inhibit two-phase natural circulation, the two phases will again be treated separately. In accident conditions, is it likely that the two phases will be divided. When the void fraction of the primary system is small, a homogeneous flow can be formed in the pipeline. If it is large, the gas phase and the liquid phase are separated. Upon the separation of the two phases, there is enough water in the primary system to allow for the free exchange between water in the nodes of the cold legs, the RPV and downcomer region, and the core nodes. Later, as the water level recedes, these different water inventories within the nodes are treated separately.

During the former of the two stages, namely when there is sufficient water in the primary circuit to allow for the free exchange of water between the different parts of the primary circuit, the masses of water in the downcomer and the cold legs are recorded and set to that value. The conservation of energy is then verified separately for all water pools with the help of the temperature differences. When the water pool is mixed with the gas phase or when there is only a slight temperature difference between water pools, the computation is executed in coupled mode. Due to the homogeneous mixture or the small temperature differences, the different working fluids are considered as one. In this mode, the system is either considered to

be saturated or solid (i.e. full of water and thus does not flow). The saturated computation is straightforward. If the system is solid, the pressure is set to the pressure of the pressurizer. If both the pressurizer and the primary system are solid, the pressure will be computed by calling another module. The gas temperature is assumed to be equal to the average water temperature at this stage. When water pools of the primary system are decoupled, the code operates in the "uncoupled" mode, allowing a temperature gradient between the primary water pool and the gas. This mode is used when the liquids are not mixed or the temperature gradient between the two is large. Now, there may be a significant temperature gradient due to superheated steam and hydrogen in the reactor core, the heating power of the reactor core water pool and the effects of the safety injection flow (if any) on the temperature of the cold legs and the downcomer. An uncommon approach is used to compute the gas temperature in the separate control volumes. Usually, one may solve the equations explicitly, without iterative calculations, however the incremental steps may not be too large, otherwise the calculations may diverge. Here, an ordinary differential equation is defined to represent the gas internal energy change rate in the total primary system. A fully implicit scheme is adopted in the code to solve the local gas temperature equations. The main advantage of this scheme is that it eliminates the numerical stiffness that may arise from separate computations of the pressure in each control volume. The mass fraction of the hydrogen in each node is treated in the same way. The steaming rate due to flashing in the reactor core and the downcomer is used to compute heat transfer and hydrogen generation. It is also used to compute the void fraction and the two-phase water level in the reactor core. This in turn will be used to determine the steaming rate induced by heat transfer from the core to water. In order to match this kind of computational loop, the computed flashing rate in the reactor core and the sub-regions of the downcomer needs to be stable and precise.

In this code, the initial step involves calculating the target steaming rate based on the existing temperature and pressure conditions. However, steam generation is restrained when there is pressurization in the primary system. To account for the pressurization resulting from steam generation, the steaming rates are accumulated throughout the time step in the code. The ultimate steaming rate is established by dividing the cumulative steaming rate by the corresponding time step.

2.1.1.3. *Hydraulics model of a primary system*

When the system is in the homogeneous state or when two phase natural circulation occurs, water transport between water pools will be adjusted to obtain the water volume in each water pool; this can be calculated as follows:

$$V_{node} = V(1 - \alpha) \quad (1)$$

where V_{node} is the total volume of a node (downcomer or cold leg), and α is the average void fraction. In the process of separating two phases (i.e. going from the coupled to the uncoupled mode), prior to the decoupling of the water pool in the code, water flow rates between water pools are adjusted to obtain the required volume. When the water pools are decoupled, the

flow rate from the cold leg to the downcomer is evaluated. The downcomer and reactor core flow rates are computed by quasi-static pressure balance. Two computations at the inlet and outlet of the primary system are usually necessary. First, the void fraction, the mass fraction of steam and hydrogen, and the enthalpy on the donor side need to be determined. Then the mass transfer rate is computed. The void fraction used is taken to specify whether the system is homogeneous or circulating and whether the inlet and outlet ports of the RPV pipelines are uncovered or covered by water. The void fraction entering the port is the associated loop void fraction α (used when the donor side of the port is homogeneous or when natural circulation is assumed to occur) or the local void fraction α_b (used when the two phases at the donor side of the port are separated). A separate computation of the void fraction entering the surge line is necessary. After the conditions of the donor side are determined, the flow rates computation is as follows:

- The flow rate is computed by calling the code's appropriate modules.
- When activated, the pressurizer spray will carry the coolant from the unbroken intermediate leg and inject it into the gas space of the pressurizer.
- When the flow through the pump bowls is blocked due to the existence of the water pool in the loop seals, counter-current natural circulation may occur in the hot leg. This phenomenon poses an important influence on heat distribution in the primary system in the early phase of the high-pressure accident sequence.
- The unidirectional flow between nodes is computed with regards to the overall pressure changes, the gas distributed source and the hydrostatic pressure head imbalances (due to the presence of gas within the primary circuit, it will produce a pressure head to drive the flow).

The computation of the gas flow rate in all parts of the primary system is like that of the water transport model.

2.1.2. Model of reactor core degradation and relocation

This section describes the model for reactor core degradation and relocation as formulated for the ESAS.

2.1.2.1. Core nodalization

The core is divided into seven radial rings (Fig. 3), and in 13 axial layers (Fig. 4). Additionally, the core is divided into three zones in axial direction: upper inactive zone, core active zone, and lower inactive zone. The upper inactive zone represents the upper grid plate, while the lower inactive zone represents the lower grid plate, support structures, core support plate and other structural parts.

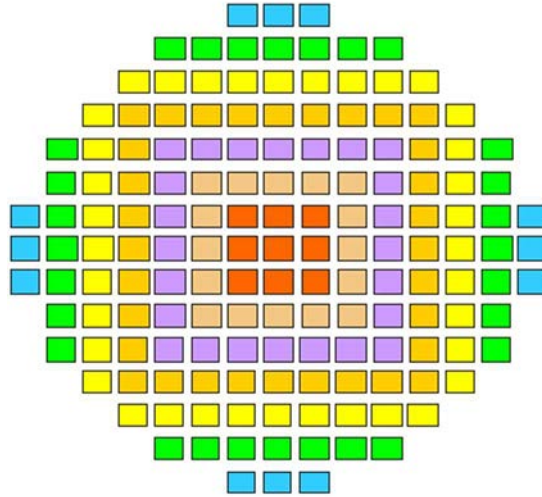


FIG. 3. Schematic of radial core nodalization (courtesy of CNPO).

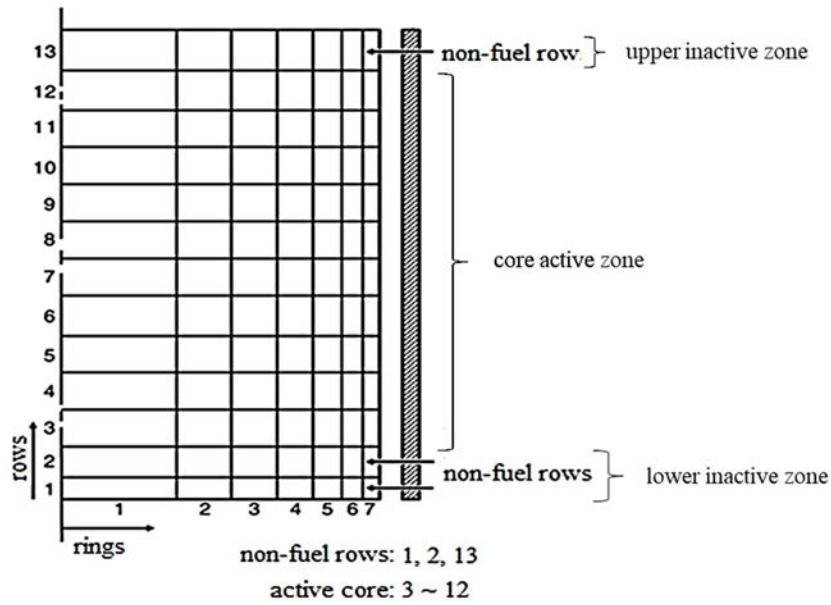


FIG. 4. Schematic of axial core nodalization (courtesy of CNPO).

2.1.2.2. Formation of reactor core molten pool and crust

To represent the transition from a thickened fuel pin structure (due to oxidation at high temperatures) to a node starting to form a molten pool and crust, the variable ICRTYP has been defined to identify a specific fuel condition. In terms of the degree of damage the following ICRTYPs are defined per node:

- (1) ICRTYP = 1: intact fuel pin structure;
- (2) ICRTYP = 2: collapsed fuel pin structure;

- (3) ICRTYP = 3: thickened fuel pin structure formed due to downward relocation (candling);
- (4) ICRTYP = 4: node filled with debris material with a porosity of less than 0.1 due to downward relocation and is no longer considered a fuel pin configuration nor is it penetrable;
- (5) ICRTYP = 5: completely molten nodes.

Note that the evolution of a fuel rod is irreversible. Once a node has changed from one ICRTYP, for example, ICRTYP = 1 to ICRTYP = 2, 3, 4 or 5, it cannot be changed back. The solid reactor core geometry (ICRTYP = 1 through 4) is illustrated in Fig. 5.

During the initial stage of the melt formation, the melt film flows downward along the fuel pin, as illustrated in Fig. 6 (a). When flowing into colder regions, the melt cools down, and the outside diameter of the fuel pin structure will increase, as illustrated in Fig. 6 (b). It is the relocation type corresponding to stages ICRTYP = 1, 2 and 3.

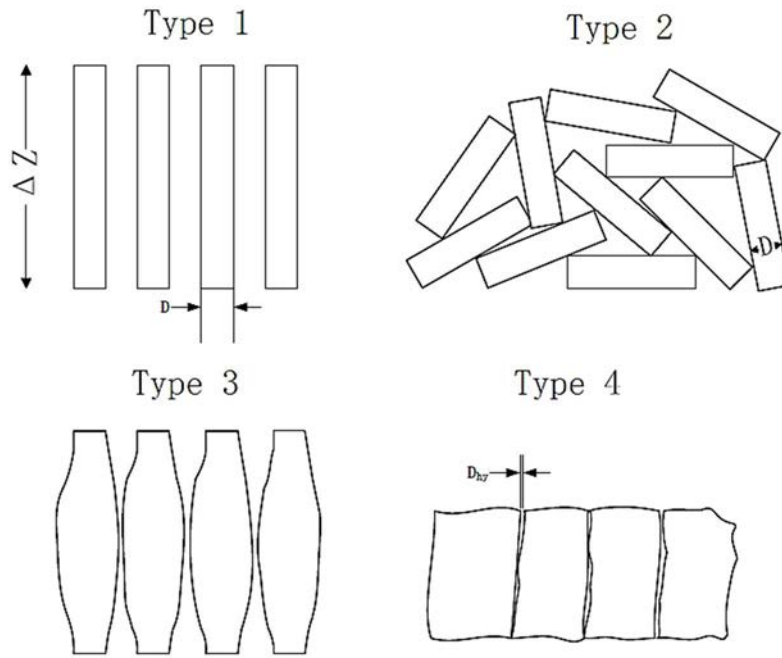


FIG. 5. Geometric types of solid core during the melting process (courtesy of CNPO).

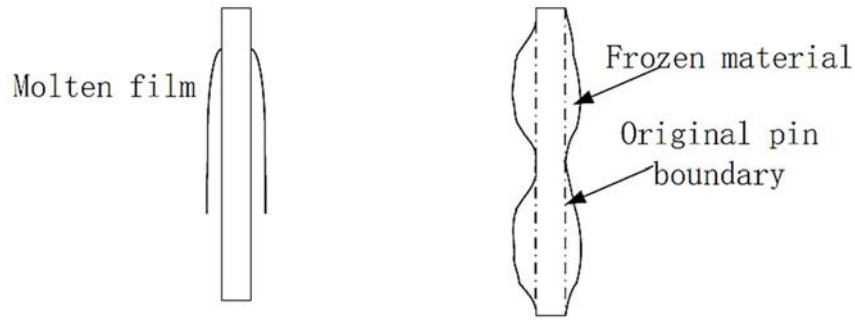


FIG. 6. Film flow model starting from ICRTYP=1: (a) melt film flows downward along the fuel pin, (b) effect of melt flowing into colder regions (courtesy of CNPO).

When frozen melt starts to accumulate at a lower situated node (ICRTYP = 3), a highly blocked flow channel is formed which limits the discharge of melt to a certain value. This value is determined by the hydraulic diameter and the hydrostatic pressure head of the melt above the blocked region. When the porosity drops below a specified value, the node type changes to ICRTYP = 4. When fuel within the nodes is melted completely, the fuel type will change to ICRTYP = 5. When the nodes are completely melted, the fuel type will change to ICRTYP = 5.

The transformation from one ICRTYP to another ICRTYP represents an irreversible change of the geometric structure of the reactor core. For example, when the axial load meets the collapse criteria of a fuel pin structure due to thermal expansion and fuel attenuation, the change from ICRTYP = 1 to ICRTYP = 2 is irreversible, which is consistent with the possible physical processes. For a structure with ICRTYP = 3, lower nodes are filled with solidified melt due to the downward relocation of the melt. If this causes the node porosity to drop to a level below 0.1, this node has likely lost its fuel pin structure completely. Therefore, this node status is considered as the initiation of the formation of crust-like structure. Depending on the node, it will melt in a particular way depending on its position in the core, as illustrated in Fig. 7.

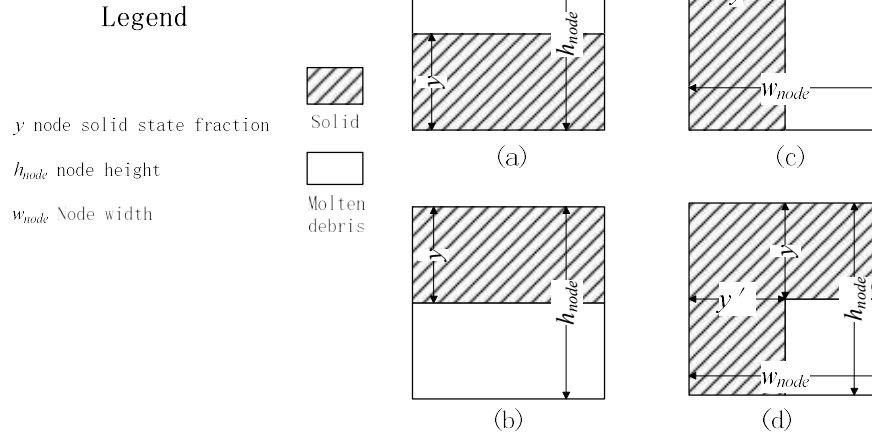


FIG. 7. Different melt - solid structures when ICRTYP=4: (a) bottom node, (b) top node, (c) outer radial node, (d) outer top node (courtesy of CNPO).

With regards to the special cases of both upward facing nodes and nodes in the outer radial region, possible physical phenomena occurring in these sub-nodes are considered. The upward heat loss is computed and the likelihood of a melt occurring along the lateral boundary of these nodes is assessed. If a node is filled to a high percentage and thus has a low porosity, it will be treated as a part of the debris crust. Then, if a melt occurs within the node, it will be treated as a layered structure as shown in Fig. 7 (crusts of a given node are part of the solid structure). Once the node has melted completely, it becomes part of the molten pool. Fig. 7 (b) and (c) show the two special structures for a node with ICRTYP = 4 (structure no longer considers fuel pin). These structures serve to assess the condition of the top and outermost nodes within a node column featuring multiple nodes categorized as either ICRTYP = 4 or ICRTYP = 5, where upper or side crusts may develop. However, their consideration is limited to nodes characterized as ICRTYP = 4. Once this condition is met, the designated structure for top nodes is utilized to calculate heat losses from the upper solid material or upper gas and heat structures.

The potential for crust formation on the top and side structure of the debris is also utilized to evaluate the potential of crust structure growth as well as melt formation that may occur at the sides or the bottom of the crust. In all cases, the frozen melt thickness is represented by the solid fraction of the node. Fig. 7 (d) illustrates another special structure, where the outer layer nodes are treated as top nodes. In this special structure, solidified debris is distributed at the top and sides of the crust according to the node aspect ratio.

Considering these different structures, reactor core nodes may differ in conditions at different stages in time. Specifically, adjacent nodes in the central region may have different ICRTYP types, as illustrated in Fig. 8. If this happens, the region is in a transient state, which likely results from different material melting temperatures (due to the relocation of mixtures) as well temperature differences due to axial and radial power distributions. However, when inhomogeneous core node regions are encountered, the energy transfer from completely

molten nodes to a node with, for example, three sides in the process of melting will rapidly cause the melting of such a node and subsequently smoothen the crust boarder.

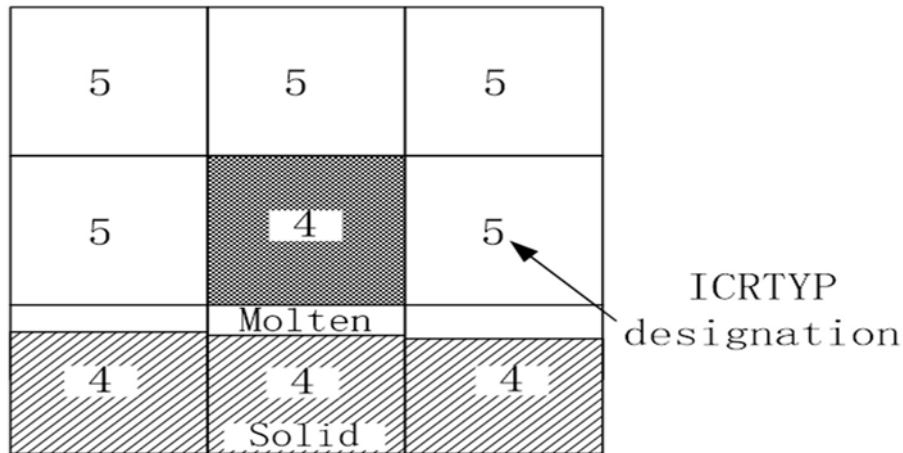


FIG. 8. Potential structure of bottom crust development (courtesy of CNPO).

Once the material meets conditions for $ICRTYP = 4$, the only way that downward flowing melt can penetrate to lower nodes is when the crust of the bottom nodes becomes thin enough to fail. Under these conditions, a criterion for crust creeping due to stress and temperature changes was developed to characterize the potential for downward melting. This criterion makes use of a time-temperature correlation to characterize the failure potential, which in turn also minimizes the numerical sensitivity related to the irreversible changes in the reactor core meltdown progression.

Note that a node does not have to be fully crusted to prevent the flow of the melt. As stated above, the downward flow rate depends on the hydraulic diameter as there may be a big flow resistance in the molten debris crevice.

2.1.2.3. Collapse of damaged reactor core nodes

There are several mechanisms which may result in the transformation of the vertical fuel pin structure ($ICRTYP=1$) to a collapsed fuel pellet bed ($ICRTYP = 2$), including cladding. The main physical processes under consideration are as follows:

- (1) High temperatures and the relocation of the metal cladding by oxidation and melting;
- (2) Fuel pin thinning leading to significant lateral displacement;
- (3) High temperatures and the relocation of metal structural components as well as the collapse of adjacent nodes;
- (4) Significant steaming or vibration within high temperature nodes;
- (5) Re-melting of blocked nodes connecting lower blocked nodes and upper intact nodes.

Processes (1)-(3) are used to calculate the Larson-Miller constant¹ (LMC) which expresses the collapse conditions. Process number (4) is associated with reactor core reflooding after large scale oxidation (includes ICRTYP = 1 and 2).

A collapse of a coolant channel occurs when the creeping determined in some reactor core nodes or channels is beyond the collapse criterion. There are four different situations:

- (1) No node collapse around;
- (2) Lower nodes collapse;
- (3) One adjacent node is empty;
- (4) All adjacent nodes are vacated.

The collapse criterion is based on the Larson-Miller creep-rupture model² including the default LMC, which is 50.0. Its value is inversely proportional to the applied stress. Parameters in the four cases are defined as LMCOL0, LMCOL1, LMCOL2 and LMCOL3. These are used for the case when the surrounding core nodes have not collapsed, a node below the node in question has collapsed, the core node is next to an empty core node or the core node is surrounded by empty core nodes, respectively. The collapse of a fuel pin occurs when the accumulated damage fraction is equal to or greater than 1. The damage fraction is computed as follows:

$$DF = \frac{\Delta t}{\frac{t_c}{f(x)}} \quad (2)$$

where:

Δt is the time step [s];

t_c is the time to collapse after applying the stress [s];

$f(x)$ $f(x) = (1 + e^{-x})^{-1}$;

$x = \beta \left(\frac{T}{T_{ref}} - 1 \right)$;

β is the sensitivity coefficient, assumed to be 50;

T is the node temperature [K];

and T_{ref} is the reference temperature [K].

¹ The Larson-Miller constant, also known as the Larson-Miller parameter, is a material property used in materials science and engineering, particularly in the field of creep behaviour analysis. The Larson-Miller constant is defined by the Larson-Miller equation, which is an empirical equation used to predict the life or time to rupture of a material subjected to elevated temperatures. The equation is often used for materials such as metals and alloys exposed to high-temperature conditions, especially in situations where traditional time-temperature parameters may not be directly applicable. It provides a useful approach for estimating the effects of temperature and time on the creep life of materials.

² In the context of creep-rupture testing, the Larson-Miller model allows for the estimation of the time to rupture based on the Larson-Miller parameter. The relationship between the Larson-Miller parameter and time to rupture is established empirically and is specific to the material being tested. Engineers and researchers use this model to make predictions about the performance of materials subjected to high-temperature and sustained loading conditions.

The variable t_c is computed by the following expression using the LMC:

$$t_c = \max\left(100, 3600 \cdot 10^{\frac{100 \cdot LMC}{T} - 20}\right) \quad (3)$$

To prevent an unreasonably sudden collapse within a small-time step, it is determined that the collapse time t_c does not fall below 100 s for any time step. The collapse time of 100 s corresponds to a fuel pin temperature of 2700 K, and thus it is assumed that the effects with temperatures greater than 2700 K can be ignored.

By default, the LMC is set to 50.0 for LMCOL0, LMCOL1, LMCOL2 and LMCOL3. As an example, if $f(x)$ is set to 1, the collapse time at 2500 K will be 1 hour. However, if $f(x)$ is computed as given, the collapse time at the same 2500 K will be 2 hours.

Channel collapse is defined as the drop of material within the channel to a lower position either within or above the current node until all node materials reach the porosity (or void fraction) of debris bed. In this case, the largest steaming rate is limited by the Kutateladze number.

At a location where ICRTYP = 4 and a crust has formed, the model provides the characteristic crust thickness at which meltdown can occur. The functional expression to describe its strength derives from the LMC which is inversely proportional to the stress. The LMC is defined with:

$$LMC = \bar{T}_c (20 + \log_{10} t_r) \times 10^{-3} \quad (4)$$

where, T_c represents the average crust temperature and t_r is the rupture time. Numerous surveys on UO₂ fuel indicate that the material is prone to creep. The stress (σ_s) experienced is related to the cumulative debris depth or crust thickness (x_c) and the effective area resisting the load (πR^2), as illustrated in Fig. 9.

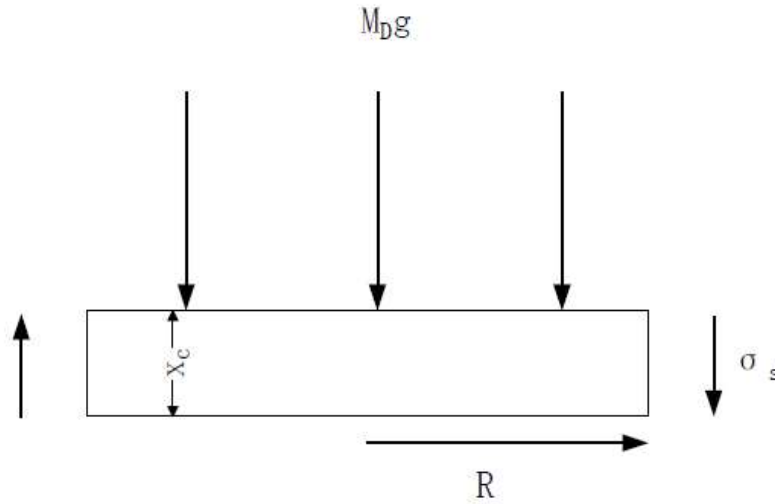


FIG. 9. Structure of stress applied on the debris crust (courtesy of CNPO).

It is assumed implicitly that when the internal nodes have all reached a similar state, the load is represented as a disk distribution along radius R and are supported by lower intact fuel pins. Therefore, the shear force applied to this disk is approximated with:

$$s_s = \frac{\rho_D g h_D x_p}{2x_c} \quad (5)$$

where x_p represents the fuel pin pitch, namely, the space between fuel pins supporting the molten pool, g the gravitational acceleration, ρ_D the debris density, and h_D the debris depth. Shear stress is utilized to evaluate the bottom crust failure.

Another variable to be computed is the average crust temperature. Under normal conditions, this value is determined by the temperatures of the overlying melt and of the nodes below. Therefore, it is approximated by the heat transfer from the crust to the lower nodes. The temperature gradient is given by:

$$\frac{dT}{dy} = \frac{T_m - T_{n-1}}{x_c + \frac{x_{node}}{2}} \quad (6)$$

Where, when the crust thickness x_c is greater than half the node thickness $\frac{x_{node}}{2}$, T_m is the node temperature in question. When the crust thickness x_c is smaller than or equal to half the node thickness $\frac{x_{node}}{2}$, T_m is the melting temperature, as illustrated in Fig. 10. In addition, T_{n-1} is temperature of the node below. Thus, the average crust temperature is evaluated as follows:

$$\bar{T}_c = T_m - \left(\frac{dT}{dy}\right)\left(\frac{x_c}{2}\right) \quad (7)$$

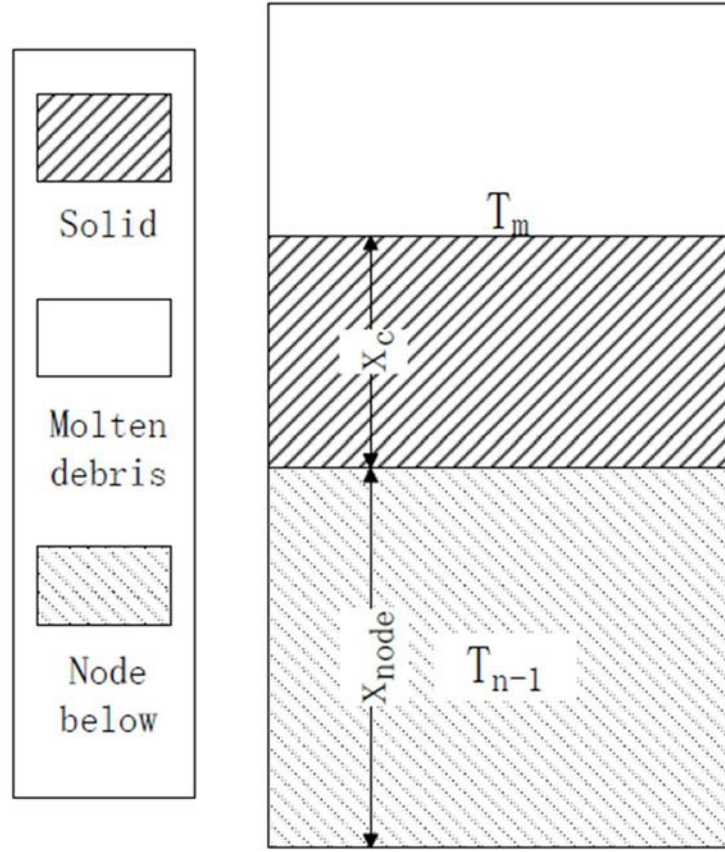


FIG. 10. Determining the average crust temperature (courtesy of CNPO).

The relation between the applied stress and the LMC is thus established. The tensile strength and rupture strength of UO_2 at room temperature are 7.5 MPa (75 kg/cm²) and 220 MPa (2 200 kg/cm²), respectively. This gives an indication of the material strength, specifically the functional relation between the stress and the crust's LMC which needs to be established. In addition, the Three Mile Island accident reveals that a stable crust is enough to withstand the weight of a debris bed ($\sim 2\,000$ kg) for more than an hour. If one assumes that the melt temperature is 3 000 K, the bottom crust temperature has that of saturated water (about 600 K) and the average crust temperature is 1 800 K with a thickness of 5 cm, a mass of 20 000 kg and a radius of 1.5 m, the corresponding bending stress is 24 MPa (based on $B = \rho_D g h_D \left(\frac{R}{x_c}\right)^2$).

Based on these two factors, the functional relationship between the applied stress and the LMC is a straight line through these points, through which the crust parameter for computing the applied stress can be acquired (Fig. 11). Therefore, the time-temperature till a rupture is computed as follows:

$$LMC = \frac{-\ln(\sigma) + LMU2A}{LMU2B} \quad (8)$$

where the nominal values of $LMU2A$ and $LMU2B$ are 19.8 and 0.083, respectively, representing the values used to define the time-temperature relation. Equation (8) gives the Larson-Miller evaluation method for downward meltdown progression resulted from lower crust failure.

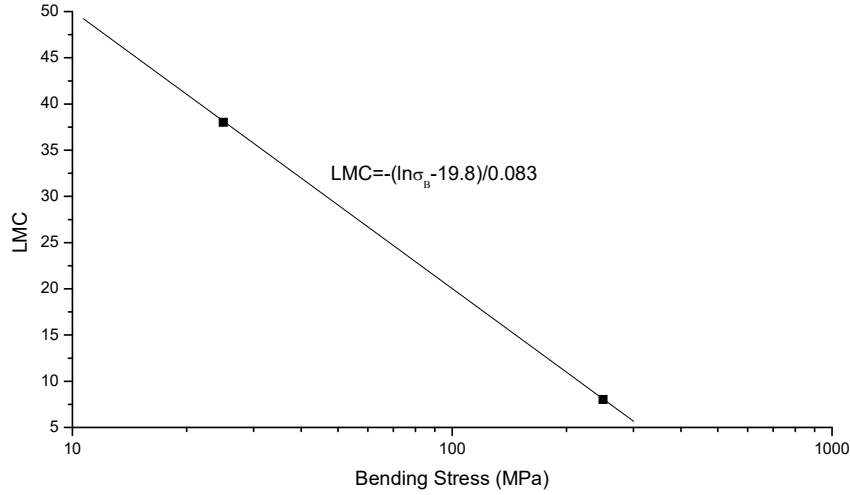


FIG. 11. Functional relation for bending-induced cladding failure (courtesy of CNPO).

Once a node reaches the condition $ICRTYP = 4$, the node failure will be addressed with the help of creep failure evaluations. The mechanism of creep failure provides the time-temperature performance, where worsening conditions are indicated by the rising of the average temperature. While this is an approximate behaviour, it provides the expected trends for all crust behaviours and minimizes possible numerical sensitivity due to switching between two models in the code (before and after failure). Crust rupture time is determined by the sum of the rupture progression time fraction in all time steps.

An approximate failure mechanism is used for the crust at the external core boundary, specifically the interface between the core and the downcomer region. A similar calculation is also performed for the bending of crust. The stress on an individual crust node is the height of the melt above the bottom of that node, meaning the total height of the melt is not necessary. This evaluation will also be done for all the nodes in the external radial region where $ICRTYP = 4$.

If the failure condition evaluates as true, treat the failure as a local failure, which permits two possible debris relocations. In case of significant bypass flow between the reactor core and the core barrel, molten debris may flow into the bypass region before entering the lower plenum, as illustrated in Fig. 12. However, if the bypass channel is small and the reactor core is directly in contact with the core barrel, then the melt can only relocate when the whole core barrel thickness is penetrated and thus flow into the downcomer and the lower plenum.

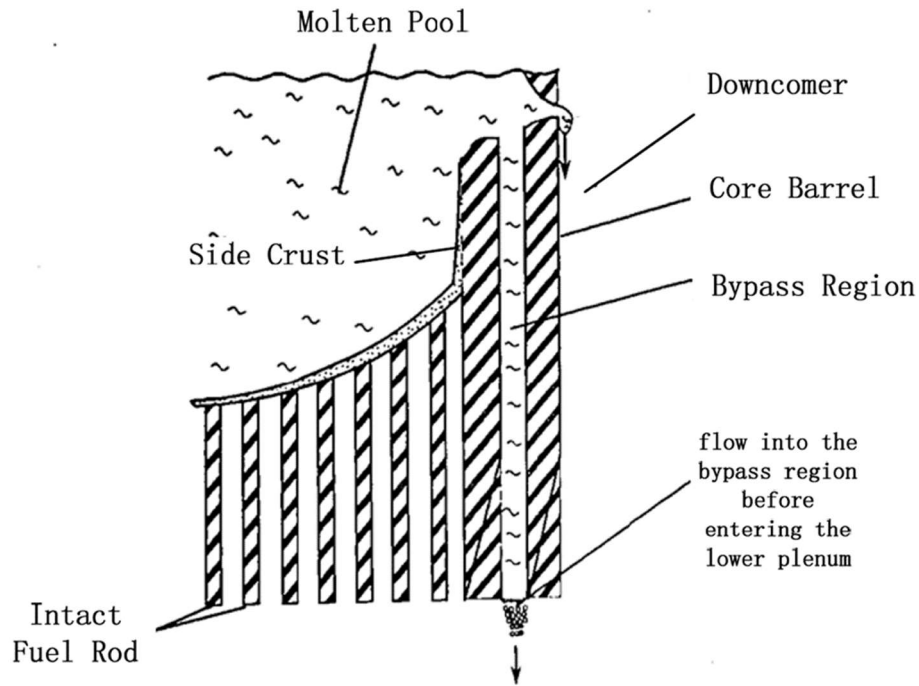


FIG. 12. Molten pool side crust break (courtesy of CNPO).

2.1.2.4. Collapse of remaining reactor core

When the reactor core mass becomes smaller than a certain proportion of the initial core mass, due to melting and relocation, the state of the core at that time is subsequently defined as completely collapsed. What remains of the reactor core will then collapse into the lower plenum in a final time step. After the large scale debris relocation to the lower plenum, a rough simulation of the degradation of the reactor core support structures will be carried out.

2.1.2.5. Relocation of molten material

In the code, downward relocation of molten material is computed in accordance with external film flow combined with internal pipe flow. When the cylindrical fuel pins are not in contact with one another (i.e., the pitch is larger than the rod diameter), the melt flow may well comply with the film flow mechanism. However, if it does not, internal pipe flow will allow for a more appropriate description of the flow. The two mechanisms are illustrated in Fig. 13. The melt flow rate is computed and determines which mechanism is used.

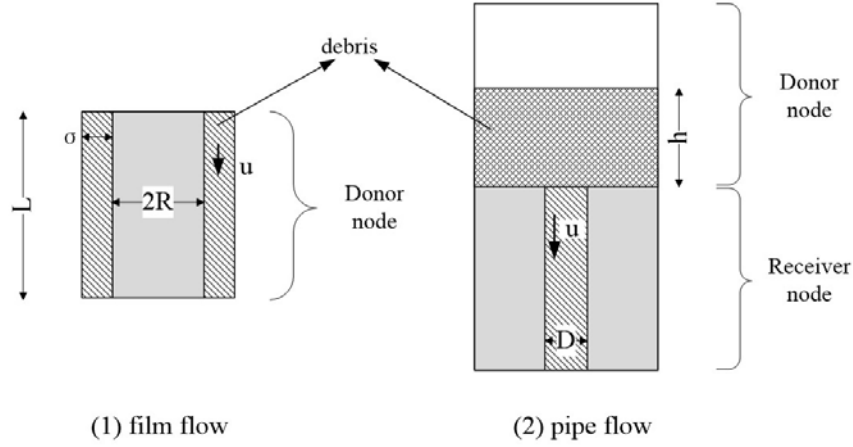


FIG. 13. Illustration of two downward flow mechanisms (courtesy of CNPO).

In case of film melt flow, the steady state film thickness δ above the cylindrical fuel pins at the source node will be computed as follows:

$$\delta = \frac{m_{pc}}{N\rho_c X_p L} \quad (9)$$

where, m_{pc} is the mass of the molten core material and ρ_c its density at the source node, N is the number of fuel pins in the source node, X_p is the wetted perimeter defined as $X_p = \frac{4A}{D_h}$, with A being the flow area and D_h the hydraulic diameter, and L is the node length. In case of a stable film flow, the film's gravitational and viscous forces are balanced, and the average melt velocity U_f and film thickness δ have the following relation:

$$U_f = \frac{\rho_c g}{3\mu_c} \delta^2 \quad (10)$$

where, μ_c is the dynamic viscosity of the melt and g is the constant of gravitational acceleration. Stable film flow rate W_f is approximated with:

$$W_f = \rho_c \delta U_f X_p N \quad (11)$$

When melting continues, some nodes may be blocked by a large amount of solidified debris. Therefore, the discharge of the melt from the source node may be restricted to very small channels thus reducing the flow (i.e., pipe flow). For internal pipe flow, the gravity momentum of the liquid in the source term node provides the potential energy to allow downward flow through the available regions in the next lower node. Thus, the driving potential is balanced by the acceleration and frictional pressure losses as follows:

$$\rho_c g h_p = \left(1 + f \frac{L}{D_h}\right) \left(\frac{W_p^2}{2\rho_c A_p^2}\right) \quad (12)$$

where, f is the friction coefficient, L the axial node length, W_p the pipe flow rate, A_p the internal flow area in the receiver node (the node below the source node), and D_h is the hydraulic diameter. The driving head is obtained with:

$$h_p = \frac{m_{\rho c}}{\rho_c A_n} \quad (13)$$

where, A_n is the node area of the source node.

For the use of the restricted internal pipe flow correlation, internal channels need to be obstructed, so that the flow is first assumed to be laminar flow. Its friction coefficient f is computed using the following:

$$f = \frac{64\mu_c}{\left(\frac{W_p}{A_p}\right) D_h} \quad (14)$$

In conclusion, the mass flow rate in the internal pipes W_p is computed as follows:

$$W_p = \frac{-B + \sqrt{B^2 - 4C}}{2} \quad (15)$$

$$U_p = \frac{W_p}{A\rho_c} \quad (16)$$

where, $B = \frac{64\mu_c A_p L}{D_h^2}$ and $C = (\rho_c A_p)^2 (2gh_p)$.

Then, the computed mass flow rate W_p is utilized to compute the Reynolds number. The Reynolds number is always greater than 640 when using this empirical formula (scope of correlation). In this case the friction coefficient is set to 0.1.

Taking these two flows into consideration, the discharge rate W of the melt from the source node into the receiver node is calculated for each time step Δt as follows:

$$W = \min\left(W_p, W_f, \frac{m_{\rho c}}{\Delta t}\right) \quad (17)$$

Similarly, one can acquire the limiting flow velocity U .

Regardless of whether film flow or a pipe flow relation are used, melt will freeze to develop a crust between the external surface of the cold wall and the internal liquid. The computation of the crust growth (i.e., frozen melt) is equivalent to the problem of freezing a liquid material at its melting point to the surface of a semi-infinite solid. For this situation, conduction theory's familiar square root growth law is used to compute the constantly growing thickness of the crust δ_c :

$$\delta_c = 2\lambda\sqrt{a_c t} \quad (18)$$

Where, a_c is the thermal diffusion coefficient of the melt, and λ is the growth constant, as shown in the implicit relation below:

$$\lambda e^{\lambda^2} \left(\frac{1}{\sigma} + \text{erf}(\lambda) \right) = \frac{1}{\sqrt{\pi}\beta} \quad (19)$$

Where, β is the dimensionless latent heat of melting:

$$\frac{1}{\beta} = \min \left(3, \frac{c_c(T_{mp} - T_w)}{h_{fs}} \right) \quad (20)$$

Here, h_{fs} is the latent heat of fusion, c_c the specific heat capacity of the melt, T_{mp} is the melting temperature, T_w is the cold wall temperature at the receiver node. In Eq. (19) variable s is the following ratio:

$$\sigma = \left(\frac{K_w C_w \rho_w}{K_c C_c \rho_c} \right)^{\frac{1}{2}} \quad (21)$$

When the melt condition is very close to that of the solid wall, s is assumed to be 1.0. When s is a constant, the growth constant λ only depends on the dimensionless latent heat b . Therefore, the growth constant solution λ is fitted by using a polynomial as follows:

$$\lambda = 0.993B - 0.961B^2 + 0.578B^3 \text{ with} \quad (22)$$

$$B = \frac{1}{\sqrt{\pi}\beta} \quad (23)$$

This polynomial applies when $T_{mp} - T_w$ results in a temperature between 1 K and 3000 K. The crust thickness increase during growth per time step is computed as follows:

$$\delta_c = 2\lambda\sqrt{a_c \Delta t} \quad (24)$$

Thus, the mass of condensed melt at the receiver node after a time step is computed as follows:

$$m_{fz} = \frac{\rho_c X_p N L \delta_c}{2} \quad (25)$$

The mass of the cumulated melt that relocates to the receiver node (the node below the source node) and may further relocate in a given time step, is the difference between the mass of the debris entering the receiver node and the solidified mass. Or, if the entire length of the node cannot be penetrated in one time step (possibly due to water or grid spacers), it is the total

mass of the melt entering the node. The mass m_r which cannot penetrate the whole receiver node length in one time step can be computed as follows:

$$m_r = \Delta t_r W \quad (26)$$

Where, Δt_r is the time required for the melt to flow through a certain length L of a node at a given velocity U , as:

$$\Delta t_r = \frac{L}{U} \quad (27)$$

For those cases where the grid spacers or water obstructions exist in the receiving node, Δt_r is set equal to Δt , the current time step (i.e. the melt flow cannot penetrate the grid spacers or the water in the receiving node within the time step). The mass leaving the source node and accumulating at the bottom of the receiving node for further relocation in the same time step is as follows:

$$m_{ac} = \Delta t W - \max(\Delta t_r W, m_{fz}) \quad (28)$$

where m_{fz} is the mass of frozen melt at the receiver node after a time step and m_{ac} is the mass leaving the source node, accumulating at the bottom of the receiving node for further relocation in the same time step.

It can be noted that this mass is added to the molten mass that already resides in the receiving node at the beginning of the time step, and the sum becomes the molten mass available for evaluating the melt relocation from the receiving node to the node below it during the same time step. That is, melt progression is evaluated from the top of the core downward, row by row. Liquid in a node in any row, regardless of how or when it appears, is available for relocation.

2.1.3. Lower head molten pool model

2.1.3.1. Model assumptions

The debris bed is divided into the particulate debris bed, the continuous, unfragmented, oxide crust, the central continuous molten pool and the overlying metal layer. The debris bed and the water distribution as applied for this PWR are illustrated in Fig. 14.

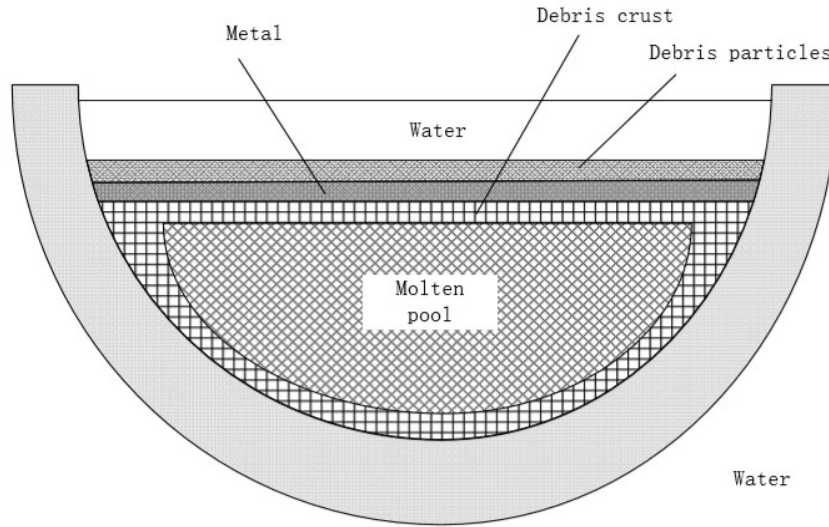


FIG. 14. Debris bed structure inside the lower head (courtesy of CNPO).

The main assumptions made in the lower head molten pool model are as follows:

- a) The debris bed is divided into the oxide molten pool in the lower part of the lower plenum and the top metal layer;
- b) The debris bed surface in contact with the upper water flow, RPV wall and the (thermal) structures can form three kinds of debris crusts: debris particles, metal layer and oxide debris crust (Fig. 14);
- c) Considering the crust's internal decay heat, the internal temperature curve is assumed to be one-dimensional and parabolic;
- d) After the metal layer has risen to the top of the oxide debris, the molten pool is deemed to be mixed uniformly and thus has the same thermal physical properties;
- e) The debris crust has the same material composition as the debris pool;
- f) The steady state equation is adopted for heat conduction;
- g) The state of the debris pool (i.e., solid, liquid or superheated liquid) will be determined according to the average debris temperature;
- h) The simulation of the debris bed quenching by water injection and the computation of the debris pool crust are separated.

2.1.3.2. Molten pool convection heat transfer

Heat in the oxide layer transfers both upwards and downwards and is affected by the decay heat in the molten pool of the lower head. When the RPV is in a state of long-term cooling, namely in a stable state of outward heat transfer, there will be a strong turbulent natural convection region in the upper region of the molten pool, while the lower region will be stable with significant thermal stratification.

The most preferred relations currently used for the description of the upward heat transfer process in the molten oxide pool are the Kulaci-Emara equation³, the Seinberner-Reineke equation⁴ and the Mayinger equation⁵.

For downward heat transfer, the main equations describing its progression in the molten oxide pool are the Mayinger equation, the Kelkar equation and the equation fitted according to the ACOPO (Advanced Core Physics and Operation) experimental data. The ACOPO experimental data refer to the dataset generated from experiments conducted using the ACOPO facility. The ACOPO experimental data typically encompass a wide range of parameters and variables related to nuclear reactor core behaviour, thermal hydraulics performance, neutron flux distribution, and other relevant aspects of reactor operation. These experiments are designed to provide valuable insights into reactor behaviour under different conditions, inform reactor design and safety assessments, and validate computational models used in reactor analysis. The ACOPO facility may utilize various instrumentation and measurement techniques to collect data, including neutron detectors, temperature sensors, pressure transducers, and flow meters. Additionally, advanced data acquisition systems are often employed to ensure accurate and reliable data recording during experiments.

According to the experiment conducted on the BALI device by Bonnet and Seiler [1], the average heat flux of the entire molten pool is expressed as:

$$q''_u = 0.466 \frac{k_{px} \Delta T}{R_{lp}} Ra^{0.229} \quad (29)$$

$$q''_d = 0.131 \frac{k_{px} \Delta T}{R_{lp}} Ra^{0.25} \left(\frac{2z_{lp}}{3R_{lp} - z_{lp}} \right)^{\frac{0.19}{3}} \quad (30)$$

$$q''_s = 0.85 \frac{k_{px} \Delta T}{R_{lp}} Ra^{0.19} \quad (31)$$

³ The Kulaci-Emara equation, also known as the Kulaci-Emara correlation, is an empirical correlation used in nuclear engineering to estimate the void fraction or void fraction distribution in two-phase flow systems, particularly in nuclear reactors. It is named after its developers, Kulaci and Emara. The equation relates the void fraction to other parameters such as mass flux, quality, pressure, and axial position in the flow channel. It is typically expressed in the form of an empirical equation, often derived from experimental data. The Kulaci-Emara equation is valuable in understanding and predicting the behaviour of two-phase flows within nuclear reactor systems.

⁴ The Seinberner-Reineke equation, also known as the Seinberner-Reineke correlation, is an empirical correlation used in nuclear engineering to estimate the void fraction or void fraction distribution in two-phase flow systems, particularly in nuclear reactors. As the Kulaci-Emara correlation, the Seinberner-Reineke equation relates the void fraction to various parameters such as mass flux, quality, pressure, and axial position in the flow channel.

⁵ The Mayinger equation, developed by Mayinger in 1977, is an empirical correlation used in nuclear engineering and thermohydraulics to predict the critical heat flux in subcooled boiling flows. Critical heat flux refers to the maximum heat flux at which boiling occurs without an unacceptable rise in wall temperature. The Mayinger equation relates the critical heat flux to various parameters such as mass flux, inlet subcooling, and flow quality. It is particularly useful in the design and analysis of nuclear reactor systems, where accurately predicting critical heat flux is crucial for ensuring safe and efficient operation. The equation is derived from experimental data and has been validated for a range of flow conditions typically encountered in nuclear reactor applications.

where

k_{px} is the thermal conductivity of the melt [$\text{W}\cdot\text{m}^{-1}\cdot\text{K}^{-1}$];

ΔT is the degree of superheat of the melt [K];

R_{lp} is the lower plenum radius [m];

and z_{lp} is the debris bed height [m].

For liquid water pools with heat sources, the Rayleigh number with the largest characteristic length can be expressed as follows:

$$Ra = \frac{g\beta q_v R_{lp}^5}{\alpha \nu k_{px}} \quad (32)$$

where

g is the gravity acceleration [$\text{m}\cdot\text{s}^{-2}$];

q_v is the volume heat production rate of the debris bed [$\text{W}\cdot\text{m}^{-3}$];

α is the thermal conductivity of the debris bed [$\text{W}\cdot\text{m}^{-1}\cdot\text{K}^{-1}$];

and ν is the kinematic viscosity of debris bed [$\text{kg}\cdot\text{m}^{-1}\cdot\text{s}^{-1}$].

The heat transfer equation is fitted in accordance with the ACOPO experiment for the upwards:

$$Nu_{up} = 1.95 Ra'^{0.18}, 10^{14} < Ra' < 10^{16} \quad (33)$$

and downwards:

$$Nu_{dn} = 0.3 Ra'^{0.22}, 10^{14} < Ra' < 10^{16} \quad (34)$$

These heat flux computation equations may be expressed in the form of heat transfer coefficients, $q'' = h\Delta T$. The upward, downward, and sideward heat transfer coefficients given by Bonnet and Seiler [1] are as follows:

$$h_u = 0.466 \frac{k_{px}}{R_{lp}} Ra^{0.229} \quad (35)$$

without a heavy
metal layer:

$$h_d = 0.131 \frac{k_{px}}{R_{lp}} Ra^{0.25} \left(\frac{2z_{lp}}{3R_{lp} - z_{lp}} \right)^{\frac{0.19}{3}} \quad (36)$$

with a heavy metal
layer:

$$h_d = 0.131 \frac{k_{px}}{R_{lp}} Ra^{0.25} \left(\frac{2z_{lp}}{3R_{lp} - z_{lp} + z_{hv}} \right)^{\frac{0.19}{3}} \quad (37)$$

$$h_s = 0.85 \frac{k_{px}}{R_{lp}} Ra^{0.19} \quad (38)$$

When the average temperature of the molten pool lies in between the solid phase and the liquid phase (i.e., between the solidus and the liquidus line on the phase diagram), the heat transfer coefficient presented above, where the two-phase mixing effect is taken into consideration, is modified to:

$$h_{2\phi} = h(1 - \Phi_{sol})^{c_{2\phi}} \quad (39)$$

where

$c_{2\phi}$ is the index, model parameter, currently set to 2.75;

and Φ_{sol} is the solid fraction in the mixture.

In the code, the solid fraction is computed from the total molten pool energy U_{pl} with the help of the following relation:

$$\Phi_{sol} = \frac{U_{liq} - U_{pl}}{U_{liq} - U_{sol}} \quad (40)$$

U_{liq} and U_{sol} correspond to the total energy at the liquidus temperature and the solidus temperature, respectively.

2.1.3.3. Debris crust dynamics and heat conduction

When the bulk of the molten debris encounters the surfaces of the various heat sinks, a debris crusts will form. The crust will form adjacent to the upper water flow, the RPV wall and the (thermal) structures. The code efficiently simulates the growth and shrinkage of the different crusts. The dynamics model for the lower debris crust with different azimuthal angles is illustrated in Fig. 15.

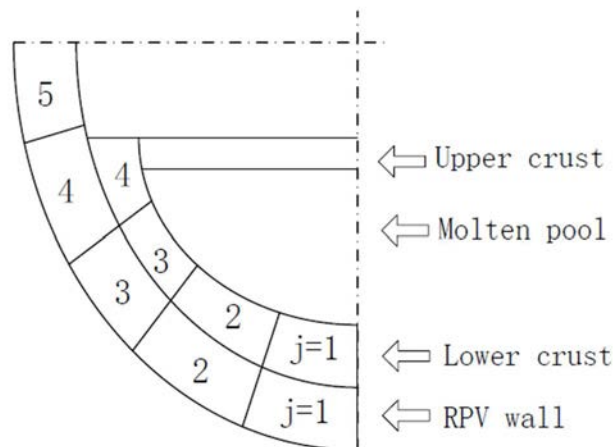


FIG. 15. Angular distribution model structure of lower head heat flux (courtesy of CNPO).

This model adopts a generalized mass and energy equation in conjunction with the node heat transfer coefficient. It is based mainly on the heat flux transferred downward from the debris bed to the lower head RPV wall. The numerical distribution is illustrated in Fig. 16.

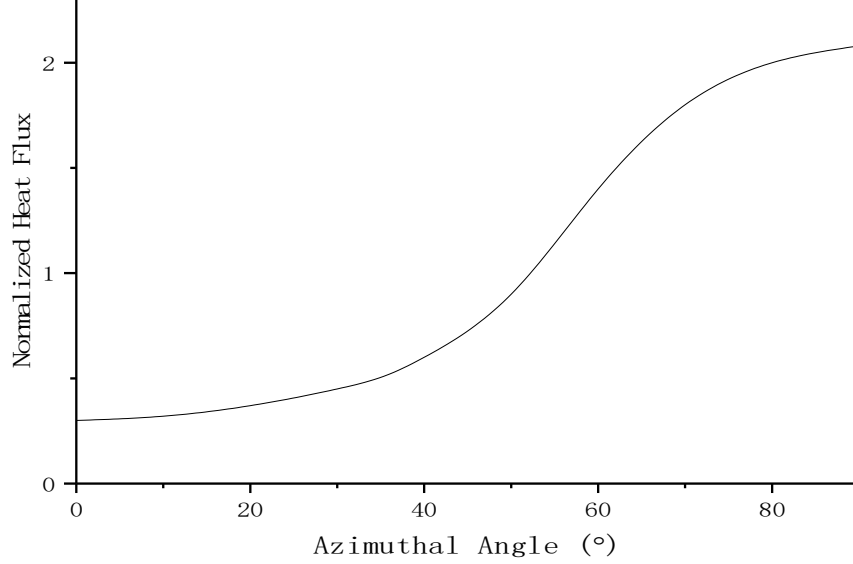


FIG. 16. Heat flux angular distribution of the molten pool lower surface (courtesy of CNPO).

The heat transfer coefficient is computed as follows:

$$h_{pl,j} = \frac{\int_{\theta_{j-1}}^{\theta_j} h_{pl}(\theta) d\theta}{\theta_j - \theta_{j-1}} \approx h_{pl} \left(\frac{\theta_j + \theta_{j-1}}{2} \right), \quad j = 1, \dots, j_{cm} \quad (41)$$

where j_{cm} is the uppermost node which the debris bed reaches. The angle θ is measured from the bottom of the lower head and θ_j corresponds to the top elevation at the lower crust node j , as indicated in Fig. 16. For segmented sphere geometries, the equation for the change in azimuthal angle can be written as follows:

$$h_{pl}(\theta) = h_d \left[C_\theta + \left(\frac{8(1 - C_\theta)(1 - \cos \phi)}{3(\phi - \cos \phi \sin \phi) - 2 \sin^3 \phi \cos \phi} \right) \sin^3 \theta \right] \quad (42)$$

where C_θ is a coefficient and $C_\theta = 0.25$. Therefore, the convection heat transfer angular distribution from the molten pool to the lower crust is expressed as follows:

$$q''_{L,j} = h_{pl,j}(T_{pl} - T_{L,j}), \quad j = 1, \dots, j_{cm} \quad (43)$$

For each node bordering on the RPV wall, the thermal resistance of the narrow gap between the crust and the wall will be ignored. Thus, the angular distribution of the heat flux is expressed as follows:

$$q''_{o,j} = \frac{k_j}{L_j} (6\bar{T}_j - 2T_{L,j} - 4T_{o,j}), \quad j = 1, \dots, j_{cm} \quad (44)$$

Due to the gap between the melt crust and the steel structure, such as the RPV lower head, steam may appear in the gap. Its heat transfer resistance is computed according to:

$$h_{gap} = \frac{k_{st}(T_{sat}, v_{st,sat})}{\delta_{gap}} \quad (45)$$

where

k_{st} is the thermal conductivity [$\text{W} \cdot \text{m}^{-1} \cdot \text{K}^{-1}$] at the saturation temperature and specific volume;
 T_{sat} is the saturation temperature [K];
 $v_{st,sat}$ is the specific volume [$\text{m}^3 \cdot \text{kg}^{-1}$];
and δ_{gap} is the distance between the crust and the steel wall, currently the model parameter is set to 100 μm .

2.1.3.4. Heat transfer computation through the metal layer

The steel structure as well as the U–Zr–O mixture start to melt due to thermal radiation of the debris bed and gradually form a metal oxide layer. In the debris bed model, the metal layer is at the top of the debris bed, which indicates a density difference among the fuel, the structural material and the control rod material. Considering the different constituents of the melt, there is a large uncertainty in the debris component distribution, due to multiple possible relocations and an unknown degree of quenching and mixing of the melt. This uncertainty will affect heat transfer from the debris bed to the RVP wall as well as the chemical reactivity with the RPV wall.

For a molten metal layer, its heat transfer coefficient will be determined by the extended Globe-Dropkin equation [2]. Where the Nusselt number computation is performed as follows:

$$Nu = 0.069Ra^{\frac{1}{3}}Pr^{0.074} \quad (46)$$

The Rayleigh number is computed as:

$$Ra = \frac{g\beta\Delta t\delta_{ml}^3}{\nu\alpha} \quad (47)$$

where δ_{ml} is the metal layer thickness [m]. The scope of application for the equation is $0.02 < Pr < 8750$ and $3 \times 10^5 < Ra < 7 \times 10^9$.

In order to take into account the effect of heat conduction and convection in the metal layer, the equation for the computation of the Nusselt number is modified to:

$$Nu = 1 + 0.069Ra^{0.333}Pr^{0.074} \quad (48)$$

Then the heat transfer coefficient is expressed as follows:

$$h_{ml} = Nu \frac{k_{ml}}{\delta_{ml}} \quad (49)$$

where, k_{ml} is the thermal conductivity of the metal layer [$W \cdot m^{-1} \cdot K^{-1}$].

As opposed to the previously selected Globe-Dropkin equation, after the modification, the model now takes the effect of sideward heat transfer from the metal layer into account. Therefore, the equation for the heat exchange of molten pool oxide layer is updated and the original equation is set as an alternative option. The modified Globe-Dropkin equation can be written as follows:

$$Nu = 1 + 0.174 Ra^{\frac{1}{3}} Pr^{0.074} \quad (50)$$

2.1.3.5. Heat transfer computation between water and reactor internals

The effects of convective and radiative heat transfer are taken into consideration for the upward heat transfer of the debris bed. In order to simplify the model, the water pool is deemed to be saturated, gas in the upper region of the debris bed absorbs no radiation energy and heat transfer from the top of the debris bed is dominated by radiation. Therefore, the upward heat flux is obtained by the following:

$$q''_{tot} = f_{wet} h_{cnv} (T_{ml} - T_{sat}) + (1 - f_{wet}) h_{rad} (T_{ml} - T_{eq}) \quad (51)$$

where

- f_{wet} is the fraction of the area covered by water on the upper surface of the debris bed;
- h_{cnv} is the convection heat transfer coefficient [$W \cdot m^{-2} \cdot K^{-1}$];
- h_{rad} is the radiation heat transfer coefficient [$W \cdot m^{-2} \cdot K^{-1}$];
- T_{ml} is the temperature of the metal layer [K];
- and T_{eq} is the temperature of the exposed heat sink [K].

The convection heat transfer coefficient h_{cnv} is computed based on nucleate boiling, critical heat flux, film boiling and the thermal radiation conditions. The upper limit of the debris bed heat transfer rate is given by the heat transfer rate required to evaporate the water inventory of the lower plenum within the current time step. Thus, the heat transfer rate will be limited to this value. The radiation heat transfer coefficient is computed with the help of the temperature in the previous time step:

$$h_{rad} = \left(\frac{\sigma}{\frac{1}{\varepsilon_{ml}} + \frac{1}{\varepsilon_{eq}} - 1} \right) (T_{ml}^2 + T_{eq}^2)(T_{ml} + T_{eq}) \quad (52)$$

where

σ is the Stefan-Boltzmann constant [$\text{W} \cdot \text{m}^{-2} \cdot \text{K}^{-4}$];
 ε_{ml} is the emissivity of the metal layer surface (model parameter);
and ε_{eq} is the emissivity of the exposed equipment heat sink surface (model parameter).

When the debris heat sink in the lower plenum has completely melted, it is assumed that the remaining heat will be transferred to the core bottom node by radiation. If the reactor core's lower node also experiences a meltdown, the heat will then be transferred upward to the upper plenum structures.

2.1.3.6. Quenching computation for the overlying water pool on the debris bed

When the debris bed is submerged in water, it is important to account for both the upward radiation heat transfer and the quenching calculations to simulate the water's effect on cooling the debris bed. This quenching term has the same structure as the critical heat flux:

$$q''_{qnc} = C_q q''_{cnf} \quad (53)$$

where, C_q is the model parameter.

The heat lost from the debris bed will be absorbed by the overlying water pool. The limit for how much heat can be absorbed is given by the heat required to evaporate the water. When the model parameter C_q is set to 0, water cannot penetrate the debris bed, thus it only cools the upper surface. When C_q is set to 1, the debris bed will not only transfer heat to the lower head wall and the upper reactor core, but there will additionally be a cooling effect on the critical heat flux. Therefore, C_q is treated as a sensitive parameter in the treatment of the lower head debris bed and can be used to analyse the uncertainty of water injection onto the debris bed.

As already mentioned, if water is present, heat flux exiting from the metal layer will be transferred to the overlying water layer; otherwise, it will be transferred to the heat sink above. In the case that there is not much water, the debris bed will not transfer heat to the heat sink in one time step. The water will initially dry-out in the next time step and later the debris bed will transfer a significant amount of heat to the heat sink. In order to avoid this sudden switch (from convective to radiative heat transfer), the concept of a minimum water layer is introduced, which is the minimum mass of water required to cover the whole debris bed surface. If the mass of the water source is greater than this value, the entire heat from the metal layer will be transferred to the upper water pool. Otherwise, only the surface covered by water

will transfer heat to the water source, while the rest of the uncovered surface will transfer heat to the upper heat sinks.

If the primary system pressurization is not taken into account in the water evaporation computation, the excessive evaporation rate of the saturated water may lead to numerical instabilities within the computations. For example, having a large amount of saturated water evaporate will cause the pressurization of the system and result in water being subcooled in the next time step and thus leading to no further evaporation. After this pressure drop, the water becomes saturated again in the next few time steps, producing another steaming spike. To avoid this instability, system pressurization due to steaming needs to be taken into account when computing the steaming rate. Under the assumption of quasi-steady conditions, the rate of pressurization in the gas phase ought to match that in the liquid phase:

$$\left(\frac{dP}{dt}\right)_g = \left(\frac{dP}{dt}\right)_l \quad (54)$$

It is assumed that the primary system gas is isothermal and follows the ideal gas law:

$$\left(\frac{dP}{dt}\right)_g \approx \frac{P_{ps}}{m_{g,ps}} (W_{st} - W_{g,out}) \quad (55)$$

where

P_{ps} is the primary system pressure [Pa];
 $m_{g,ps}$ is the primary system gas mass [kg];
 W_{st} is the unknown steaming rate of the upper water pool to be solved [$\text{kg}\cdot\text{s}^{-1}$];
and $W_{g,out}$ is the effective steam flow out of the primary system [$\text{kg}\cdot\text{s}^{-1}$].

The rate of pressure change in the water phase is written as:

$$\left(\frac{dP}{dt}\right)_w = \frac{dP}{dT_w} \frac{dT_w}{dt} \quad (56)$$

It is further assumed that the water's parameters evolve along the saturation line. For this purpose, one utilizes the Clausius-Clapeyron equation, where $\frac{dP}{dT_w}$ is defined as follows:

$$\frac{dP}{dT_w} \approx \frac{dP}{dT_{w,sat}} = \frac{h_{fg}}{T_{sat} v_{fg}} \quad (57)$$

where

h_{fg} is the latent heat of vaporization [$\text{J}\cdot\text{kg}^{-1}$];
and v_{fg} is the specific volume difference between saturated water and saturated steam [$\text{m}^3\cdot\text{kg}^{-1}$].

The rate of change in water temperature obtained by solving the energy conservation equation of water is as follows:

$$\frac{d(mu)_w}{dt} = m_w \frac{du_w}{dt} + u_w \frac{dm_w}{dt} = Q_{cm} + W_{w,in}h_{in} - W_{st}h_{st} \quad (58)$$

where

$$m_w \frac{du_w}{dt} = m_w c_{v,w} \frac{dT_w}{dt} \quad (59)$$

$$u_w \frac{dm_w}{dt} = u_w (W_{w,in} - W_{st}) \quad (60)$$

and

m_w is the mass of water [kg];
 u_w is the specific internal energy [$\text{J} \cdot \text{kg}^{-1}$];
 $c_{v,w}$ is the specific heat at a constant volume [$\text{J} \cdot \text{kg}^{-1} \cdot \text{K}^{-1}$];
 Q_{cm} is the heat transfer rate from the debris bed to the upper water pool [W];
and $W_{w,in}$ is the water flow rate into the water pool [$\text{kg} \cdot \text{s}^{-1}$].

In summary, the following equation is obtained:

$$\frac{dT_w}{dt} = \frac{Q_{cm} + W_{w,in}(h_{in} - u_w) - W_{st}(h_{st} - u_w)}{m_w c_{v,w}} \quad (61)$$

By substituting the water specific internal energy h_w into the equation for computing the steaming rate, it follows:

$$W_{st} = \frac{\frac{P_{ps}}{m_{g,ps}} + \frac{h_{fg}}{T_{sat} v_{fg}} \left[\frac{Q_{cm} + W_{w,in}(h_{in} - h_w)}{m_w c_{v,w}} \right]}{\frac{P_{ps}}{m_{g,ps}} + \frac{h_{fg}}{T_{sat} v_{fg}} \frac{(h_{st} - h_w)}{m_w c_{v,w}}} \quad (62)$$

2.1.3.7. Gap cooling computation under the RPV lower head

During the accident that occurred at unit two of the Three Mile Island nuclear power station, molten core material dropped to the lower plenum and resulted in the RPV wall reaching temperatures of around 1100°C in a region of about 1 m in diameter. However, after the temperature is reached, the wall was cooled rapidly. The explanation of this phenomenon lies within the creep properties of the material, which can cause the accelerated cooling process. This cooling mechanism model is introduced below.

Generally, when the RPV wall is heated to the extent that significant creeping occurs, a gap will form between the wall and the debris bed. This separation is most obvious when the debris

does not adhere to the wall tightly (see Fig. 17). The heat transfer resistance will increase due to the evaporation of water in surface cavities. This will, in a typical reactor system where material creep of the RPV wall is observed, result in a relative displacement of the melt away from the RPV wall and a narrow gap between the debris and the RPV wall (see Fig. 18).

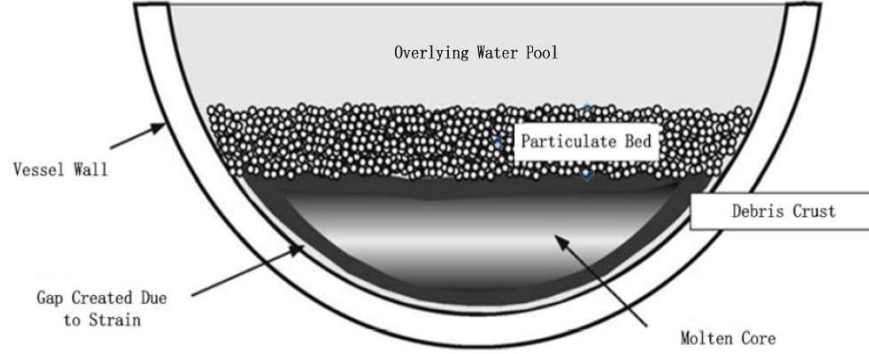


FIG. 17. Diagram for water injection quenching of the debris bed (courtesy of CNPO).

To determine how large a gap would need to be in order to allow for enough water ingress and thus sufficient cooling of the RPV wall to avoid further creep, one uses the creep rupture model. This model represents material creep as a fractional approach to rupture for each time step, which is related to the strain resulting from creep. A typical value for ductile materials at their failure strain ϵ_f is 0.2. As an approximation, one can assume that the strain is linearly related to the damage fraction, with a value of unity corresponding to the strain at failure. Hence, if the cumulative damage fraction is 10^{-3} , the corresponding strain would be 20 000.

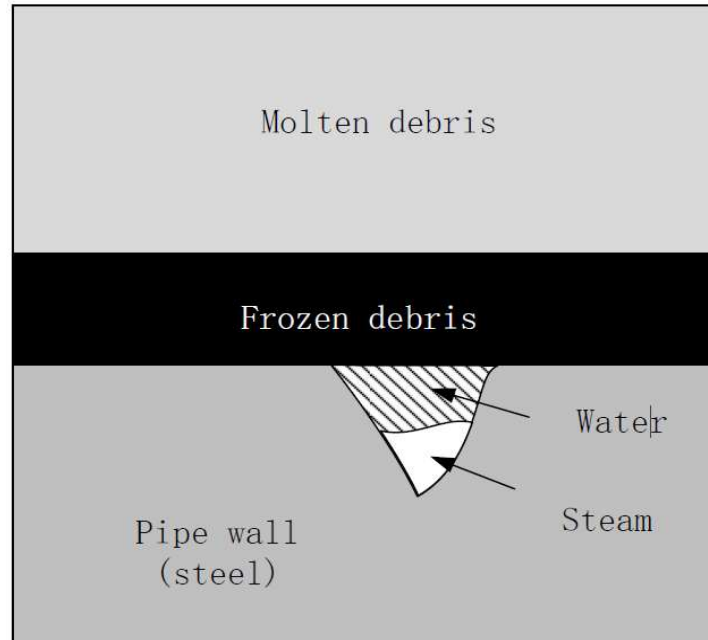


FIG. 18. Narrow gap between the debris and the RPV wall due to strain effect (courtesy of CNPO).

The emerging gap δ_{gap} between the RPV wall and the core debris is then as follows:

$$\delta_{gap} = R_{lp}\varepsilon_f f_{gap} + d_{gap,o} \quad (63)$$

where f_{gap} is the creep damage fraction.

Once a gap is formed, water will flow through it and, by boiling, the heat of the debris bed will be removed. The maximum heat flux that can be transferred to the water source in the gap is computed by the following equation:

$$q''_{gap} = Ch_{fg}\sqrt{\rho_g}^4\sqrt{g\sigma(\rho_f - \rho_g)} \quad (64)$$

where

ρ_f is the saturated water density [$\text{kg}\cdot\text{m}^{-3}$];

ρ_g is the saturated steam density [$\text{kg}\cdot\text{m}^{-3}$];

h_{fg} is the latent heat of vaporization [$\text{J}\cdot\text{kg}^{-1}$];

g is the acceleration of gravity [$\text{m}\cdot\text{s}^{-2}$];

and σ is the surface tension at the steam-water interface [$\text{N}\cdot\text{m}^{-1}$].

The coefficient C is computed as follows:

$$C = 0.16F_{gap} \left[1 + 6.7 \times 10^{-4} \left(\frac{\rho_f}{\rho_g} \right)^{0.6} \frac{l}{\delta} \right] \quad (65)$$

where

δ is the gap thickness [m];

l is the gap length [m];

and F_{gap} is the cooling efficiency in the gap with the model parameter ranging from 0 to 1.

When F_{gap} adopts the recommended value 1, the computed gap heat flow rate is at its maximum. The rate of gap heat transfer under these hydraulic limitations is computed as follows:

$$Q_{gap} = 2q''_{gap}\pi - R_{lp}l \quad (66)$$

The boiling heat transfer in the gap cools down both the inner surface area of the RPV and the outer surface of the melt crust. The equations for the heat transfer rates of these surfaces are as follows:

$$q''_{wo} = k_w \frac{dT}{dr} \Big|_{w,lp} \quad (67)$$

$$q''_{co} = k_c \frac{dT}{dr} \Big|_{c,lp} \quad (68)$$

Equation (67) describes the heat flux of the RPV wall and Eq. (68) specifies the heat flux of the core debris, where k is the thermal conductivity. Both temperature gradients are computed under the assumption that the heat transfer surface temperature is equal to the lower head water temperature. If the sum of these two heat fluxes is less than the maximum heat flux in the gap, then the computed heat flux will serve as a reference value and the temperature on these two surfaces is equal to the lower head water temperature:

$$q''_{gap} > q''_{wo} + q''_{co} \quad (69)$$

If the sum of these two heat fluxes is greater than the maximum heat flux, the maximum heat flux will be distributed across two terms according to the computed value ratio (see Eqs (70) and (71)), so that the total heat flux cannot exceed the maximum value determined by the experiment. The distribution ratio is defined as follows:

$$K_w = \frac{q''_{wo}}{q''_{wo} + q''_{co}} \quad (70)$$

$$K_c = \frac{q''_{co}}{q''_{wo} + q''_{co}} \quad (71)$$

The computation equations for the heat fluxes on both sides of the gap are:

$$q''_w = K_w q''_{gap} \quad (72)$$

$$q''_c = K_c q''_{gap} \quad (73)$$

In the crust model, it is assumed that the crust temperature distribution is parabolic:

$$T = C_0 x^2 + C_1 x + C_2 \quad (74)$$

And the bulk crust temperature is defined as follows:

$$\bar{T} = \frac{1}{L} \int_0^L T dx \quad (75)$$

Coefficient C_0 , acquired by combining the above two equations, is given with:

$$C_0 = \frac{3}{L^2} \left(\bar{T} - \frac{C_1}{2} L - C_2 \right) \quad (76)$$

The temperature gradient of the crust acquired by taking the derivative of the crust internal temperature T is as follows:

$$\frac{dT}{dx} = 2C_0 x + C_1 \quad (77)$$

Taking the gap thermal resistance and the heat transfer rate between the crust and the RPV wall into account, the above equation may be adapted as follows:

$$\left(\frac{dT}{dx}\right)_0 = \frac{h_f}{k}(T_0 - T_f) + \frac{1}{k}q_c'' \quad (78)$$

where

h_f is the heat transfer coefficient of the gap [$\text{W}\cdot\text{m}^{-2}\cdot\text{K}^{-1}$];
 T_0 is the outer surface temperature of the crust [K];
 T_f is the inner surface temperature of the RPV wall [K];
and q_c'' is the crust outer surface heat flux [$\text{W}\cdot\text{m}^{-2}$].

Then C_1 is solved for as:

$$C_1 = \frac{h_f}{k}(T_0 - T_f) + \frac{1}{k}q_c'' \quad (79)$$

And the other two coefficients are computed as follows:

$$C_2 = \frac{1}{2}\left[3\bar{T} - \frac{h_f L}{2k}(T_0 - T_f) - T_L - \frac{L}{2k}q_c''\right] \quad (80)$$

$$C_0 = \frac{3}{4L^2}\left[2T_L - 2\bar{T} - \frac{h_f L}{k}(T_0 - T_f) - \frac{L}{k}q_c''\right] \quad (81)$$

The average temperature T_0 is related to the heat transferred to the water within the gap and the RPV wall and is solved by the temperature distribution equation. For its computation the following equation is used:

$$T_0 = \frac{3\bar{T} - T_L + \frac{h_f L}{2k}T_f - \frac{L}{2k}q_c''}{2 + \frac{h_f L}{2k}} \quad (82)$$

The average temperature T_0 , as calculated in Eq. (82), enables a smooth transition from a condition where there is no significant heat transfer rate to one where the heat transfer to the gap is sufficient enough to remove all the heat.

It is assumed that all heat transferred to the gap is absorbed by water:

$$Q_{gap} = 2(q_w'' + q_c'')\pi R_{lp}l \quad (83)$$

If the heat released to the crust is not completely transferred to water in the gap, the remaining heat will be transferred to the RPV wall:

$$Q_{wall} = Q_{out,crust} - Q_{gap} \quad (84)$$

Therefore, the water in the gap plays a part in cooling the melt and the RPV wall, however it may not be sufficient to prevent the RPV wall temperature from rising. Yet, a higher wall temperature will lead to additional strain in the wall leading to a larger gap and allowing for more water to flow between the RPV wall and the melt. This in turn will lead to intensified cooling and the mitigation of creep failure. Thus, as long as there is a water source in the lower head, creeping of the RPV wall can essentially restrict itself.

2.1.4. RPV failure model

The code takes the following four mechanisms resulting in the initial failure of the RPV lower head into account:

- a) Continuous heating by the accumulated debris bed and attack of the molten core debris may weaken the penetration support welds and subsequently result in penetration ejection;
- b) Internal pressure combined with the weight of the debris and high temperatures may cause a creep failure of the RPV wall;
- c) Direct attack of the lower head by combined debris jets of mixed melt may lead to the local ablation of the lower head;
- d) Thermal attack of the vessel wall by the molten metal layer at the top of the debris bed in the lower plenum leads to the weakening of the vessel wall and potentially to the vessel failure.

It is assumed that the failure of the RPV is initialised by a local failure rather than a large-scale creep failure of the lower head. In high-pressure accident sequences, if a local failure occurs on the side of the vessel, only the debris above the failure position will be dislodged and expelled from the RPV, while most of the debris will be left in the lower plenum. In addition, the pressure inside the vessel will drop and the pressure load acting on the lower head will decrease significantly. This in turn results in the remaining debris staying enclosed in the RPV for an increased time period. The debris will therefore continue to heat the lower plenum which may eventually lead to a large-scale creep failure of the lower head. In this case, the remaining debris is then released into the containment. Thus, the extent of a large-scale creep failure is not significant, as long as it is large enough to rapidly dislodge the remaining debris from the lower plenum.

In this code, the criteria for large-scale failures are simplified. After a local failure, the lower head node next to the local failure node is evaluated for material creeping. When the creeping damage fraction of any node exceeds 0.4, a large-scale failure occurs. The failure node is fully discharged and is thus left with no residual debris.

2.1.4.1. Creep rupture of lower head

Hoop stress imposed on the lower head will be treated as stress imposed on each lamina of the lower head in the computations. All laminas will be assumed to have the same strain rate. Given the stress curve and temperature of each lamina, the corresponding creep rupture time can be evaluated. The creep rupture time fraction is obtained by dividing the time step by the creep rupture time. The fraction will be added to in subsequent time steps until it reaches 1. At that point, the lower head fails due to material creeping. Local creep failures may occur in the lower head near the top of the debris bed along the circumferential direction of the reactor (where the heat flux is highest). The position of the RPV failure is evaluated by the creep model. In case of a creep failure, the model will implement a break at the first node whose cumulative damage fraction exceeds 1.

2.1.4.2. Jet impingement

This mechanism is considered only when the reactor core debris relocates the lower head for the first time, because any accumulated debris will form a protective crust layer on the lower head surface as well as form a molten pool on the upper part of the crust. In conservative calculation, it is assumed that the molten debris is discharged in the form of an uninterrupted jet. First, the free fall velocity of the jet and the diameter of the jet while entering the lower plenum water pool are calculated. The entrained material can cause the formation of particulate debris which will fall onto the debris bed. Then, while passing through the pool, the entrainment rate on the jet surface is calculated by the Epstein model, and it is considered that the entrained materials cause the formation of particle debris, which will fall onto the debris bed. The remaining jet will impact on the bottom head (with diameter, superheat and velocity determined). Finally, the Epstein model is used to estimate the bottom head erosion rate caused by the molten material jet impact. This rate is integrated during the jet release period to determine whether the RPV wall is penetrated or not. Upon the completion of the jet release, the erosion calculation will stop.

The Epstein model for the erosion rate is summarized below. For melt and oxide impingement on molten steel, the steel melting velocity is computed by the following:

$$\frac{v_m}{\alpha_w} \left[\frac{v_w}{2a} \left(\frac{\rho_w}{\rho_j} \right)^{\frac{1}{2}} \right]^{\frac{1}{2}} = 0.1 \ln(1 + 10N) \quad (85)$$

where, N is the melting parameter, defined as follows:

$$N = \frac{c_{p,j}(T_j - T_{mp,j})}{\lambda_w + c_{p,w}(T_{mp,w} - T_0)} \frac{k_j}{k_w} \left[\frac{v_w}{v_j} \left(\frac{\rho_w}{\rho_j} \right)^{\frac{1}{2}} \right]^{\frac{1}{2}} \theta'(o) \quad (86)$$

where

v_m is the steel melting velocity [$\text{m}\cdot\text{s}^{-1}$];
 a_w is the wall thermal diffusivity [$\text{m}^2\cdot\text{s}^{-1}$];
 v_w is the kinematic viscosity of molten wall [$\text{kg}\cdot\text{m}^{-1}\cdot\text{s}^{-1}$];
 v_f is the kinematic viscosity of the jet [$\text{kg}\cdot\text{m}^{-1}\cdot\text{s}^{-1}$];
 r_w is the wall density [$\text{kg}\cdot\text{m}^{-3}$];
 r_j is the jet density [$\text{kg}\cdot\text{m}^{-3}$];
 k_w is the wall thermal conductivity [$\text{W}\cdot\text{m}^{-1}\cdot\text{K}^{-1}$];
 k_j is the jet thermal conductivity [$\text{W}\cdot\text{m}^{-1}\cdot\text{K}^{-1}$];
 c_w is the specific heat of the wall [$\text{J}\cdot\text{kg}^{-1}\cdot\text{K}^{-1}$];
 c_j is the specific heat of the jet [$\text{J}\cdot\text{kg}^{-1}\cdot\text{K}^{-1}$];
 T_j is the jet temperature [K];
 $T_{mp,w}$ is the wall melting point temperature [K];
 $T_{mp,j}$ is the jet melting point temperature [K];
 T_0 is the wall temperature [K];
 and λ_w is the latent heat of fusion for the wall [$\text{J}\cdot\text{kg}^{-1}$].

In the above equation, a is the stagnation-point velocity gradient:

$$a \approx \frac{u_j}{D} \quad (87)$$

where

u_j is the impinging jet velocity [$\text{m}\cdot\text{s}^{-1}$];
 and D is the jet diameter [m].

The dimensionless temperature gradient of the surface $\theta'(o)$ is a function of the Prandtl number of the melt jet. This function is approximated as follows:

$$\begin{cases} \theta'(o) = 0.549Pr_j^{0.411} & Pr_j \leq 0.5 \\ \theta'(o) = 0.55Pr_j^{0.35} & Pr_j > 0.5 \end{cases} \quad (88)$$

2.1.4.3. Attack of the vessel wall by the metal layer of the debris bed

One of the main assumptions of the lower head molten pool model is that the debris bed is divided into two parts: the oxide molten pool below and the metal layer on top. For the metal layer, it is assumed that there is an identical convective circulation to that of the molten oxide pool. This circulation allows for the upward transfer of the decay heat from the lower lying debris bed (oxide melt), and results in the sideward heat transfer between the metal layer and the RPV wall. Therefore, the sideward heat flux of the metal layer can be computed. This heat flux needs to be conducted through the RPV wall adjacent to the metal layer.

The following steps are used to determine the sideward heat flux from the overlying metal layer to the RPV wall. As proposed by Globe and Dropkin [2], the relational expression for natural convection heat transfer in a metal layer per Eq. (89) is:

$$Nu = 0.069 Ra^{\frac{1}{3}} Pr^{0.074} \quad (89)$$

For a material layer without an internal heat source, the Rayleigh number (Ra) and Nusselt number (Nu) are defined in the conventional way, as follows:

$$Ra = \frac{g\beta\Delta T x_{ml}^3}{\alpha\nu} \quad (90)$$

$$Nu = \frac{h_c x_{ml}}{k} \quad (91)$$

where x_{ml} is the thickness of the metal layer. By substituting the definitions of the Reynolds number (Eq. (90)) and the Nusselt number (Eq. (91)) into Eq. (89), one can obtain the expression for the heat transfer coefficient of a circulating cell in the metal layer is:

$$h_c = 0.069k \left(\frac{g\beta\Delta T}{\alpha\nu} \right) Pr^{0.074} \quad (92)$$

Assuming typical properties for molten steel and a Prandtl number Pr of 0.16, the equation simplifies as follows:

$$h_c = 930 \Delta T^{\frac{1}{3}} \quad (93)$$

The heat flux transferred from the debris pool of oxidic melt surrounded by the adjacent crust to the bottom surface of the metal layer is q''_{max} as shown in Fig. 19. This heat flux is then removed from the metal layer by upward radiation towards RPV internal heat sinks or by sideward convection towards RPV wall. It is assumed that the upward radiation is comparable to the heat transfer to RPV wall, and the horizontal dimension of the circulation cell (see Fig. 19) is equal to the height of the metal layer. Therefore, the heat flux to the RPV wall is approximated as half of the heat flux transferred from the oxidized crust, $q''_{side} = \frac{q''_{max}}{2}$.

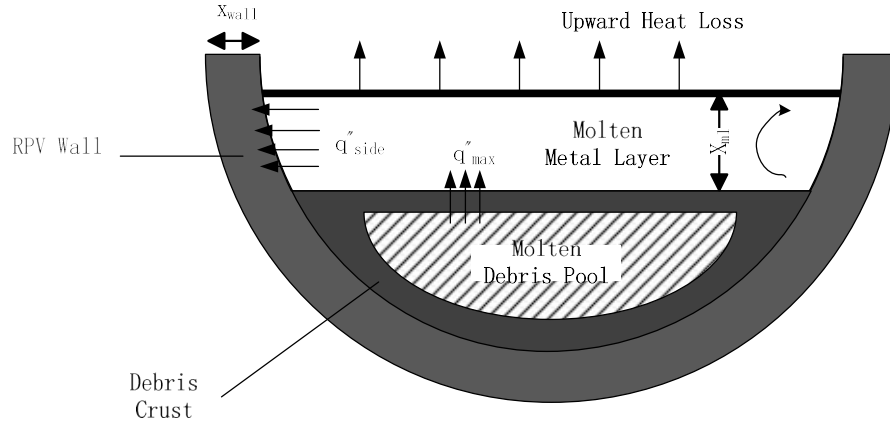


FIG. 19. Impact of the metal layer on RPV wall (courtesy of CNPO).

The temperature gradient ΔT_L across the metal layer thickness is required to drive the circulation to the upper and side boundaries of the layer. This can be characterized in the conventional manner:

$$q''_{max} = h_c \Delta T_L \quad (94)$$

By substituting Eq. (94) into the Eq. (93), one obtains the following:

$$q''_{max} = 930 \Delta T_L \quad (95)$$

$$\Delta T_L = 930^{-\frac{3}{4}} q''_{max}^{\frac{3}{4}} \quad (96)$$

$$\Delta T_L = \left(\frac{10^{18}}{930^3} \right)^{\frac{1}{4}} \left(\frac{q''_{max}}{10^6 \text{ W/m}^2} \right)^{3/4} \quad (97)$$

$$\Delta T_L = 188 \text{ K} \left(\frac{q''_{max}}{10^6 \text{ W/m}^2} \right)^{3/4} \quad (98)$$

Then, the effective temperature difference ΔT_{eff} , which causes sideward convective heat transfer from the metal layer to the RPV wall, is computed as follows:

$$\Delta T_{eff} = \text{Min} \left[188 \text{ K} \left(\frac{q''_{max}}{10^6 \text{ W/m}^2} \right)^{0.75}, \max(0, T_{SSPS} - T_{AVSSI}) \right] \quad (99)$$

where

T_{SSPS} is the average temperature of the metal layer [K];

and T_{AVSSI} is the surface temperature of the wall in contact with the metal layer [K].

Likewise, the effective sideward heat transfer coefficient is given with:

$$H_{side} = 5324 \text{ W/m}^2 \text{ K} \left(\frac{q''_{max}}{10^6 \text{ W/m}^2} \right)^{0.25} \quad (100)$$

As outlined above, the actual sideward heat flux is approximated as half of q''_{max} and expressed as follows:

$$q''_{side} = \frac{H_{side} \Delta T_{eff}}{2} \quad (101)$$

2.1.5. Model for molten corium concrete interaction

This section details the models developed for the molten corium concrete interactions during the severe accident conditions.

2.1.5.1. Model assumptions

The assumptions used in the model for the molten corium concrete interaction (MCCI) are:

- a) The energy produced in the process of the concrete phase-transformation and in the endothermic reactions are combined and treated as a single effective latent heat;
- b) The temperature distribution in the heat sink is assumed to be one-dimensional in the ablation direction;
- c) The heat sink temperature curve uses a fine nodalization on the surface where the thermal boundary layer resides, while the internal nodalization is relatively coarse;
- d) Mixing of the debris pool is homogeneous;
- e) The debris crust and debris pool have the same composition;
- f) The steady-state expression is applicable to changes in heat transfer and water level swell;
- g) The chemical reaction between the corium and the concrete is treated by an equilibrium model.

Refer to Fig. 20 for representation of the model features.

2.1.5.2. Heat transfer and ablation of the heat sink

Fig. 20 shows the concrete ablation process during MCCI. The molten debris comes into contact with the floor and the sidewalls, radiating heat to the upper wall and undergoing convective heat transfer with the atmosphere. The temperature distribution in the heat sink is obtained by solving the fully implicit one-dimensional heat conduction equation, which utilizes the heat flux from the core debris to the heat sink. The debris pool relocates downward (see Fig. 21), causing the bottom and side crusts of the solidified corium to have different thicknesses due to variations in their convective heat transfer coefficients.

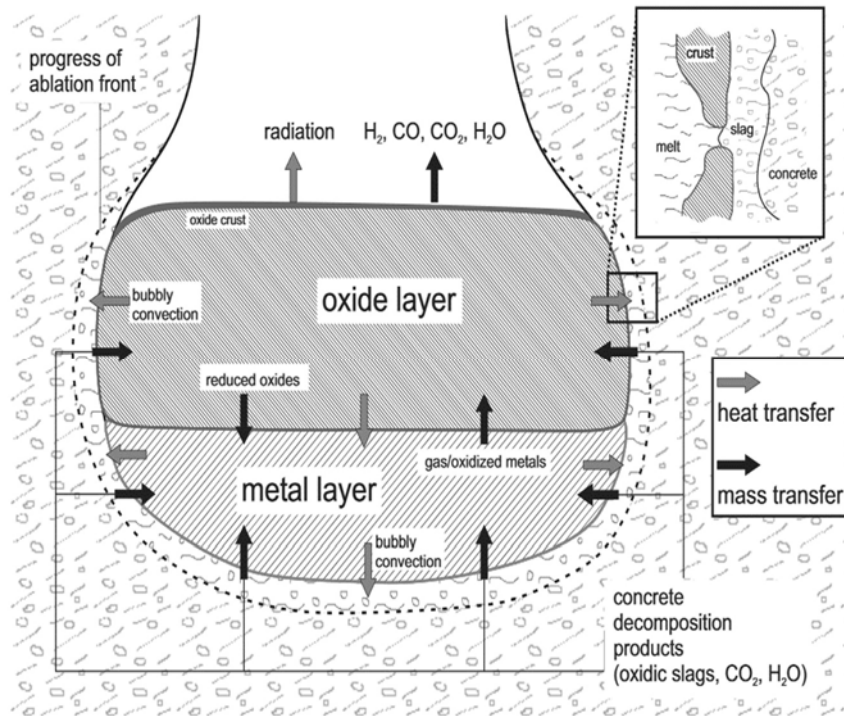


FIG. 20. Schematic diagram of the MCCI process (courtesy of CNPO).

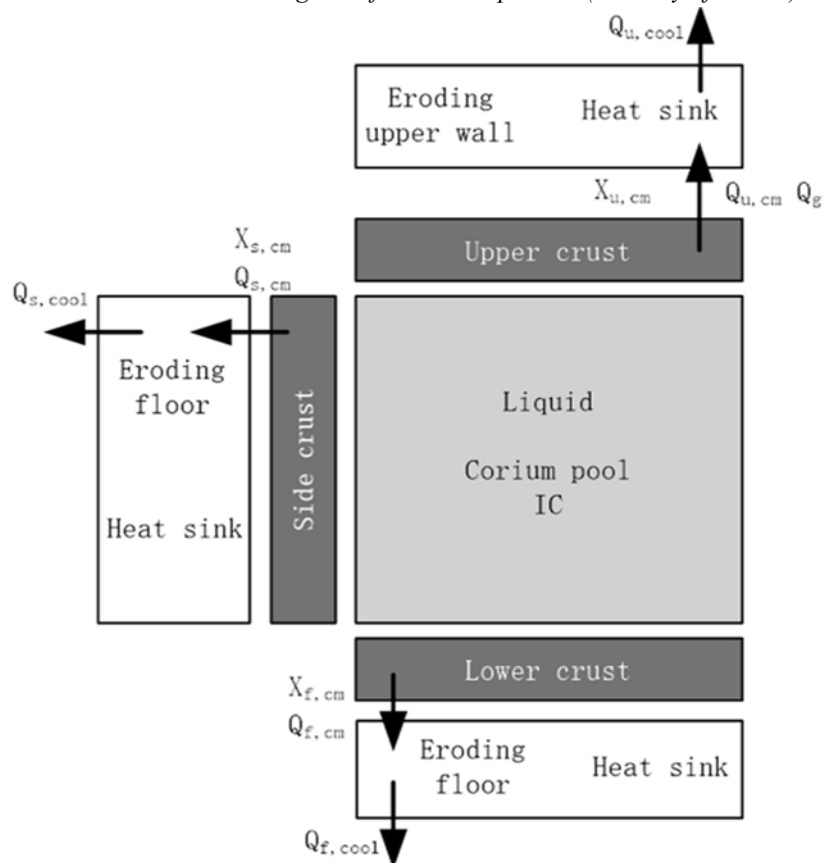


FIG. 21. Schematic diagram of debris pool and sub-compartment (courtesy of CNPO).

The heat flux to the floor and sidewall heat sinks is a result of the convective heat transfer from the molten debris to the sideward and downward crusts as well as the heat generation within the crusts. In quasi-steady conditions one can thus write the following:

$$q_d'' = h_d(T_F - T_{F,m}) + q_v x_{cd} \quad (102)$$

$$q_s'' = h_s(T_F - T_{F,m}) + q_v x_{cs} \quad (103)$$

where

- q_d is the downward heat flux [$\text{W} \cdot \text{m}^{-2}$];
- q_s is the sideward heat flux [$\text{W} \cdot \text{m}^{-2}$];
- h_d is the downward heat transfer coefficient [$\text{W} \cdot \text{m}^{-2} \cdot \text{K}^{-1}$];
- h_s is the sideward heat transfer coefficient [$\text{W} \cdot \text{m}^{-2} \cdot \text{K}^{-1}$];
- T_F is the bulk temperature of the molten debris [K];
- $T_{F,m}$ is the debris melting temperature [K];
- q_v is the volumetric heat generation rate [W/m^3];
- x_{cd} is the thickness of the bottom crust [m];
- and x_{cs} is the thickness of the side crusts [m].

The convective heat transfer coefficient of the molten corium h_d and h_s are affected by changes in the viscosity of the melt and the viscosity increases sharply with the increase of the debris solid fraction. The solid fraction of the oxidic melt may be treated as a pseudo-binary system composed of core oxides (i.e., UO_2 , ZrO_2) and concrete oxides (including SiO_2 , CaO , MgO , Al_2O_3) as illustrated in Fig. 22. The solid fraction is determined by the system temperature, which in turn is determined by the heat transfer from the debris pool. When the debris pool is 100% liquid, the heat flux reaches its maximum. When the debris pool is completely solidified, the convection term goes to zero.

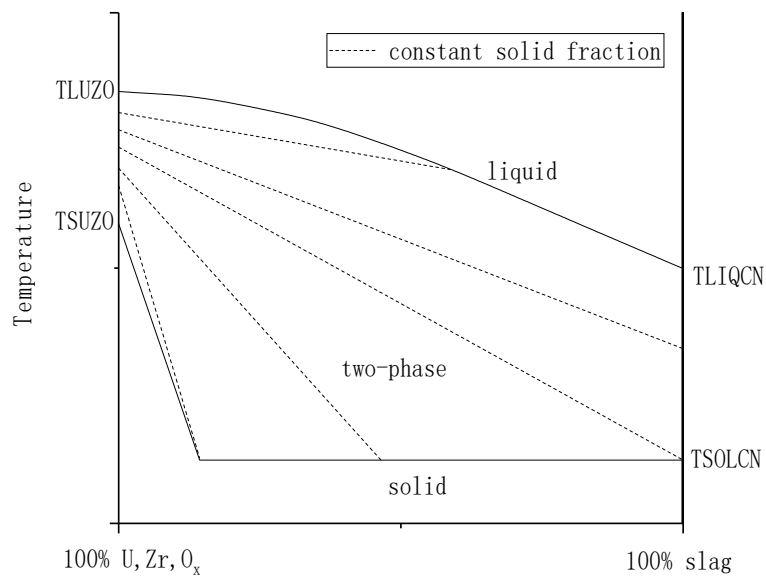


FIG. 22. Diagram of the pseudo-binary system considered in this code; the solid lines represent the solidus and liquidus lines; the dotted lines represent a constant solid fraction (courtesy of CNPO).

The sideward and downward heat transfer coefficients are both a function of the solid fraction of the debris pool. They are expressed by the following mathematical relation:

$$h = h_0(1 - f_s)^n \quad (104)$$

where, f_s is the solid fraction of the debris pool and h_0 is the nominal heat transfer coefficient of the fully molten debris. The downward and sideward nominal heat transfer coefficients are model parameters which affect the rate at which the concrete is eroded, and their values typically range from 1 000 to 10 000 W·m²·K⁻¹. The value of the exponent n ranges from around 1-3. The heat transfer coefficients in the downward and sideward directions are generally different and thus the ablation rates in these two directions are usually different as well. In ESAS they are set to 3 500 and 3 000, respectively.

2.1.5.3. Debris pool and crust

The debris pool has the capability to perform lumped energy and a mass balance calculation for up to 50 condensed phase compounds. Oxide debris is regarded as a pseudo-binary system composed of core oxides and concrete oxides. If the heat flux is sufficient to induce melting of the concrete, it is assumed that the concrete slag enters the debris pool immediately. All gases released from the ablation of the lower lying concrete and some of the gases (the gases released due to ablation of the side walls may escape directly without passing through the debris pool) released due to the ablation of the sidewalls enter the debris pool and chemically react there. The fraction of gas entering the debris pool from the sidewall is set to 1. It is assumed that the released gases completely bypass the solid debris pool, without undergoing any chemical reactions.

As illustrated in Fig. 21, the bottom and side crusts of the solidified corium may have different thicknesses due to their different convective heat transfer coefficients. The upper crust is treated separately because it transfers energy by radiation to the cavity wall and by convection to the gases in the cavity. Because of the debris' internal heat source, it is assumed that the three independent crusts (i.e., upper, side, and lower crust) have parabolic temperature distributions. For example, the temperature distribution of the lower crust can be expressed by the following steady-state expression:

$$\frac{T - T_i}{T_{F,m} - T_i} = 1 - \left(\frac{x}{x_c}\right)^2 \quad (105)$$

where $T_{F,m}$ is the melting temperature of the molten mixture and T_i is the temperature of the interface between the crust and the concrete. It is assumed that T_i is equal to the concrete surface temperature. This temperature distribution is only used for crust-concrete, crust-gas, or crust-interface temperature gradients, and is added to the dynamic equation of crust growth or shrinkage. If the crust is thin enough to transfer all the decay heat to the interface through thermal conduction, the parabolic equation will converge to an appropriate temperature

distribution. Please note that the temperature at the interface between the molten debris and its crust corresponds to the melting temperature of the debris.

If the pool of the melt-concrete mixture is too deep to transfer the heat produced by thermal conduction, the central zone of the debris pool will start to melt as previously described. Under these conditions, the heat flux from the central region of molten pool to the outer crust may be expressed by a convection term. The heat transfer from the crust is computed by the following thermal conduction equation:

$$q'' = -k_F \left. \frac{dT}{dx} \right|_{x=x_c} \quad (106)$$

It can be evaluated by using the following assumption for the in-crust steady-state parabolic temperature distribution:

$$-k_F \left. \frac{dT}{dx} \right|_{x=x_c} = \frac{2k_F(T_{F,m} - T_i)}{x_c} \quad (107)$$

where k_F is the thermal conductivity of the debris. The above equation may also be expressed as follows:

$$q'' = \frac{3k_F(\bar{T}_c - T_i)}{x_c} \quad (108)$$

where \bar{T}_c is the average temperature of the crusts. This equation is also applicable in the case where the debris is completely solid. Similarly, the temperature distribution of as well as the heat transfer from side crust may be determined.

The heat flux from the upper crust is equal to the sum of heat radiation and convective heat losses:

$$q' = [(1/(\varepsilon_i + 1/\varepsilon_w - 1))\sigma(T_i^4 - T_w^4) + h_g(T_i - T_g)] \quad (109)$$

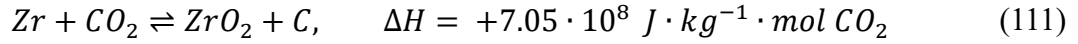
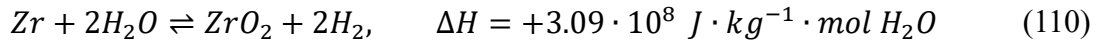
Where, ε_i is the emissivity of the crust-atmosphere interface, and ε_w and T_w are the emissivity and the temperature of surrounding concrete walls, respectively. Variable s is the Boltzmann constant, T_g is the gas temperature, and h_g is the convective heat transfer coefficient between the interface and the atmosphere. In this method, it is assumed that gas does not absorb radiant energy but eventually receives heat from the concrete walls, which leads to essentially the same results. For the concrete wall surface, the applied heat flux increases the wall temperature and eventually causes it to melt.

An overall heat balance on the debris (including the crusts and molten region) is formed by subtracting the energy loss rate from the energy generation rate. Energy losses are due to heat transfer to the concrete and the surroundings as discussed above, the addition of molten

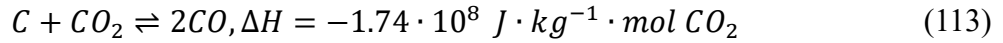
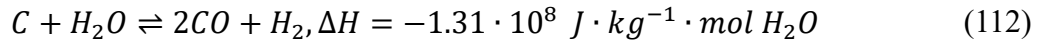
concrete at its melting temperature to the corium-concrete pool mixture, and heating of the gases which are transported through the pool. Energy generation results from the internal decay power and the oxidation heat produced by the reaction metallic constituents in the melt with the steam and/or carbon dioxide released from the concrete.

2.1.5.4. Chemical reaction

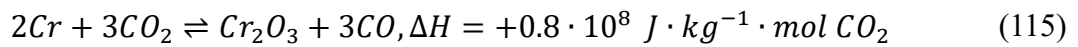
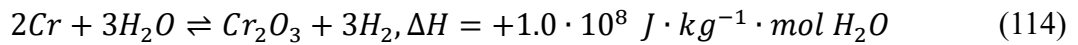
Chemical reactions between gases released from the concrete and the core debris are very important because they are the source terms of flammable gases and fission products exiting the debris pool. The equilibrium model utilized allows all reactions to proceed at the same time and the equilibrium constants of some important oxidation reactions cause continuous oxidation reactions of the main metal pool constituents. The reactions and approximate heat released by these reactions are listed below as a reference for the expected sequence of reactions:



Please note that Zr may also react with SrO_2 , and that this reaction does not necessarily produce carbon, instead it may produce CO. If elementary carbon is produced, the free carbon will react with steam or gas after the complete depletion of Zr, which will result in a near full conversion:



The Cr nearly fully converts with regards to the following reactions:



It is concluded that:

$$\dot{n}(\text{H}_2\text{O})|_{eq} = \dot{n}(\text{H}_2\text{O})|_0 \cdot (1 + k_1)^{-1} \quad (116)$$

$$\dot{n}(\text{H}_2)|_{eq} = \dot{n}(\text{H}_2\text{O})|_0 \cdot k_1 \cdot (1 + k_1)^{-1} \quad (117)$$

$$\dot{n}(\text{CO}_2)|_{eq} = \dot{n}(\text{CO}_2)|_0 \cdot (1 + k_2)^{-1} \quad (118)$$

$$\dot{n}(\text{CO})|_{eq} = \dot{n}(\text{CO}_2)|_0 \cdot k_2 \cdot (1 + k_2)^{-1} \quad (119)$$

where \dot{n} is the molar flow rate (mol/s), and k_1 and k_2 are equilibrium constants. The subscripts "0" and "eq" represent the initial and equilibrium states, respectively. The

equilibrium constants are temperature dependent and the orders of magnitude of k_1 and k_2 are 1.0 and 10.0, respectively.

It is assumed that all gases released from the downward MCCI will enter the debris pool. This assumption does not always apply to the sidewall, as mentioned above. Some gases released from the reactions at the sidewall may bypass the debris pool and enter the containment atmosphere directly. The fraction of gases released from the sidewalls and enter the debris pool can significantly affect the extent of MCCI reactions. In particular, the released gases will increase the oxidation of Zr and subsequent concrete ablation as well as the amount of non-condensable gas, such as H_2 , in containment. The fraction of gases released from sidewalls and entering the debris pool is a model parameter. Set it to 1 in the model.

2.1.5.5. Debris pool solidification

If the average temperature of the core materials in each region as well as the thickness of the upper, sidewall and lower crusts are known, the state of the debris pool at any point in space and time can be computed. In particular, the change rate in the crust thickness can be expressed with the help of the energy transferred from the debris pool to the crust, the heat generation inside the crust and the energy transferred to the crust-concrete interface as well as the growth rate of the crust:

$$U_{crust} = - \frac{\left[h(T_F - T_{f,m}) + q_v x_c - \frac{2k_F(T_{F,m} - T_i)}{x_c} \right]}{\sum x_i \rho_i L_i} \quad (120)$$

where x_i , ρ_i and L_i represent the mass fraction, density and latent heat of constituent i , respectively. Variable q_v represents the volumetric decay heat source. If the crust is so thick that the energy of the molten pool and the heat generated by the crust itself cannot be transferred, the inner surface of the crust will melt, thinning out the crust. On the other hand, if the crust is thin enough to transfer more heat than the sum of heat transferred from the molten pool plus heat generated inside the crust, the inner surface of the crust will solidify, increasing the crust's thickness.

The evaluation of the solidified debris pool is consistent with that of the molten pool, except for the crust thickness which is assumed to be half of the debris pool thickness and that the inner surface temperature of the crust is unknown. Since the average temperature of the melt \bar{T}_{CM} can be obtained from different regions by integrating the parabolic temperature distribution within the crust over the direction of the crust thickness, it can be used to express the temperature gradient on the outer surface.

When the solidified debris pool is evaluated, it is assumed that the sidewalls have the same thermal conductivity as the lower edge of the pool. However, the conduction resistances of the two may be different due to their difference in thickness. As in the evaluation of the molten pool, if the crust-concrete interface temperature is higher than or equal to the concrete melting

temperature, concrete ablation will be computed. Therefore, under certain conditions and configurations, solid debris can also ablate concrete.

In order to calculate the heat transferred to the concrete, the implicit equation is used to improve the numerical stability for large time steps. By expanding the heat flux as a function of the average temperature of the debris and the average temperature of the concrete surface nodes, the following equation is obtained:

$$q''(\bar{T}_c - T_w^4) = q''(\bar{T}_{co}, T_{io}) + \frac{\partial q''}{\partial \bar{T}_c} \Delta T + \frac{\partial q''}{\partial \bar{T}_i} \Delta T \quad (121)$$

The relationship between the temperature change and the heat flux is shown below:

$$\Delta T_j = \frac{q'' \Delta t}{C_j}, \quad j = c \text{ or } i \quad (122)$$

where C_j is the heat capacity and Δt is the time step. Through further simplification, we obtain:

$$q'' = \frac{q_0''}{1 + a_c + a_i} \quad (123)$$

where

$$a_j = \left(\frac{3k_{cm}}{x_c} \right) \left(\frac{\Delta t}{C_j} \right) \quad (124)$$

2.1.5.6. *Effect of coolant*

For water covered debris cases, the heat flux off the top of the pool is determined by several different limits. Any one of which could be a limiting value depending upon the specific circumstances. The first limit considered is the water addition rate since the vaporization rate cannot exceed this value. Secondly, if the water addition rate represents a vaporization heat flux in excess of that which can be lost through the upper crust of the pool, then water accumulates and the flux to the water is limited through the hydrodynamic stability of the water or by the combination of convection and radiation in a film boiling mode. For simplicity, the hydrodynamic stability calculations consider only two different levels (i.e., a quenching rate for a dispersed water phase and one for any overlying pool). In the dispersed phase, the energy conducted through the upper crust needs to be sufficient to exceed the hydrodynamic limit posed by the pool phase, such that the overlying water is dispersed above the pool as fine droplets with the dispersed phase receiving energy from the surface of the pool as a result of convection and radiation. In this calculation, the energy flux to the water is determined by the droplet fluidization velocity as follows:

$$u_{gd} = \frac{3.7^4 \sqrt{g\sigma(\rho_f - \rho_g)}}{\sqrt{\rho_g}} \quad (125)$$

The heat flux is then:

$$q_d'' = 3.7 h_{fg} \sqrt{\rho_g}^4 \sqrt{g\sigma(\rho_f - \rho_g)} \quad (126)$$

In addition to the hydraulic restrictions, the code also computes the surface heat flux of the debris pool during film boiling – q_{fb} determined by convection and radiation from the surface to the water:

$$q_{fb}'' = h_{fb}(T_i - T_{sat}) + \varepsilon\sigma(T_i^4 - T_{sat}^4) \quad (127)$$

where

$$\varepsilon = \frac{1}{\varepsilon_{cm}} + \frac{1}{\varepsilon_w} \sim 1 \quad (128)$$

If the heat flux is lower than the droplet fluidization heat flux, but higher than the characteristic steady-state limit of the pool, its value will be used for the heat transfer from the top of the debris pool to the water. The heat flux decreases as the surface temperature drops and eventually drops below the characteristic hydraulic restriction value of the pool phase.

When the debris pool is fully covered by water and the debris surface temperature is sufficiently low, the heat flux in the droplet and film boiling modes will be lower than that of the pool boiling phase. The energy flux is obtained from the Kutateladze flat plate critical heat flux:

$$q_k'' = 0.14 h_{fg} \sqrt{r_g}^4 \sqrt{gs(r_f - r_g)} \quad (129)$$

As long as the average temperature of the debris pool exceeds the saturation temperature of water, the quenching rate will be assumed to remain unchanged.

During water injection, the energy balance of the molten pool is:

$$\frac{2k_F(T_{F,m} - T_i)}{x_c} = q_{st}'' \quad (130)$$

where q_{st}'' represents the evaporation rate. Once the amount of heat flux transferred to the water is determined, the heat flux balance of the upper crust surface will be computed iteratively to determine the upper surface temperature in each time step. This temperature

ranges between the lowest value, the saturation temperature of water, and the upper limit, the melting temperature of the core material.

2.1.6. Hydrogen combustion model

Hydrogen deflagration and explosions are two important combustion processes in severe accident analyses. Deflagration is the process in which the combustion front of a hydrogen cloud propagates in subsonic speed relative to the unburned gas, while an explosion is a process in which the combustion front propagates at sonic or supersonic speeds. Factors such as fuel type, oxidant, inert gas concentration, initial temperature and pressure, geometry disturbance and type of ignition determine the type of combustion and the subsequent pressure. The gas composition as well as the initial thermal hydraulic state will limit flammability and explosibility, while geometry and the type of disturbance will determine the possibility of explosion. The combustion mechanism model in ESAS deals with four basic phenomena. Firstly, it deals with the inherent flammability of gas mixtures at specific temperatures and pressures. Secondly, it computes the extent and duration of combustion to compute the temperature and pressure of the affected region. Thirdly, it is necessary to calculate the ignition criterion without an ignition source. Finally, the code deals with the extension of flammability limits in the event of temperature variations as well as solves the problem of spontaneous combustion. The deflagration to detonation transition and flame acceleration are not simulated in this code.

2.1.6.1. Incomplete combustion

The use of appropriate geometry is advocated for employing the asymptotic behaviour curve of flammability in mole fraction coordinates. Variable x represents the mole fraction of fuel (in this case hydrogen) and y represents the mole fraction of the inertant (any inert gas). The asymptotic and longitudinal axes of the lower and higher fuel limits intersect at:

$$y_l = m_l x + b_l \quad (131)$$

$$y_r = m_r x + b_r \quad (132)$$

These functions are shown in Fig. 23. The intercept represents the lower and upper flammability limits in the absence of an inertant. By considering points with low inertant concentration and joining them with the intercept, one may achieve the dotted line as in Fig. 23 and the slope of a given set of flammability limit data can be derived. The inertant concentration reaches the maximum at the "nose" of the flammability limit curve (denoted as the inert point in the figure) which is represented by coordinates $(X_i$ and $Y_i)$.

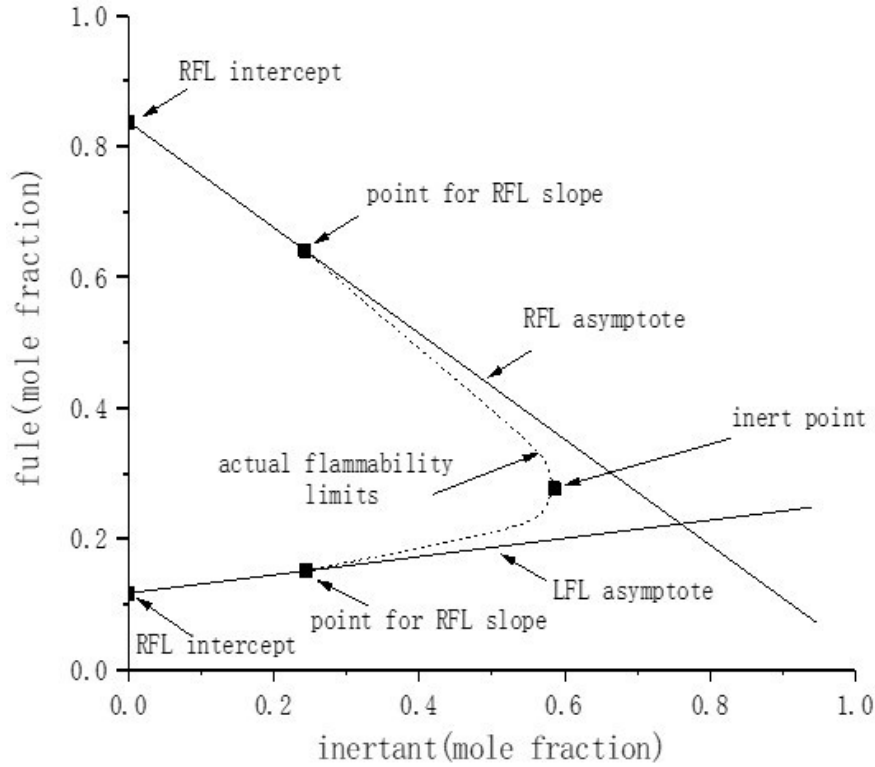


FIG. 23. Drawing of flammability limit curve (courtesy of CNPO).

Two asymptotes of the flammability limit curve are expressed in an exponential form:

$$y^{-a} = b[y_l^{-a} + y_r^{-a}] \quad (133)$$

If $b = 1$, when x is close to the lean flammability limit intercept and y_l is close to zero, then $\frac{1}{y_l}$ will be much greater than $\frac{1}{y_r}$, so y will be close to asymptote y_l . When x is close to the rich flammability limit intercept, the situation is reversed. The use of a scaling factor b enables both the inert point and derivatives at the inert point to be included in the flammability limits.

Exponent a is obtained by derivation. The concentration of inertant at the inert point reaches the maximum value, thus:

$$a = \frac{\ln\left(-\frac{m_l}{m_r}\right)}{\ln\left(\frac{y_{li}}{y_{ri}}\right)} - 1 \quad (134)$$

where y_{li} and y_{ri} are obtained by substituting x_i , and m_r is negative. The scale factor b is obtained by making the inert point lie on the flammability limit curve:

$$b = \frac{y_i^{-a}}{y_{li}^{-a} + y_{ri}^{-a}} \quad (135)$$

This method of establishing the flammability limit curve uses the values of five data points, which may be the best-fit average values of actual data and the maximum physical limit values at the inert points. This method has been successfully applied to fuel-oxidant-inertant mixtures, such as H_2 –air– H_2O and CO –air– CO_2 systems. When the temperature rises, the zero-inertant intercepts will be extrapolated. However, the slopes of the lower and higher flammability limit lines will remain constant, and the inert point will move towards the 100% inertant point. This phenomenon is summarized in Fig. 24.

The change of the zero-inertant intercept value with temperature is obtained by method of linear interpolation:

$$X_{Lu} = X_{LLu} + M_{Lu}(T - 298) \quad (136)$$

$$X_{Ru} = X_{RLu} + M_{Ru}(T - 298) \quad (137)$$

where X_{LLu} and X_{RLu} represent the lean flammability limit and the rich flammability limit at standard pressure, respectively, X_{Lu} and X_{Ru} represent the lean flammability limit and the rich flammability limit at temperature T , respectively, and the slopes M_{Lu} and M_{Ru} are obtained from data fitting. The slopes of the asymptotes remain constant.

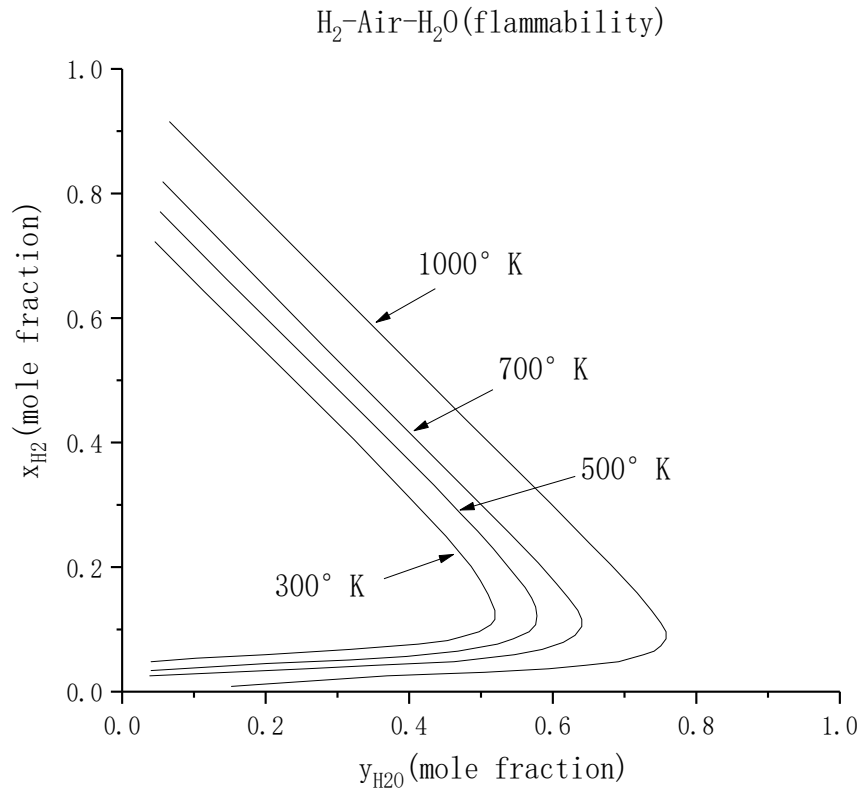


FIG. 24. Change of flammability limits with temperature (courtesy of CNPO).

The position of the inert point is uncertain because it moves along the curve of different situations. It is hypothesized that this point will shift towards the 100% inertant mark, resulting

in a lower maximum inertant concentration during the early stages of spontaneous combustion. For an H₂–air–H₂O system, the auto-ignition temperature T_{auto} and steam inertant concentration Y_{auto} at T_{auto} are specified as 983 K and 0.75. It is assumed that the inert point varies linearly with temperature; from standard pressure ($y_{i,stp}$, $x_{i,stp}$) to the inert concentration point $y_{st,ia}$ at the specified temperature T_{auto} , and the corresponding fuel concentration point x_i on the $y=100\%$ inertant line:

$$y_i = y_{i,stp} + \frac{(y_{st,ia} - y_{i,stp})(T - 298)}{(T_{auto} - 298)} \quad (138)$$

$$x_i = x_{i,stp} - \frac{x_{i,stp}(y_i - y_{i,stp})}{1 - y_{i,stp}} \quad (139)$$

At the auto-ignition temperature, the flammability limit curve is discontinuous because at this temperature any mixture is flammable. With the general method above, ternary mixture flammability limit fitting has been developed for fuel–air–inertant systems (H₂–air–H₂O, H₂–air–N₂, CO–air–CO₂ and CO–air–N₂). Some applicable constants are given in Table 2 and Table 3. Compared with the parameters in the literature, these fittings are in good agreement with the parameter ranges.

TABLE 2. FLAMMABILITY LIMIT DATA OF TERNARY MIXTURES WITH UPWARD FLAME PROPAGATION

| | | |
|--|--|-------------------------|
| 1. Zero inertant point, with upward propagation [at 298 K, unit: mole%] | H ₂ lower limit | 4.5 |
| | CO lower limit | 12.5 |
| | H ₂ upper limit | 78 |
| | CO upper limit | 72 |
| 2. Slope of temperature dependence curve of zero inertant point [Note: $X(T) = X(298) + M \times (T - 298)$, X = mole%, T = temperature] | H ₂ lower limit | -6.45×10^{-3} |
| | CO lower limit | -1.425×10^{-2} |
| | H ₂ upper limit | b |
| | CO upper limit | b |
| 3. Slope of asymptote of upward propagation flammability limit curve with inertant added [D (mole number of inertant) / D (mole number of fuel)] | H ₂ lower limit, with H ₂ O added | 22.5 |
| | CO lower limit, with CO ₂ added | 8.0 |
| | H ₂ upper limit, with H ₂ O added | -0.8452 |
| | CO upper limit, with CO ₂ added | -0.811 |
| | H ₂ lower limit, with N ₂ added | 1000 |
| | CO lower limit, with N ₂ added | -1.0 |
| | H ₂ upper limit, with N ₂ added | 1000 |
| | CO upper limit, with N ₂ added | -1.0 |
| 4. Coordinates of inert points, for upward propagation [unit: mole%] | H ₂ O in H ₂ –air–H ₂ O | 52 |
| | H ₂ in H ₂ –air–H ₂ O | 12 |
| | CO in CO–air–CO ₂ | 40 |
| | CO ₂ in CO–air–CO ₂ | 20 |
| | N ₂ in H ₂ –air–N ₂ | 70 |
| | H ₂ in H ₂ –air–N ₂ | 6 |
| | N ₂ in CO–air–N ₂ | 56.5 |
| | CO in CO–air–N ₂ | 14.5 |

TABLE 3. FLAMMABILITY LIMIT CURVE COEFFICIENT AT STANDARD PRESSURE

| System compositions | Constant coefficient | |
|--------------------------------------|----------------------|-------|
| | a | b |
| H ₂ -air-H ₂ O | 2.057 | 1.041 |
| H ₂ -air-N ₂ | 1.420 | 1.023 |
| CO-air-CO ₂ | 5.494 | 1.168 |
| CO-air-N ₂ | 0.946 | 0.983 |

In case of more than one inertant, the average flammability limit curve is obtained by averaging the slopes of all asymptotes:

$$M_l = \left(\frac{f_1}{M_{l1}} + \frac{f_2}{M_{l2}} \right)^{-1} \quad (140)$$

$$M_r = f_1 M_{r1} + f_2 M_{r2} \quad (141)$$

where f_1 and f_2 are relative inertant fractions ($f_1 + f_2 = 1$). After the combustion of the mixture, the fraction of nitrogen in the air will increase. The excess nitrogen concentration y_{N_2x} is obtained by the following equation:

$$y_{N_2x} = y_{N_2} - \frac{x_{O_2}}{r_a} \quad (142)$$

where y_{N_2x} is the mole fraction of nitrogen, x_{O_2} is the mole fraction of oxygen and r_a is the ratio of oxygen to nitrogen in air, which is about 0.21/0.79=0.266. The effective inert point is obtained by weighting the fuel and inertants:

$$x_i = f_1 x_{i1} + f_2 x_{i2} \quad (143)$$

In the case of more than one type of fuel, Le Chatelier's principle is used to obtain both the slope of the flammability limit curve and the inert points:

$$M_l = \left(\frac{f_1}{M_{l1}} + \frac{f_2}{M_{l2}} \right)^{-1} \quad (144)$$

$$x_i = \frac{1}{\frac{f_1}{x_{i1}} + \frac{f_2}{x_{i2}}} \quad (145)$$

A generalized H₂-CO-air-H₂O-CO₂-N₂ flammability limit curve can be created by the application of (143) to the slopes found with (140) and (141) for single fuels, so that inertant averaging is performed prior to application of Le Chatelier's law. This order is followed for calculation of the inert point using firstly (143) for each fuel and secondly (145). In principle, each fuel has its own autoignition temperature at which each fuel-inertant mixture has its own inert point. In order to limit the number of free parameters, the temperatures T_{auto} corresponding to each fuel are assumed to be the same and the inert point of each fuel-inertant

mixture is proportional to that of H_2-H_2O . This assumption is to be reasonable for light water reactors (LWRs) because in the application of this model, CO will not appear without H_2 , and H_2O is the dominant inertant. By direct proportion to the H_2-H_2O inert point fraction movement, the inertant point $y_{N_2,ia}$ of H_2-N_2 moves towards 100% inert point under T_{auto} :

$$y_{N_2,ia} = y_{N_2,i} + \left(\frac{1 - y_{N_2,i}}{1 - y_{st,i}} \right) (y_{st,ia} - y_{st,i}) \quad (146)$$

where $y_{st,i}$ and $y_{N_2,i}$ represent the concentrations of H_2O and N_2 , respectively, at their respective inert points under standard pressure.

2.1.6.2. Complete combustion

The flammability limit for downward flame propagation is managed as a sperate criterion for combustion completeness. This criterion is designed to address cases where the combustion completeness model predicts incomplete combustion, despite the mixture experiencing downward flammability that normally results in complete combustion. To deal with such conflict, when the conditions under the ignition criterion are satisfied to trigger combustion, the downward combustion will occur first and thus allow for the combustion to be completed. Under saturated conditions, the Westinghouse flame-temperature relationship provides a basis for variation of downward propagation limit with steam concentration. To preserve the Westinghouse saturated steam concentration data, Coward and Jones dry data [3], and the inert point variation characteristics for upward flammability, the flammability limits for downward flame propagation are plotted in a straight line.

Constructing the curve in this way allows for the downward limits to always lie below the upward propagation limits. Low and high flammability limits for downward propagation are obtained by combining the zero-inertant intercept and the inert points on the straight line. These points are initially adjusted for temperature, as are the upward propagation limits. Some of the constants used for the fuels are listed in Table 4.

An example of this method being applied at different temperatures is shown in Fig. 25. It is assumed that the autoignition temperature is 1034 K, and the maximum steam inerting limit is 75%. The saturated upward propagation limit curve is used as a reference line.

For complex mixtures, the inertant averaging method is used to acquire inert points, and Le Chatelier's principle is applied to the individual limits of each fuel computation. Each limit corresponds to a straight line, so extrapolation beyond the nominal inert point of each fuel is possible for the downward propagation limits.

TABLE 4. FLAMMABILITY LIMIT DATA OF TERNARY MIXTURES FOR DOWNWARD FLAME PROPAGATION

| | | |
|--|--|-------------------------|
| 1. Zero inertant point, for downward propagation [at 298 K, unit: mole%] | H ₂ lower limit | 8.5 |
| | CO lower limit | 15.9 |
| | H ₂ upper limit | 71.5 |
| | CO upper limit | 68.0 |
| 2. Slope of temperature curve of zero inertant point [Note: $X(T) = X(298) + M \times (T_{298})$ X=mole%, T=temperature] | H ₂ lower limit | -8.4×10^{-3} |
| | CO lower limit | -1.425×10^{-2} |
| | H ₂ upper limit | 2.667×10^{-2} |
| | CO upper limit | 2.0×10^{-2} |
| 3. Coordinates of inert point, for upward propagation [unit: mole%] | H ₂ O in H ₂ -AIR-H ₂ O | 52 |
| | H ₂ in H ₂ -AIR-H ₂ O | 12 |
| | CO in CO-AIR-CO ₂ | 40 |
| | CO ₂ in CO-AIR-CO ₂ | 20 |
| | N ₂ in H ₂ -AIR-N ₂ | 62 |
| | H ₂ in H ₂ -AIR-N ₂ | 11 |
| | N ₂ in CO-AIR-N ₂ | 50 |
| | CO in CO-AIR-N ₂ | 17 |

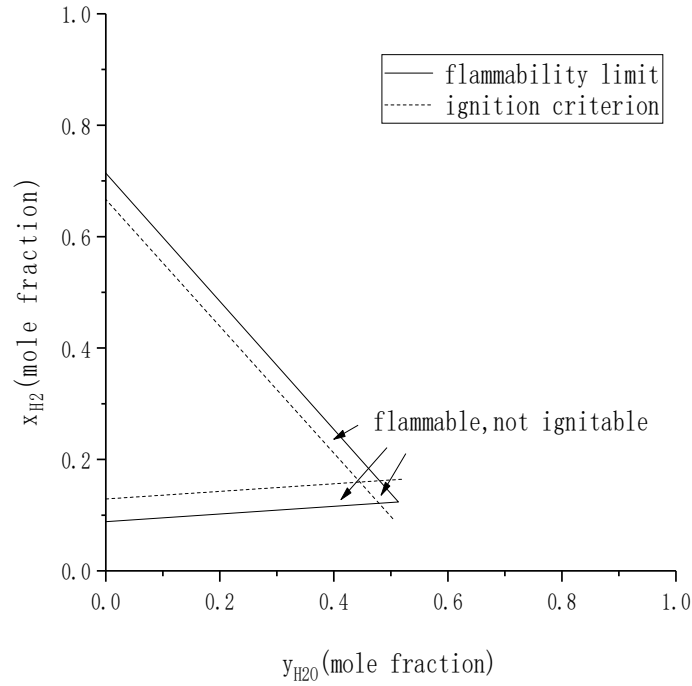


FIG. 25. Ignition criterion of H₂-air-H₂O (courtesy of CNPO).

2.1.6.3. Ignition criteria

In case that an igniter is present and active, the mixture can be ignited whenever flammability limits are met. The presence of another ignition source (such as sparks generated by a device) can be simulated as an igniter that was suddenly triggered.

The ignition criterion compensates for the downward flammability limit and is defined as the mole fraction of hydrogen above or below the temperature-steam concentration dependent limits. This compensation Δx_{IG} is added to the lower limit value of the hydrogen concentration in the downward flammability limit curve, while $-\Delta x_{IG}$ is added to the upper limit value in the downward flammability limit curve, as illustrated in Fig. 25, where Δx_{IG} is positive. This means that igniting a low concentration mixture requires a higher hydrogen concentration than the lower limit in the flammability limit curve, while igniting a high concentration mixture requires a lower hydrogen concentration than the upper limit in the flammability limit curve. Note that the steam ignition inerting limit is less than the limit in the corresponding flammability limit curve. The diamond-shaped region located in the flammable zone but outside of the ignition area is not combustible. The inert point $(x_{i,IG}, y_{i,IG})$ is determined by solving the following equations:

$$x_{i,IG} = (x_{RD} - \Delta x_{IG}) + y_{i,IG} M_{R,IG} \quad (147)$$

$$x_{i,IG} = (x_{LD} + \Delta x_{IG}) + y_{i,IG} M_{L,IG} \quad (148)$$

The analysis shows that igniting a lower concentration mixture requires meeting the following condition:

$$x > x_{L,IG} = (x_{LD} + \Delta x_{IG}) + y M_{L,IG} \quad (149)$$

where x represents the fuel concentration, y represents the inertant concentration and LD represents the zero-inertant lower intercept at a given temperature. The slope is expressed as:

$$M_{L,IG} = \frac{x_i - x_{LD}}{y_i} \quad (150)$$

To consider the correction of temperature for the inert point the following procedure is used: Let (x_i, y_i) be the inert point for the downward propagating flammability limit at a given temperature. This is a known parameter and can be obtained from data. Similarly, to the ignition of the upper concentration mixture, the following condition needs to be met:

$$x < x_{R,IG} = (x_{RD} - \Delta x_{IG}) + y M_{R,IG} \quad (151)$$

$$M_{R,IG} = \frac{x_i - x_{RD}}{y_i} \quad (152)$$

where RD represents the upper limit intercept point of the zero inertant after the temperature correction is considered. The inertant averaging method and Le Chatelier's principle are used in the ignition criterion just as for the downward propagation limits.

2.1.6.4. Passive autocatalytic recombiner module

The hydrogen depletion rate correlation of the passive autocatalytic recombiner (PAR) is hard-wired in the code as follows:

$$W_d = \frac{FEPAR [0.029883(C - C_0) + 0.001009(C - C_0)]P}{T} \quad (153)$$

where

W_d is the hydrogen depletion rate [kg/h];
 $FEPAR$ is the scale factor parameter for a reference PAR unit;
 C is the hydrogen volume fraction at the PAR inlet;
 P is the total pressure [bar];
 T is the gas temperature at the PAR inlet [K];
and C_0 is the limiting hydrogen volume fraction.

The equation is valid for any PAR unit that is similar in configuration and design to the NIS PARs [4]. $FEPAR$ is a scale factor in the hydrogen depletion rate equation. A $FEPAR$ value of 5 596 037 is recommended for a full-scale PAR unit developed by NIS [4]. The C_0 is a limiting hydrogen volume fraction below which the hydrogen depletion rate by the PAR is zero. $C_0 = 0.0$ is recommended as a nominal severe accident depletion rate.

The depletion rate established by the equation applies only when the PAR unit is in thermal equilibrium with its environment. The time required to establish thermal equilibrium is called the startup time. The startup time is short in a dry atmosphere but can be much longer if the PAR is exposed to moisture. The startup time is also a function of the hydrogen concentration in the atmosphere surrounding the PAR unit; a higher hydrogen concentration can lead to a faster heat-up of the PAR unit. During the startup time, the hydrogen depletion by the PAR is treated as negligible. At the end of the startup time, the PAR unit reaches thermal equilibrium and starts consuming hydrogen at the rate dictated by the depletion correlation (see Eq. (153)). In the code for ESAS, the simplifying assumption is made so that the PAR will become fully functional by the end of the start-up time.

Note: The SimFlow model (introduced Section 2.2.3) would run together with these models introduced above, however, SimFlow model does not belong to the part of the severe accident model, there is just some data exchange between SimFlow model and severe accident model.

2.2. NUCLEAR POWER PLANT MODELS FOR NORMAL OPERATION

2.2.1 Core physics

The reactor core neutron kinetics simulation software SimCore is an advanced real-time reactor core neutron dynamics simulation software with the following main characteristics:

- Two-group, three-dimensional and spatio-temporal kinetic equation with six groups of delayed neutrons makes up the basic model of the system;
- It adopts the "quasi-static method", namely dividing the temporal and spatial variation of the neutron flux to be the product of the amplitude and the shape function:

$$\phi_g(r, t) = \Phi_g(r, t)T(t) \quad g = 1, 2 \text{ (energy group);}$$

- Influences on reactivity, such as control rod movement, boron concentration change, fuel and burnable poison depletion, fission product concentration change, moderator temperature and density effect, Doppler effect, etc. are all taken into account by the two-group neutron cross-section node in three-dimensional space;
- Influences of the reflecting layer on neutron-flux distribution is heterogeneous in different core regions, which is considered by albedo distribution;
- Decay heat from the reactor core is calculated by 11 groups of decay heat models.

2.2.1.1. Mathematical model

Fission power and power distribution solution is a two-group three-dimensional diffusion equation:

$$\frac{1}{V_g} \frac{\partial \phi_g(r, t)}{\partial t} = \nabla D_g \nabla \phi_g(r, t) - \Sigma_{r.g} \phi_g(r, t) \quad (154)$$

$$+ \chi_g (1 - \beta) \sum_{g=1}^2 (v \Sigma_f)_g \phi_g(r, t)$$

$$+ \chi_g \sum_{m=1}^6 \lambda_m C_m(r, t) + X_g S(r, t)$$

$$\frac{\partial C_m(r, t)}{\partial t} = \beta_m \sum_{g=1}^2 (v \Sigma_f)_g \phi_g(r, t) - \lambda_m C_m(r, t) \quad (155)$$

where

| | |
|------------------|---|
| g | denotes the energy group symbol, $g = 1, 2$; |
| m | is the delayed neutron precursor element label, $m = 1, 2, \dots, 6$; |
| V_g | is the neutron velocity of group [g]; |
| ϕ_g | is the neutron flux of group [g]; |
| $(v \Sigma_f)_g$ | is the neutron fission cross section of group [g]; |
| D_g | is the neutron diffusion coefficient of group [g]; |
| $\Sigma_{r.g}$ | is the neutron cross section, equal sum of the absorption cross section and the downward scattering cross section; |
| C_m | is the delayed neutron precursor nuclear concentration of group [m]; |
| λ_m | is the delayed neutron precursor nuclear decay constant of group [m]; |
| β_m | is the group m delayed neutron portion of group m , $\beta = \sum \beta_m$; |
| $S(r, t)$ | is the neutron source; |
| and χ_g | is the discriminant function, $\chi_g = \begin{cases} 1, & \text{if } g = 1 \\ 0, & \text{if } g = 2 \end{cases}$. |

The following express the respective quantities:

| | |
|---|-------------------------------------|
| $\frac{1}{V_g} \frac{\partial \phi_g(r,t)}{\partial t}$ | is the neutron density growth rate; |
| $\nabla D_g \nabla \phi_g(r,t)$ | is the neutron diffusion; |
| $\Sigma_{r,g} \phi_g(r,t)$ | is the neutron absorption; |
| $\chi_g(1 - \beta) \sum_{g=1}^2 (\nu \Sigma_f)_g \phi_g(r,t)$ | is the instant neutron source; |
| $\chi_g \sum_{m=1}^6 \lambda_m C_m(r,t)$ | is the delayed neutron source; |
| and $\chi_g S(r,t)$ | is the external neutron source. |

Separation variable processing: several variables are required to solve equations (154) and (155) directly. Thus, it is assumed that the neutron flux change over time can be divided into the product of an amplitude and a shape function as shown according to the quasi-static method:

$$\phi_g(r,t) = \Phi_g(r,t)T(t), \quad g = 1, 2 \quad (156)$$

Substituting this into the above two equations (Eqs (154) and (155)) results in the shape function and the amplitude function. After obtaining the shape function and the amplitude function, the total fission power can be obtained from the integral over the entire core.

After inserting the Eq. (156) into equations (154) and (155) and introduce the corresponding shape function normalization conditions, the shape function is obtained as follows:

$$\begin{aligned} \frac{1}{V_g} \frac{\partial \Phi_g(r,t)}{\partial t} &= \nabla D_g \nabla \Phi_g(r,t) - \left[\Sigma_{r,g} + \frac{1}{V_g} \frac{dT(t)}{Tdt} \right] \Phi_g(r,t) \\ &+ \chi_g(1 - \beta) \sum_{g=1}^2 (\nu \Sigma_f)_g \Phi_g(r,t) + \frac{\chi_g}{T} \sum_{m=1} \lambda_m C_m(r,t) \\ &+ \frac{\chi_g}{T} S(r,t) \\ \frac{\partial C_m(r,t)}{\partial t} &= \beta_m \sum_{g=1}^2 (\nu \Sigma_f)_g \Phi_g(r,t) - \lambda_m C_m(r,t) \end{aligned} \quad (157)$$

$$(158)$$

The amplitude function is then as follows:

$$\frac{dT}{dt} = \frac{\rho - \beta}{\Lambda} T + \sum_{m=1} \lambda_m C_m + S \quad (159)$$

$$\frac{dC_m(t)}{dt} = \frac{\beta_m}{\Lambda} T - \lambda_m C_m(t) \quad (160)$$

where

ρ is the reactivity;

and Λ is the neutron generation time.

The shape function is solved using an adiabatic model. For this all the derivative terms in the shape function are ignored:

$$-\nabla D_1 \nabla \Phi_1(r, t) + \Sigma_{r,1} \Phi(r, t) = \frac{1}{k_{eff}} \left(v \Sigma_{f1} \Phi_1(r, t) + v \Sigma_{f2} \Phi_2(r, t) \right) \quad (161)$$

$$-\nabla D_2 \nabla \Phi(r, t) + \Sigma_{r,2} \Phi_2(r, t) = \Sigma_{1,2} \Phi_1(r, t) \quad (162)$$

By inputting the cross-section data and performing the iterative calculations one can obtain the reactivity.

The software SIMCORE uses 11 groups of decay heat models to calculate the core decay heat:

$$\frac{dC_i(r, t)}{dt} = b_i \left(f_1(r, t) S_{f1}(r, t) + f_2(r, t) S_{f2}(r, t) \right) - l_i C_i(r, t) \quad (163)$$

$$i = 1, 2, \dots, 11$$

The decay heat generated by the metamorphosis of the i element is: $F_{di} = e_i l_i C_i(r, t)$

The total decay heat is thus:

$$F_d = \sum_{i=1}^{11} e_i l_i C_i(r, t) \quad (164)$$

where

- C_i is the decay concentration of group i ;
- l_i is the decay constant of group i ;
- b_i is the portion of fission generation of i ;
- S_f is the macroscopic fission cross section of fuel;
- f is the neutron flux;
- F_d is the decay heat;
- and e_i is the energy released by one decay of group i .

Using the implicit finite difference method, it follows:

$$\frac{dF_{di}}{dt} = \varepsilon_i \lambda_i \beta_i (\phi_1 \Sigma_{f1} + \phi_2 \Sigma_{f2}) - \lambda_i F_{di} \quad (165)$$

By substituting $k_i = \varepsilon_i \beta_i$ into Eq. (165):

$$\frac{F_{di}^{n+1} - F_{di}^n}{\Delta t} = \lambda_i k_i (\phi_1 \Sigma_{f1} + \phi_2 \Sigma_{f2}) - \lambda_i F_{di}^{n+1} \quad (166)$$

$$F_{di}^{n+1} = \frac{F_{di}^n + \Delta t \lambda_i k_i (\phi_1 \Sigma_{f1} + \phi_2 \Sigma_{f2})}{1 + \lambda_i \Delta t} \quad (167)$$

SimCore contains calculation models for the concentration of iodine, promethium, xenon and samarium in three-dimensional space. The change in iodine concentration over time is obtained with:

$$\frac{dC_I(r, t)}{dt} = \beta_I [\Phi_1(r, t) \Sigma_{f1}(r, t) + \Phi_2(r, t) \Sigma_{f2}(r, t)] - \lambda_I C_I(r, t) \quad (168)$$

The xenon concentration over time is obtained with:

$$\begin{aligned} \frac{dC_{Xe}(r, t)}{dt} = & \lambda_I C_I(r, t) + \beta_{Xe} [\Phi_1(r, t) \Sigma_{f1}(r, t) + \Phi_2(r, t) \Sigma_{f2}(r, t)] \\ & - \sigma_{Xe} C_{Xe}(r, t) \Phi_2(r, t) - \lambda_{Xe} C_{Xe}(r, t) \end{aligned} \quad (169)$$

The promethium concentration over time is calculated as follows:

$$\frac{dC_{Pm}(r, t)}{dt} = \beta_{Pm} [\Phi_1(r, t) \Sigma_{f1}(r, t) + \Phi_2(r, t) \Sigma_{f2}(r, t)] - \lambda_{Pm} C_{Pm}(r, t) \quad (170)$$

The samarium concentration over time is obtained with:

$$\frac{dC_{Sm}(r, t)}{dt} = \lambda_{Pm} C_{Pm}(r, t) - \sigma_{Sm} * C_{Sm}(r, t) \Phi_2(r, t) \quad (171)$$

where

- I is iodine;
- X is xenon;
- Pm is promethium;
- Sm is samarium;
- $\beta_I, \beta_{Xe}, \beta_{Pm}$ is the fission yield portion of iodine, xenon and promethium;
- $\lambda_I, \lambda_{Xe}, \lambda_{Pm}$ is the decay constant for iodine, xenon and promethium;
- σ_{Xe}, σ_{Sm} is the microscopic absorption cross-section of xenon and samarium;
- Σ_{f1}, Σ_{f2} is the macroscopic neutron fission cross-section of the fuel;
- and Φ_1, Φ_2 is the neutron flux of the thermal and fast neutron group.

Promethium is a kind of transition nuclide during the generation of samarium, the nuclear fission first generates promethium, then promethium decays to be samarium.

2.2.1.2. Input data

To establish the three-dimensional neutron kinetics simulation model, the following two-group parameters are considered. They are applicable for various assembly types and under all burn-up steps for the first and equilibrium cycle (minimum nine burn-up points are required for each type of assembly).

- Σ_{a1} is the fast neutron absorption cross-section;
- $\Sigma_{1 \rightarrow 2}$ is the moderation cross-section of fast to thermal neutrons;
- D_1 is the fast group diffusion coefficient;
- $V_1 \Sigma_{f1}$ is the fast group source cross-section;
- Σ_{f1} is the fast neutron fission cross-section;
- $V_2 \Sigma_{f2}$ is the thermal group source cross-section;
- Σ_{f2} is the thermal neutron fission cross-section;
- Σ_{a2} is the thermal neutron absorption cross-section;
- D_2 is the thermal neutron diffusion coefficient;
- σ_{Xe} is the microscopic cross-section of xenon;
- and σ_{Sm} is the microscopic cross-section of samarium.

The following kinetic parameters are used in the calculation:

- V_1, V_2 are the neutron velocity;
- Λ is the average neutron lifetime;
- λ_e is the decay constant of the delayed neutron precursor;
- and β_f is the delayed fission neutron fraction

The fission product and burn-up distribution include:

- Fission yield;
- Metamorphic constants of Xe, Sm, I and Pm;
- Three-dimensional burn-up distribution (BOL, MOL, EOL).

SimCore code calculation process and system interface are shown in Fig. 26 and Fig. 27, respectively.

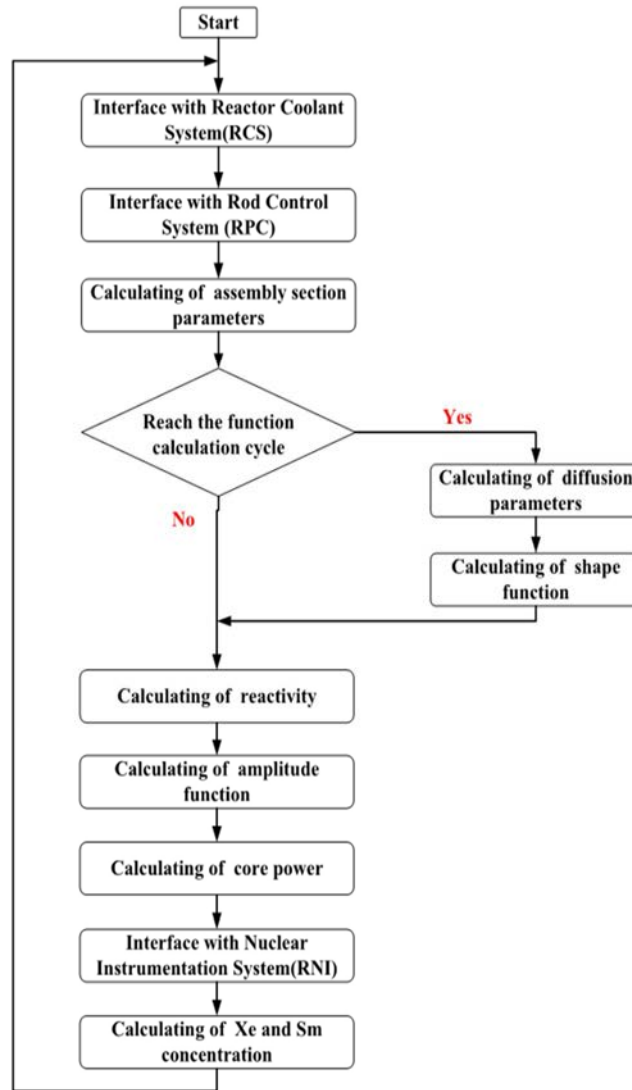


FIG. 26. Core physics calculation process in normal operation mode (courtesy of CNPO).

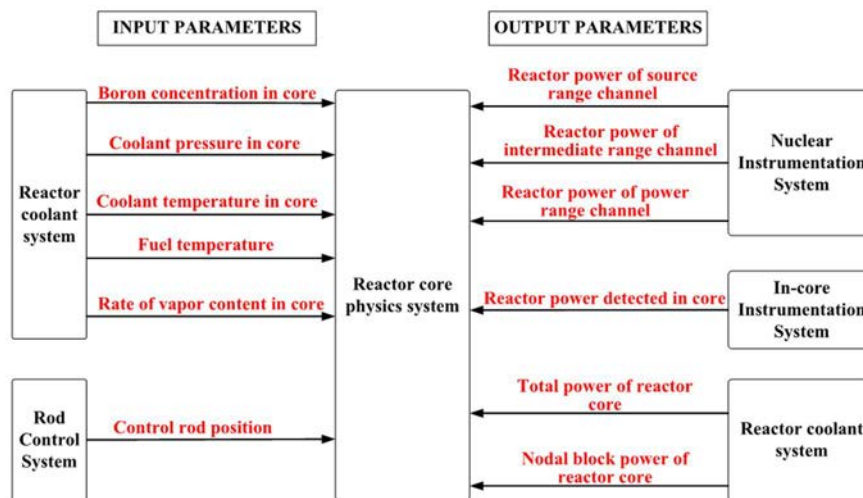


FIG. 27. Core physics system interface (courtesy of CNPO).

2.2.2. Thermal hydraulics real time simulation code

The SimTherm code (Thermal Hydraulic Engineering Analysis Tool in Real-Time) is a generalized thermal hydraulic code developed for real time operator training as well as for best-estimate engineering analysis in both nuclear and non-nuclear power plants. It can be used for the simulation of thermal, non-equilibrium, non-homogeneous, two-phase flow systems involving a steam-water mixture, non-condensable gases and non-volatile solutes. The range of simulation scenarios includes a wide range of normal, abnormal, and accidental operations of interest in LWRs. The SimTherm applications are versatile, however the present scope of simulation for SimTherm is as follows:

- PWR primary systems: RPV, hot legs, cold legs, steam generator tubes, pressurizers, reactor coolant pumps, valves, and fuel elements;
- PWR secondary systems: boilers, downcomers, steam separators, steam domes (up to feedwater and main steam line inlet nozzles).

SimTherm is developed as a best-estimate code for real-time simulation and thus the models used require rigorous assessment and verification. A significant amount of effort has been made to meet these requirements, which can be categorized into three phases:

- Corroborating the code with idealized problems, which may have analytical or conceptualized solutions;
- Verification of the code against separate effect test data;
- Validation of the code against integral system test data or actual plant data.

Counterpart calculation results are used as benchmark data whenever actual plant data or test facility data are not available. The assessment of the SimTherm code is an ongoing effort. At this point in time, an extensive amount of assessment has been completed for the above three phases.

2.2.2.1. Field equations

The SimTherm code contains six field equations, including conservation equations for non-condensable gas mass, vapor mass, liquid mass, vapor energy, liquid energy and mixture (sum) momentum:

Non-condensable gas mass:

$$\frac{\partial}{\partial t}(\alpha_g \rho_g X_n) + \frac{1}{A} \frac{\partial}{\partial x}(\alpha_g \rho_g v_g X_n A) = \frac{\delta S_n}{A} \quad (172)$$

Vapor mass:

$$\frac{\partial}{\partial t}(\alpha_g \rho_g) + \frac{1}{A} \frac{\partial}{\partial x}(\alpha_g \rho_g v_g A) = \Gamma + \frac{\delta S_g}{A} \quad (173)$$

Liquid mass:

$$\frac{\partial}{\partial t}(\alpha_f \rho_f) + \frac{1}{A} \frac{\partial}{\partial x}(\alpha_f \rho_f v_f A) = -\Gamma + \frac{\delta S_g}{A} \quad (174)$$

Vapor energy:

$$\begin{aligned} \frac{\partial}{\partial t}(\alpha_g \rho_g u_g) + \frac{1}{A} \frac{\partial}{\partial x}(\alpha_g \rho_g u_g v_g A) + P \frac{\partial \alpha_g}{\partial t} + \frac{P}{A} \frac{\partial}{\partial x}(\alpha_g v_g A) \\ = q_{wg} + q_{ig} + (\Gamma - \Gamma_w) h_g^* + \Gamma_w h_g^s + DISS_g + \frac{\delta S_{gQ}}{A} \end{aligned} \quad (175)$$

Liquid energy:

$$\begin{aligned} \frac{\partial}{\partial t}(\alpha_f \rho_f u_f) + \frac{1}{A} \frac{\partial}{\partial x}(\alpha_f \rho_f u_f v_f A) + P \frac{\partial \alpha_g}{\partial t} + \frac{P}{A} \frac{\partial}{\partial x}(\alpha_f v_f A) \\ = q_{wf} + q_{if} + (\Gamma - \Gamma_w) h_f^* + \Gamma_w h_f^s + DISS_f + \frac{\delta S_{fQ}}{A} \end{aligned} \quad (176)$$

Mixture (sum) momentum:

$$\begin{aligned} \alpha_g \rho_g \frac{\partial v_g}{\partial t} + \alpha_f \rho_f \frac{\partial v_f}{\partial t} + \frac{1}{2} \alpha_g \rho_g \frac{\partial v_g^2}{\partial x} + \frac{1}{2} \alpha_f \rho_f \frac{\partial v_f^2}{\partial x} \\ = -\frac{\partial P}{\partial x} + \rho B_x - \alpha_g \rho_g v_g FWG - \alpha_f \rho_f v_f FWF \\ - \Gamma(v_g - v_f) + \delta P_p + \delta S_v \end{aligned} \quad (177)$$

In order to solve the six given field equations above (Eqs (172) – (177)), seven independent variables are required. These variables include the pressure p , liquid and gas internal energies u_f and u_g , respectively, void fraction (α_g), non-condensable gas (air) mass fraction (X_n), gas and liquid velocity (v_g and v_f). A drift equation is used to balance the number of field equations and the number of independent variables:

$$(1 - \alpha_g C_0) v_g - \alpha_g C_0 v_f = v_{gj} \quad (178)$$

The solution of the set of seven field equations requires closure correlations to compute the interfacial heat and mass transfer (h_{ig}, h_{if} and Γ), wall heat transfer (q_{wg}, q_{wf}), wall energy dissipation ($DISS_f, DISS_g$), wall friction (FWF, FWG), distribution parameter (C_0) and drift velocity (V_{gj}). The equations of state are also required to calculate the five dependent thermodynamic variables, namely the liquid temperature (T_f), gas temperature (T_g), saturation temperature (T_s), liquid density (D_f) and the gas density (D_g). The linearized state equations are as follows:

$$\tilde{\rho}_f - \rho_f = \left(\frac{\partial \rho_f}{\partial P} \right) (\tilde{P} - P) + \left(\frac{\partial \rho_f}{\partial u_f} \right) (\tilde{u}_f - u_f) \quad (179)$$

$$\tilde{T}_f - T_f = \left(\frac{\partial T_f}{\partial P} \right) (\tilde{P} - P) + \left(\frac{\partial T_f}{\partial u_f} \right) (\tilde{u}_f - u_f) \quad (180)$$

$$\tilde{\rho}_g - \rho_g = \left(\frac{\partial \rho_g}{\partial P} \right) (\tilde{P} - P) + \left(\frac{\partial \rho_g}{\partial u_g} \right) (\tilde{u}_g - u_g) + \left(\frac{\partial \rho_g}{\partial X_n} \right) (\tilde{X}_n - X_n) \quad (181)$$

$$\tilde{T}_g - T_g = \left(\frac{\partial T_g}{\partial P} \right) (\tilde{P} - P) + \left(\frac{\partial T_g}{\partial u_g} \right) (\tilde{u}_g - u_g) + \left(\frac{\partial T_g}{\partial X_n} \right) (\tilde{X}_n - X_n) \quad (182)$$

$$\tilde{T}^s - T^s = \left(\frac{\partial T^s}{\partial P} \right) (\tilde{P} - P) + \left(\frac{\partial T^s}{\partial u_g} \right) (\tilde{u}_g - u_g) + \left(\frac{\partial T^s}{\partial X_n} \right) (\tilde{X}_n - X_n) \quad (183)$$

$$\Gamma_g = \Gamma_w - \frac{h_{if}(T^s - T_f) + h_{ig}(T^s - T_g)}{h_s^* - h_f^*} \quad (184)$$

2.2.2.2. Two-phase flow model

Two flow regime maps are used in the SimTherm code: a vertical and a horizontal flow regime map. A schematic of the vertical flow regime map as coded in SimTherm is shown in Fig. 28.

$$\begin{aligned} 15^\circ \leq \varphi \leq 90^\circ & \quad \text{Vertical flow} \\ 0^\circ \leq \varphi \leq 15^\circ & \quad \text{Horizontal flow} \end{aligned}$$

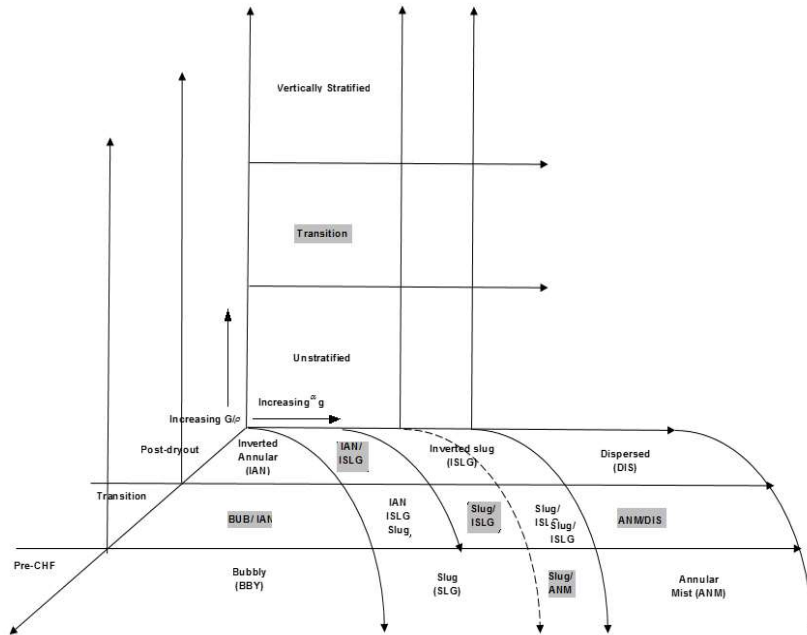


FIG. 28. Vertical volume flow regime map (courtesy of CNPO).

The map consists of bubbly, slug, annular mist, and dispersed (droplet or mist) flows in the pre-critical heat flux (CHF) regime. Inverted annular, inverted slug and dispersed (droplet or

mist) flows post dry-out are vertically stratified for sufficiently low mixture velocity $\frac{G}{\rho}$. Transition regions provided in the code are also shown in Fig. 28, and details of the interpolating functions are given in the sections dealing with the actual heat and mass transfer as well as drag correlations.

The values for the parameters governing the flow regime transitions are:

$$\alpha_{AB} = \begin{cases} \alpha_{AB}^* & G \leq 2000 \\ \alpha_{AB}^* + \frac{0.5 - \alpha_{AB}^*}{1000}(G - 2000) & 2000 < G < 3000 \\ 0.05 & G \geq 3000 \end{cases} \quad (185)$$

$$\alpha_{AB}^* = \max(0.25 \min(1, (0.045D^*)^8), 10^{-3}) \quad (186)$$

where the mixture flow rate is:

$$G = \alpha_g \rho_g |v_g| + \alpha_f \rho_f |v_f| \quad (187)$$

The dimensionless Taylor bubble diameter D^* is:

$$D^* = D \left[\frac{g(\rho_f - \rho_g)}{\sigma} \right]^{\frac{1}{2}} \quad (188)$$

where D is the hydraulic diameter of the volumes, and σ is the surface tension according to the pressure and internal energy:

$$\alpha_{CD} = \alpha_{AB} + 0.2 \quad (189)$$

$$\alpha_{AC} = \max(\alpha_{AM}^{min}, \min(\max(\alpha_{crit}^f, 0.75), \alpha_{crit}^e, \alpha_{BS}^{max})) \quad (190)$$

$$\alpha_{crit}^f = \begin{cases} \frac{1}{v_g} \left[\frac{qD(\rho_f - \rho_g)}{\rho_g} \right]^{\frac{1}{2}} & \text{for upflow} \\ 0 & \text{for downflow and countercurrent flow} \end{cases} \quad (191)$$

where $\alpha_{AM}^{min} = 0.5$, $\alpha_{BS}^{max} = 0.9$ and the following relations hold true:

$$\alpha_{DE} = \alpha_{AC} - 0.05 \quad (192)$$

$$\alpha_{AD} = 10^{-7} \quad (193)$$

The Taylor bubble flow velocity can then be written as in Eq. (194).

$$v_{TB} = 0.35 \left[\frac{gD(\rho_f - \rho_g)}{\rho_f} \right]^{\frac{1}{2}} \quad (194)$$

The transition from bubbly flow to slug flow is based on Taitel, Bornea and Dukler [5], according to which the transition occurs when the rise velocity of the bubbles in the bubbly flow regime exceeds the Taylor bubble rise velocity, since the bubbles will approach the trailing edges of the Taylor bubbles and coalesce:

$$v_0 > v_{TB} \quad (195)$$

$$v_0 = 1.53 \left[\frac{g(\rho_f - \rho_g)\sigma}{\rho_f^2} \right]^{\frac{1}{4}} \quad (196)$$

When $D < D_{crit}$, the above equations always hold. D_{crit} is defined as in Eq. (197).

$$D_{crit} = 19.11 \left[\frac{\sigma}{g} (\rho_f - \rho_g) \right]^{\frac{1}{2}} \quad (197)$$

The critical dimensionless diameter for bubbly flow is then $D_{crit} = 19.11$.

The transition from slug flow to annular mist flow is based on the postulate that annular flow will occur in a vertical pipe when the upward drag forces are sufficient to overcome gravity and can lift the liquid droplets in the core flow region as well as those which may be created by shattering wave crests in the wall-adjacent liquid film. The transition criterion is defined as:

$$\alpha_{AC} = \min (\alpha_{crit}^f, \alpha_{crit}^e) \quad (198)$$

where

$$\alpha_{crit}^f = \begin{cases} \frac{1}{v_g} \left[\frac{qD(\rho_f - \rho_g)}{\rho_g} \right]^{\frac{1}{2}} & \text{for upflow} \\ 0.75 & \text{for downward and countercurrent flow} \end{cases} \quad (199)$$

$$\alpha_{crit}^e = \frac{1.6}{v_g} \left[\frac{gD(\rho_f - \rho_g)}{\rho_g^2} \right] \quad (200)$$

Due to that the Eq. (198) (α_{AC} is unreasonably low, or $\alpha_{AC} > 1$) when the vapor velocity is too low or too high, an additional requirement is added to the code:

$$\alpha_{AM}^{min} \leq \alpha_{AC} \leq \alpha_{BS}^{max} \quad (201)$$

Finally, α_{AC} is obtained as shown below:

$$\alpha_{AC} = \max(\alpha_{AM}^{min}, \min(\alpha_{crit}^f, \alpha_{crit}^e, \alpha_{BS}^{max})) \quad (202)$$

When flow encounters the departure from nucleate boiling (DNB) phenomenon within a flow channel, it can lead to various flow regimes, including inverted flow regimes downstream. These inverted flows exhibit complex and typically unstable flow geometries, and their boundaries are not well-defined. However, the post-CHF flow regimes may be influenced by the pre-CHF regime of the flow, indicating a dependence on its flow history. It is important to note that the mechanisms governing transitions post-CHF are distinct from those pre-CHF, implying that transition criteria for the former may not directly apply to the latter. Despite this distinction, the code currently employs pre-CHF flow regime criteria for post-CHF regime determination due to the lack of a suitable post-CHF flow regime model.

When the flow mixture velocity in a vertical conduit is so low that an identifiable gas or liquid interface is present, the vertically stratified flow regime is applied in the SimTherm code.

The first requirement for the vertical stratification is that the mixture velocity is lower than the Taylor-bubble rise velocity, $v_m < v_{TB}$, where:

$$v_m = \frac{\alpha_g \rho_g |v_g| + \alpha_f \rho_f |v_f|}{\rho_m} \quad (203)$$

$$\rho_m = \alpha_g \rho_g + \alpha_f \rho_f \quad (204)$$

$$\alpha_{g,L} > 0.7 \quad (205)$$

$$\alpha_{g,L} - \alpha_{g,K} > 0.2 \text{ or } \alpha_{g,K} - \alpha_{g,I} > 0.2 \quad (206)$$

$$\alpha_{g,I} \leq \alpha_{g,K} \leq \alpha_{g,L} \quad (207)$$

2.2.3. SimFlow code

The SimFlow code is used for the modelling of the secondary loop and the balance of plant systems. It can be used in various systems such as the main steam, feedwater, service water, and off gas systems. SimFlow is also used in severe accident mode. It is designed to model the hydraulic systems in real time simulation. In addition to obtaining system flows and pressures, it allows for the calculation of temperatures and the transport of substances dissolved and in suspension.

The resolution of a hydraulic network relies on fundamental equations, including the continuity equation (or conservation of mass), conservation of momentum equation, and conservation of energy equation. To simplify these equations for application in hydraulic networks, certain assumptions are made:

- One-dimensional flow is assumed, neglecting volumetric effects. This implies that properties vary in only one direction, with all properties remaining constant across a flow section but possibly varying across different sections;
- Homogeneity is assumed within each node, meaning that all properties within a node are considered uniform. This assumption is valid as node sizes and numbers can be adjusted to simulate non-homogeneous phenomena effectively;
- Steam and non-condensable gases are treated as an ideal gas mixture;
- The air temperature is considered equal to the vapor temperature;
- Hydraulic networks are simplified into a flow network comprising inner nodes, boundary nodes, and junctions. Inner nodes represent the flow space of the medium, assumed to be uniformly mixed, while boundary nodes allow independent changes in physical parameters. Nodes are interconnected via junctions.

The schematic provided in Fig. 29 illustrates a closed duct representing a node with multiple junctions, showcasing the arrangement of inner and boundary nodes connected by junctions.

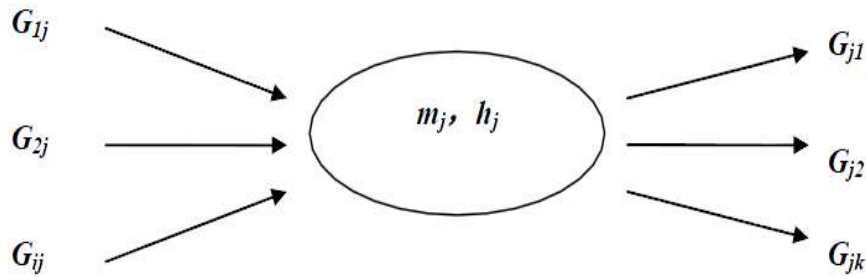


FIG. 29. SimFlow node and junction schematic (courtesy of CNPO).

2.2.3.1. Basic equations

Hydraulic networks are modelled with SimFlow. All fluid dynamics and thermodynamics calculations are performed, including fluid flows, pressures, thermodynamic properties, material concentrations and transport. The heat exchange with pipe walls and the surroundings, as well as the pipe wall temperatures are also calculated. For the flow in a closed conduit, the continuity equation is as follows:

$$\frac{dm_j}{d\tau} = \sum_i G_{ij} - \sum_k G_{jk} \quad (208)$$

where

m_j is the mass of node j ;

and G_{ij} is the mass flow of the junction between node i and j .

The momentum balance equation is:

$$\frac{L}{S} \frac{dG}{d\tau} = P_i - P_j + \rho g h_{ij} + P_{pump} - f_{ij} \quad (209)$$

where

- ρ is the fluid density [kg/m³];
- g is the acceleration of gravity [m/s²];
- L is the length of junction [m];
- S is the cross-sectional area of junction [m²];
- τ is the time [s];
- P_i is the pressure of node i [Pa];
- h_{ij} is the height difference between node i and j [m];
- and P_{pump} is the pump head [Pa].

The term f_{ij} represents the load losses due to friction in the piping, changes in cross-section, and changes in direction. This term may generally be expressed as being proportional to the velocity squared:

$$f_{ij} = \frac{G^2}{2S^2 k_{SI}^2 \rho} \quad (210)$$

Where k_{SI} is the conductivity of the junction, and G is the mass flow rate [kg/s].

The calculation of the pump pressure term P_{pump} is very specific to the type of pump and its size. Fig. 30 shows a typical centrifugal pump curve.

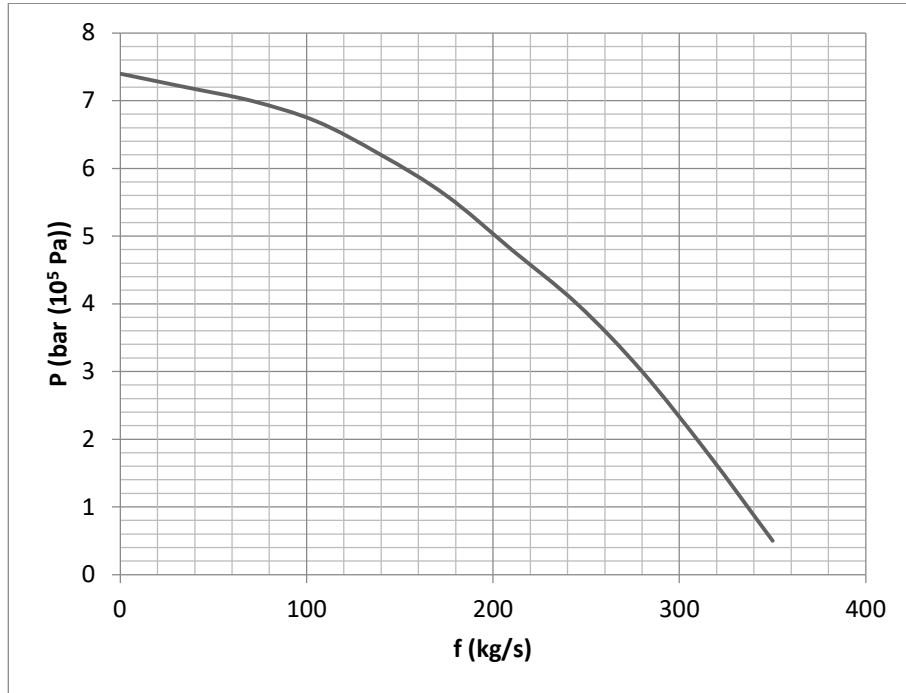


FIG. 30. Pump curve showing the pump pressure in relation to the flow rate (courtesy of CNPO).

The pump pressure is obtained with:

$$P_{pump} = k_1 n^2 + k_2 nG + k_3 G^2 \quad (211)$$

Where k_1, k_2, k_3 represent the characteristic coefficients of the pump, and n is the pump speed.

The energy balance equation for a fluid can be written as follows:

$$\frac{d\left(m_j \left(h_j - \frac{P_j}{\rho_j}\right)\right)}{d\tau} = \sum_i (G_{ij} h_i) - \sum_k (G_{jk} h_j) - W_j + Q_j \quad (212)$$

The heat transfer term Q_j is composed of several different parts: the heat transfer to the tube wall and external heat sources. The output power W_j is only calculated in the turbine nodes.

2.2.3.2. Transport properties equations

The soluble chemicals are assumed to have no heat capacity and occupy no volume. This is a valid assumption because the concentrations are low enough to have no significant effect on the physical properties of the fluid.

$$\frac{d(m_j C_j^n)}{d\tau} = \sum_i (G_{ij} C_i^n) - \sum_k (G_{jk} C_j^n) + J \quad (213)$$

where C_j^n is concentration of soluble chemicals at node I , and J is the source item of chemicals which could generate the chemical at a constant rate. By applying the continuity equation, the following is obtained:

$$\left(\sum_i G_{ij} - \sum_j G_{jk}\right) C_j^n + m_j \frac{dC_j^n}{d\tau} = \sum_i (G_{ij} C_i^n) - \sum_k (G_{jk} C_j^n) + J \quad (214)$$

Equation (214) can also be written as:

$$\frac{dC_j^n}{d\tau} = \frac{\sum_i [G_{ij} (C_i^n - C_j^n)] + J}{m_j} \quad (215)$$

where

$$m_j = m_j^c + \left(\sum_i G_{ij} - \sum_j G_{jk}\right) d\tau \quad (216)$$

2.2.3.3. Physical property equations

The momentum balance equation can be written as:

$$\frac{L}{S} \frac{dG}{d\tau} + \frac{G^2}{2S^2 k_{SI}^2 \rho} - (P_i - P_j + \rho g h_{ij}) - P_{pump} = 0 \quad (217)$$

To solve this equation, it has to be linearized:

$$G_{ij} = f(p_i, p_j, \rho_i, \rho_j) \quad (218)$$

$$\Delta G_{ij} = \frac{\partial G_{ij}}{\partial p_i} \Delta p_i + \frac{\partial G_{ij}}{\partial p_j} \Delta p_j + \frac{\partial G_{ij}}{\partial \rho_i} \Delta \rho_i + \frac{\partial G_{ij}}{\partial \rho_j} \Delta \rho_j \quad (219)$$

where

$$\Delta p_i = \frac{dp_i}{d\tau} \Delta \tau \beta \quad (220)$$

$$\Delta p_j = \frac{dp_j}{d\tau} \Delta \tau \beta \quad (221)$$

$$\Delta \rho_i = \frac{d\rho_i}{d\tau} \Delta \tau \beta \quad (222)$$

$$\Delta \rho_j = \frac{d\rho_j}{d\tau} \Delta \tau \beta \quad (223)$$

For the flow in a closed conduit the continuity equation gives:

$$\frac{d(V_i \rho_i)}{d\tau} = \sum_i G_{ij} - \sum_k G_{jk} \quad (224)$$

where

$$\rho_i = f(p_i, h_i, C_i^k) \quad (225)$$

$$\frac{d\rho_i}{d\tau} = \frac{\partial \rho_i}{\partial p_i} \frac{dp_i}{d\tau} + \frac{\partial \rho_i}{\partial h_i} \frac{dh_i}{d\tau} + \sum_k \left(\frac{\partial \rho_i}{\partial C_i^k} \frac{dC_i^k}{d\tau} \right) \quad (226)$$

$$\frac{d(V_i \rho_i)}{d\tau} = V_i \frac{\partial \rho_i}{\partial p_i} \frac{dp_i}{d\tau} + V_i \frac{\partial \rho_i}{\partial h_i} \frac{dh_i}{d\tau} + V_i \sum_k \left(\frac{\partial \rho_i}{\partial C_i^k} \frac{dC_i^k}{d\tau} \right) \quad (227)$$

$$-\frac{dm_i}{d\tau} = \sum_j G_{ij}^c + \sum_j \Delta G_{ij} \quad (228)$$

According to the momentum balance equation and the continuity equation, the linearization would give the following:

$$\begin{aligned} \frac{dp_i}{d\tau} \left\{ \left(\sum_j \frac{\partial G_{ij}}{\partial p_i} + \left(\sum_j \frac{\partial G_{ij}}{\partial \rho_i} \right) \frac{d\rho_i}{dp_i} \right) \Delta\tau \beta + V_i \frac{\partial \rho_i}{\partial p_i} \right\} \\ + \frac{dp_j}{d\tau} \left(\sum_j \frac{\partial G_{ij}}{\partial p_j} + \left(\sum_j \frac{\partial G_{ij}}{\partial \rho_j} \right) \frac{d\rho_j}{dp_j} \right) \Delta\tau \beta = C^* \end{aligned} \quad (229)$$

where

$$\begin{aligned} C^* = & - \sum_j G_{ij}^c - V_i \left(\frac{\partial \rho_i}{\partial h_i} \frac{dh_i}{d\tau} + \sum_k \left(\frac{\partial \rho_i}{\partial C_i^k} \frac{dC_i^k}{d\tau} \right) \right) - \left(\sum_j \frac{\partial G_{ij}}{\partial \rho_i} \right) \frac{\partial \rho_i}{\partial h_i} \frac{dh_i}{d\tau} \Delta\tau \beta \\ & - \left(\sum_j \frac{\partial G_{ij}}{\partial \rho_j} \right) \frac{\partial \rho_j}{\partial h_j} \frac{dh_j}{d\tau} \Delta\tau \beta \\ & - \left(\sum_j \frac{\partial G_{ij}}{\partial \rho_i} \right) \sum_k \left(\frac{\partial \rho_i}{\partial C_i^k} \frac{dC_i^k}{d\tau} \right) \Delta\tau \beta \\ & - \left(\sum_j \frac{\partial G_{ij}}{\partial \rho_j} \right) \sum_k \left(\frac{\partial \rho_j}{\partial C_j^k} \frac{dC_j^k}{d\tau} \right) \Delta\tau \beta \end{aligned} \quad (230)$$

The resulting equation is as follows:

$$\begin{aligned} \frac{dp_i}{d\tau} \left(\left(\sum_j \frac{\partial G_{ij}}{\partial p_i} + \left(\sum_j \frac{\partial G_{ij}}{\partial \rho_i} \right) \frac{d\rho_i}{dp_i} \right) \Delta\tau \beta + V_i \frac{\partial \rho_i}{\partial p_i} + kass \times (1 - \varphi) \right) \\ + \frac{dp_j}{d\tau} \left(\sum_j \frac{\partial G_{ij}}{\partial p_j} + \left(\sum_j \frac{\partial G_{ij}}{\partial \rho_j} \right) \frac{d\rho_j}{dp_j} \right) \Delta\tau \beta = C^* \end{aligned} \quad (231)$$

Here *kass* is a compressibility factor, and φ is the void fraction. Therefore, the system of equations is a symmetrical, real and positive matrix:

$$A \cdot \overline{\Delta P} = B \quad (232)$$

where $\overline{\Delta P}$ is the vector of the unknown pressure changes of the system. Once the pressures have been determined, the calculation of mass flows between nodes can be performed by applying the momentum balance equation.

By applying the continuity equation and the energy conservation equation, the following enthalpy equation is obtained:

$$\frac{dh_j}{d\tau} = \frac{(\sum_i G_{ij} - \sum_k G_{jk}) \frac{p_j}{\rho_j} + V_j \frac{dp_j}{d\tau} + Q_j - W_j + \sum_i [G_{ij}(h_i - h_j)]}{m_j} \quad (233)$$

where

$$m_j = m_j^c + \left(\sum_i G_{ij} - \sum_j G_{jk} \right) d\tau \quad (234)$$

The average specific enthalpy of fluid can be written as follows:

$$h = h_L(1 - X) + h_v \left(X - \sum_n C^n \right) + \sum_n C^n h_g^n \quad (235)$$

The liquid density is calculated with the help of the average enthalpy, liquid enthalpy, non-condensable gas enthalpy, steam enthalpy and the soluble chemicals concentrations:

$$X = \frac{h - h_L - \sum_n C^n (h_g^n - h_v)}{h_v - h_L} \quad (236)$$

If steam and a non-condensable gas make up an ideal gas mixture, then the following equation is obtained from the ideal gas state equation:

$$\frac{T}{V_{mix}} = \frac{p_v}{m_v R_v} = \frac{p_{mix}}{m_{mix} R_{mix}} \quad (237)$$

where

V_{mix} is the volume of steam and non-condensable gas [m^3];

v is the subscript indicating parameters of steam;

mix is the subscript indicating parameters of mixed fluid;

and T is the temperature of mixed fluid [K].

In general, the gas constants R_g for non-condensable gases are assumed to be constant. This is a valid assumption over the range of temperature encountered in the power plant simulation in normal operation mode. Consequently, the following general equation may be written for R_{mix} :

$$R_{mix} = R_v \frac{X - \sum_n C^n}{X} + \sum_n R_g^n \frac{C^n}{X} = \frac{1}{X} \left(R_v \left(X - \sum_n C^n \right) + \sum_n R_g^n C^n \right) \quad (238)$$

Finally, the gas pressure can be determined by the following two equations

$$p_v = p_{mix} \frac{(X - \sum_n C^n) R_v}{(X - \sum_n C^n) R_v + \sum_n C^n R_g^n} \quad (239)$$

$$p_g^n = p_{mix} \frac{C_g^n R_g^n}{(X - \sum_n C^n) R_v + \sum_n C^n R_g^n} \quad (240)$$

where g is the subscript indicating parameters of non-condensable gas.

The node density is then calculated from the liquid density, the gas density and the steam quality:

$$\rho = \frac{1}{\frac{1-X}{\rho_L} + \frac{X}{\rho_{gas}}} = \frac{1}{\frac{1-X}{\rho_L} + \frac{X}{p/RT}} = \frac{1}{\frac{1-X}{\rho_L} + \frac{RXT}{p}} \quad (241)$$

where

$$RX = R_v \left(X - \sum_k C_k \right) + \sum_k (C_k R_k) \quad (242)$$

3. USER MANUAL

The User Manual provides detailed instructions on the ESAS installation, start of the software, initializations with error list and how to resolve them. Additionally, the User Manual provides explanations on how to activate desired NPP conditions and interpret the simulator results.

3.1. GENERAL INSTRUCTIONS

This section provides comprehensive guidance on the installation process of ESAS, along with instructions for utilizing the software effectively. Additionally, it includes an error list with suggested solutions to address any encountered issues.

3.1.1. Installation

The ESAS is available as an executable installer. To install it, the user needs to double click on the installer application, after which the user can then customize the installation path. The installation usually takes around 3 minutes.

The simulator was tested on the Windows 11 operating system. However, it is also compatible with earlier versions of Windows. Although it is a 32-bit application, it runs efficiently on 64-bit processors as well.

The ESAS is capable of running simulations in real time on standard desktops and laptops with a CPU speed of at least 1.5 GHz, 4 GB of RAM, and 50 GB of storage. For users seeking an optimized software experience, it is advisable to use a computer with higher specifications, such as a CPU speed of 3 GHz, 8 GB of RAM, or better. To simulate at 4× real-time speed, a computer with higher configurations is required. This might include a CPU speed of 4 GHz, 16 GB of RAM, or superior specifications.

The magnitude of outputs from the 3D severe accidents simulation model may vary depending on the regional settings of the computer. Thus, it is important to adjust the appearance of decimal data types to “.” (rather than for example “;”). In Windows, this can be achieved by clicking the “Start” button and then clicking on or searching for “Control Panel”. Here, for Windows 10, select the settings under “Change date, time, or number format,” and for Windows 7, navigate through “Clock, Language, and Region” to “Regional and Language Options.” Next, open the “Formats” tab. In Windows 10, choose the “Additional settings” button and adjust the decimal symbol to “.” in the window that appears. In Windows 7, click on “Customize this format” under “Current Format,” which opens a new window where the decimal settings can be adjusted to “.”. Changing the region to English (United States) also helps to resolve the issue.

3.1.2. ESAS start-up

Once the simulator is installed, a shortcut will appear on the user’s screen. To run the simulator, the following steps are required:

- (1) Double click the launcher (shortcut on the desktop) as shown in Fig. 31.



FIG. 31. ESAS desktop launcher icon.

- (2) The loading progress of the simulator is visible in the progress bar within the application window, as illustrated in Fig. 32.



FIG. 32. Loading screen after ESAS initialization and startup.

- (3) In the subsequent step, users can choose the simulator mode via the mode selection interface, opting for either “Normal Operation Mode” or “Severe Accident Mode,” as depicted in Fig. 33.

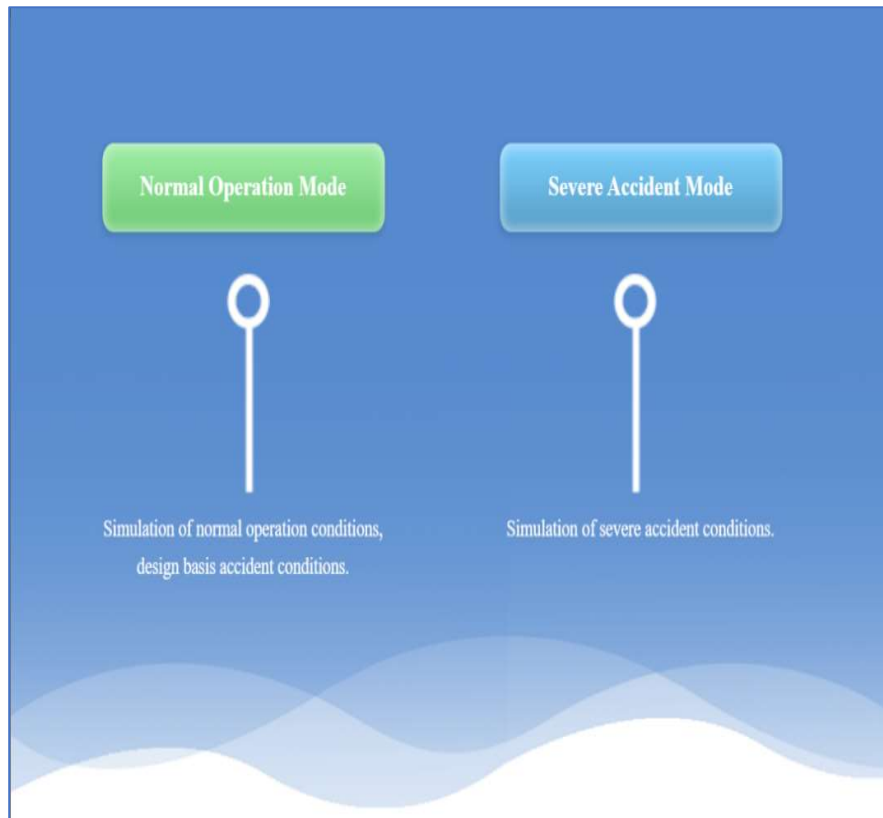


FIG. 33. ESAS interface to select the mode.

- (4) By default, the application loads initial condition 1 (I001), representing 100% power at the start of fuel life, as shown in Fig. 34.

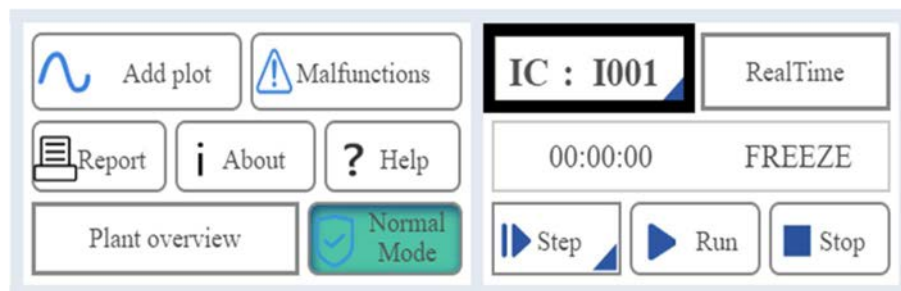


FIG. 34. ESAS menu panels: initial conditions (IC in the screen) enclosed by a bold rectangle.

- (5) To transition to another simulation frame, navigate to the “Plant Overview” tab (refer to Fig. 35) located in the second panel from the right. From there, select different views by clicking on either the name of the new view or the + button adjacent to the name, as demonstrated in Fig. 36. The view opens either in the same window or in a new one, depending on the selection.



FIG. 35. ESAS menu panels: plant overview drop-down button enclosed by a bold rectangle.



FIG. 36. Drop-down list of different simulator windows.

- (6) Equipment operation: pumps, valves and values set in blue can be selected and their values and modes can be modified by the user. Additionally, some control modes can be changed from automatic to manual by turning the switch on the interface as highlighted by bold rectangles in Fig. 37.

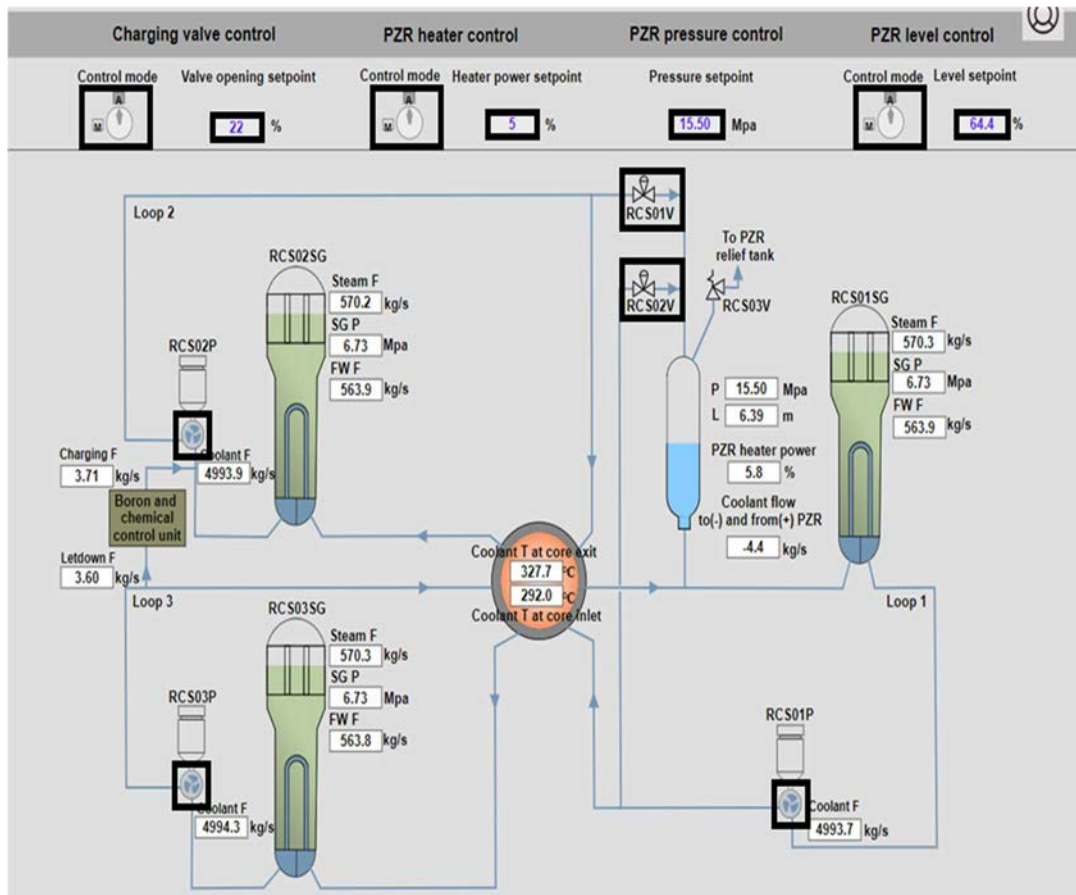


FIG. 37. Reactor coolant system simulator window: pumps, valves and switches enclosed by bold rectangles.

- (7) Plotting: click “Add plot” as highlighted in Fig. 38. Choose up to six parameters to be displayed in the plot (see Fig. 39). Click “CreatePlot”, a new window will open displaying the plot.



FIG. 38. ESAS menu panels: add plot button enclosed by a bold rectangle.

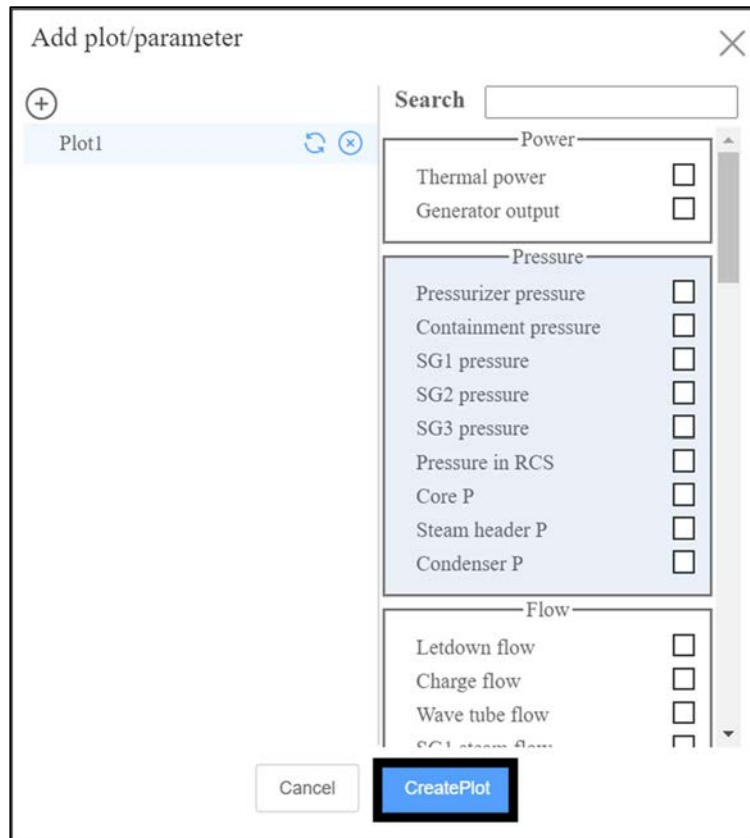


FIG. 39. Plotting window with a list of selectable variables for the graph: CreatePlot button enclosed by a bold rectangle.

- (8) Inserting a malfunction: click “Malfunction” (highlighted in Fig. 40) and choose malfunctions to insert. In severe accident mode only one scenario can be selected at the same time. Click “Insert” to make the failure effective (see Fig. 41).



FIG. 40. ESAS menu panels: malfunctions button enclosed by a bold rectangle.

| Malfunctions | |
|--------------------------|--|
| <input type="checkbox"/> | Reduction in feedwater temperature (loss of feedwater heating) |
| <input type="checkbox"/> | Abnormal increase in feedwater flow |
| <input type="checkbox"/> | Loss of normal feedwater flow (feedwater pumps trip) |
| <input type="checkbox"/> | Loss of condenser vacuum |
| <input type="checkbox"/> | Condenser coolant pumps trip |
| <input type="checkbox"/> | Inadvertent opening of main steam safety valve (SG1) |
| <input type="checkbox"/> | Inadvertent opening of main steam safety valve (SG2) |
| <input type="checkbox"/> | Inadvertent opening of main steam safety valve (SG3) |
| <input type="checkbox"/> | Turbine trip |
| <input type="checkbox"/> | Turbine trip with bypass valve failed closed |
| <input type="checkbox"/> | Spurious turbine run-back |
| <input type="checkbox"/> | 001PO reactor coolant pump tripping |
| <input type="checkbox"/> | 002PO reactor coolant pump tripping |
| <input type="checkbox"/> | 003PO reactor coolant pump tripping |
| <input type="checkbox"/> | Inadvertent SIS valve opening |
| <input type="checkbox"/> | Uncontrolled control rod assembly withdrawal at power |
| <input type="checkbox"/> | Control rod stuck |
| <input type="checkbox"/> | Control rod drop |
| <input type="checkbox"/> | Inadvertent actuation of PRS |
| <input type="checkbox"/> | Earthquake induced equipment or component failures |
| <input type="checkbox"/> | Main steam pipeline break outside containment |
| <input type="checkbox"/> | Steam generator tube rupture(SG1) |
| <input type="checkbox"/> | Steam generator tube rupture(SG2) |
| <input type="checkbox"/> | Steam generator tube rupture(SG3) |
| <input type="checkbox"/> | The loop 1 hot leg rupture |
| <input type="checkbox"/> | The loop 2 hot leg rupture |
| <input type="checkbox"/> | The loop 3hot leg rupture |
| <input type="checkbox"/> | Inadvertent reactor isolation – closure of all main steam isolation valves |
| <input type="checkbox"/> | Inadvertent opening of a pressure relief valve |

| | | | | | |
|---------------|---------|-----|-------|---------------|--------|
| Time Delay(s) | 00 : 00 | Set | Reset | Insert | Clear |
| | | | | GlobalClear | Return |

FIG. 41. Drop-down list of possible reactor system malfunctions: insert button enclosed by a bold rectangle.

- (9) Severe accident mode: when the user selects ‘Severe accident mode’, the severe accident 3D display interface will open additionally to the normal 2D plant interface. Users can choose the screen resolution, the display size and the graphics quality; Fig. 42 shows the window of the 3D reactor representation.

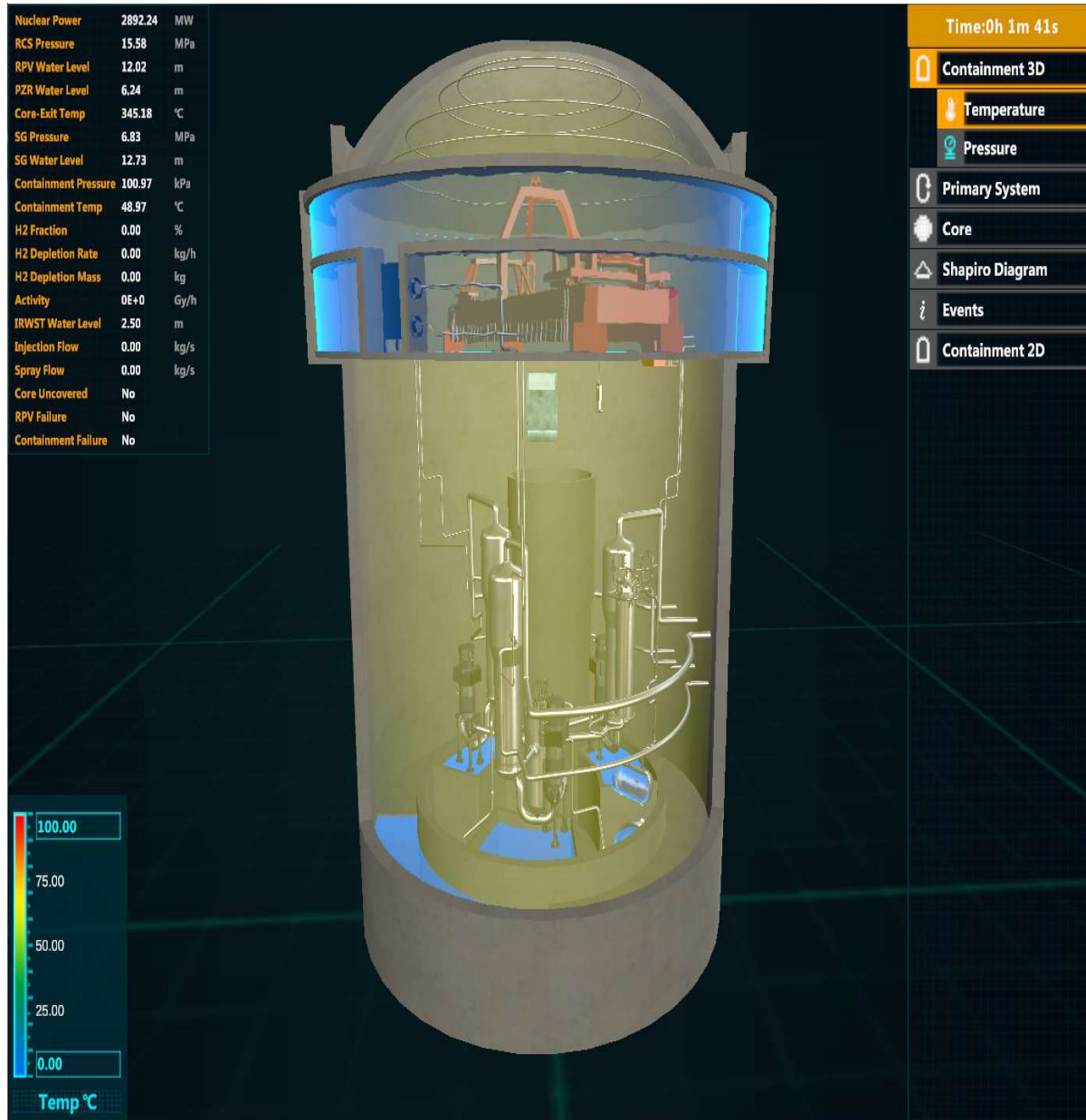


FIG. 42. 3D severe accident window showing the containment.

- (10) The simulation can be started by clicking the “Run” button as can be seen in Fig. 43.

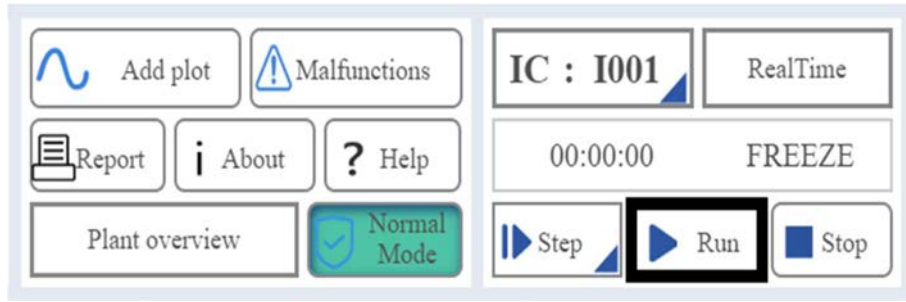


FIG. 43. ESAS menu panels: Run button enclosed by a bold rectangle.

3.1.3. Initialization

By default, the initial condition (abbreviated as IC in the simulator) in normal operation mode is I001 and S001 in severe accident mode, however, the user can load any of the other initial conditions available.

The following are the initial conditions available in the simulator (the abbreviation FP used in the simulator refers to full power):

- (1) S001: 100% FP;
- (2) I001: 100% FP, beginning of core life;
- (3) I002: 100% FP, middle of core life;
- (4) I003: 100% FP, end of core life;
- (5) I004: 50% FP (Xenon balance);
- (6) I005: 10% FP (release interlock of reactor-turbine);
- (7) I006: hot standby state (<2% FP);
- (8) I007: hot shutdown state;
- (9) I008: reach criticality;
- (10) I009: 8% FP (ready to speed up);
- (11) I010: mini load after synchronization;
- (12) I011: ready to interlock reactor-turbine;
- (13) I012: raising load (320 MW);
- (14) I013: raising load to 65% FP;
- (15) I014: raised to 100% FP.

3.1.4. Error resolution

If an error occurs when trying to open the application, as shown in Fig. 44, the user may need to wait for around 30 s and then try to start the simulator again. This is due to background processes which are not automatically killed when closing the software. While these are still running in the background, the application cannot be restarted.

If a pop-up appears and reads “Port 9001: port check failed” or “Port 6397: port check failed”, the user is required to restart the computer in order to release the port. Then restart the software.



FIG. 44. Error message.

3.2. REFERENCE NUCLEAR POWER PLANT DESCRIPTION

The design used in ESAS is a simplified version of a typical advanced PWR. The primary system consists of three loops, each of them including a reactor coolant pump and a steam generator (SG). A pressurizer is connected to one of the hot legs. The reactor has a rated power of approximately 3000 MW(th) and 1100 MW(e). Fig. 45 shows a simplified scheme of the reference NPP.

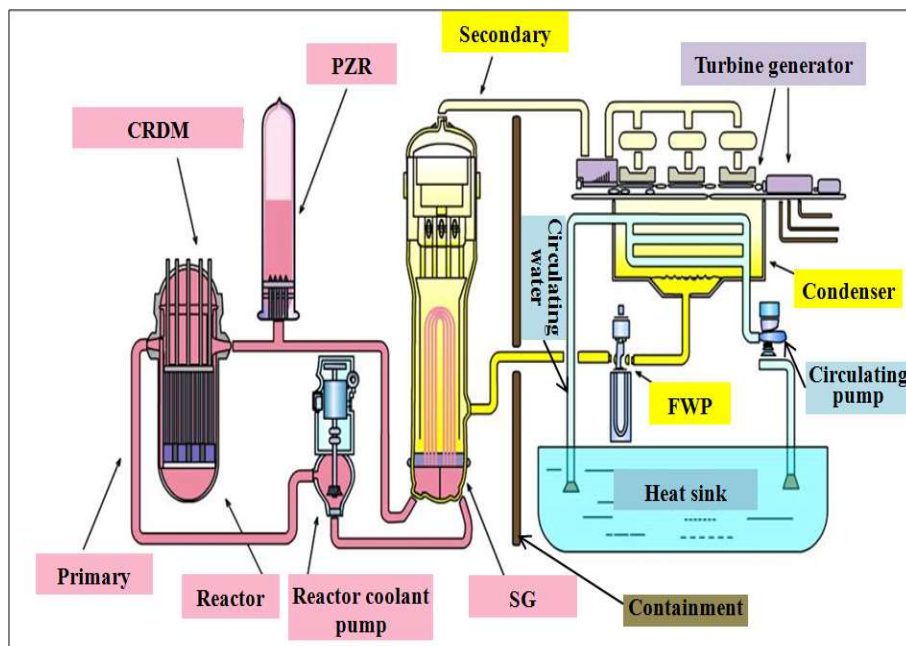


FIG. 45. Scheme of the reference NPP based on an advanced PWR (courtesy of CNPO).

For educational purposes the user can induce a series of normal operation scenarios as well as transient events. The simulator can be an effective tool to help users understand the general operating principles of a PWR type NPP along with some hands-on experience with respect to operator actions in various scenarios.

To understand the behaviours of the reactor in different scenarios, the following systems are incorporated in the simulator:

- Reactor coolant system;

- Core physics system;
- Containment system;
- Active and passive safety systems.

3.2.1. Reactor coolant system

The reactor coolant system (RCS), along with the reactor control and protection system, is designed to realize several main functions:

- Heat transfer from the reactor to the SGs;
- Reactivity control;
- Neutron moderation;
- Pressure control;
- Act as the second barrier during fission product release; the first one being the fuel cladding.

The reactor coolant acts not only as the heat conducting medium but also as the neutron moderator. The PZR acts as a pressure controlling device with the help of electrical heaters and spray valves. In normal operation conditions, it is mainly used to maintain the RCS pressure at a reference setpoint (15.5 MPa). It can also be used to regulate the reactor coolant pressure with respect to different requirements. The PZR also has relief valves to prevent the RCS pressure from exceeding the design value of 17.2 MPa. The reactivity can be changed by regulating the boron concentration in the reactor coolant. All the systems and pipes of the RCS together form a closed pressure boundary and act as a barrier against the release of radioactive materials.

The RCS includes the following components: RPV, reactor core, three primary loops each including a SG and a reactor coolant pump, and a PZR including its internal electric heaters, PZR spray valves, PZR relief valves, PZR relief pipe and tank as well as the surge line between the PZR and the coolant pipe. Instrumentation is used for determining the PZR level, its pressure and temperature, the reactor coolant temperature, and the reactor coolant flowrate which are used for monitoring the system or the operational state of devices and to control the PZR level and pressure. Fig. 46 shows a simplified 3D representation of the RCS of the reference plant.

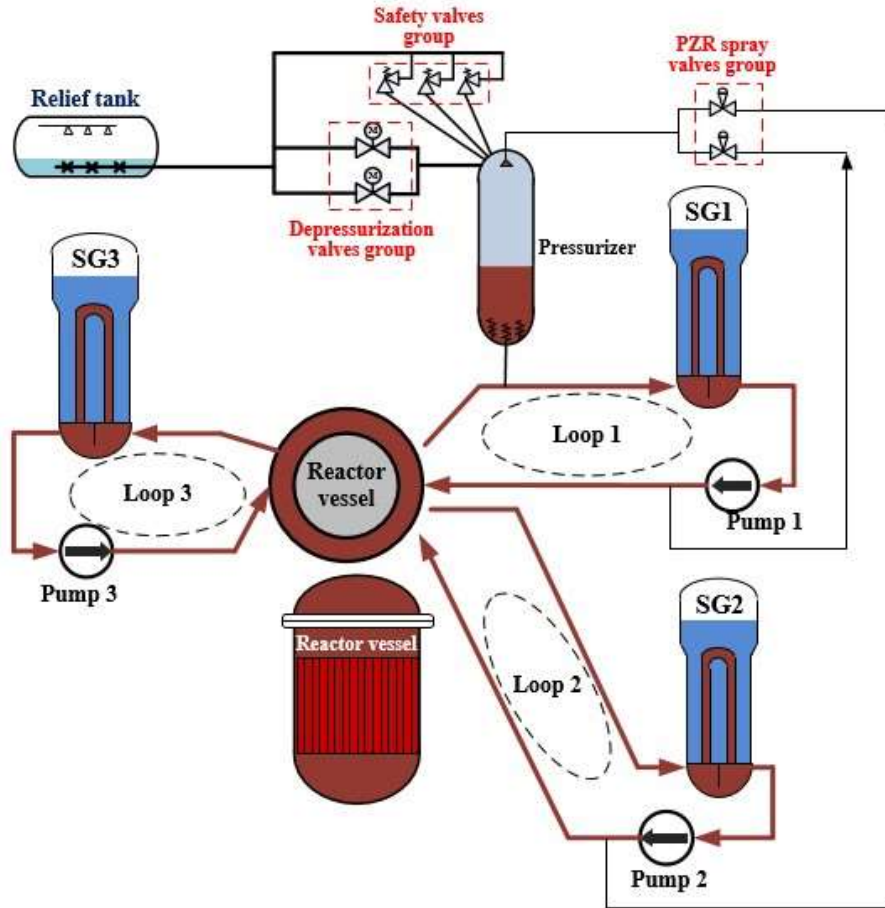


FIG. 46. Simplified representation of the RCS of the reference NPP (courtesy of CNPO).

The thermal energy produced in the RPV core by fission reactions within the fuel pellets (about 5% ^{235}U enrichment) is transferred to the reactor coolant. It is in turn circulated through the reactor core to the SGs by forced circulation induced by the reactor coolant pumps. The heated reactor coolant then undergoes heat exchange in the SGs by transferring the heat to the secondary feedwater.

The parameters of the RCS under normal operating conditions are shown in Table 5.

TABLE 5. OPERATING PARAMETERS OF THE REACTOR COOLANT SYSTEM UNDER NORMAL CONDITIONS

| Parameter | Rated value (100% FP) |
|--|--------------------------|
| Nominal pressure | 15.5 MPa |
| Design flow rate (cold leg) | 6608 kg/s (in each loop) |
| Inlet temperature of the reactor core | 292.2°C |
| Outlet temperature of the reactor core | 327.8°C |
| Primary circuit average temperature | 310.0°C (in each loop) |
| Steam pressure at SG outlet | 6.7 MPa |
| Steam flow at SG outlet | 570 kg/s (at each SG) |
| Main feedwater temperature | 224.5°C |

3.2.2. Core system

The main function of this system is to provide heat to the RCS under normal operation conditions in order to produce electric power. The reactor power level can be influenced by different factors, including:

- Control rod insertion;
- Change in boron concentration;
- Burn-up state;
- Xenon concentration.

The reactor core consists of 177 fuel assemblies of a standard 17×17 grid size. A typical core layout is shown in Fig. 47. The numbers within the squares represent the peaking factors; the local power density divided by average power density.

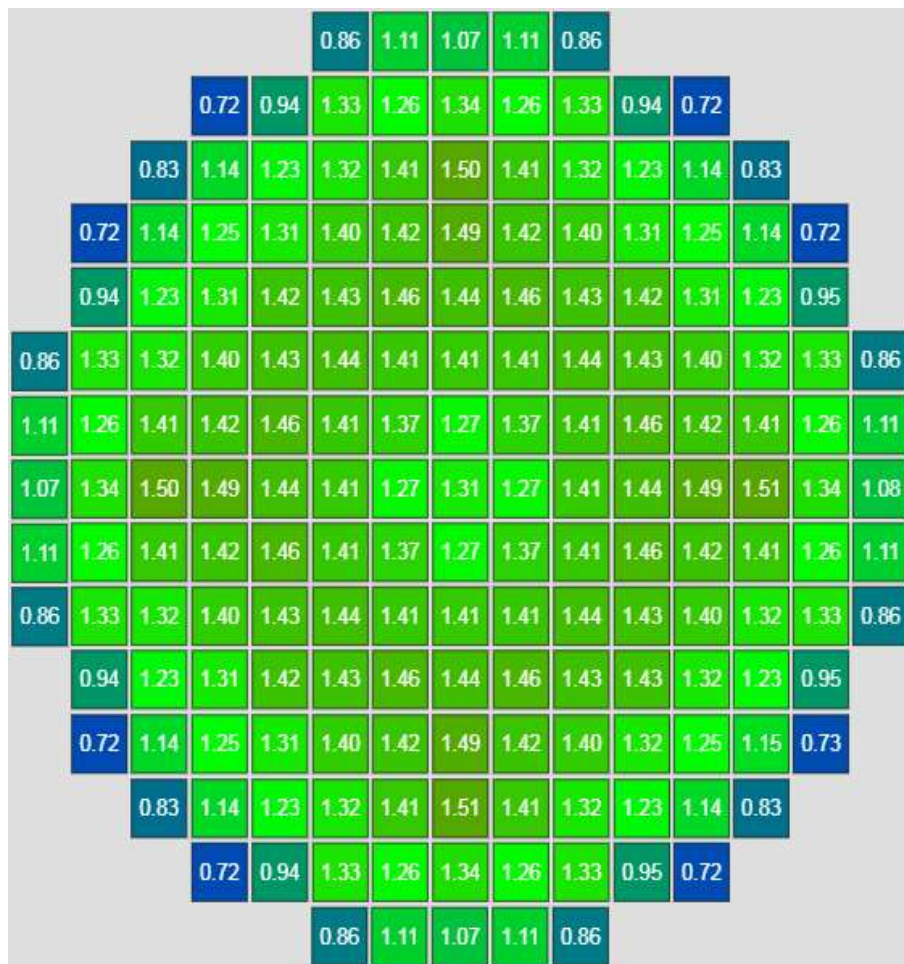


FIG. 47. Reactor core layout with peaking factors for each assembly (courtesy of CNPO).

Reactivity control is achieved with the help of control rods and by adjusting the boron concentration in the primary coolant. The control rods are organized by design function into three groups: the shutdown rod group (S bank), the temperature rod group (R bank) and the power rod group (G bank). The shutdown rod group is designed to ensure a safe and stable

state after shutdown of the reactor in the case of an emergency by inserting enough negative reactivity including a safety margin. The temperature rod group is used mainly to control the average temperature of the primary system and to keep it at the value required according to the load demand. The power rod group is used to rapidly regulate the prescribed reactor power level to follow changes in secondary load. However, all the rod groups fall into the core after a reactor trip signal is issued to provide a sufficient shutdown margin for any operating condition. ESAS includes a shutdown bank, a temperature bank and four power banks. The four groups of power rod banks are moved together in overlapping mode.

The principle of the overlapping movement of the different power banks is shown in Fig. 48. As shown, the N2 group is retracted first in the withdrawal process. When the N2 group reaches 140 steps (point A in Fig. 48) from the bottom 5 step, the simultaneous withdrawal of the N1 group is initiated. The groups G2 and G1 are withdrawn with respect to the same principle. The overlapping step is counted from 0 to 615 steps, which is the sum of moving steps required for all four power bank groups to reach the top (225 step). The overlapping steps are not counted.

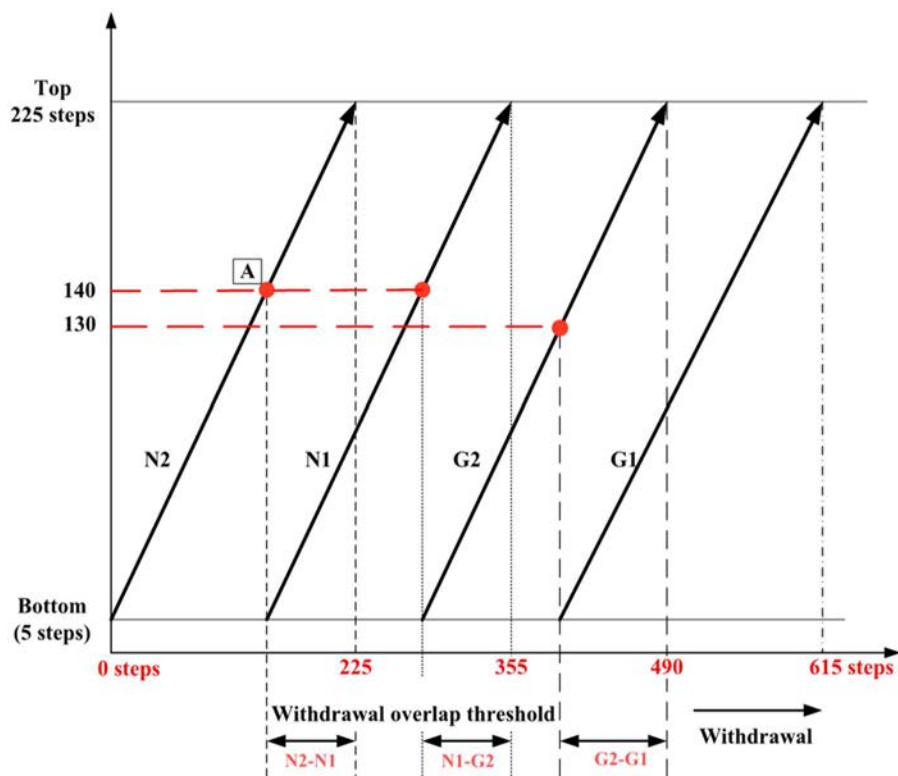


FIG. 48. Power bank overlapping principle during the withdrawal process (courtesy of CNPO).

During the insertion, the four groups of power banks are moved in overlapping mode as shown in Fig. 49. This process starts with the group G1. When the G1 group reaches 100 steps (point A in Fig. 49) from the top (225 step), insertion of G2 group is coincidentally started. N1 and N2 are inserted analogously. The overlapping steps are counted from 615 to 0 until all power

rods reach 5 steps. Similar to the withdrawal process, the steps in the overlapping areas are not counted.

This system allows reactor power manoeuvring in two normal operation modes: reactor leading mode and turbine leading mode. The two transient reactor power manoeuvring modes are stepback and setback.

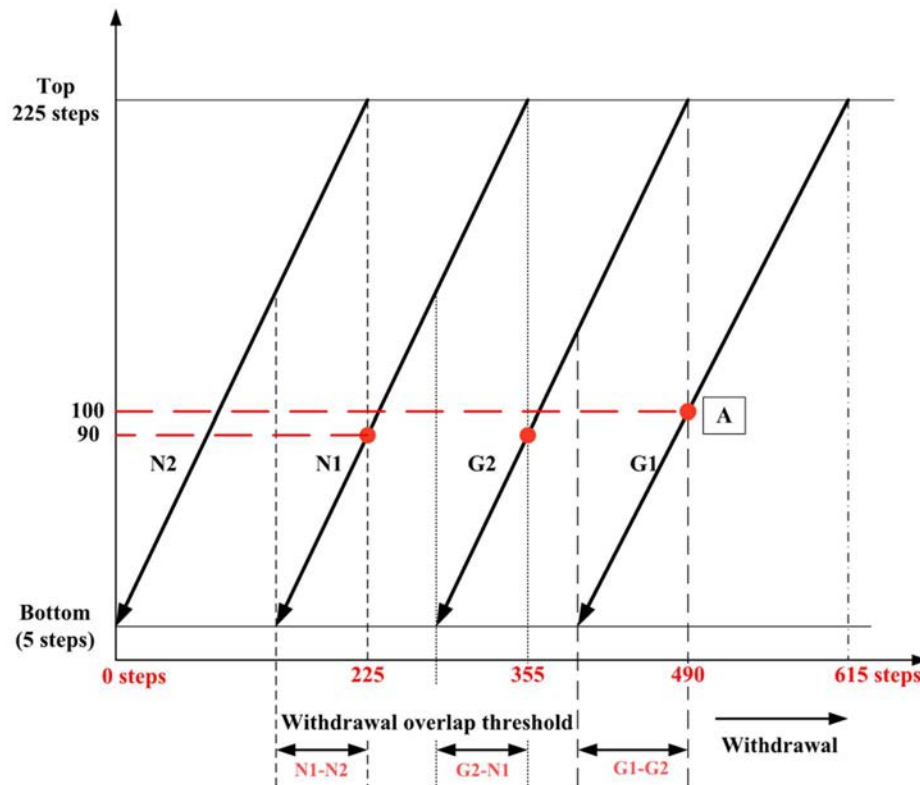


FIG. 49. Power bank overlapping principle during the insertion process (courtesy of CNPO).

3.2.3. Secondary circuit system

The secondary circuit system is an integrated system comprised of the main steam line, turbine generator, condenser, turbine bypass and feedwater systems. A simplified sketch of the secondary system is shown in Fig. 50.

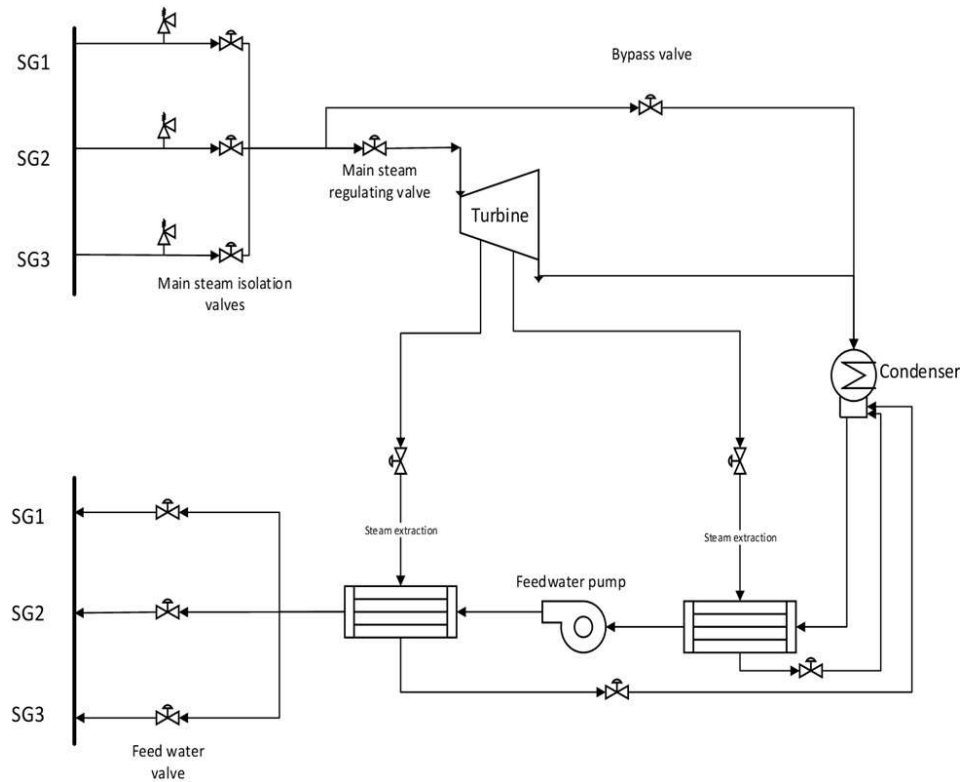


FIG. 50. Scheme of the secondary circuit system (courtesy of CNPO).

The steam system is used to transfer saturated steam from the SG to the steam turbine and its auxiliary equipment, as well as to the condenser via the steam turbine bypass exhaust system. As it is shown in Fig. 50, it includes three main steam lines from the SG to the main steam header, the main steam safety release valves, the main steam isolation valves, the steam lines and the steam control valves from the main steam header to the inlet of the steam turbine, the steam turbine bypass exhaust system from the main steam header to the condenser.

The function of the isolation valves is to prevent the flow of steam to the turbine. On each steam line, there is a steam safety valve (8.5 MPa), which releases steam to the atmosphere if the steam pressure exceeds the design value. The steam control valves are used to regulate the steam flow to the turbine in normal operation and during turbine speed up (from 5 rpm to synchronization speed, 1500 rpm).

The turbine bypass system allows steam to pass directly from the SG to the condenser via a control valve. It is necessary as the reactor power cannot adapt to rapid changes in the turbine generator load. Thus, when the turbine load drops significantly, the system discharges steam directly into the condenser, thereby providing an artificial load for the reactor and reducing the change in amplitude of both the temperature and the pressure in the steam system. This allows for the cooling of the reactor to be maintained even in the event of a turbine trip (does not necessarily coincide with a reactor trip), load rejection or during the startup and shutdown processes. The condenser has a capacity of 100%.

There are steam flow rate and steam pressure instruments for turbine load control, SG level control and bypass control. In full power conditions, the steam pressure and temperature at the outlet of the SG are 6.7 MPa and 283°C, respectively. The flow rate in the steam line at the outlet of a single SG is 570 kg/s, and the pressure of the main steam header is 6.4 MPa.

The turbine drives the alternator with the mechanical power required to satisfy the load demands of the grid, maintaining a frequency of 50 Hz and a speed of 1500 r/min. Its maximum capacity amounts to 1100 MW(e).

In normal operation conditions, the condenser system receives and cools the spent steam coming from the turbine and other steam users, while providing back pressure for the turbine. The spent steam is cooled by circulating water from an external water source (ultimate heat sink) and condensates. This process makes sure the condenser vacuum is maintained. When the turbine bypass system is in service, the condenser receives bypass steam after being cooled and depressurized by spray water. In full power conditions, the condenser pressure is 4.3 kPa and the condenser temperature amounts to 30°C.

The feedwater system provides a flow of preheated water to the SGs. Feedwater is heated and evaporated within the SGs, and the subsequent saturated steam exits via the SG outlet. A simplified simulation scheme is implemented in ESAS.

The condensate from the condenser is extracted by condensate pumps (out of the scope of ESAS) and preheated in seven stages by heat exchangers (simplified simulation within ESAS) which preheat the condensate with steam extracted at different points from the turbine to increase the thermal efficiency of the secondary circuit. After preheating, the water is pumped into the SGs by feedwater pumps, which have a large delivery head. Before being injected into the SGs, the feedwater flow rate is regulated by the control valves so that the SG level stays at the required value with respect to the secondary load.

At full power, the feedwater header pressure is 7.3 MPa and the temperature is 224.5°C. The feedwater inlet flow of a single SG is set to 570 kg/s.

3.2.4. Containment system

The containment is an enclosure surrounding the RPV, components of the primary system, components of the cooling system and parts of the passive and active safety systems.

At the bottom of the containment is the containment sump which, in normal operation conditions, is filled with borated water and is also used to collect any water leaking from the primary circuit or a break in the event of an accident.

3.2.4.1. Passive and active systems

The active and passive safety systems maintain the cooling of the core and the integrity of the containment as well as limit the progression and mitigate the consequences of a potential

accident. The main systems include the safety injection system (SIS), the containment spray system (CSS), the passive residual heat removal system on the secondary side (PRS), the passive containment heat removal system (PCS) and the cavity injection and cooling system (CIS). Fig. 51 presents a simplified diagram of the safety systems discussed.

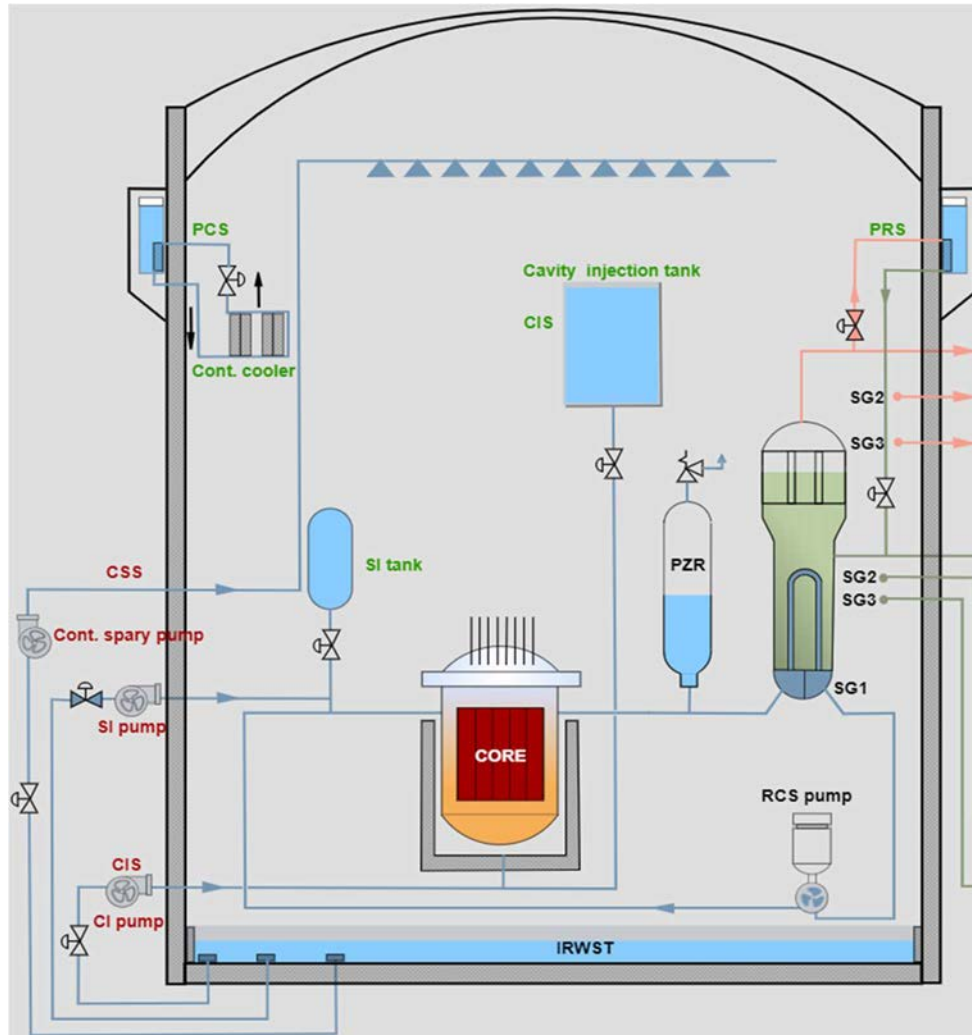


FIG. 51. Safety systems used in ESAS.

3.2.4.2. Safety injection system

The SIS is designed to mitigate some potential DBAs. It is mainly used to inject borated water into the primary system, in particular the RPV, in the case of a break in the primary system, the main steam line or in similar scenarios. This is done to ensure that the reactor core is always covered and to prevent the reactor core from melting.

The SIS includes active and passive components. The active part consists of injection pumps. With them, borated water can be extracted from the internal refuelling water storage tank (IRWST) which is a containment sump with 2400 m³ and injected into the hot and cold legs of each loop in the primary circuit via connecting pipes. The injection pressure is almost 10 MPa. The passive part includes three accumulators (65 m³) filled with borated water and

pressurized by nitrogen at 4.3 MPa. In the case of a LOCA, the SIS is actuated. The active part starts injecting when the primary pressure drops below 10 MPa. The injection from the passive part is automatically induced when the pressure falls below 4.3 MPa.

3.2.4.3. Containment spray system

The CSS is designed to protect the containment. It incorporates pumps, heat exchangers and spray ring nozzles. The spray pumps extract borated water from the IRWST (i.e. containment sump). In the event of an accident (e.g., a LOCA), the pressure and the temperature within the containment may increase to values which are deemed unsafe. If the pressure reaches 240 kPa, the CSS is actuated to help decrease the pressure as well as the temperature inside the containment to an acceptable level in order to protect the integrity of the containment.

3.2.4.4. Passive containment heat removal system

The PCS is designed to maintain the pressure and temperature of the containment at an acceptable level during the severe accident conditions where the CSS failed. This system consists of heat exchangers distributed at the top of the containment and pipes connecting the cooling water storage tank outside the containment to these heat exchangers. The cooling water flows through the heat exchangers due to natural circulation, thus removing the heat from the containment.

3.2.4.5. Passive residual heat removal system on the secondary side

The PRS is designed to supply cooling water to the SGs on the secondary side in the case of loss of all feedwater supply. This system consists of heat exchangers submerged in a water storage tank located outside the containment. Pipes connect the steam outlet of the SG with these heat exchangers and reconnect the condensed steam to the feedwater inlet of the SG. The PRS thus assures the continuous cooling of the primary circuit.

3.2.4.6. Cavity injection and cooling system

Severe accidents requiring the CIS often experience a serious threat to the integrity of the RPV. The CIS is designed to mitigate severe accidents that would lead to the failure of the RPV by cooling the vessel from the outside.

This system consists of active and passive components. The active system includes a motor driven pump which is connected to the passive system's IRWST (volume of 2200 m³) by connecting pipes. Once the CIS is actuated, the pump extracts borated cooling water from the IRWST (i.e. containment sump) and injects the water into the annular space between the insulation and the outer surface of the RPV. The cooling water from the passive storage tank is also injected by force of gravity. This helps remove the heat from the RPV and can prevent overheating and failure.

3.2.4.7. Control and protection systems

Control and protection systems of an NPP are required to mitigate the consequences of transients and accidents that may occur during operation. Based on the operational scenarios in normal ESAS operation mode, the following control functions are required and implemented:

- Reactor power control;
- Primary average temperature control;
- PZR pressure control;
- PZR water level control;
- Turbine generator load control;
- Turbine bypass control;
- Feedwater flow control.

3.2.4.8. Reactor power control

The reactor power control is designed to execute the automatic power rod (G bank) movements according to the demand. The demand is determined by the turbine load in turbine leading mode (Fig. 52) or by the manually defined setpoint in reactor leading mode (Fig. 53).

In turbine leading mode, the control logic for the G bank is as follows: the control system generates an overlapping step value as setpoint for the G bank according to the secondary load.

The actual value of the overlapping step of the G bank is compared to the setpoint. The deviation indicates the direction and the speed of the G bank movement which is subsequently initiated.

In reactor leading mode, the control logic for the G bank is as follows: the control system compares the actual reactor power value to the manually adjusted power level setpoint and calculates the necessary direction and speed of the movement for G bank.

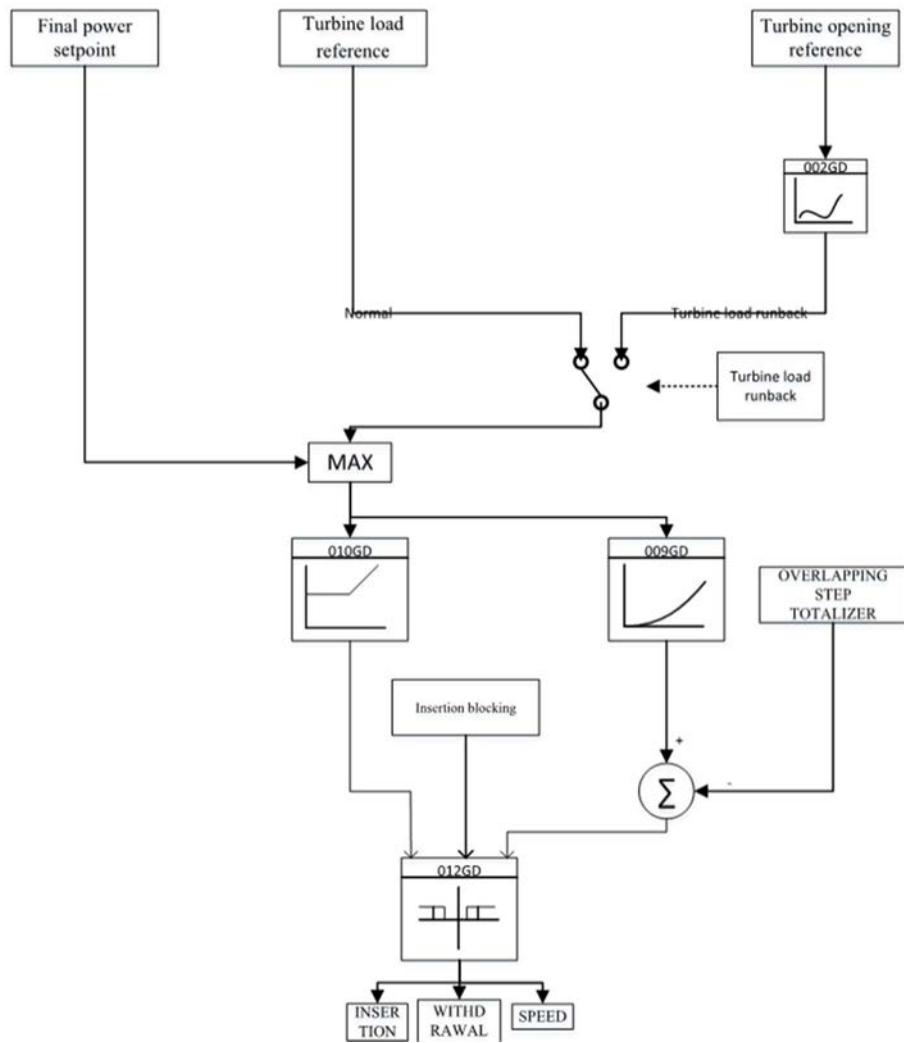


FIG. 52. Scheme of the reactor power control principal in turbine leading mode (courtesy of CNPO).

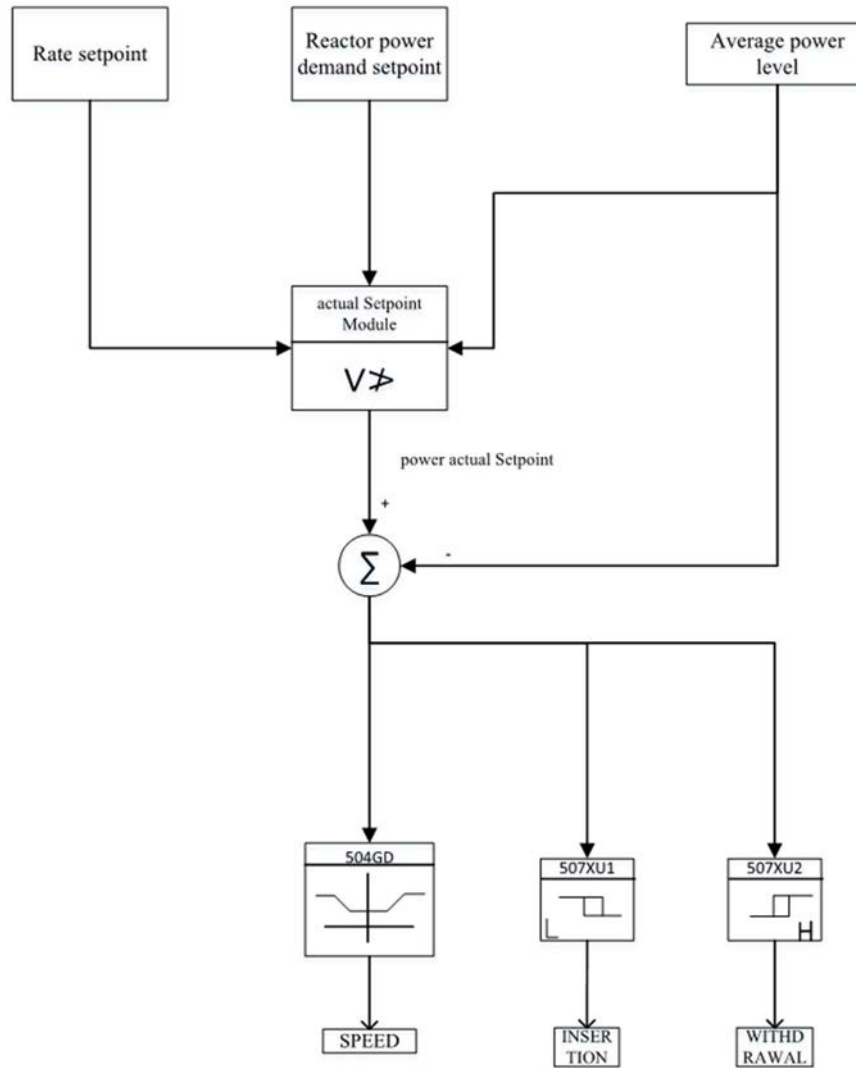


FIG. 53. Scheme of the reactor power control principal in reactor leading mode (courtesy of CNPO).

3.2.4.9. Primary average temperature control

The primary average temperature control is designed to adjust the automatic temperature rod (R bank) movement in accordance with the deviation of the current primary average temperature value from the reference value. This reference value is calculated based on the secondary steam load. The set value for the reference temperature T_{ref} is 291.4°C at zero power and 310°C at full power. The power level variations with T_{ref} can be viewed in Fig. 54. The R bank will move automatically according to the temperature difference ΔT which is defined as $T_{ref} - T_{ave}$. When $\Delta T > 0.83^\circ\text{C}$ the R bank will withdraw, if $\Delta T < -0.83^\circ\text{C}$ the R bank rods will insert. If the R bank is outside of the manoeuvring band (180–204 steps) during the routine power increase of the unit, users can manually adjust the boron concentration (indicated as BC in the simulator) to keep the R bank within manoeuvring band.

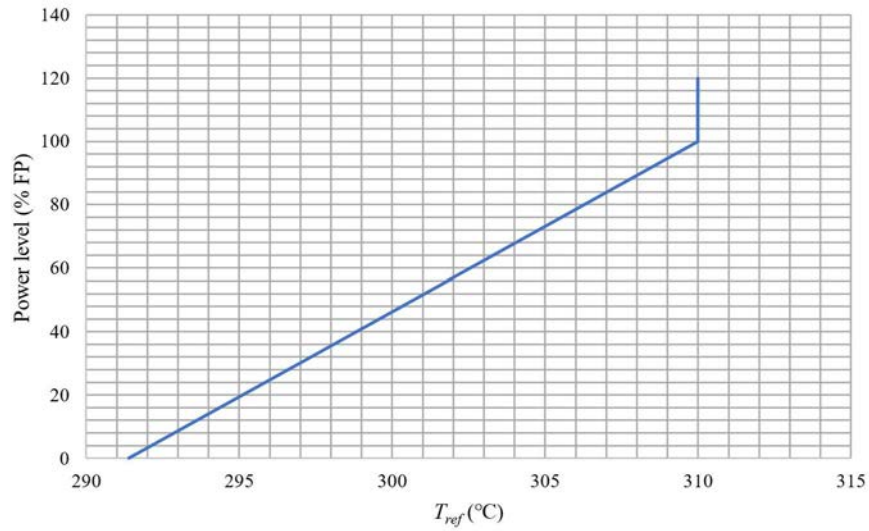


FIG. 54. Variation of power level with the change in reference temperature.

The control logic for the R bank is as follows: the control system generates an average temperature reference as a setpoint (T_{ref}) according to the secondary load, it then compares the setpoint with the value of the average temperature. The temperature difference is used to generate the direction and speed information for the R bank. The primary average temperature control logic is shown in Fig. 55.

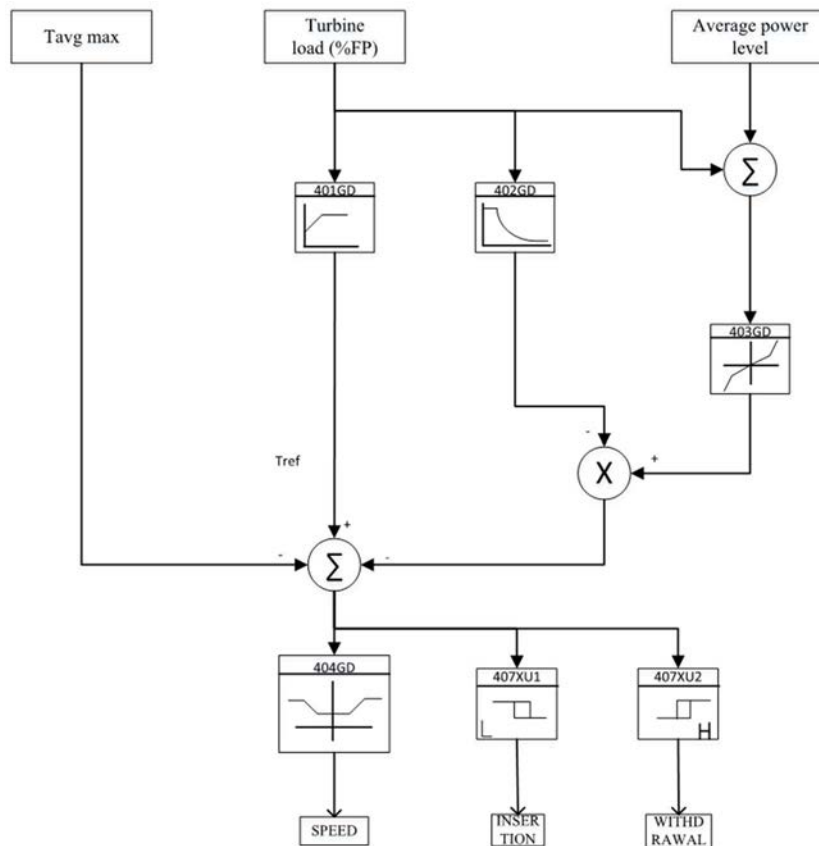


FIG. 55. Primary average temperature control logic diagram (courtesy of CNPO).

The xenon reactivity override function is implemented to accelerate the xenon depletion and save training time for users. Two operation buttons are located on the graphical user interface (GUI) tab “Control rod and reactivity” and are labelled as “Equilibrium Xe” and “Calculate Xe”.

“Calculate Xe” is used to supply a choice for users to determine whether to freeze the Xenon concentration calculation. If the button pops up, it will stop calculating the xenon concentration which will be frozen at current value. This function is mainly used while manoeuvring the reactor power to avoid the influence of xenon on the reactivity. Thus, it reduces the compensation operations by adjusting the boron concentration frequently.

“Equilibrium Xe” is used to bring the xenon concentration to a balanced state quickly only when the reactor is critical (e.g. after manoeuvring the reactor power). The boron concentration will be adjusted at the same time to maintain the critical state of the reactor. This function can potentially reduce the simulation time significantly as the evolution of the xenon concentration process usually takes 10–20 hours to reach a balanced state after manoeuvring the reactor power.

3.2.4.10. PZR level control

The PZR level control is designed to maintain the PZR level at a programmed value based on T_{avg} . This system is necessary to compensate for the volume change of the reactor coolant. The coolant level in the PZR is controlled by charge and letdown flows from the chemical and volume control systems (simplified simulation).

Fig. 56 shows the variation of the PZR level as a function of T_{avg} . The PZR water level control logic diagram is shown in Fig. 57.

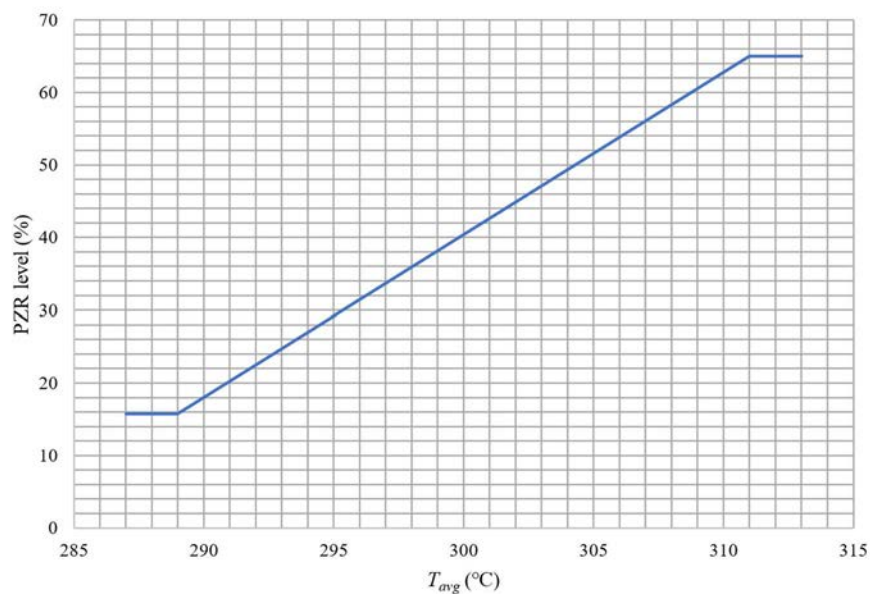


FIG. 56. Variation of PZR level with the average temperature.

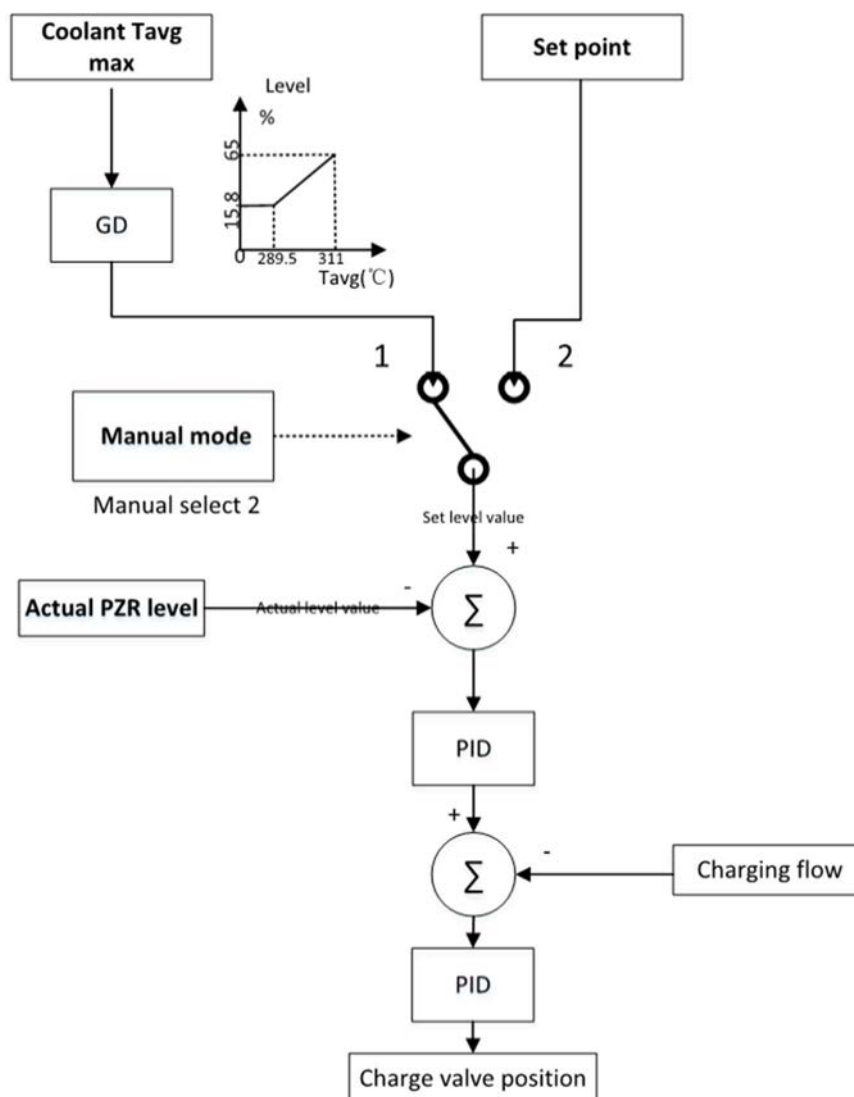


FIG. 57. PZR water level control logic diagram (courtesy of CNPO).

The PZR level control is accomplished with the help of the charging flow control valve. The control logic for the charging valve is as follows: the control system generates a PZR level reference as a setpoint based on the current average temperature of the primary circuit, then the setpoint is compared to the measurement of PZR level. The observed difference is converted to a compensatory flow which is added to the system and the charging flow measurement is changed to the new charging flow reference (flow setpoint). The control system continues to compare the flow setpoint with the actual charging flow value and any deviation is compensated by the change in the opening of the charging flow control valve.

3.2.4.11. PZR pressure control

The PZR pressure control is designed to maintain a constant reactor coolant pressure of 15.5 MPa during operation. This is achieved by using electrical heaters installed at the bottom of the PZR and spray valves installed at the top. Fig. 58 shows the power level with respect to the PZR pressure variation.

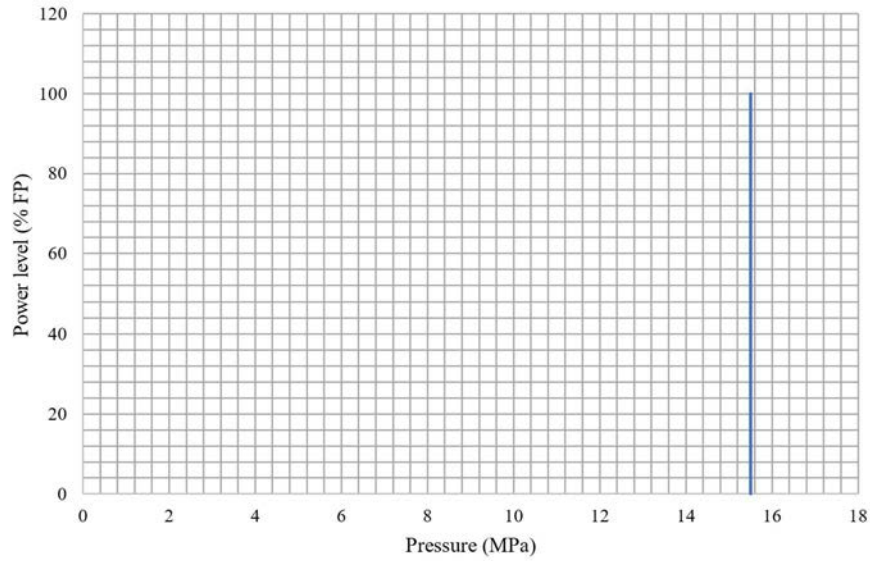


FIG. 58. PZR pressure variation with power level.

Fig. 59 shows the PZR pressure control logic diagram. The PZR pressure control is implemented by the spray valves and the electric heaters. The control logic is as follows: the control system compares the pressure setpoint with the measured pressure, the deviation is then converted to the required opening of the spray valves.

Pressures of 0.17 MPa and 0.52 MPa are linearly mapped to openings of 0% and 100%, respectively. Similarly, the deviation is also used to generate control order for heaters in the case of a required pressure increase.

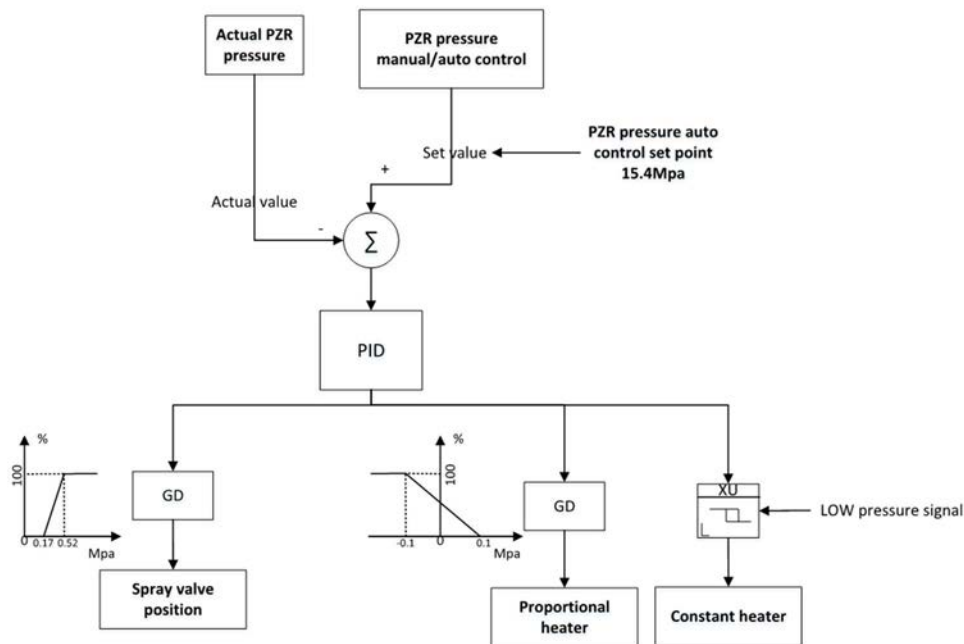


FIG. 59. PZR pressure control logic diagram (courtesy of CNPO).

3.2.4.12. Turbine load control

The turbine load control is designed to maintain the turbine generator output at the setpoint by automatically adjusting the opening of the turbine inlet valves. Fig. 60 shows the turbine load control logic diagram that is realized by turbine inlet valves. The control logic is as follows: in turbine leading mode, the control system compares the load demand which is set manually with the actual load measurement. In reactor leading mode, the control system compares the reactor power level with the turbine load level. The difference is then used to calculate the required opening of the turbine inlet valves.

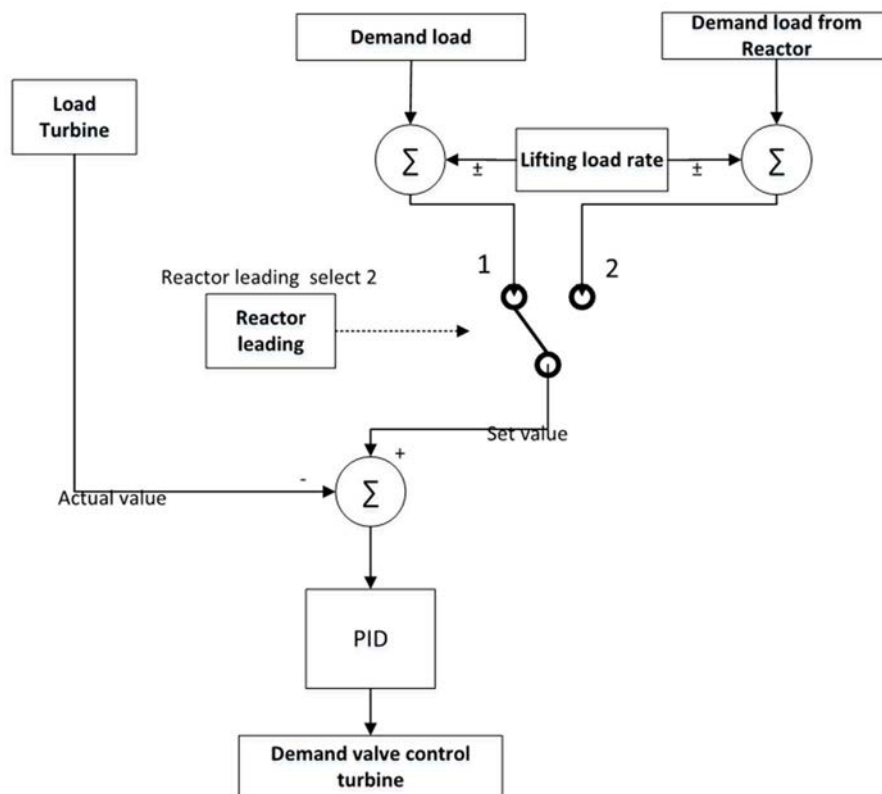


FIG. 60. Turbine control logic diagram (courtesy of CNPO).

3.2.4.13. Turbine bypass control

The turbine bypass control is designed to maintain either the average temperature of the reactor coolant or the steam pressure of the main steam, depending on the chosen operation mode. The turbine bypass system is used to allow for reactor cooling to be maintained in the event of a turbine trip, load rejection and during a startup or programmed shutdown procedure. This is achieved by controlling either the temperature excess in RCS or the pressure excess in main steam system, depending on the turbine bypass mode chosen. The turbine bypass system has a capacity of 100%.

The turbine bypass control system has two operating modes: average temperature control mode (T mode) and pressure control mode (P mode). In T mode, the bypass valve is controlled

with respect to the difference between T_{ref} and T_{avg} . If T_{ref} is higher than T_{avg} by a certain threshold, the bypass valve will start to open, otherwise it will remain closed. In P mode, the bypass valve is controlled with respect to the deviation of the steam header pressure value to the pressure setpoint (the default value is set to 7.5 MPa). When the steam header pressure is higher than the setpoint the bypass valve will start to open, otherwise it will remain closed. Fig. 61 shows the turbine bypass control logic diagram.

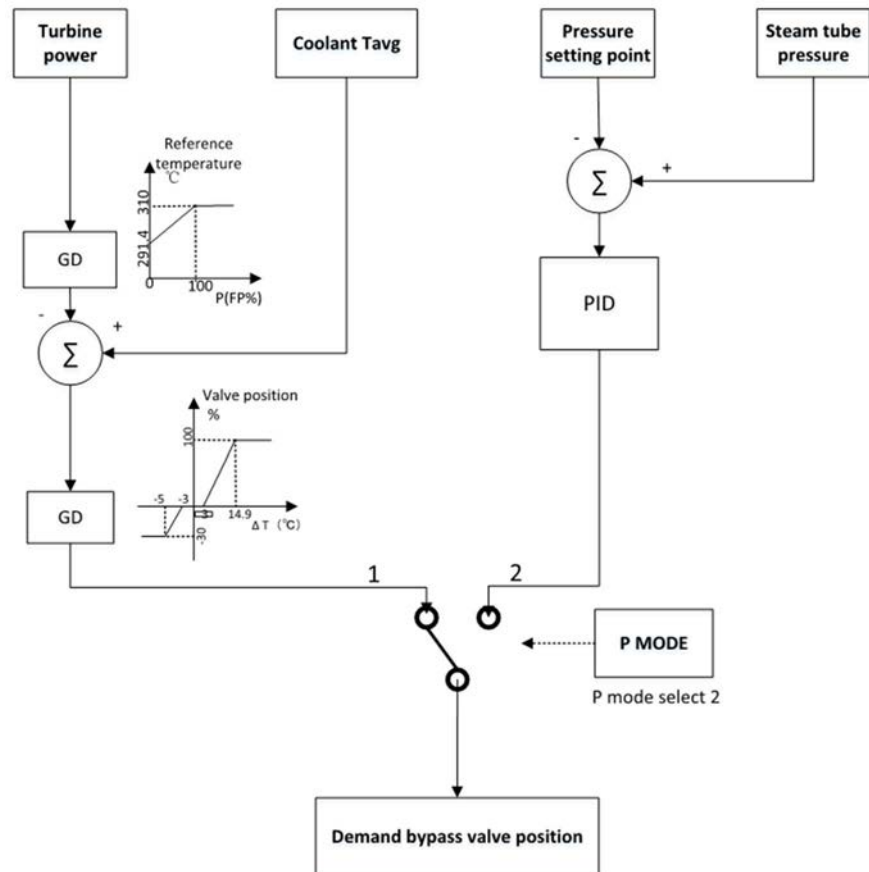


FIG. 61. Turbine bypass control logic diagram (courtesy of CNPO).

3.2.4.14. Feedwater flow control

The feedwater flow control is designed to adjust the feedwater flowrate to the SG by adjusting the valve position of the feedwater regulating valves. This enables the control of the water level of the SG in secondary load change conditions.

The SG level reference value is calculated with respect to the secondary load level. Fig. 62 shows the SG reference level variation as a function of the secondary load level. The SG feedwater flow control logic diagram is shown in Fig. 63.

The feedwater flow is regulated by the feedwater flow adjustment valves. The control logic is as follows: the control system generates a SG level setpoint according to the secondary load

level, this is then compared to the SG level measurement. The control system also compares the total steam flow and the total feedwater flow. The difference in both the level and the flow are then used to determine the position of the feedwater flow adjustment valves.

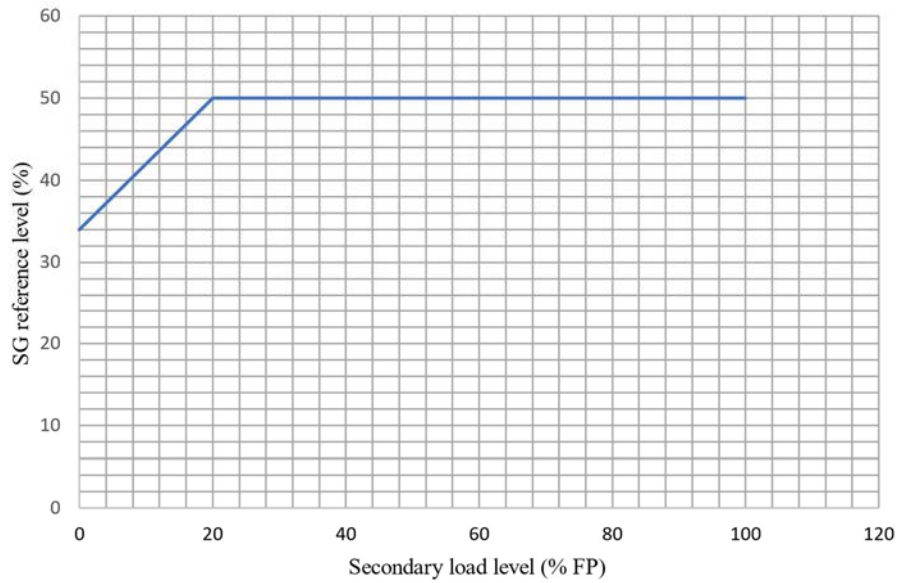


FIG. 62. SG reference level variation with secondary load level.

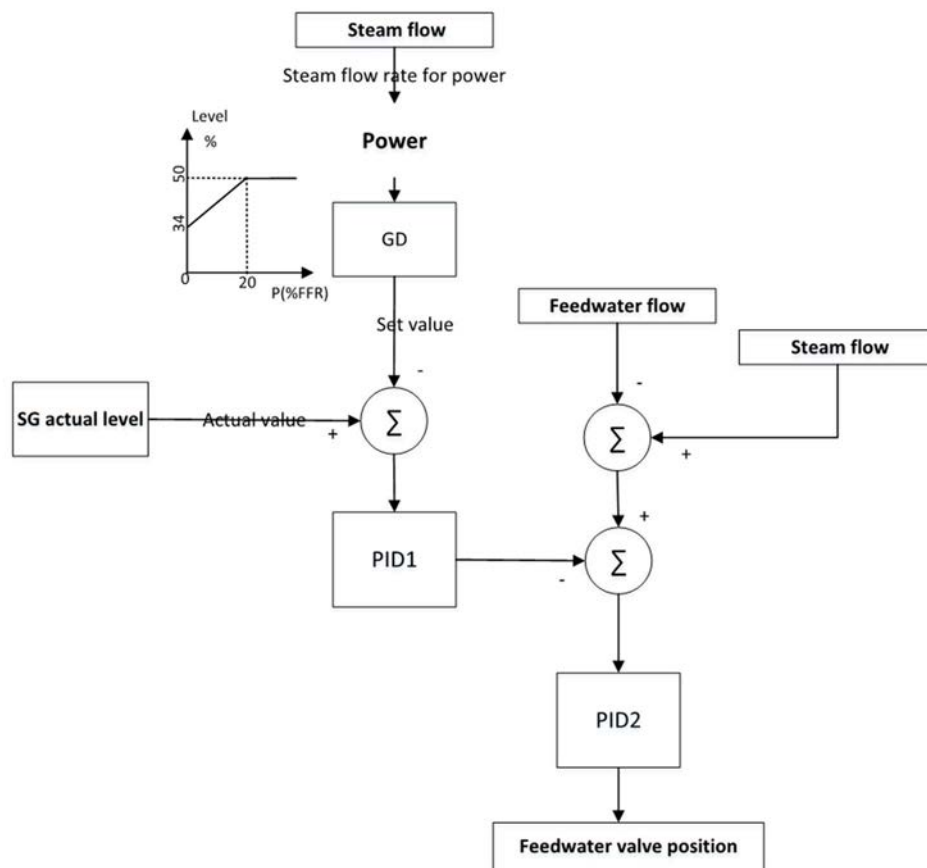


FIG. 63. SG feedwater flow control logic diagram (courtesy of CNPO).

3.2.4.15. Protection systems control

The protection systems are used to actuate the reactor and the turbine trip or other safety systems in emergency or accident conditions. These measures are implemented in order to protect the integrity of the three main safety barriers, namely the fuel cladding, the RCS and the containment.

The protection signals are:

- Reactor trip signal;
- Reactor setback, reactor stepback signal;
- Safety injection signal;
- Containment spray signal;
- PCS, PRS and CIS startup signals.

3.2.5. Reactor trip signal

The reactor trip signal initiates the rapid insertion of all the control rods into the reactor core by force of gravity. This simulator uses simplified trip signals tailored to its requirement.

Table 6 shows the reactor trip signals and their thresholds.

TABLE 6. REACTOR TRIP SIGNAL CONFIGURATION

| No. | Signal | Threshold |
|-----|--|--|
| 1 | Low pressurizer pressure | < 13 MPa |
| 2 | High pressurizer pressure | > 16.45 MPa |
| 3 | High pressurizer water level | > 2.43 m |
| 4 | Low water level of SG | < -1.26 m |
| 5 | High water level of SG | > 0.9 m |
| 6 | Shutdown at a high setpoint of power | > 109% |
| 7 | Main pump trips | Main pump trips |
| 8 | Low circulation flow of coolant | < 88.8% FP |
| 9 | ATWT (Anticipated Transients Without Trip) | Nuclear power level > 30% full power while main feedwater flow <6% |
| 10 | Earthquake | True |
| 11 | Safety injection | True |
| 12 | Manual | True |
| 13 | High reactor power change rate | > $\pm 5\%$ full power/2 s |

3.2.6. Reactor setback and stepback

The setback function is designed to reduce the reactor power to 10% of full power at a rate of 10% FP/min. This is initiated by the automatic power control system after the setback signal is triggered manually. The setback function only works in Reactor leading mode.

The stepback function is designed to reduce the reactor power to 50% of full power by rapidly inserting a part of the rod groups after the stepback signal is manually activated.

In both setback or stepback conditions, users may need to intervene in order to maintain the R bank rod within the specified range (setpoint –12, setpoint +12) by adjusting the boron concentration. When the R bank rod is higher than the setpoint, the boron concentration needs to be decreased, otherwise, when the R bank is lower than the setpoint, the boron concentration needs to be increased. This is due to the destabilisation effects the setback and stepback conditions have on the reactor core which is reflected in the movements of the R bank rod.

3.2.7. Safety injection

The safety injection signal is designed to instruct the SIS to inject borated water into the RCS. The safety injection signals implemented in this simulator are listed in Table 7 and are similar to the ones used in the reference NPP.

TABLE 7. SAFETY INJECTION SIGNALS CONFIGURATION

| No. | Signal | Threshold |
|-----|--|--|
| 1 | Low pressurizer pressure | < 11.83 MPa |
| 2 | High containment pressure | > 130 kPa |
| 3 | High steam pipe flow & low steam pipe pressure | > 0 kg/s (the difference between the flow corresponding to the steam turbine load and the flowmeter) < 3.45 MPa |
| 4 | High differential pressure of steam pipe | > 0.7 MPa |
| 5 | Manual | True |

3.2.8. Containment spray

The containment spray function is designed to protect the integrity of the containment. The containment spray can be actuated by two signals, either when the containment pressure reaches a value higher than 240 kPa or when the system is activated manually. The containment spray signals implemented in ESAS are the same as in reference NPP.

3.2.9. Startups heat removal systems

There are three passive safety systems taken from the reference NPP and implemented in this simulator: the PCS, the PRS and the CIS.

The PCS, or passive containment heat removal system, is designed for long term heat removal from the containment in beyond DBA scenarios. Such scenarios can include SBOs or the failure of the CSS. This system can be actuated manually or by an automated signal when the containment temperature exceeds 115°C.

The PRS, or passive residual heat removal system, is designed to remove both the decay heat and the sensible heat from the reactor and the primary circuit. The system can provide cooling and thus ensure a stable plant state for 72 hours in the case of an SBO and/or a loss of both normal and auxiliary feed water. This system can be activated either manually or by the

relevant value exceeding its predetermined threshold. Fig. 64 shows the PRS automatic startup logic.

The CIS, or cavity injection and cooling system, is designed to externally reduce the temperature of the RPV and prevent it from being damaged by molten corium during a severe accident. The CIS can be activated manually or by the automated signal which occurs when the core exit temperature exceeds 650°C. The CIS consists of an active and a passive part which activate simultaneously as soon as the startup signal is triggered.

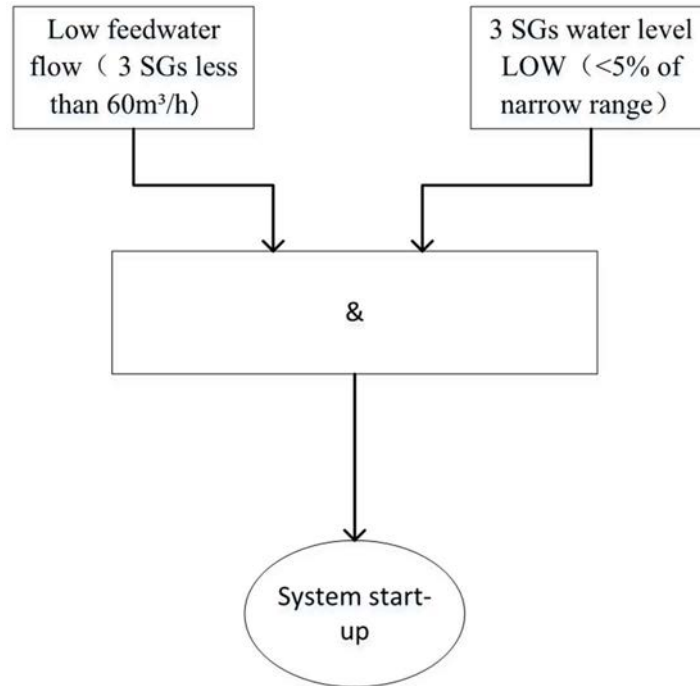


FIG. 64. PRS automatic startup logic (courtesy of CNPO).

3.3. MAIN FEATURES OF THE SIMULATOR

This section details main features of the simulator and provides the screen shots per described modes of operation.

3.3.1. Simulator operation

3.3.1.1. Mode selection

ESAS offers two modes of operation: normal operation mode and severe accident mode. Normal operation mode is used for the simulation of normal operation conditions and DBAs. Severe accident mode is used for the simulation of severe accident scenarios. Users can choose the corresponding mode according to the aim of their simulation. Fig. 33 shows the interface for mode selection.

3.3.1.2. Initial screen

After selecting the normal operation mode, the ESAS displays the screen as shown in Fig. 65 showing the plant overview with the ESAS menu panels on the top. From this screen the user can navigate to all relevant information and other windows as available. These can be selected from drop-down lists which open by clicking on some of the menu buttons in the ESAS menu panels.

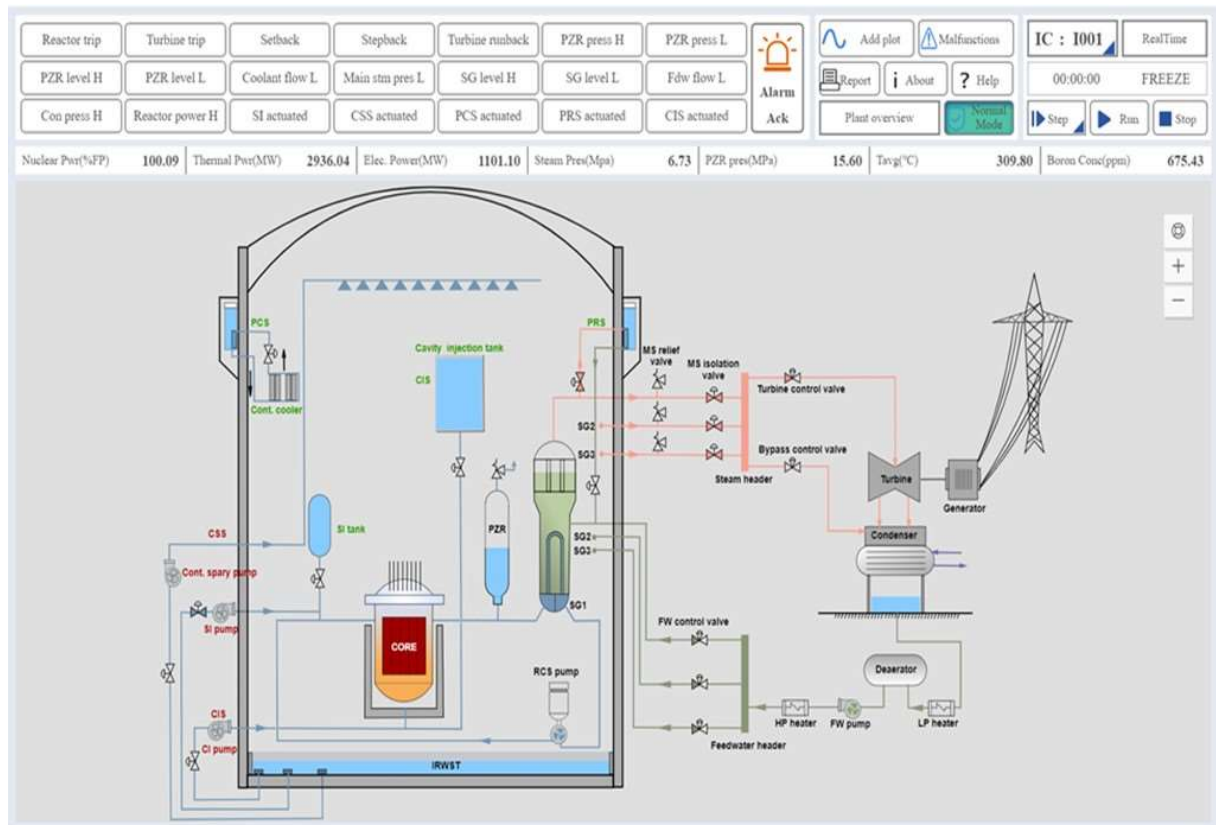


FIG. 65. Plant overview; ESAS initial screen after opening normal operation mode.

3.3.1.3. IC list

Selecting the IC button on the top right corner of the main interface opens a list of predefined initial conditions is shown in Fig. 66. These include the sets of variables necessary to initialize the mathematical models of the simulator for a particular state of the plant. Before initiating the simulation, it is necessary to load an initial condition. By default, the initial condition IC001 is selected.

Users can select an initial condition to either reset, snap, edit or delete. Selecting the reset button will select and load a predefined initial condition.

In order to access the initial conditions, user can also select the small arrow in the corner of the IC button on the main interface which opens the quick IC reset drop-down list as shown in Fig. 67. Then users can choose any predefined initial conditions from this list. By selecting

the snap button, the current state of the simulator is saved as an initial condition. The edit button allows the user to edit the description of the selected initial condition. Selecting the delete button deletes the selected initial condition.

Some initial conditions have a lock icon to their left. To execute the snap, edit, or delete functions for these initial conditions, the user needs to input a password. Initially, the password is 1234 and can be changed by clicking the Change IC edit password button (as shown in Fig. 68). The password can be up to 8 digits long and can be composed of numbers and letters.

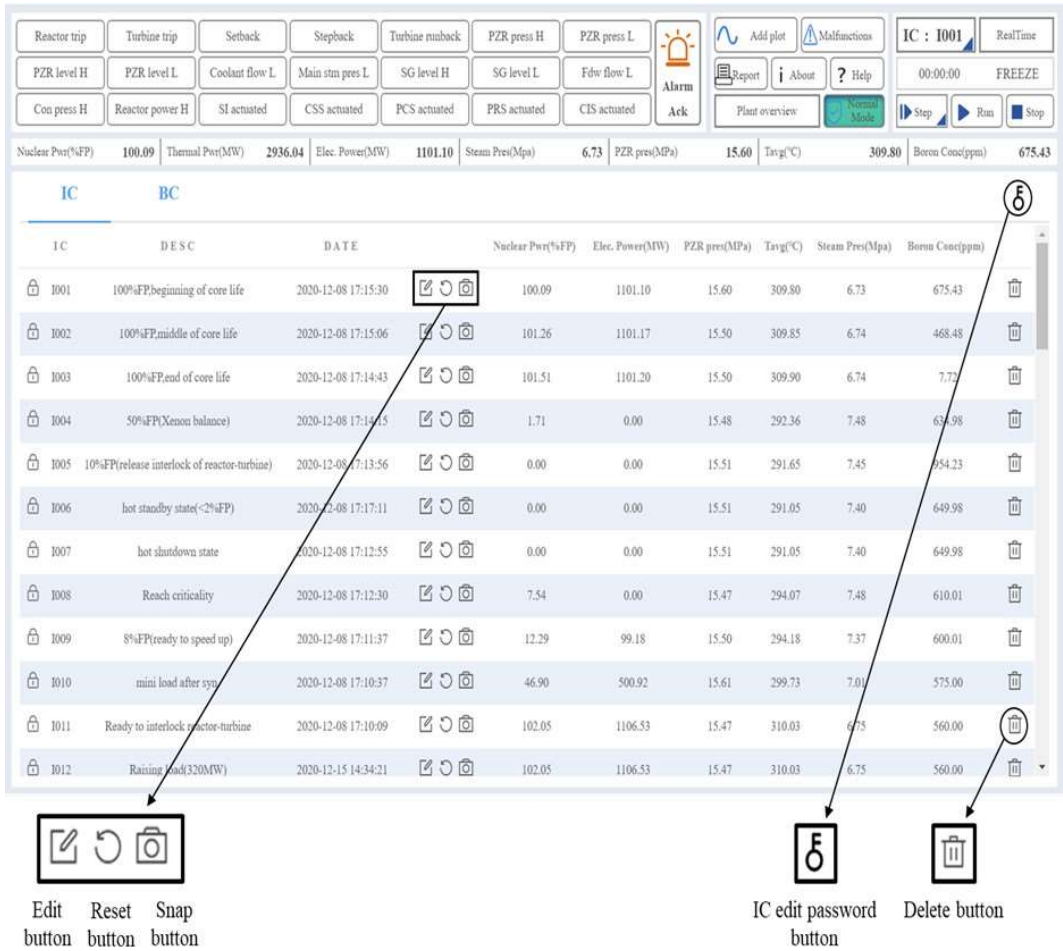


FIG. 66. IC list in ESAS normal operation mode.

Reactor trip

Turbine trip

Setback

Stopback

Turbine runback

PZR press H

PZR press L

Alarm

Ack

Add plot

Malfunctions

IC : 1001

RealTime

PZR level H

PZR level L

Coolant flow L

Main stm press L

SG level H

SG level L

Fdr flow L

Con press H

Reactor power H

SI actuated

CSS actuated

PCS actuated

PRS actuated

CIS actuated

Report

ICNames

Plant

Name

Description

Nuclear Power(%FP)

100.09

Thermal Power(MW)

2936.84

Elec. Power(MW)

1101.10

Steam Press(Mpa)

6.73

PZR press(MPa)

15.60

IC

BC

IC

DESC

DATE

Nuclear Power(%FP)

Elec. Power(MW)

PZR press(MPa)

1001

100%FPbeginning of core life

2020-12-08 17:15:30

100.09

1101.10

15.60

1002

100%FPmiddle of core life

2020-12-08 17:15:06

101.26

1101.17

15.50

1003

100%FPend of core life

2020-12-08 17:14:43

101.51

1101.20

15.50

1004

50%FP(Xenon balance)

2020-12-08 17:14:15

1.71

0.00

15.48

1005

10%FP(release interlock of reactor-turbine)

2020-12-08 17:13:56

0.00

0.00

15.51

1006

hot standby state(<2%FP)

2020-12-08 17:17:11

0.00

0.00

15.51

1007

hot shutdown state

2020-12-08 17:12:55

0.00

0.00

15.51

1008

Reach criticality

2020-12-08 17:12:30

7.54

0.00

15.47

1009

8%FP(ready to speed up)

2020-12-08 17:11:37

12.29

99.18

15.50

1010

mini load after syn.

2020-12-08 17:10:37

46.90

500.92

15.61

1011

Ready to interlock reactor-turbine

2020-12-08 17:10:09

102.05

1106.53

15.47

1012

Raising load(3200MW)

2020-12-15 14:34:21

102.05

1106.53

15.47

294.07

7.48

610.01

294.18

7.37

600.01

299.73

7.61

575.00

310.03

6.75

560.00

310.03

6.75

560.00

FIG. 67. IC reset drop-down list.

Reactor trip

Turbine trip

Setback

Stopback

Turbine runback

PZR press H

PZR press L

Alarm

Ack

PZR level H

PZR level L

Coolant flow L

Main steam press L

SG level H

SG level L

Fdr flow L

Alarm

Report

Alarm

Help

Con press H

Reactor power H

SI actuated

CSS actuated

PCS actuated

PRS actuated

CIS actuated

Plant overview

Freeze

Stop

Run

Stop

Nuclear Power(%FP)

100.09

Thermal Power(MW)

2936.84

Elec. Power(MW)

1101.10

Steam Press(Mpa)

6.73

PZR press(MPa)

15.60

Temp(°C)

309.80

Reactor CoreTemp

675.43

IC

BC

IC

DESC

DATE

Temp(°C)

Steam Press(Mpa)

Reactor CoreTemp

1001

100%FPbeginning of core life

2020-12-08 17:15:30

309.80

6.73

675.43

1002

100%FPmiddle of core life

2020-12-08 17:15:06

309.85

6.74

668.48

1003

100%FPend of core life

2020-12-08 17:14:43

309.90

6.74

7.72

1004

50%FP(Xenon balance)

2020-12-08 17:14:15

282.34

7.48

634.98

1005

10%FP(release interlock of reactor-turbine)

2020-12-08 17:13:56

291.67

7.45

654.23

1006

hot standby state(<2%FP)

2020-12-08 17:17:11

291.07

7.48

643.98

1007

hot shutdown state

2020-12-08 17:12:55

291.07

7.48

643.98

1008

Reach criticality

2020-12-08 17:12:30

7.54

0.00

15.47

294.87

7.48

638.81

1009

8%FP(ready to speed up)

2020-12-08 17:11:37

12.29

99.18

15.50

294.13

7.37

680.01

1010

mini load after syn.

2020-12-08 17:10:37

46.90

500.92

15.61

299.73

7.60

571.06

1011

Ready to interlock reactor-turbine

2020-12-08 17:10:09

102.05

1106.53

15.47

310.03

6.75

560.00

1012

Raising load(3200MW)

2020-12-15 14:34:21

102.05

1106.53

15.47

310.03

6.75

560.00

Change Password

old Password

new Password

re-enter Password

Confirm

FIG. 68. Change IC edit password via IC edit password change button.

3.3.1.4. Backtrack condition list

The backtrack condition (the button is indicated as BC on the simulator screen) allows the user to go back to a certain stage of the previous calculation. Users can select the backtrack

condition button on the screen with the IC list of initial conditions to switch to the backtrack condition list as shown in Fig. 69. From this list, users can choose which backtrack conditions to load. The interval at which the backtracking conditions are saved is determined by the backtrack interval. It can be set to 1, 5, 10, 20 or 30 minutes and can be changes throughout the running of the simulation (see Fig. 70).











| | | | | | | | | | | | | | | | | |
|------------------|---------------------|----------------|-----------------|--------------------|------------------|--------------|---|--|--|---|--|--|-----------------|--|-----------------|--|
| Reactor trip | Turbine trip | Setback | Stepback | Turbine runback | PZR press H | PZR press L |  Alarm Ack |  Add plot |  Malfunctions | IC : 1001 | RealTime | | | | | |
| PZR level H | PZR level L | Coolant flow L | Main stm pres L | SG level H | SG level L | Fdr flow L | |  Report |  About | | |  Help | 00:00:00 | FREEZE | | |
| Con press H | Reactor power H | SI actuated | CSS actuated | PCS actuated | PRS actuated | CIS actuated | |  Plant overview |  Step |  Run |  Stop | | | | | |
| Nuclear Pwr(%FP) | | 100.09 | Thermal Pwr(MW) | 2936.04 | Elec. Power(MW) | 1101.10 | | Steam Pres(Mpa) | 6.73 | PZR pres(MPa) | 15.60 | Tavg(°C) | 309.80 | Boron Conc(ppm) | 675.43 | |
| IC | | BC | | Backtrack Interval | | | | | | | | | | <input type="text" value="Please select #"/> | | |
| B C | DATE | | TIME | | Nuclear Pwr(%FP) | | Elec. Power(MW) | | PZR pres(MPa) | | Tavg(°C) | | Steam Pres(Mpa) | | Boron Conc(ppm) | |
| B001 | 2022-11-28 09:11:04 | | 00:00:00 | | 100.00 | | 1101.28 | | 15.50 | | 310.92 | | 6.83 | | 675.60 | |
| B002 | 2022-11-28 09:12:04 | | 00:01:00 | | 100.00 | | 1103.33 | | 15.42 | | 310.22 | | 6.85 | | 675.60 | |
| B003 | 2022-11-28 09:13:04 | | 00:02:00 | | 100.00 | | 1101.62 | | 15.46 | | 310.12 | | 6.85 | | 675.60 | |
| B004 | 2022-11-28 09:14:04 | | 00:03:00 | | 100.00 | | 1101.28 | | 15.51 | | 310.12 | | 6.85 | | 675.60 | |
| B005 | 2022-11-28 09:15:05 | | 00:04:00 | | 100.00 | | 1101.30 | | 15.56 | | 310.15 | | 6.85 | | 675.60 | |
| B006 | 2022-11-28 09:16:04 | | 00:05:00 | | 100.00 | | 1101.40 | | 15.61 | | 310.19 | | 6.86 | | 675.60 | |
| B007 | 2022-11-28 09:17:05 | | 00:06:00 | | 100.00 | | 1101.49 | | 15.66 | | 310.23 | | 6.86 | | 675.60 | |
| B008 | 2022-11-28 09:18:04 | | 00:07:00 | | 100.00 | | 1101.53 | | 15.67 | | 310.27 | | 6.87 | | 675.60 | |
| B009 | 2022-11-28 09:19:04 | | 00:08:00 | | 100.00 | | 1101.55 | | 15.67 | | 310.31 | | 6.87 | | 675.60 | |
| B010 | 2022-11-28 09:20:04 | | 00:09:00 | | 100.00 | | 1101.56 | | 15.66 | | 310.33 | | 6.87 | | 675.60 | |

FIG. 69. Backtrack condition list in normal operation mode.

| | | | | | | | | | | | | |
|------|---------------------|----------|---|--------------------|-----------------|---------------|----------|-----------------|--|--|--|--|
| IC | | BC | | Backtrack Interval | | 5 Minutes ^ | | | | | | |
| B C | DATE | TIME | | Nuclear Pwr(%FP) | Elec. Power(MW) | PZR pres(MPa) | Tavg(°C) | Steam Pres(Mpa) | | | | |
| B001 | 2023-01-18 12:00:07 | 00:00:00 | 🕒 | 101.22 | 1101.10 | 15.50 | 309.80 | 6.73 | | | | |
| B002 | 2023-01-18 12:00:51 | 00:01:00 | 🕒 | 88.03 | 483.54 | 15.26 | 308.06 | 6.75 | | | | |
| B003 | 2023-01-18 12:01:11 | 00:02:00 | 🕒 | 73.68 | 499.46 | 15.08 | 304.96 | 6.75 | | | | |
| B004 | 2023-01-18 12:01:31 | 00:03:00 | 🕒 | 52.18 | 549.14 | 15.01 | 302.62 | 7.06 | | | | |

FIG. 70. Backtrack interval dropdown list enclosed in a bold rectangle.

3.3.1.5. Plot

By selecting the “Add plot” button on the main interface a list of plot parameters opens as shown in Fig. 71. Here the user can select parameters to display in a graph. Subsequently, a plot is created by selecting the “CreatePlot” button at the bottom of the window, see Fig. 71.

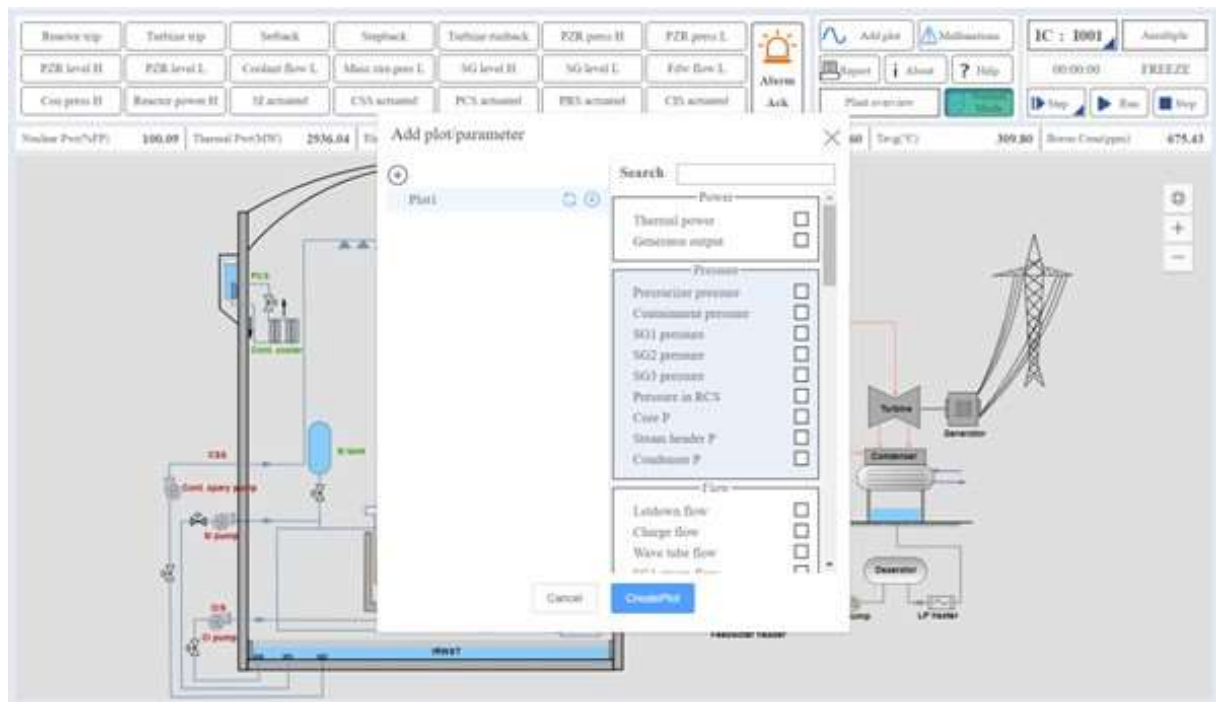


FIG. 71. Parameter selection for plotting.

Users can export the established plot to as .csv file or an image file (see left and right of Fig. 72, respectively). The .csv file can be found in the directory where the simulator is installed \\ESAS\\WEB\\php\\api. The user can select where to save the image file.



FIG. 72. Icons for different export options as found in the top left corner of the plot window.

Each plot can display the curves of up to six parameters (a list of all the parameters can be found in I-1 of the Annex I), as shown in Fig. 73.

The y-axis shows the percentage as well as the absolute values. By default, the absolute value is only shown for the initially selected parameter, all other parameters are shown in percentage. In order to change from percentage to the absolute value for any of the other parameters, one can select the appropriate name in the legend above the graph. Both the selected parameter name and the corresponding curve are highlighted when pressed.

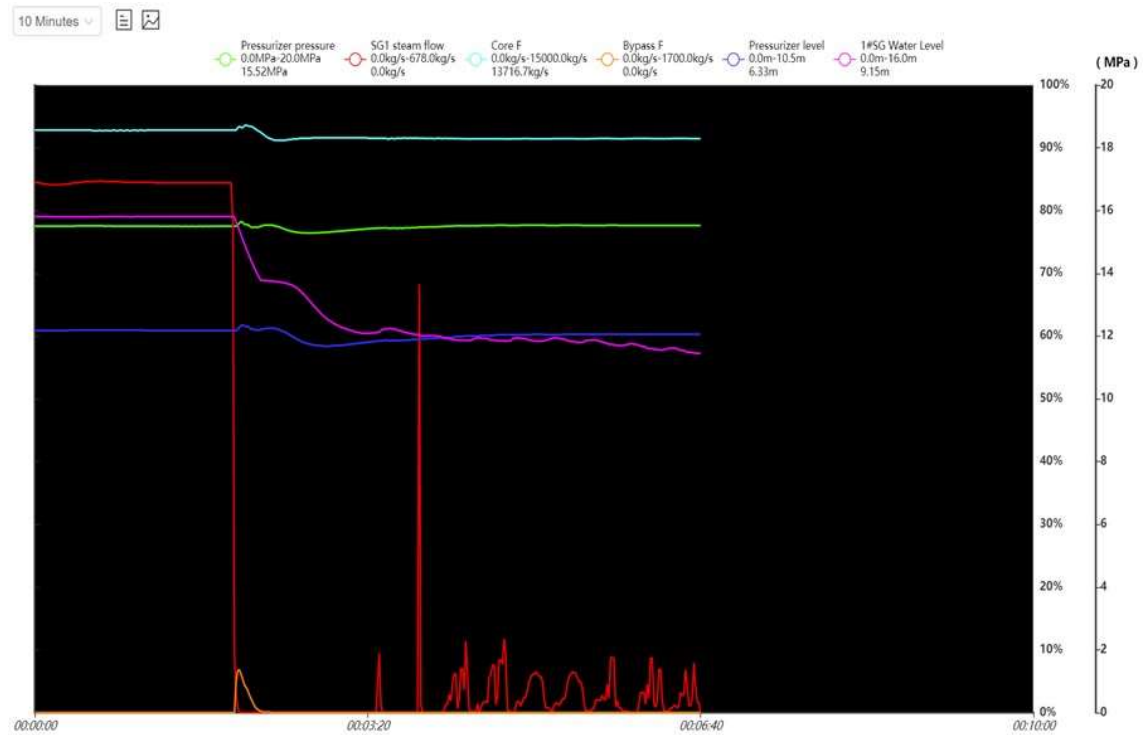


FIG. 73. Plotting window.

It is advised not to keep the plot window open while running long transients. Instead, it is recommended to view plots of interesting variables later in groups of three variables per plot, for example. Users can choose the axis range by selecting a time interval from the drop-down list (see Fig. 74) choosing button.

By selecting the plot area and keeping the mouse pressed, one can move through the timeline in the selected axis scale by pulling the screen to either side. In order to zoom in or out of the plot one can either use the mouse scroll wheel or pinch in or outward on the touchpad, respectively.

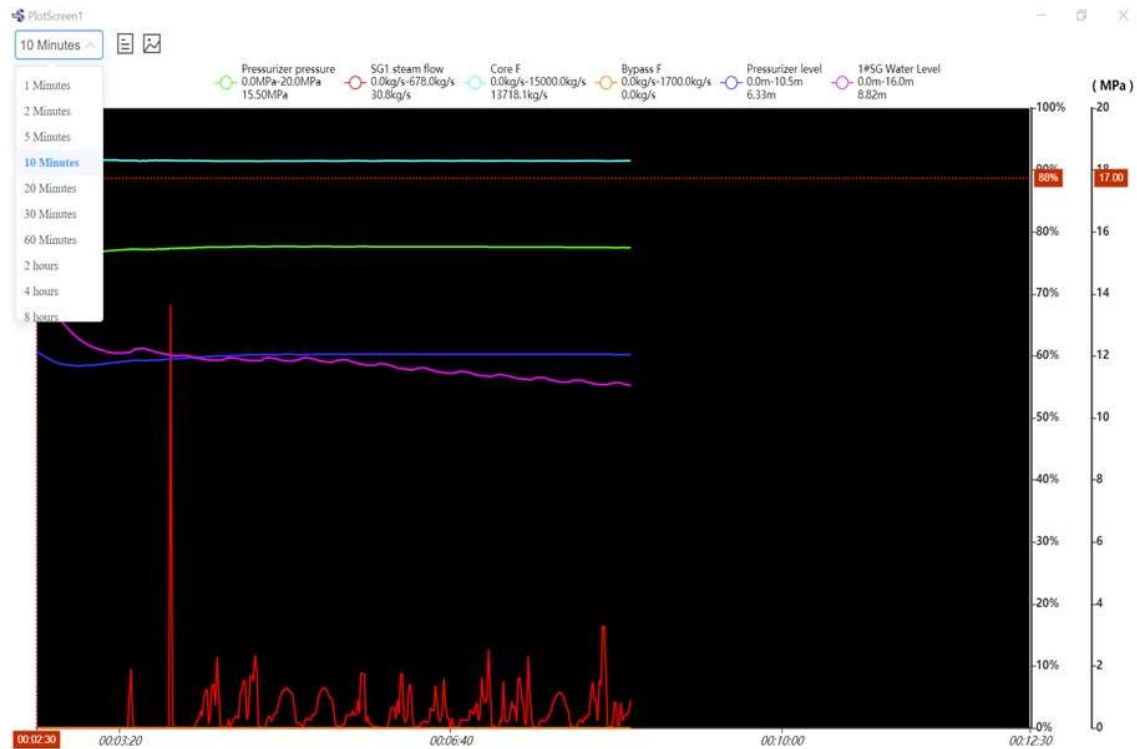


FIG. 74. Plot axis range change drop-down list.

3.3.1.6. Malfunctions

Users can select the malfunction button on the main interface to open the malfunction list. Here malfunctions can be selected or deselected as shown in Fig. 75. Selecting the check box, the malfunction is selected. It can be activated by clicking the insert button.

Users can set a time delay after which the malfunction will take effect. Users can click the clear button to disable the malfunction. Selecting the global clear button disables all the selected malfunctions. Selecting the return button serves as an exit from the malfunction list.

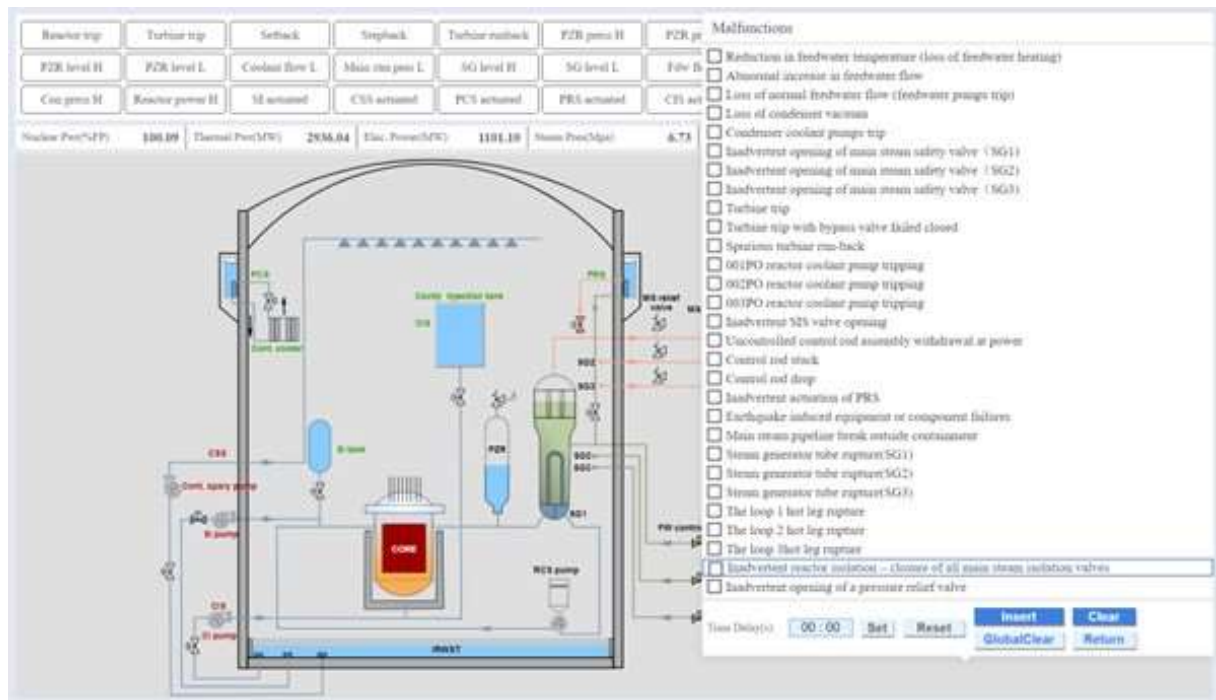


FIG. 75. List of malfunctions.

3.3.1.7. Speed control

The speed control button is used to determine the calculation speed. By selecting the button initially labelled “RealTime” on the main interface, one can select the desired speed of the simulation. There are eight different simulation speeds to choose from. The slowest possible speed is “SlowTime 1/4x” and will execute the simulation at a quarter of the speed that is expected in reality.

The quickest possible speed is “FastTime 4x” which executes the simulation at four times the real time speed. When selecting “Amultiple” the code performs the fastest calculations capable at that point in time. The drop-down list for the time selection is shown in Fig. 76.

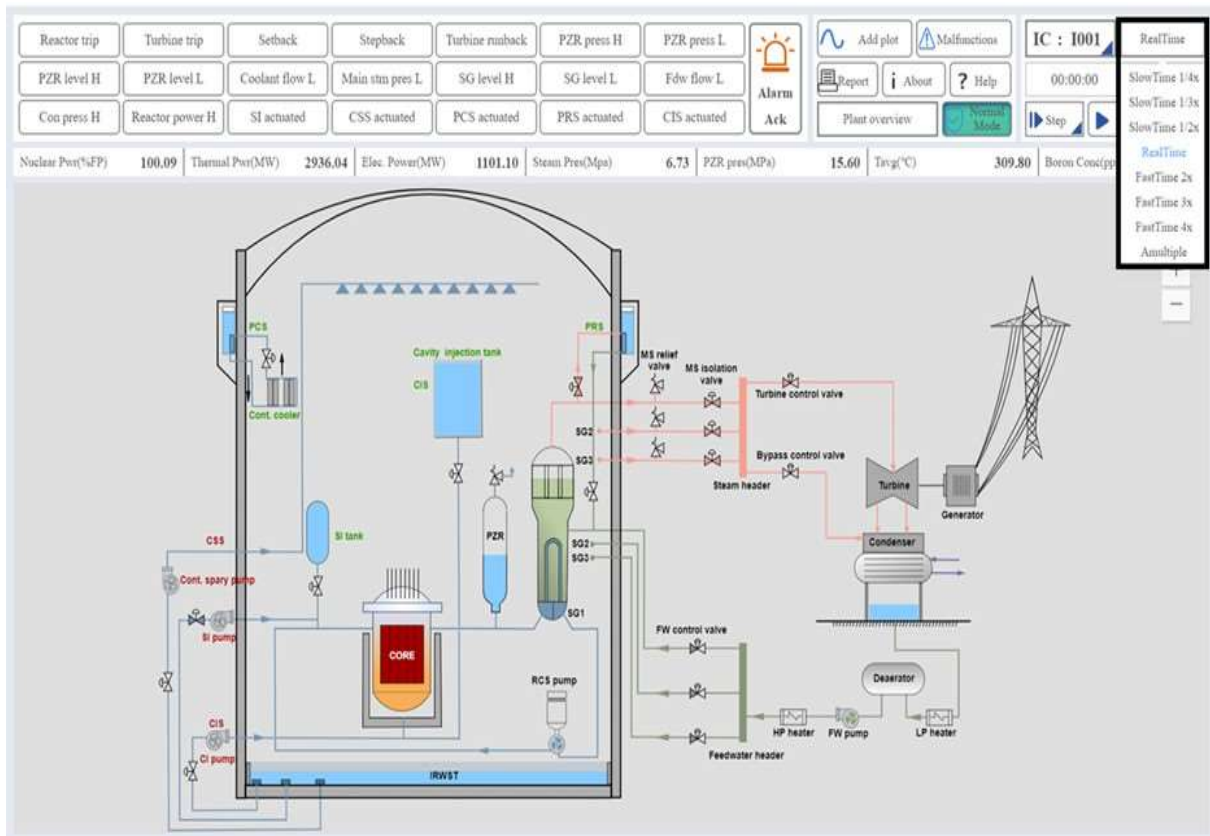


FIG. 76. Choice of calculation speeds enclosed in a bold rectangle.

3.3.1.8. Alarms

The alarm display area of the main interface in the leftmost panel is shown in Fig. 77. The setpoints at which the various alarms will go off are shown in Table 8. Here, “H” stands for high, “L” for low, “press” for pressure, “stm” for steam, “Fwd” for forward and “Con” for containment. Note that an audible alarm signal will start when an alarm is triggered.

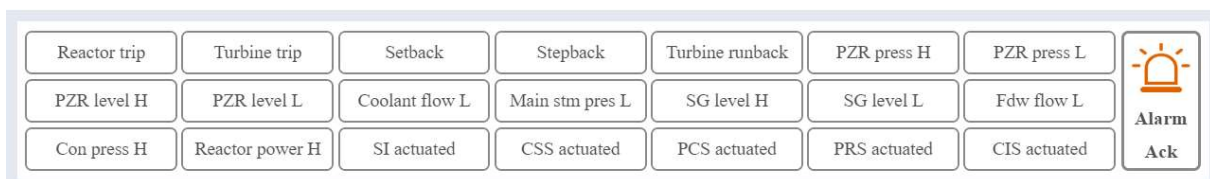


FIG. 77. Alarms display panel.

TABLE 8. SETPOINTS AND ALARMS

| Number | Alarm name | Setpoints | Unit |
|--------|------------------|-----------|------|
| 1 | PZR press H | 16.45 | MPa |
| 2 | PZR press L | 13 | MPa |
| 3 | PZR level H | 8.43 | m |
| 4 | PZR level L | 1.37 | m |
| 5 | Coolant flow L | 4440 | kg/s |
| 6 | Main stm press L | 3.45 | MPa |
| 7 | SG level H | 13.55 | m |
| 8 | SG level L | 11.39 | m |
| 9 | Fwd flow L | 42 | kg/s |
| 10 | Con press H | 240 | kPa |

3.3.1.9. Readouts and inputs

There are two types of readouts in the simulator's GUI those which are used for monitoring, and which cannot be changed, and values that can be altered by the user. The values can be changed by selecting the value and entering a new value in the pop-up window. The fixed values are shown in black font, values that the user can change are in blue. Different types of inputs can be seen in the left panel of Fig. 78.

The GUI also includes switches and buttons which can be activated by the user. A few examples can be seen in Fig. 78. Both buttons and switches are used to change mode settings. By selecting either the label A or M on the switch (see switch next to "R bank mode" in Fig. 78), the dial will turn to either the automatic or the manual mode, respectively. Buttons can be used to activate values input by the user (see Fig. 79(a)) or to activate and deactivate specific safety systems as shown in Fig. 79(b).

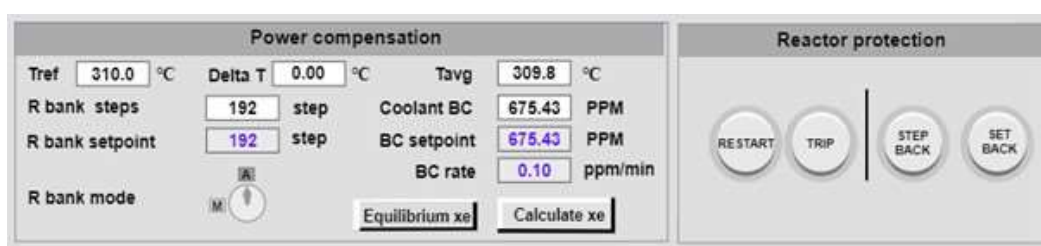


FIG. 78. Readout types, switches and buttons found in ESAS.

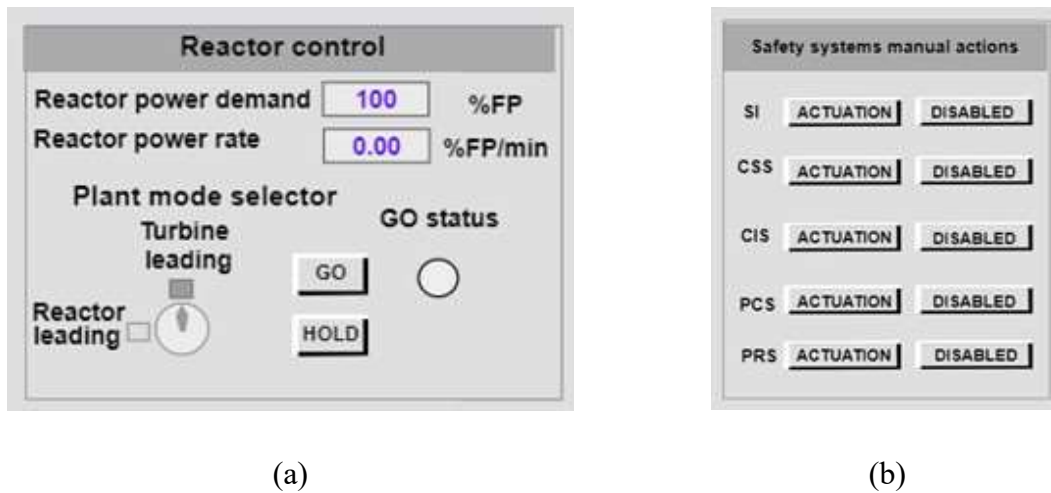




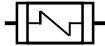
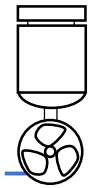



FIG. 79. Example of inputs toggled by buttons.

A list of thermal hydraulics symbols used in the GUI can be found in Table 9. The symbols change their graphical representation slightly according to use (on or off etc.) in the simulator GUI.

TABLE 9. THERMAL HYDRAULICS SYMBOLS USED IN ESAS

| Symbol | Meaning |
|---|-----------------|
|  | Relief valve |
|  | Pneumatic valve |
|  | Control valve |
|  | Pump |
|  | Heater |
|  | Reactor pump |
|  | Circuit breaker |

3.3.1.10. Help

Users can select the “Help” button on the main interface to access the ESAS user manual (Fig. 80).

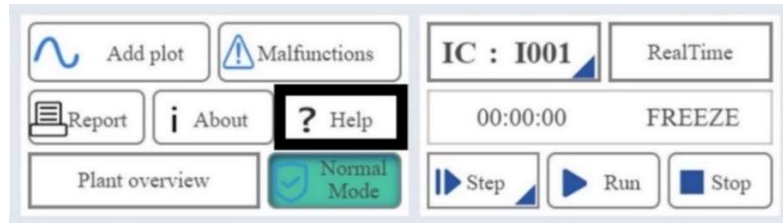


FIG. 80. ESAS menu panels: help enclosed by a bold rectangle.

3.3.1.11. About

Users can select the “About” button on the main interface to access information on the software and its developers as shown in Fig. 81.



FIG. 81. Software information.

The user can find the name of the simulator, the current version, the developer as well as a contact e-mail address and the simulator website.

3.3.2. Display screens

3.3.2.1. Description of valves and pumps on display screens

The names, acronyms and default status of the devices as well as the display screens on which they can be found are listed in Table 10.

TABLE 10. LIST OF VALVES AND PUMPS

| Number | Device name | Acronyms | Default status | Display |
|--------|----------------------------|----------|----------------|------------------------|
| 1 | Pressurizer spray valve 01 | RCS01V | Closed | Reactor coolant system |
| 2 | Pressurizer spray valve 02 | RCS02V | Closed | Reactor coolant system |
| 3 | Pressurizer safety valve | RCS03V | Closed | Reactor coolant system |
| 4 | Reactor coolant pump 01 | RCS01P | Running | Reactor coolant system |
| 5 | Reactor coolant pump 02 | RCS02P | Running | Reactor coolant system |
| 6 | Reactor coolant pump 03 | RCS03P | Running | Reactor coolant system |

TABLE 10. LIST OF VALVES AND PUMPS (cont.)

| Number | Device name | Acronyms | Default status | Display |
|--------|---|----------|----------------|------------------------------|
| 7 | Passive containment heat removal valve | PCS01V | Closed | Safety system |
| 8 | Passive residual heat removal system valve 01 | PRS01V | Open | Safety system |
| 9 | Passive residual heat removal system valve 02 | PRS02V | Closed | Safety system |
| 10 | Safety injection valve 01 | SIS01V | Open | Safety system |
| 11 | Safety injection valve 02 | SIS02V | Closed | Safety system |
| 12 | Safety injection pump | SIS01P | Stopped | Safety system |
| 13 | Containment spray valve | CSS01V | Closed | Safety system |
| 14 | Containment spray pump | CSS01P | Stopped | Safety system |
| 15 | Cavity injection valve 01 | CIS01V | Closed | Safety system |
| 16 | Cavity injection valve 02 | CIS02V | Closed | Safety system |
| 17 | Cavity injection pump | CIS01P | Stopped | Safety system |
| 18 | Main steam isolation valve 01 | MS01V | Open | NPP secondary circuit system |
| 19 | Main steam isolation valve 02 | MS02V | Open | NPP secondary circuit system |
| 20 | Main steam isolation valve 03 | MS03V | Open | NPP secondary circuit system |
| 21 | Main steam relief valve 04 | MS04V | Closed | NPP secondary circuit system |
| 22 | Main steam relief valve 05 | MS05V | Closed | NPP secondary circuit system |
| 23 | Main steam relief valve 06 | MS06V | Closed | NPP secondary circuit system |
| 24 | Turbine load control valve | TC01V | Open | NPP secondary circuit system |
| 25 | Turbine bypass control valve | BC01V | Closed | NPP secondary circuit system |
| 26 | Feed water valve 01 | FW01V | Open | NPP secondary circuit system |
| 27 | Feed water valve 02 | FW02V | Open | NPP secondary circuit system |
| 28 | Feed water valve 03 | FW03V | Open | NPP secondary circuit system |
| 29 | Feed water pump | FW01P | Running | NPP secondary circuit system |

3.3.2.2. Plant overview (in both modes)

The plant overview is shown in Fig. 82 displaying the main devices, pipelines and system compositions of the reference NPP.

With the help of the zoom function on the right-hand side of the display, one can increase or decrease the size of the GUI. The concentric circles above the plus and minus buttons restore the view to the original display size.

3.3.2.3. Control rod and reactivity (in normal operation mode only)

The “Control rod and reactivity” screen is shown in Fig. 82 and contains a depiction of the RPV with the control rod position and coolant flow direction indicator, a map of the core, the power peak diagram, a list of the main core parameters, the power control function area, the power compensation function area, the reactor control function area and the reactor protection function area.

Values highlighted in blue instead of in the default black can be selected and subsequently changed by the user. These values are setpoints for the G bank and R bank positions as well as the boron concentration and its rate of change. The reactor power and its rate of change can also be adjusted.

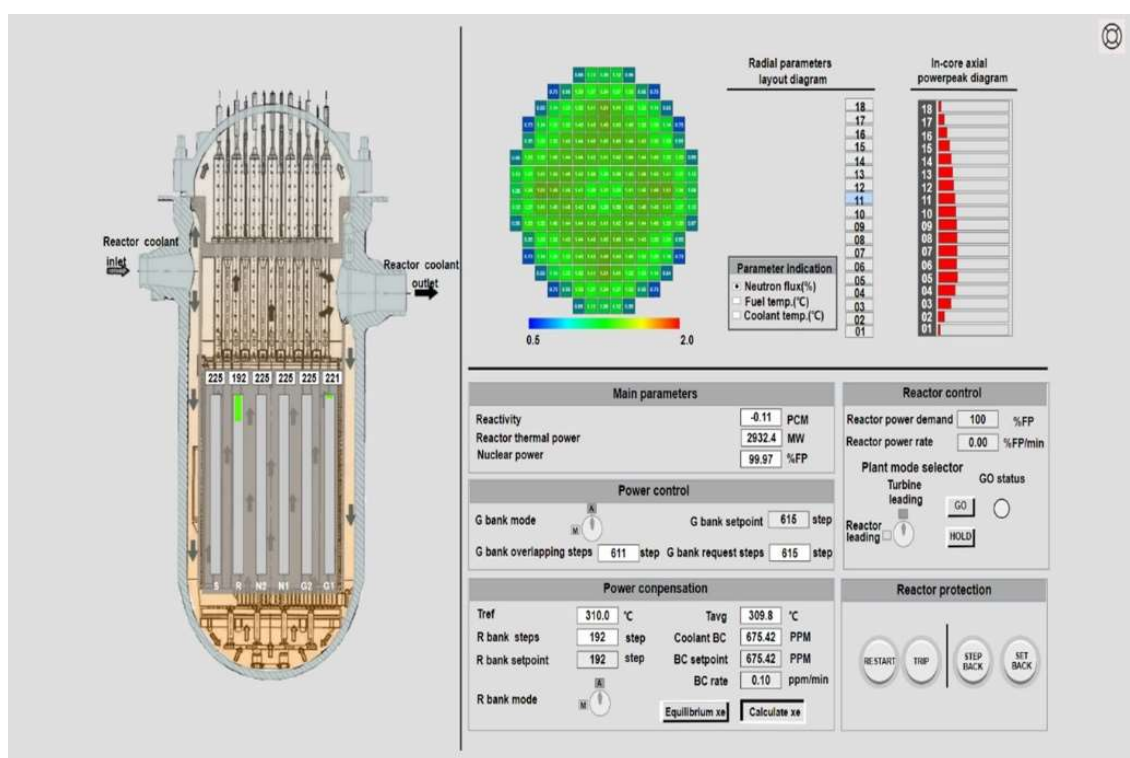


FIG. 82. Control rod and reactivity window.

3.3.2.4. Reactor coolant system (in both modes)

The “Reactor coolant system” window can be opened by selecting it from the available reactor overview displays and is shown in Fig. 83. It contains the main components and parameters of the primary circuit. Users can control the charging flow, the PZR heater control, the PZR pressure and PZR level on this screen.

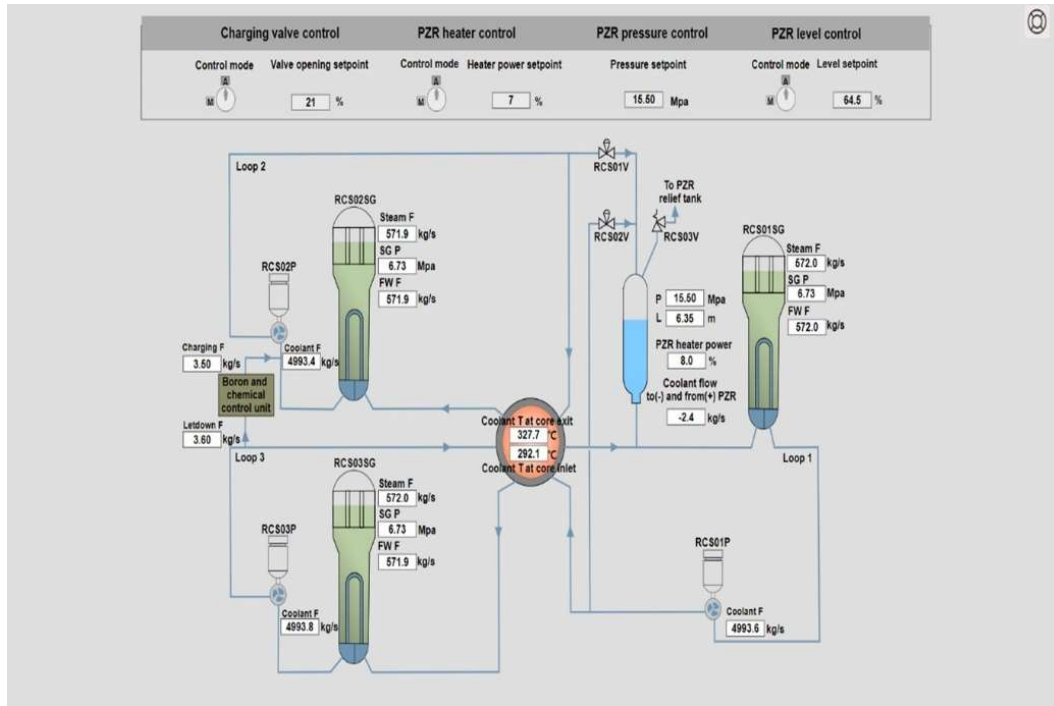


FIG. 83. Reactor coolant system window.

3.3.2.5. Safety systems (in both modes)

The “Safety systems” window is shown in Fig. 84 and contains the SIS, CSS, PRS, PCS, CIS and some selected parameters of the primary circuit. Here, safety systems can be manually actuated or disabled. One can also observe the opening and closing of safety valves and the movement of the injection pumps.

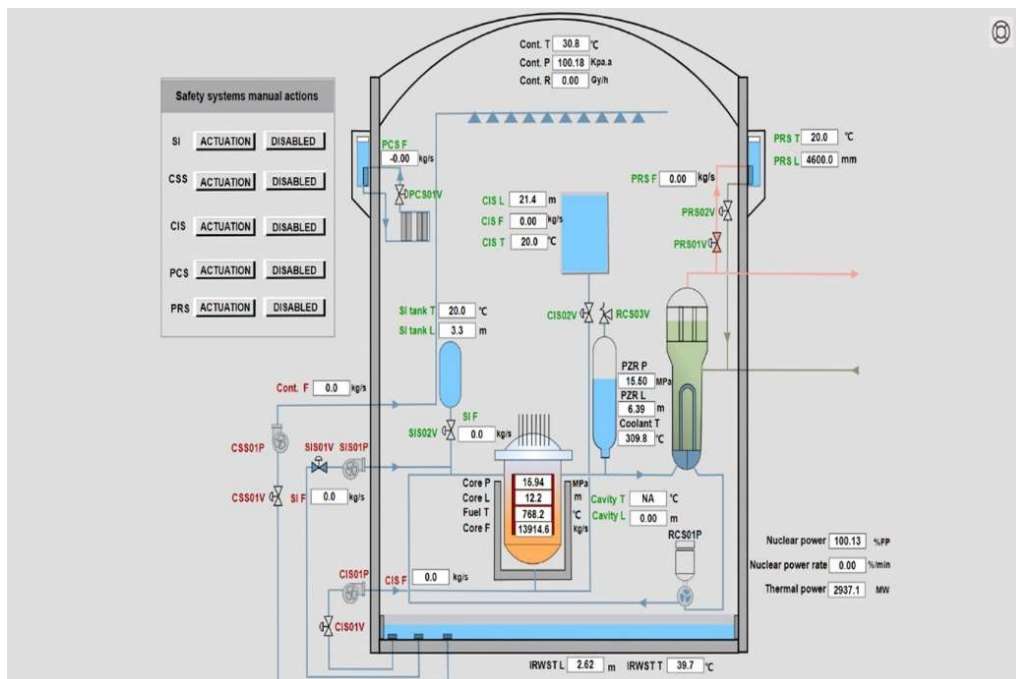


FIG. 84. Safety systems window.

3.3.2.6. Trip parameters (in both modes)

The screen “Trip parameters” is shown in Fig. 85 and includes the reactor trip signals, the turbine trip signals, the safety injection signals, the containment spray signals, the PRS actuation signal, the CIS actuation signal and the PCS actuation signal.

Next to each signal, the real value of the variable and the setpoint at which the action takes place are displayed. The light of the signal that is triggered first will be illuminated in order to help the user identify the cause of the trip.

For example, for a reactor trip, there are 13 possible variables which may have caused it. If the trip is due to high pressure in the PZR, the light next to “High PZR pressure” will come on. After this signal no other light will be activated although other trip parameters may have been triggered since the trip initiation. This helps the user to determine the first fault.

The screenshot displays the 'Trip parameters' window, organized into several sections:

- REACTOR TRIPS:** Contains 13 signals. The first six are on the left, and the last seven are on the right. Each signal has a radio button, a text label, a numerical value, a comparison operator, and a setpoint. For example, 'Low PZR pressure' shows 18.50 Mpa < 13 Mpa. The 'High reactor power' signal shows 99 %FP > 100% FP. A 'Manual' radio button and a 'RESET' button are at the bottom right of this section.
- TURBINE TRIP:** Contains three signals: 'Reactor trip', 'High condenser pressure' (4 Kpa > 23 Kpa), and 'Manual'. A 'RESET' button is at the bottom right.
- SAFETY INJECTION:** Contains four signals: 'Low PZR pressure' (18.50 Mpa < 11.53 Mpa), 'High steam differential pressure between SGs' (> 0.7 Mpa), 'High containment pressure' (100 KPa > 120 KPa), and 'High steam flow with low steam pressure'. A 'Manual' radio button and a 'RESET' button are at the bottom right.
- CONTAINMENT SPRAY:** Contains two signals: 'High containment pressure' (100 KPa > 240 KPa) and 'Manual'. A 'RESET' button is at the bottom right.
- PRS ACTUATION:** Contains one signal: 'Low SGs level with loss of feedwater' (12.55 < 11.53 m). A 'RESET' button is at the bottom.
- CIS ACTUATION:** Contains one signal: 'High reactor core temperature' (> 650 °C). A 'RESET' button is at the bottom.
- PCS ACTUATION:** Contains one signal: 'High containment temperature' (> 115 °C). A 'RESET' button is at the bottom.

FIG. 85. Trip parameters window.

3.3.2.7. Nuclear power plant secondary circuit system (in both modes)

The “NPP secondary circuit system” screen shown in Fig. 86 contains the main components of the secondary circuit, the key parameters and the turbine control function area. From this screen the turbine can be controlled as well as some of the secondary circuit valves, such as the turbine bypass valve. This screen also shows the outgoing generator circuit breaker, visualized as the connection between the generator and the utility pole, which detaches from the grid in the case of a turbine trip.

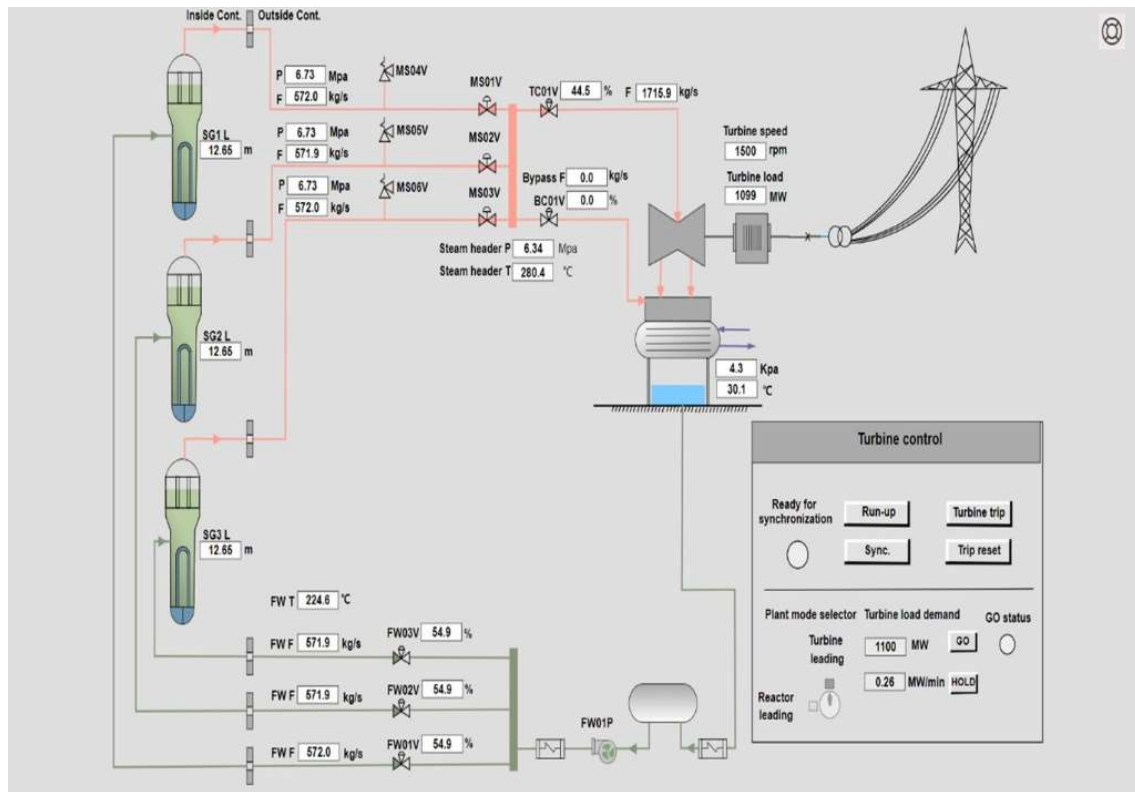


FIG. 86. NPP secondary circuit system window.

3.3.2.8. Parameters for severe accident mode (in severe accident mode only)

The parameters for the severe accident mode are shown in Fig. 87. The box titled “Main Parameters” shows the most important parameters of the NPP, including general status and safety relevant parameters for both process control and safety systems, respectively.

Under “Debris Behaviour” one can find information on the condition of the core as well as the debris distribution. The “Events” window shows the most important time points of the accident, namely the core uncover, the time at which the core debris relocated to the lower head, the failure of the RPV and the failure of the containment.

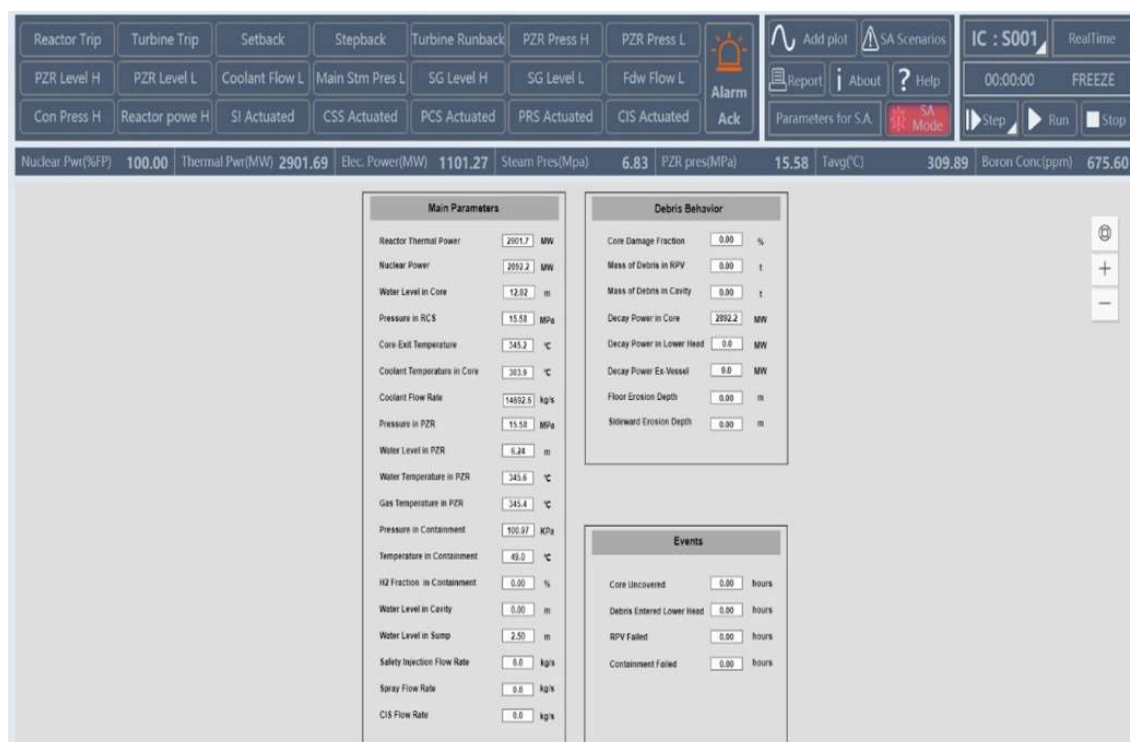


FIG. 87. Parameters for SA mode list.

3.3.2.9. 3D containment representation (in severe accident mode only)

The 3D containment representation is shown in Fig. 88; it consists of the dome, the SG compartment, where the RCS break is located and the lower compartment. Users can select a system within these areas in order to see the temperature, pressure, H₂ fraction and fission product activity released inside the containment. Various water tanks, such as the PCS tank, the IRWST, the quench tank and the accumulators are included in the 3D representation. The current water level in these tanks is indicated by the tone of colour. The PCS tank can be selected to display the water level and temperature within the tank. Other water tanks cannot be selected within this window.



FIG. 88. Containment in the 3D NPP representation.

3.3.2.10. 3D primary system representation (in severe accident mode only)

The RCS, the SGs, the PZR, the quench tank, the IRWST and the CIS tanks are all shown in the primary system screen as can be seen in Fig. 89. One can see the water as well as steam represented in pipes and vessels as in Fig. 89. The water movement within the system indicates the real liquid flow rate within the pipes.

Users can select equipment to view the parameters related to operation. These include the SGs, the PZR, the quench tank, the RPV and the cavity. Within the RPV, the core and the lower head can additionally be selected.

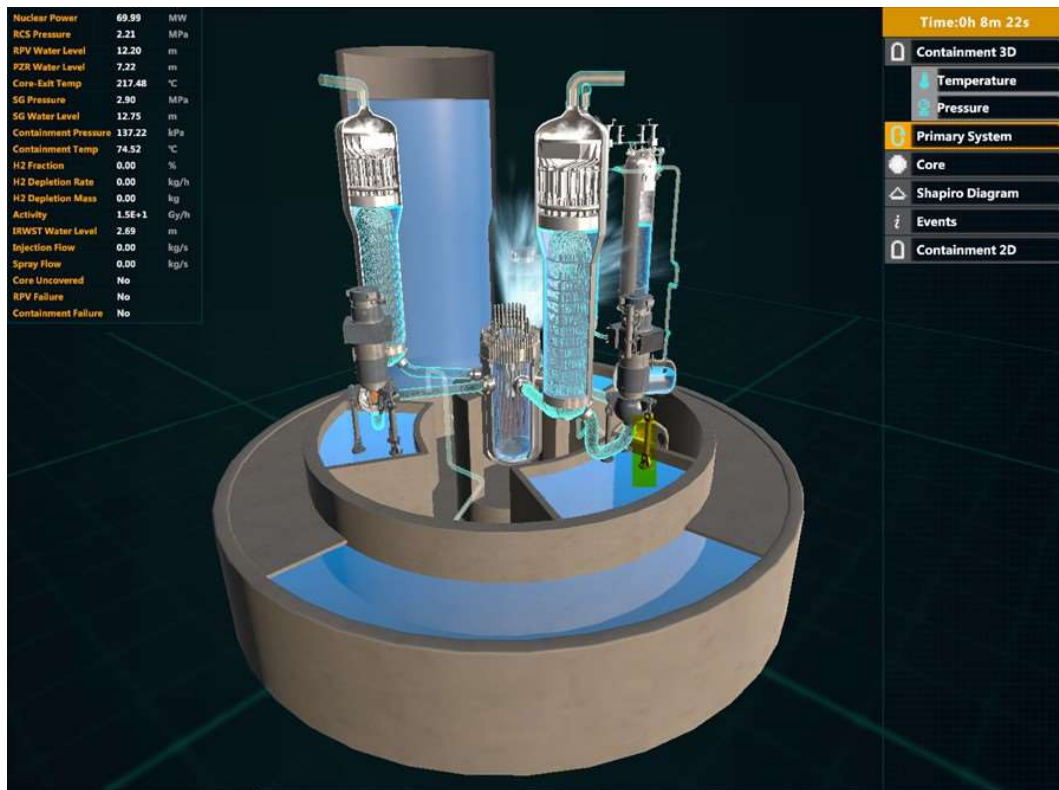


FIG. 89. Primary system in the 3D NPP representation.

3.3.2.11. Reactor core in 3D representation (in severe accident mode only)

In the 3D reactor representation, the tab “Core” can be selected and a 2D map of the core is then displayed for different core heights. Two main parameters are shown for each node within the core representation: the temperature and the normalized mass, defined as the ratio of the current mass to the initial mass. The colour indicates the temperature of the nodes within the core.

The power or mass distribution can be displayed on the right hand side of the screen as shown in Fig. 90. Users can open the drop-down list to select whether to display the distribution of power or mass in the RPV. The distribution can be viewed for all 13 layers of the core. The user can switch to a different layer by selecting the appropriate layer button.

- Layer 01 and layer 02 represent the lower grid plate, the support structures and the core support plate (i.e. the non-fuel parts);
- Layers 03–12 represent the active core;
- Layer 13 represents the upper grid plate (non-fuel part);
- The lower head represents the parameters at the lower end of the RPV.

In the event of molten corium concrete interaction, the process is displayed below the layers indicating power or mass distribution.

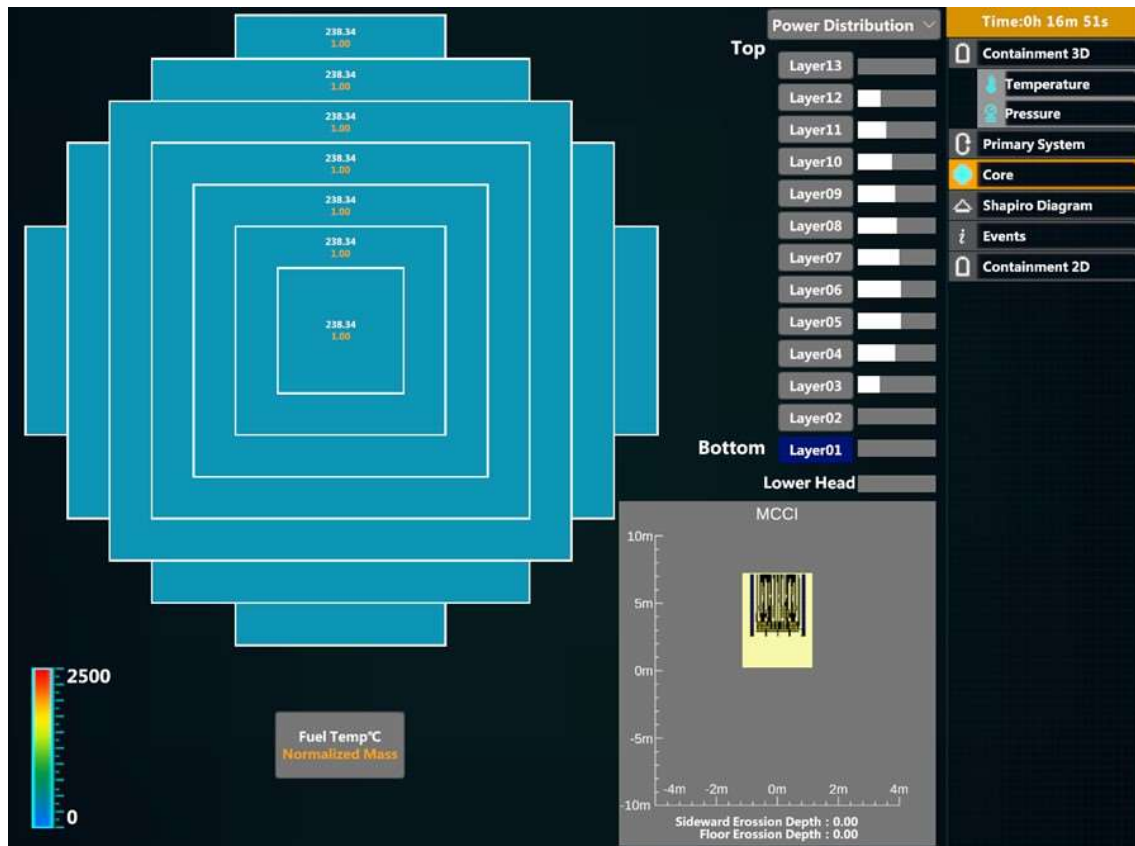


FIG. 90. Core representation in the 3D NPP representation (MCCI: molten corium concrete interaction).

3.3.2.12. Shapiro diagram in 3D representation (in severe accident mode only)

The Shapiro diagram shown in Fig. 91 is used to display the hydrogen risk conditions. Four regions are visible in the displayed diagram: black, yellow, orange and red region:

- When the indicated point is displayed in the black region, no hydrogen risk is imminent;
- Yellow region indicates that the hydrogen in containment may undergo slow burning;
- Orange region indicates the potential of fast burning of hydrogen;
- Red region implies a risk of hydrogen detonation.

The diagram includes three different gas fractions, CO₂, steam, N₂, O₂, CO and H₂, displayed on the left side of the diagram.

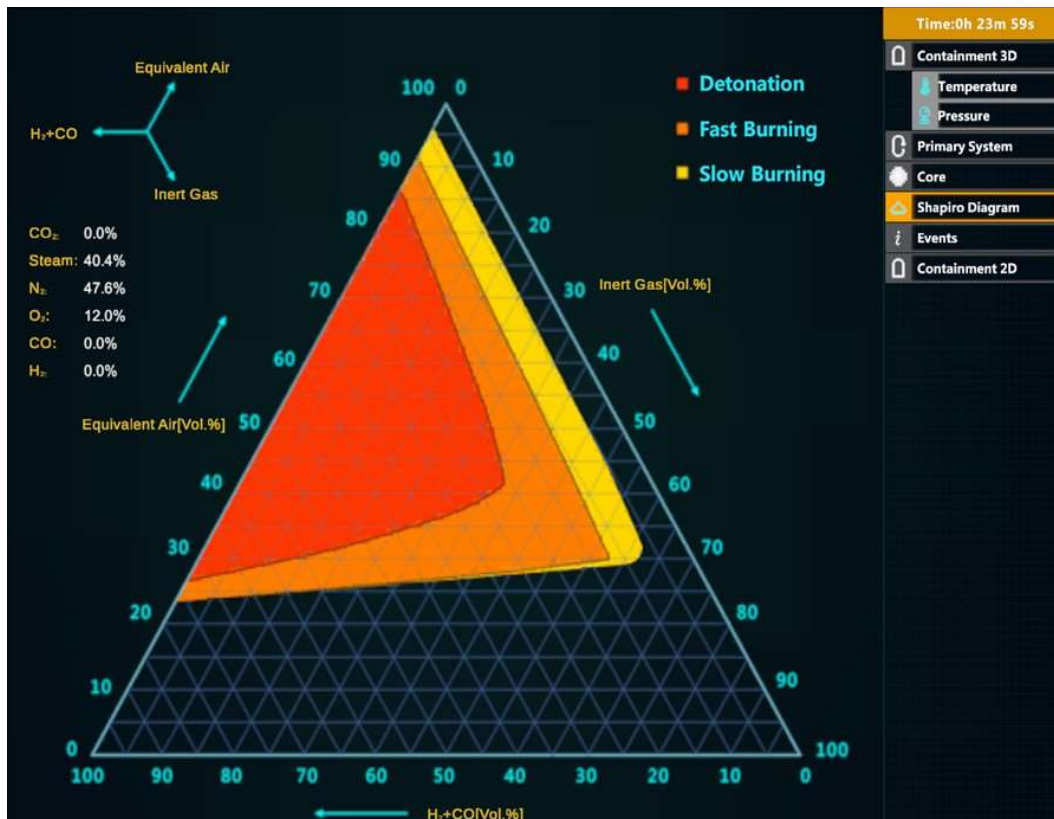


FIG. 91. Shapiro diagram in the 3D NPP representation.

3.3.2.13. Events tab in 3D representation (in severe accident mode only)

Fig. 92 shows the “Events” screen with examples for possible occurrences that would be displayed.

| Time | Event |
|--------------------|--------------------------------|
| 0 hr 00 min 02 sec | RCS Break |
| 0 hr 00 min 02 sec | Cold Leg Break |
| 0 hr 00 min 41 sec | Reactor Scram |
| 0 hr 03 min 04 sec | Accumulator Activated |
| 0 hr 03 min 33 sec | PZR Safety Valve Open |
| 0 hr 23 min 26 sec | RCP Stop |
| 0 hr 35 min 29 sec | Core Uncovered |
| 0 hr 53 min 29 sec | Containment Spray Activated |
| 1 hr 09 min 24 sec | Core-Exit Temp exceeds 650°C |
| 2 hr 00 min 23 sec | Debris Relocates to Lower Head |
| 2 hr 14 min 20 sec | RPV Dry Out |

Time: 8h 45m 1s

- Containment 3D
- Temperature
- Pressure
- Primary System
- Core
- Shapiro Diagram
- Events
- Containment 2D

FIG. 92. Events in the 3D NPP representation.

The most important events and their time stamps are listed as shown in Table 11.

TABLE 11. LIST OF POSSIBLE SEVERE ACCIDENT EVENTS

| Number | Event |
|--------|-----------------------------------|
| 1 | RCS Break |
| 2 | Cold Leg Break |
| 3 | SG Tubes Rupture |
| 4 | Feed Water Lost |
| 5 | Reactor trip |
| 6 | RCP Stop |
| 7 | Core Uncovered |
| 8 | Core Exit Temp exceeds 650°C |
| 9 | Debris Relocates to Lower Head |
| 10 | RPV Dry Out |
| 11 | RPV Failure |
| 12 | Debris Enters Cavity |
| 13 | Containment Failure |
| 14 | High Pressure Injection Activated |
| 15 | Low Pressure injection Activated |
| 16 | Accumulator Activated |
| 17 | Containment Spray Activated |
| 18 | PZR Safety Valve Open |
| 19 | PZR Relief Valve Open |

3.3.2.14. Containment 2D tab in 3D representation (in severe accident mode only)

The tab “Containment 2D” as shown in Fig. 93 displays the node partitioning of the containment model.

Each box represents a compartment in the containment. The colour in the boxes ranges from blue to red and indicates the H₂ fraction within compartments. Each compartment also indicates a few parameters and their values, such as the pressure and the gas temperature. The water temperature and the water level are additionally displayed for compartments that contain water tanks.

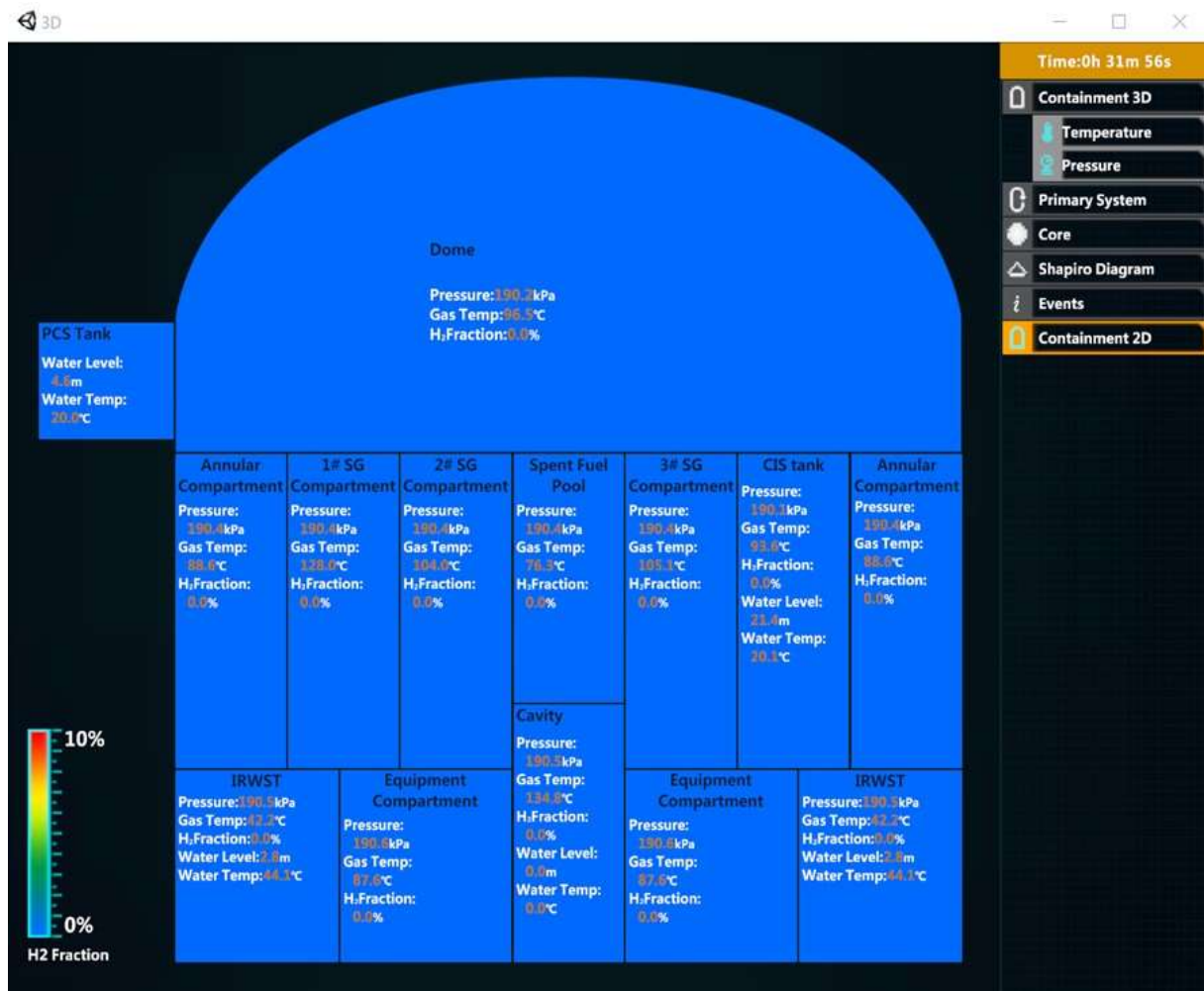


FIG. 93. 2D containment representation in the 3D NPP representation.

REFERENCES

- [1] BONNET, J. M., SEILER, J. M., "Thermal-Hydraulic Phenomena in Corium Pools for Ex-Vessel Situations: the BALI Experiment", Proceedings of the international conference on Nuclear Engineering (ICONE 7), Tokyo, Japan (1999).
- [2] GLOBE, S., DROPKIN, D., Natural Convection Heat Transfer in Liquids Confined by Two Horizontal Plates and Heated From Below, ASME Journal of Heat Transfer, **81** (1959) 24.
- [3] COWARD, H. F., JONES, G. W., Limits of flammability of gases and vapors, Bureau of mines, **503** (1952).
- [4] EPRI, NIS PAR Depletion Rate Equation of Hydrogen Recombination During an AP600. Design Basis Accident, EPRI ALWR Program Report (1995).
- [5] TAITEL, Y., BORNEA, D., DUKLER, A.E., Modelling Flow Pattern Transitions for Steady Upward Gas-Liquid Flow in Vertical Tubes, AIChE Journal **26** (1980), 345-354.

ANNEX I

ESAS PLOTTING VARIABLES

This Annex provides a list of ESAS variables that can be plotted and analyzed as shown in Table I-1.

TABLE I-1. VARIABLES FOUND IN THE PLOTTING WINDOW OF ESAS

| Number | Variable | Number | Variable |
|--------|-----------------------------|--------|----------------------------------|
| 1 | Thermal power | 35 | Condenser T |
| 2 | Generator output | 36 | IRWST T |
| 3 | Pressurizer pressure | 37 | SI tank T |
| 4 | Containment pressure | 38 | CIS T |
| 5 | SG1 pressure | 39 | PRS T |
| 6 | SG2 pressure | 40 | Steam header T |
| 7 | SG3 pressure | 41 | Cavity T |
| 8 | Pressure in RCS | 42 | Delta T |
| 9 | Core P | 43 | Tref |
| 10 | Steam header P | 44 | Pressurizer level |
| 11 | Condenser P | 45 | 1#SG Water Level |
| 12 | Letdown flow | 46 | 2#SG Water Level |
| 13 | Charge flow | 47 | 3#SG Water Level |
| 14 | Wave tube flow | 48 | Core L |
| 15 | SG1 steam flow | 49 | IRWST L |
| 16 | SG2 steam flow | 50 | CIS tank L |
| 17 | SG3 steam flow | 51 | SI tank L |
| 18 | Core F | 52 | PRS L |
| 19 | CIS Passive F | 53 | Cavity L |
| 20 | CIS F | 54 | Turbine Speed |
| 21 | SIS F | 55 | G bank overlapping steps |
| 22 | SIS Passive F | 56 | R bank steps |
| 23 | Containment spray F | 57 | Coolant BC |
| 24 | PCS F | 58 | Xenon |
| 25 | PRS F | 59 | Reactivity |
| 26 | Bypass F | 60 | TC01V position |
| 27 | Coolant F1 | 61 | BC01V position |
| 28 | Coolant F2 | 62 | FW01V position |
| 29 | Coolant F3 | 63 | FW02V position |
| 30 | Steam header F | 64 | FW03V position |
| 31 | Average coolant temperature | 65 | Cont. R |
| 32 | Containment temp. | 66 | PZR level set point |
| 33 | Fuel T | 67 | PZR heater power set point |
| 34 | FW T | 68 | Charging valve opening set point |

ANNEX II

ESAS EXAMPLES: NPP NORMAL OPERATION

II-1. INITIAL CONDITION VERIFICATION

This section describes the initial state of the main parameters under 100% full power condition for normal operation mode (Table II-1). Figure II-1 shows the NPP main display of ESAS which appears when the simulator is launched in normal operation mode.

TABLE II-1. DETAILS OF INITIAL CONDITION VERIFICATION

| Parameter description | GUI sheet | Reference value or state | Allowable deviation |
|---|-----------------------------------|--------------------------|---------------------|
| Nuclear power | Fixed column | 100% FP | ±2 |
| Thermal power | | 2900 MW | ±40 |
| Electric power | | 1100 MW | ±12 |
| Steam pressure | | 6.6 MPa | ±0.2 |
| PZR pressure | | 15.4 MPa | ±0.2 |
| Reactor coolant average temp. (T _{avg}) | | 310°C | ±2 |
| Reactor coolant boron concentration | | 675 ppm | ±10 |
| PZR heater control | Reactor coolant system | Auto | n.a. ^a |
| PZR level control | | | |
| Steam flow (Steam F) | | 571 kg/s/SG | ±6 |
| Feedwater flow (FW F) | | 571 kg/s/SG | ±6 |
| PZR level | | 6.6 m | ±0.4 |
| PZR spray valve (RCS0xV) | | Auto | n.a. |
| Charging flow | | 3.56 kg/s | ±0.3 |
| Let-down flow | Running when simulator is running | 3.58 kg/s | ±0.2 |
| Reactor coolant pumps | | | n.a. |
| Plant mode | Secondary system | Turbine leading | |
| Feedwater pumps (FW01P) | | Running | |
| Feedwater control valves (FW0xV) | | Auto | n.a. |
| Turbine load control valve (TC01V) | | Auto | |
| Turbine bypass valve (BC01V) | | Closed (0%) | |
| G bank mode | Control rods | Auto | n.a. |
| R bank mode | | Auto | |
| G bank overlapping steps | | 615 steps | ±5 |
| R bank steps | | 192 steps | ±5 |
| ^a n.a.: not applicable | | | |

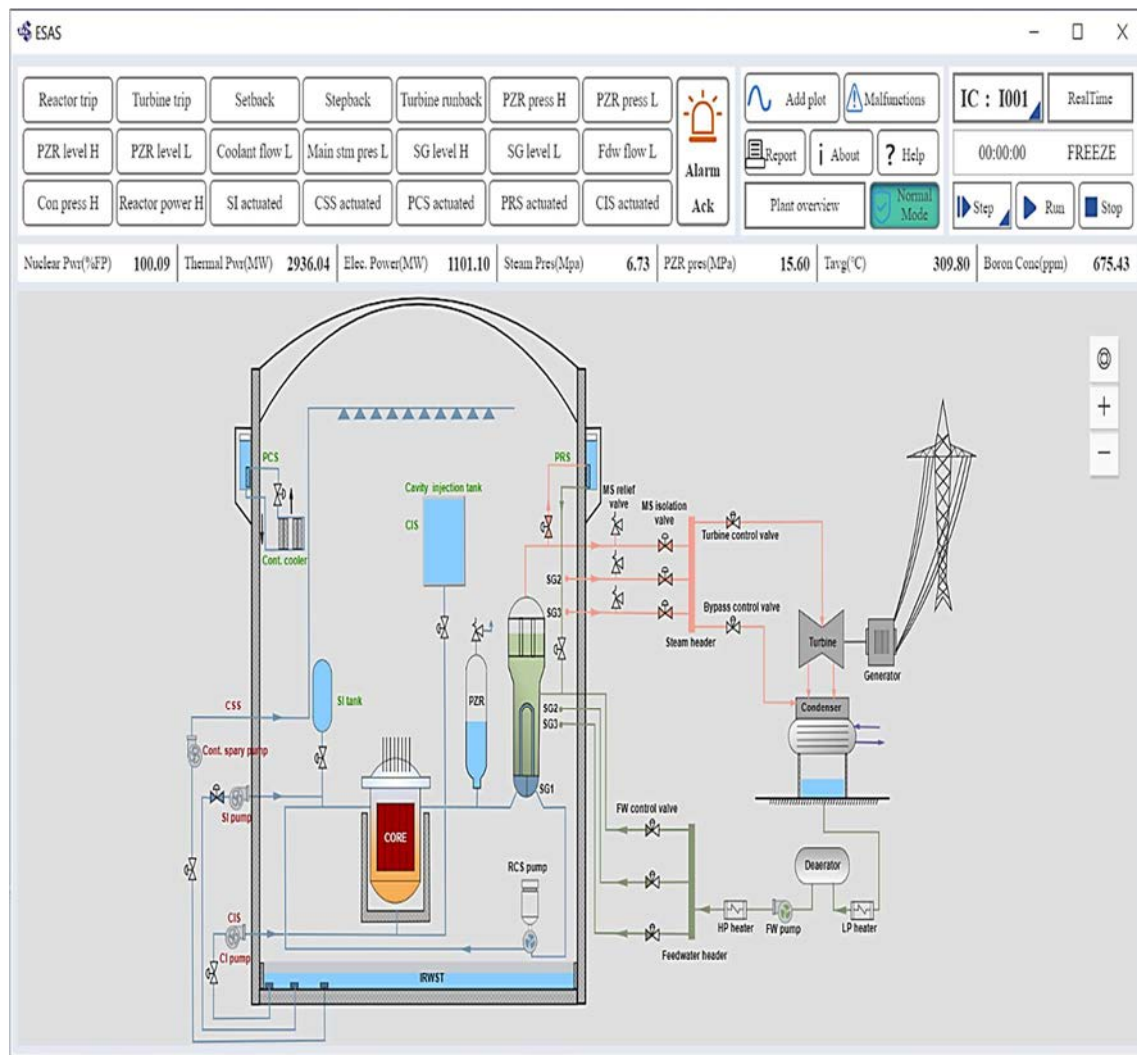


FIG. II-1. Main system screen of ESAS.

II-2. LOAD MANOEUVRING (50% FULL POWER) IN TURBINE LEADING MODE

The ESAS steps and parameters for a load manoeuvring (50 % full power) in turbine mode are shown in Table II-2.

TABLE II-2. DETAILS OF LOAD MANOEUVRING (50% FULL POWER) IN TURBINE LEADING MODE

| No. | Step | GUI sheet | Expected response |
|-----|---|------------------------|--|
| 1 | Load the IC 100% FP | IC | IC loaded successfully |
| 2 | Run simulator | n.a ^a | Simulator time begins to run |
| | Check the following parameters: | | Each parameter is stable near the following value: |
| | 1) Reactor power (% FP) | | 100±2% FP |
| | 2) Turbine generator output (MW) | Fixed column | 1100±5 MW |
| | 3) T _{avg} (°C) | | 310±1°C |
| | 4) PZR pressure (MPa) | | 15.4 ±0.2 MPa |
| | 5) PZR level (m) | Reactor coolant system | 6.6±0.2 m |
| | 6) Feed water flow (kg/s) | | 571±10 kg/s (for each SG) |
| 3 | 7) Steam pressure (MPa) | | 6.7±0.5 MPa |
| | 8) Steam flow (kg/s) | | 571±10 kg/s (for each SG) |
| | 9) SG level (m) | Secondary system | 12.65±0.2 m (for each SG) |
| | 10) Turbine speed (rpm) | | 1500±5 rpm |
| | 11) Turbine bypass valve opening (%) | | 0±1% |
| | 12) R bank position (steps) | | 192±10 steps |
| | 13) G bank overlapping position (steps) | Control rods | 615±7 steps |
| | 14) Boron concentration (ppm) | | 675±20 ppm |
| 4 | Check plant is in “turbine leading” mode | Secondary system | Switch turned to “turbine leading” mode |
| | Start load reduction: | | — Turbine load demand is changed to 550 MW; |
| 5 | 1) Set target load to 550 MW (50% FP); | Secondary | — Turbine load rate becomes 30 MW/min; |
| | 2) Set load reduction rate to 30 MW/min; | | — Turbine generator load starts to decrease. |
| | 3) Release: Press GO button. | | |
| | Check the trend of the following parameter during load reduction: | | |
| | 1) Reactor power | Fixed column | Reactor power starts to decrease |
| | 2) Turbine inlet valve | Secondary system | Turbine inlet valve opening starts to decrease |
| 6 | 3) Steam flow | | Steam flow starts to decrease |
| | 4) Feed water flow | RCS | Feed water flow starts to decrease |
| | 5) T _{avg} | Fixed column | T _{avg} starts to decrease due to T _{ref} being programmed on the secondary load |

TABLE II-2. DETAILS OF LOAD MANOEUVRING (50% FULL POWER) IN TURBINE LEADING MODE (cont.)

| No. | Step | GUI sheet | Expected response |
|-----|---|------------------|--|
| 7 | During turbine load reduction, check that the R bank moves according to the following principle: $\Delta T = T_{avg} - T_{ref}$ <i>If $\Delta T > 0.83^{\circ}\text{C} \rightarrow R$ bank withdraws</i> <i>If $\Delta T < -0.83^{\circ}\text{C} \rightarrow R$ bank inserts</i> | Control rods | R bank moves correctly |
| 8 | If necessary, adjust the boron concentration (BC) to keep the R bank within the manoeuvring band (180 – 204 steps): — If the R bank is near the upper limit (204): Dilution is required, reduce the BC setpoint: 3 – 5 ppm at a time BC change rate of 0.1 – 0.5 ppm/min; — If the R bank is near the lower limit (180): Increasing the boron concentration is required, increase the BC setpoint: 3 – 5 ppm at a time BC change rate of 0.1 – 0.5 ppm/min. Perform these actions until the R bank becomes stable within the ban (180 – 240). It may be helpful to increase the speed of calculations. | Control rods | — Boron concentration adjusted correctly; — R bank stays within the manoeuvring band. |
| 9 | Verify that the load becomes stable near 550 MW | Secondary system | — Turbine generators load stable near 550 MW; — Reactor power stable near 50% FP. |
| | Check the following parameters: | | Each parameter is stable near the following value: |
| | 1) Reactor power (% FP) | | 50±5% FP |
| | 2) Turbine generator output (MW) | Fixed column | 550±10 MW |
| | 3) T_{avg} ($^{\circ}\text{C}$) | | 300±2 $^{\circ}\text{C}$ |
| | 4) PZR pressure (MPa) | | 15.4±0.2 MPa |
| | 5) PZR level (m) | | 4.3±0.5 m |
| 10 | 6) Feed water flow (kg/s) | RCS | 280±20 kg/s (for each SG) |
| | 7) Steam pressure (MPa) | | 6.67±0.1 MPa |
| | 8) Steam flow (kg/s) | Secondary system | 280±20 kg/s (for each SG) |
| | 9) SG level (m) | | 0±0.2 m (for each SG) |
| | 10) R bank position (steps) | | 180 ~ 204 steps |
| | 11) G bank overlapping position (steps) | Control rods | 413±10 steps |
| | 12) Boron concentration (ppm) | | 675±20 ppm |
| 11 | Bring turbine back to 100% FP: 1) Set target load to 1100 MW (100% FP) ; 2) Set load rate to 30 MW/min ; 3) Release: Press GO button. | | — Turbine load demand becomes 1100 MW; — Turbine load rate become 30 MW/min; — Turbine generator load start to rise. |

TABLE II-2. DETAILS OF LOAD MANOEUVRING (50% FULL POWER) IN TURBINE LEADING MODE (cont.)

| No. | Step | GUI sheet | Expected response |
|-----|---|------------------|---|
| 12 | <p>If necessary, adjust the boron concentration (BC) to keep the R bank within the manoeuvring band (180–204 steps):</p> <ul style="list-style-type: none"> — If the R bank is near the upper limit (204): Dilution is required, reduce the BC setpoint: 3 – 5 ppm at a time BC change rate of 0.1–0.5 ppm/min; — If the R bank is near the lower limit (180): Increasing the boron concentration is required, increase the BC setpoint: 3-5 ppm at a time BC change rate of 0.1–0.5 ppm/min. <p>Perform these actions until the R bank becomes stable within the ban (180–240). It may be helpful to increase the speed of calculations.</p> | Control rods | <ul style="list-style-type: none"> — Boron concentration adjusted at set point correctly; — R bank is controlled within manoeuvring band. |
| | Check the trend of the following parameter during load increase: | | |
| 13 | 1) Reactor power | Fixed column | Reactor power starts to rise |
| | 2) PZR level | RCS | PZR level starts to rise following the programmed reference value |
| | 3) Main steam flow | Secondary system | Main steam flow starts to rise |
| | 4) G bank overlapping steps | | G bank position start to rise |
| | 5) T_{avg} | Control rods | T_{avg} starts to rise following T_{ref} programmed by the R bank movement or change in boron concentration |
| 14 | When the turbine generator load reaches the target set point, check the following parameters: | | Each parameter is stable near the following value: |
| | 1) Reactor power (% FP) | Fixed column | 100±2% FP |
| | 2) Turbine generator output (MW) | | 1100±5 MW |
| | 3) T_{avg} (°C) | | 310±2°C |
| | 4) PZR pressure (MPa) | | 15.4±0.2 MPa |
| | 5) PZR level (m) | RCS | 6.88±0.2 m |
| | 6) Feed water flow (kg/s) | | 571±10 kg/s (for each SG) |
| | 7) Steam pressure (MPa) | | 6.7±0.2 MPa |
| | 8) Steam flow (kg/s) | Secondary system | 571±10 kg/s (for each SG) |
| | 9) SG level (m) | | 12.65±0.2 m (for each SG) |
| | 10) R bank position (steps) | | 192±10 steps |
| | 11) G bank overlapping position (steps) | Control rods | 615±7 steps |
| | 12) Boron concentration (ppm) | | 675±20 ppm |

Figure II–2 shows the secondary circuit system which consists of a window for changing the turbine leading mode.

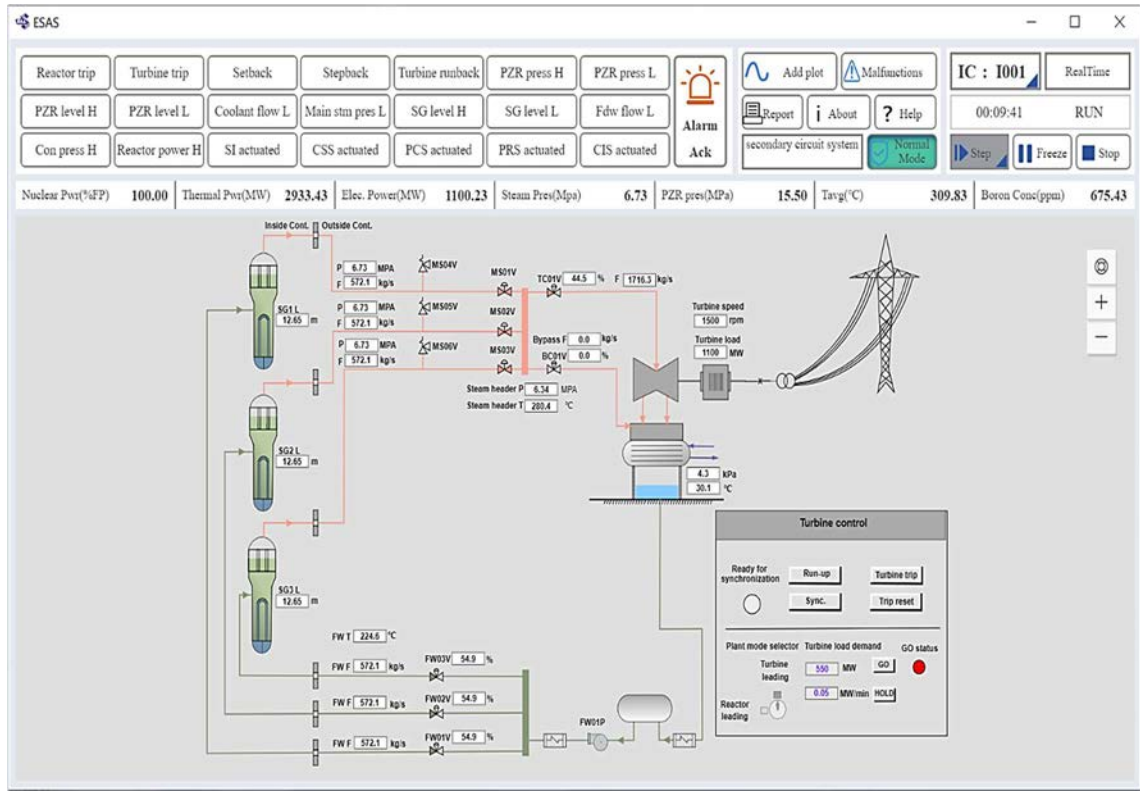


FIG. II–2. Power reduction (turbine leading mode) from 100% to 50%.

II-3. LOAD MANOEUVRING (50% FP) IN REACTOR LEADING MODE

The ESAS steps and parameters for a load manoeuvring (50 % full power) in reactor leading mode are shown in Table II-3.

TABLE II-3. DETAILS OF LOAD MANOEUVRING (50% FP) IN REACTOR LEADING MODE

| No. | Step | GUI sheet | Expected response |
|-----|---|----------------------------------|---|
| 1 | Load a 100% FP IC | IC | IC loaded successfully |
| 2 | Put simulator in running | Run/Freeze | Run state shown and simulator time begins |
| 3 | Check the following parameters: | | Each parameter is stable near the following value: |
| | 1) Reactor power (% FP) | Fixed column | 100±2% FP |
| | 2) Turbine generator electric output (MW) | | 1100±5 MW |
| | 3) T_{avg} (°C) | | 310±1°C |
| | 4) PZR pressure (MPa) | | 15.4±0.2 MPa |
| | 5) PZR level (m) | Reactor coolant system | 6.88±0.2 m |
| | 6) Feed water flow (kg/s) | | 571±10 kg/s (for each SG) |
| | 7) Steam pressure (MPa) | Secondary system | 6.7±0.2 MPa |
| | 8) Steam flow (kg/s) | | 571±10 kg/s (for each SG) |
| | 9) SG level (m) | | 12.65±0.2 m (for each SG) |
| | 10) Turbine speed (rpm) | | 1500±5 rpm |
| | 11) Turbine bypass valve opening (%) | | 0±2% |
| | 12) R bank position (steps) | Control rods | 192±10 steps |
| | 13) G bank overlapping position (steps) | | 615±7 steps |
| | 14) Boron concentration (ppm) | | 675±20 ppm |
| 4 | Change plant to “Reactor leading” mode | Control rods | Switch to “Reactor leading” mode |
| 5 | Start power reduction: | | — Reactor power demand become 50% FP; |
| | 1) Set target power at (50% FP) ; | Secondary | — Reactor power rate become 3% FP/min; |
| | 2) Set power reduction rate at 3% FP/min ; | | — Reactor power starts to decrease according to required rate. |
| 6 | Check the trend of each parameter during power reduction: | Fixed column Secondary system | — G bank starts to insert; |
| | | | — Turbine generator load starts to decrease along with reactor power reduction; |
| | | | — Steam flow starts to decrease; |
| | | | — Feed water flow starts to decrease; |
| 7 | During turbine load reduction, check R bank moving automatically according to the deviation that $T_{ref}-T_{avg}$ ($\Delta T > 0.83^\circ\text{C}$, withdrawing ; $\Delta T < 0.83^\circ\text{C}$ inserting) | Control rods | — T_{avg} starts to decrease along with T_{ref} programmed on secondary load. |
| | | | R bank moves correctly |

TABLE II-3. DETAILS OF LOAD MANOEUVRING (50% FP) IN REACTOR LEADING MODE (cont.)

| No. | Step | GUI sheet | Expected response |
|-----|--|-----------------|--|
| 8 | If necessary, adjust BC to maintain R bank within manoeuvring band (180-204 steps): | Fixed column | <ul style="list-style-type: none"> — Boron concentration adjusted at set point correctly ; — R bank is controlled within manoeuvring band. |
| | <ul style="list-style-type: none"> — If R bank withdraw near high limit (204), perform dilution: Reduce BC set point (3-5 ppm for each time): and set a proper BC rate (0.1-0.5 ppm/min recommended), until R bank become stable within band; — If R bank inserts near low limit (180), perform boration: Increase BC set point (3-5 ppm for each time) ;and set a proper BC rate (0.1-0.5 ppm/min recommended), until R bank become stable within band. | | |
| 9 | When reactor power decreases to 50% FP , verify reactor power become stable | Control rod | <ul style="list-style-type: none"> — Reactor power stable near 50% FP; — Turbine generator load stable near 550 MW. |
| 10 | Check the following parameters: | Fixed column | Each parameter is stable near the following value: |
| | 1) Reactor power (% FP) | | 50±2% FP |
| | 2) Turbine generator electric output (MW) | | 550±5 MW |
| | 3) T _{avg} (°C) | | 300±2 °C |
| | 4) PZR pressure (MPa) | | 15.4±0.2 MPa |
| | 5) PZR level (m) | Reactor coolant | 4.3±0.5 m |
| | 6) Feed water flow (kg/s) | system | 280±20 kg/s (for each SG) |
| | 7) Steam pressure (MPa) | Secondary | 6.7±0.2 MPa |
| | 8) Steam flow (kg/s) | | 280 kg/s (for each SG) |
| | 9) SG level (m) | Control rods | 12.65±0.2 m (for each SG) |
| | 10) R bank position (steps) | | 180~204 steps |
| | 11) G bank overlapping position (steps) | | 413±7 steps |
| | 12) Boron concentration (ppm) | | 675±80 ppm |
| 11 | Bring reactor back to 100%FP: | | — Reactor power demand become 100% FP; |
| | 1) Set target power at 100% FP ; | | — Reactor power rate become 3% FP/min; |
| | 2) Set power rate at 3% FP/min ; | | — Reactor power starts to rise according to required rate. |
| 12 | 3) Release : push button GO. | Control rods | <ul style="list-style-type: none"> — Boron concentration adjusted at set point correctly — R bank is controlled within manoeuvring band. |
| | If necessary, adjust BC to maintain R bank within manoeuvring band (180-204 steps) during increasing load: | | |
| 12 | <ul style="list-style-type: none"> — If R bank withdraw near high limit (204), perform dilution, reduce BC set point (3-5ppm for each time) and set a proper BC rate (0.1-0.5 ppm/min recommended), until R bank become stable within band; — If R bank inserts near low limit (180), perform boration: increase BC set point (3-5 ppm for each time) and set a proper BC rate (0.1-0.5 ppm/min recommended), until R bank become stable within band. | | |
| | | | |

TABLE II-3. DETAILS OF LOAD MANOEUVRING (50% FP) IN REACTOR LEADING MODE (cont.)

| No. | Step | GUI sheet | Expected response |
|-----|---|----------------------------------|--|
| 13 | Check the trend of each parameter during power rising: | Fixed column Secondary system | — G bank position start to rise; |
| | | | — Turbine generator load starts to rise; |
| | | | — Main steam flow starts to rise; |
| | | | — T_{avg} starts to rise following the T_{ref} by R bank movement or boron concentration change; |
| | | | — PZR level starts to rise following the programmed reference value. |
| 14 | When turbine generator load reach target set point, check the following parameters: | Fixed column Secondary System | Each parameter is stable near the following value: |
| | 1) Reactor power (% FP) | | 100% FP |
| | 2) Turbine generator electric output (MW) | Fixed column | 1100 MW |
| | 3) T_{avg} (°C) | | 310°C |
| | 4) PZR pressure (MPa) | | 15.4 MPa |
| | 5) PZR level (m) | Reactor coolant system | 6.88 m |
| | 6) Feed water flow (kg/s) | | 571 kg/s (for each SG) |
| | 7) Steam pressure (MPa) | | 6.7 MPa |
| | 8) Steam flow (kg/s) | Secondary system | 571 kg/s (for each SG) |
| | 9) SG level (m) | | 12.65 m (for each SG) |
| | 10) R bank position (steps) | | 192 steps |
| | 11) G bank overlapping position (steps) | Control rods | 615 steps |
| | 12) Boron concentration (ppm) | | 675 ppm |

Figure II–3 shows the secondary circuit system which consists of a window for changing the reactor leading mode.

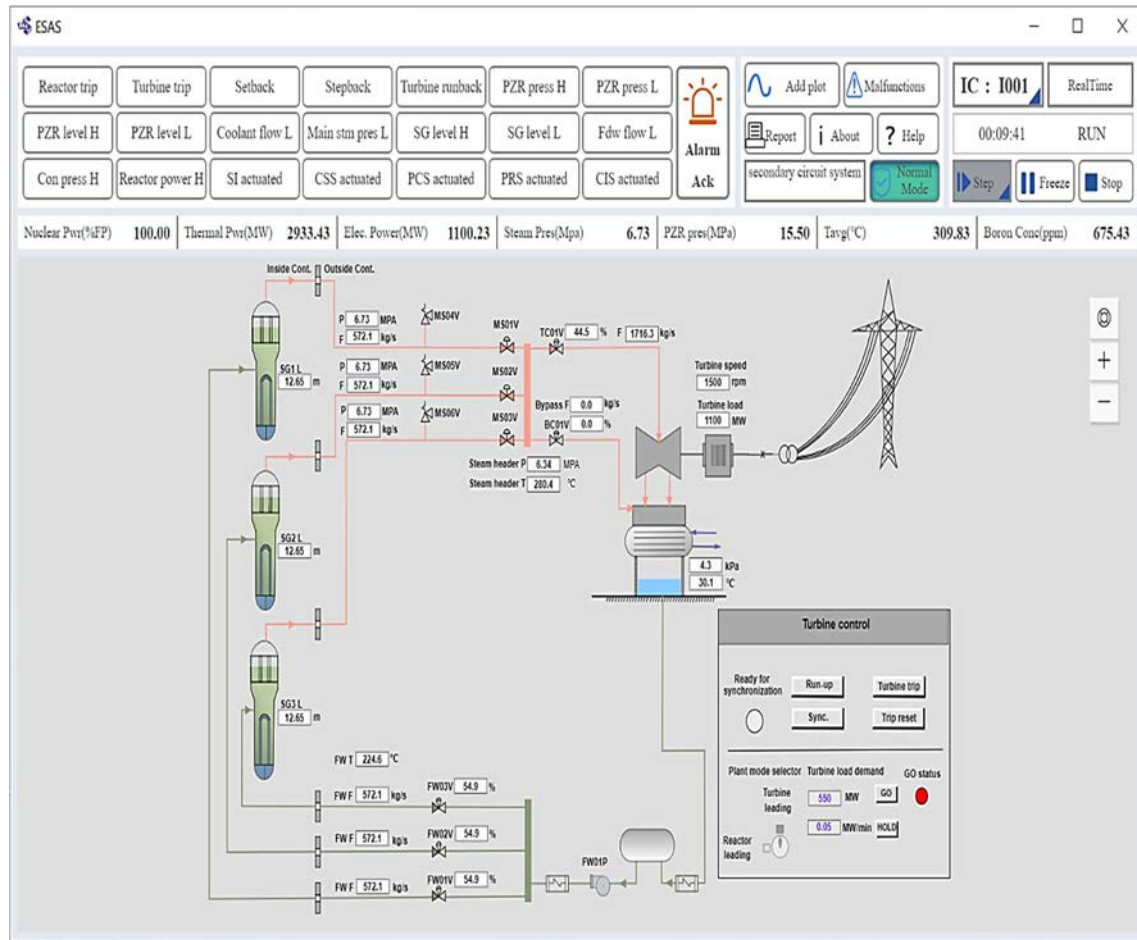


FIG. II–3. Power reduction (reactor leading mode) from 100% to 50%.

II-4. REACTOR POWER DECREASE FROM 100% FP TO HOT SHUTDOWN CONDITION

The ESAS steps and parameters for reducing reactor power from 100% FP to hot shutdown condition mode are shown in Table II-4.

TABLE II-4. DETAILS OF REACTOR POWER DECREASE FROM 100% FP TO HOT SHUTDOWN CONDITION

| No. | Step | GUI sheet | Expected response |
|-----|--|------------------|---|
| 1 | Load a 100% FP IC | IC | IC loaded successfully |
| 2 | Put simulator in running | Run/Freeze | Run state shown and simulator time begins |
| 3 | Check the following parameters: | | Each parameter is stable near the following value : |
| | 1) Reactor power (% FP) | Fixed column | 100±2% FP |
| | 2) Turbine generator electric output (MW) | | 1100±5 MW |
| | 3) T _{avg} (°C) | | 310±1°C |
| | 4) PZR pressure (MPa) | | 15.4±0.2 MPa |
| | 5) PZR level (m) | Reactor coolant | 6.6±0.2 m |
| | 6) Feed water flow (kg/s) | system | 571±10 kg/s (for each SG) |
| | 7) Steam pressure (MPa) | Secondary system | 6.7±0.5 MPa |
| | 8) Steam flow (kg/s) | | 571±10 kg/s (for each SG) |
| | 9) SG level (m) | | 12.65±0.2 m (for each SG) |
| | 10) Turbine speed (rpm) | | 1500±5 rpm |
| | 11) Turbine bypass valve opening (%) | | 0±1% |
| | 12) R bank position (steps) | Control rods | 192±10 steps |
| | 13) G bank overlapping position (steps) | | 615±7 steps |
| | 14) Boron concentration (ppm) | | 675±20 ppm |
| 4 | Check plant control state: | | |
| | 1) Change to “turbine” mode; | Control rods | — switch to “turbine” mode; |
| | 2) G bank in auto control mode; | | — G bank mode selector in AUTO Switch; |
| | 3) R bank in auto control mode; | | — R bank mode selector in AUTO; |
| | 4) Feedwater control valve in auto control; | | — Feedwater valve in auto state; |
| | 5) Turbine bypass control valve in auto control; | Secondary system | — Bypass valve in auto state; |
| | 6) There is no alarm. | | — No alarm. |
| 5 | Start load reduction: | | — Turbine load demand become |
| | 1) Set target load at 110 MW (10% FP); | Secondary system | 110 MW; |
| | 2) Set load reduction rate at 30 MW/min; | | — Turbine load rate become |
| | 3) Release : push button GO. | | 30 MW/min; |
| | | | — Turbine load starts to decrease. |

TABLE II-4. DETAILS OF REACTOR POWER DECREASE FROM 100% FP TO HOT SHUTDOWN CONDITION (cont.)

| No. | Step | GUI sheet | Expected response |
|-----|--|----------------------------------|---|
| 6 | Check the parameters trend during load reduction: | | |
| | 1) Turbine inlet valve starts to close due to turbine load control system; | Fixed column Secondary system | — Turbine inlet valve opening starts to decrease; |
| | 2) G bank starts to insert due to reactor power control system along with turbine load; | | — G bank starts to insert; |
| | 3) T_{avg} starts to decrease and matched with T_{ref} programmed according to turbine load by R bank; | | — Reactor power starts to decrease |
| | 4) PZR level starts to decrease and matched with reference level programmed according to T_{avg} by charging flow. | | — Feed water flow starts to decrease; |
| | | | — T_{avg} starts to decrease along with T_{ref} programmed on secondary load; |
| | | | — PZR level starts to decrease. |
| 7 | During turbine load reduction, check R bank moving automatically according to the deviation that $T_{ref}-T_{avg}$ (if $\Delta T > 0.83^{\circ}\text{C}$, R bank would withdraw automatically; if $\Delta T < -0.83^{\circ}\text{C}$, R bank would insert automatically) | Control rods | — R bank moves correctly |
| 8 | If necessary, adjust BC to maintain R bank within manoeuvring band (180-204 steps): | | |
| | — If R bank withdraw near high limit (204), perform dilution: Reduce BC set point (3-5 ppm for each time); and set a proper BC rate (0.1-0.5 ppm/min recommended), until R bank become stable within band; | Control rods | — Boron concentration adjusted at set point correctly: |
| | — If R bank inserts near low limit (180), perform boration: Increase BC set point (3-5 ppm for each time); and set a proper BC rate (0.1-0.5 ppm/min recommended), until R bank become stable within band. | | — R bank is controlled within manoeuvring band. |
| 9 | When turbine generator load decreases to 110 MW (10% FP), check load stable | Control rods | — Turbine generator load stable near 110 MW; — Reactor power stable near 11% FP; — 'Fdw Flow L' alarm activate. |
| 10 | Check the following parameters: | | |
| | Each parameter is stable near the following value : | | |
| | 1) Reactor power (% FP) | Fixed column | 11% FP |
| | 2) Turbine generator electric output (MW) | | 110 MW |
| | 3) T_{avg} ($^{\circ}\text{C}$) | | 293.2 $^{\circ}\text{C}$ |
| | 4) PZR pressure (MPa) | | 15.4 MPa |
| | 5) PZR level (m) | Reactor coolant system | 2.38 m |
| | 6) Feed water flow (kg/s) | | 57.1 kg/s (for each SG) |
| | 7) Steam pressure (MPa) | Secondary system | 7.4 MPa |
| | 8) Steam flow (kg/s) | | 57.1 kg/s (for each SG) |
| | 9) SG level (m) | | 12.36 m (for each SG) |
| | 10) R bank position (steps) | Control rods | 180~204 steps |
| | 11) G bank overlapping position (steps) | | 331 steps |
| | 12) Boron concentration (ppm) | | 675 ppm |

TABLE II-4. DETAILS OF REACTOR POWER DECREASE FROM 100% FP TO HOT SHUTDOWN CONDITION (cont.)

| No. | Step | GUI sheet | Expected response |
|-----|--|----------------------------------|--|
| 11 | Uncouple reactor and turbine : | Control rods | — |
| | 1) Adjust G bank set point at current step; | | — G bank setpoint become 331 steps; |
| | 2) Adjust R bank set point at current step; | | — R bank setpoint become 190 steps; |
| | 3) Put G bank in manual mode; | | — G bank in manual mode; |
| 12 | 4) Put R bank in manual mode. | Secondary system Control rods | — R bank in manual mode. |
| | Continue to reduce turbine generator load: | | — Turbine generator load continue to decrease; |
| | 1) Set turbine load at 50 MW (5% FP) ; | | — Reactor power still stable at 11% FP; |
| | 2) Set load reduction rate at 30 MW/min; | | — G bank does not move; |
| 13 | 3) Release : push button GO. | Control rods | — Turbine bypass valve would start to open. |
| | During load reduction, maintain T_{avg} at T_{ref} by | | — Boron concentration changed correctly; |
| | adjusting boron concentration (refer to step 8), | | — Reactor power always stable at 11% FP. |
| | and maintain reactor power near 11% FP | | — |
| 14 | When turbine generator load reach 50 MW, manually trip the turbine: Push turbine trip button | Secondary system Control rods | — Turbine inlet valve fully closed; |
| | | | — Turbine generator load drop to 0 MW; |
| | | | — Reactor power still stable at 11% FP; |
| | | | — Turbine bypass valve further opens; |
| 15 | Bring reactor to hot standby state (2% FP): Continue to insert G bank by manual: Reduce G bank setpoint manually | Control rods | — Turbine trip alarm activated; |
| | | | — Turbine speed starts to decrease and would be stable at 5 rpm finally. |
| | | | — G bank overlapping steps starts to decrease; |
| | | | — Reactor power continue to decrease. |
| 16 | When reactor power reduced to 2% FP: Stop inserting G bank | Control rods | — |
| | | | — Reactor power stable at 2% FP |
| | | | — |
| | | | — |
| 17 | Bring reactor to hot shutdown state (0% FP and subcritical): 1) Continue to insert G bank by manual: Set G bank overlapping setpoint at 0 steps; | Control rods | — G bank starts to move to the bottom (5 steps for each rod group); |
| | | | — Reactor power continue to decrease to 0% FP; |
| | | | — R bank starts to move to the bottom (5 steps); |
| | | | — Boron concentration starts to rise and would be stable at 950 ppm finally. |
| | 2) Insert R bank by manual: Set R bank setpoint at 5 steps; | | |
| | | | |
| | | | |
| | | | |
| | 3) Perform boration to 950 ppm: Adjust BC setpoint at 950 ppm; Adjust BC rate at 1 ppm/min. | | |
| | | | |
| | | | |
| | | | |

TABLE II-4. DETAILS OF REACTOR POWER DECREASE FROM 100% FP TO HOT SHUTDOWN CONDITION (cont.)

| No. | Step | GUI sheet | Expected response |
|-----|--|------------------|---|
| | Wait for stable state of the following parameters: | | Each parameter stable near the following values : |
| | 1) Reactor power (% FP) | | 0% FP |
| | 2) Turbine generator electric output (MW) | | 0 MW |
| | 3) T_{avg} (°C) | Fixed column | 291.4°C |
| | 4) PZR pressure (MPa) | | 15.4 MPa |
| 18 | 5) PZR level (m) | Reactor coolant | 1.97 m |
| | 6) Feed water flow (kg/s) | system | <20 kg/s (for each SG) |
| | 7) Steam pressure (MPa) | | 7.5 MPa |
| | 8) Steam flow (kg/s) | Secondary system | <20 kg/s (for each SG) |
| | 9) SG level (m) | | 12.1 m (for each SG) |
| | 10) R bank position (steps) | | 5 steps |
| | 11) G bank overlapping position (steps) | Control rods | 0 steps |
| | 12) Boron concentration (ppm) | | 950 ppm |
| 19 | Based on the check of step 18, reactor hot shutdown state can be confirmed | n.a. | Hot shutdown state reached |

The secondary circuit system also consists of a window for setting the target power and target rate as shown in Figure II-4.

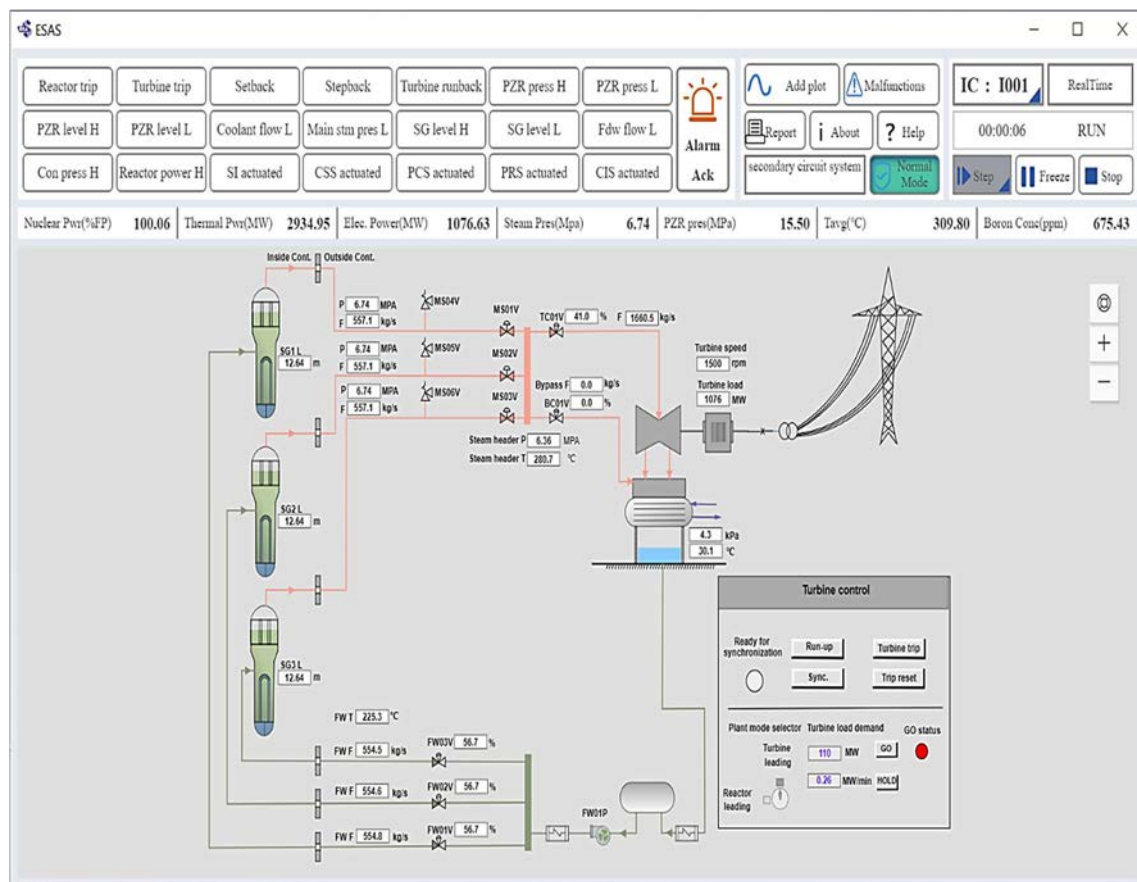


FIG. II-4. Reactor power reduction decrease from 100% FP to hot shutdown condition.

II-5. REACTOR POWER RISE FROM HOT SHUTDOWN CONDITION TO 100% FP

The ESAS steps and parameters for increasing reactor power from hot shutdown condition to 100% FP mode are shown in Table II-5.

TABLE II-5. DETAILS OF REACTOR POWER RISE FROM HOT SHUTDOWN CONDITION TO 100% FP

| No. | Step | GUI sheet | Expected response |
|-----|--|------------------------|---|
| 1 | Load a “hot shutdown state” IC | IC | IC loaded successfully |
| 2 | Put simulator in running | Run/Freeze | Run state shown and simulator time begins |
| 3 | Check the following parameters: | | Each parameter is stable near the following value : |
| | 1) Reactor power (% FP) | Fixed column | 0% FP |
| | 2) Turbine generator electric output (MW) | | 0 MW |
| | 3) T _{avg} (°C) | | 291.4°C |
| | 4) PZR pressure (MPa) | | 15.4 MPa |
| | 5) PZR level (m) | Reactor coolant | 1.97 m |
| | 6) Feed water flow (kg/s) | system | <20 kg/s (for each SG) |
| | 7) Steam pressure (MPa) | Secondary system | 6.7 MPa |
| | 8) Steam flow (kg/s) | | <20 kg/s (for each SG) |
| | 9) SG level (m) | | 12.1 m (for each SG) |
| | 10) Turbine speed (rpm) | | 0 rpm |
| | 11) Turbine bypass valve opening (%) | | <2% |
| | 12) S bank position (steps) | Control rods | 225 steps |
| | 13) R bank position (steps) | | 5 steps |
| | 14) G bank overlapping position (steps) | | 0 steps |
| | 15) Boron concentration (ppm) | | 855±50 ppm |
| | 16) Reactivity (pcm) | | <3000 pcm |
| 4 | Check the control systems state: | | |
| | 1) Change to “Turbine leading” mode; | Control rods | — Switch to “turbine leading” mode; |
| | 2) G bank in manual control mode; | | — G bank mode selector in MANUAL; |
| | 3) R bank in manual control mode; | | — R bank mode selector in MANUAL; |
| | 4) Feed water control valve in auto control; | Secondary system | — Feed water valve in auto state; |
| | 5) Turbine bypass valve in auto control; | Reactor coolant system | — Bypass valve in auto state; |
| | 6) PZR pressure control in auto mode; | | — PZR spray valve and heaters in AUTO; |
| | 7) PZR level control in auto mode. | | — PZR level control mode switch to AUTO. |
| 5 | Reactor start-up to critical state: Push reactor RESTART button | | — G bank overlapping position initiated to 315 steps; |
| | | | — R bank position initiated to 190 steps; |
| | | | — Reactivity rises (still negative); |
| | | | — About 10 s later, boron concentration initiated to critical value (upon the xenon state); |
| | | | — Reactivity rises to critical value (positive and about 0 pcm). |

TABLE II-5. DETAILS OF REACTOR POWER RISE FROM HOT SHUTDOWN CONDITION TO 100% FP (cont.)

| No. | Step | GUI sheet | Expected response |
|-----|---|--|---|
| 6 | Start to increase reactor power: 1) Withdraw G bank: Adjust G bank set point (add 3 steps and wait several minutes for each time, then repeat the operation until reactivity stable at a positive value). | Control rods | — G bank position starts to rise; — Reactivity rises to a positive value and stable (at 49 pcm recommended). |
| | | | |
| 7 | Wait for 10-20 minutes, check the reactor power level by nuclear power | Fixed column Control rods Secondary system | — Nuclear power indication starts to rise from 0; — T_{avg} starts to rise; — Reactivity starts to decrease; — Turbine bypass valve further opens. |
| 8 | Bring reactor to hot standby state (2% FP): 1) When reactor power rises to 2% FP, stop withdrawing G bank (if exceeding 2% FP, insert G bank by several steps). | Control rods | — Reactor power stable at approximately 2% FP; — Reactivity near 0 pcm (± 5 pcm); — T_{avg} stable at approximately 292.5°C. |
| | | | |
| 9 | Continue to increase reactor power to 8% FP: 1) Withdraw G bank: Adjust G bank set point (add 3 steps and wait several minutes for each time). | Control rods | — G bank overlapping position rises; — Reactivity rises to a positive value, then decreases slowly; — Nuclear power indication continues to rise; — T_{avg} continue to rise; — Turbine bypass valve further opens. |
| 10 | When reactor power rises to 8% FP, stop withdrawing G bank (if exceeding 8% FP too much, insert G bank by several steps) | Fixed column | — Reactor power stable at approximately 8% FP; — Reactivity near 0 pcm (± 5 pcm); — T_{avg} stable at approximately 295°C. |
| 11 | Turbine speed-up: a) Reset turbine trip signal: Push trip reset button. b) Start turbine speed-up: Push Run-up button. | Secondary system | — Turbine trip alarm disappears — Turbine speed starts to rise and stable at 1500 rpm finally |
| | | | |
| 12 | Continue to increase reactor power to 15% FP: Check G bank overlapping step and request steps: 1) If overlapping step is higher than request value, decrease BC: Adjust BC set point (reduce set point by 3 ppm and wait several minutes for each time); 2) Otherwise, withdraw G bank: Adjust G bank set point (add 3 steps and wait several minutes for each time, then repeat the operation). | Control rods | — G bank overlapping position rises or BC decreases; — Reactivity rises to a positive value, then decreases slowly; — Nuclear power indication continues to rise; — T_{avg} continue to rise; — Turbine bypass valve further opens. |
| | | | |

TABLE II–5. DETAILS OF REACTOR POWER RISE FROM HOT SHUTDOWN CONDITION TO 100% FP (cont.)

| No. | Step | GUI sheet | Expected response |
|-----|---|---|---|
| 13 | When reactor power rises to 15% FP, stop withdrawing G bank (if exceeding 15% FP too much, insert G bank by several steps) or adjusting BC set point (if exceeding 15% FP too much, increase BC set point by several ppm) | Control rods | <ul style="list-style-type: none"> — Reactor power stable at approximately 15% FP; — Reactivity near 0 pcm (± 5 pcm); — T_{avg} stable at approximately 296.3°C. |
| 14 | <p>Synchronization:</p> <ol style="list-style-type: none"> 1) Check synchronization indicator; 2) Push sync. Button. | Secondary system | <ul style="list-style-type: none"> — Lamp of ready for synchronization light; — Generator outgoing break closed automatically; — Generator have a minimum load (approximately 50 MW); — Turbine bypass valve opening decreases automatically. |
| 15 | <p>Increase turbine generator load, and ready to changeover G bank and R bank to auto mode:</p> <ol style="list-style-type: none"> 1) Increase turbine generator load; 2) Set turbine load demand at 150 MW; 3) Set load rate at 30 MW/min; 4) Release : push GO button. | <p>Secondary system</p> <p>Control rods</p> | <ul style="list-style-type: none"> — Turbine load starts to rise ; — G bank request step starts to rise; — T_{ref} value starts to rise; — Turbine bypass valve opening further decreases automatically. |
| 16 | <p>When G bank request step become near the overlapping step and T_{ref} become near T_{avg}:</p> <ol style="list-style-type: none"> 1) Changeover G bank to auto mode; 2) Changeover R bank to auto mode. | Control rods | <ul style="list-style-type: none"> — G bank in auto mode; — R bank in auto mode; — G bank request step near overlapping step (deviation <3 steps); — T_{ref} near T_{avg} (deviation < 0.9°C). |
| 17 | <p>Continue increase turbine load to 100% FP:</p> <ol style="list-style-type: none"> 1) Increase turbine generator load; 2) Set turbine load demand at 1100 MW; 3) Set load rate at 30 MW/min; 4) Release : push GO button. | Control rods | <ul style="list-style-type: none"> — Turbine load starts to rise; — G bank overlapping steps rises automatically; — T_{ref} starts to rise and T_{avg} is controlled by T_{ref}; — Turbine bypass valve opening decreases to 0%. |
| 18 | <p>During turbine load increasing, check R bank moving automatically according to the deviation that $T_{ref}-T_{avg}$ ($\Delta T > 0.83^\circ\text{C}$, withdrawing ; $\Delta T < 0.83^\circ\text{C}$, inserting)</p> | Control rods | <ul style="list-style-type: none"> — R bank moves correctly |
| 19 | <p>If necessary, adjust BC to maintain R bank within manoeuvring band (180-204 steps):</p> <ol style="list-style-type: none"> 1) If R bank withdraw near high limit (204), perform dilution: Reduce BC set point (3-5 ppm for each time); and set a proper BC rate (0.1-0.5 ppm/min recommended), until R bank become stable within band; 2) If R bank inserts near low limit (180), perform boration: Increase BC set point (3-5 ppm for each time); and set a proper BC rate (0.1-0.5 ppm/min recommended), until R bank become stable within band. | Control rod | <ul style="list-style-type: none"> — Boron concentration adjusted at set point correctly; — R bank is controlled within manoeuvring band. |

TABLE II-5. DETAILS OF REACTOR POWER RISE FROM HOT SHUTDOWN CONDITION TO 100% FP (cont.)

| No. | Step | GUI sheet | Expected response |
|---|---|--|---|
| 20 | Check the following auto control: | | — PZR level rises and maintained near reference value programmed based on T_{avg} ; |
| | 1) PZR level control; | | — Feed water flow rises along with turbine load; |
| | 2) Feed water flow control; | | — PZR pressure always controlled 15.4 MPa. |
| | 3) PZR pressure control. | | |
| When turbine load reach 1100MW, check the following parameters: | | All parameters stable at the following values: | |
| 21 | 1) Reactor power (% FP) | | 100±2% FP |
| | 2) Turbine generator electric output (MW) | Fixed column | 1100±5 MW |
| | 3) T_{avg} (°C) | | 310±1°C |
| | 4) PZR pressure (MPa) | | 15.4±0.2 MPa |
| | 5) PZR level (m) | Reactor coolant system | 6.6±0.2 m |
| | 6) Feed water flow (kg/s) | | 571±10 kg/s (for each SG) |
| | 7) Steam pressure (MPa) | Secondary system | 6.7±0.2 MPa |
| | 8) Steam flow (kg/s) | | 571±10 kg/s (for each SG) |
| | 9) SG level (m) | | 12.65±0.2 m (for each SG) |
| | 10) R bank position (steps) | Control rods | 180~204 steps |
| | 11) G bank overlapping position (steps) | | 615 steps |
| | 12) Boron concentration (ppm) | | 600-900 ppm |

Figure II-5 shows the control rods and reactivity screen which consists of reactor power control window.

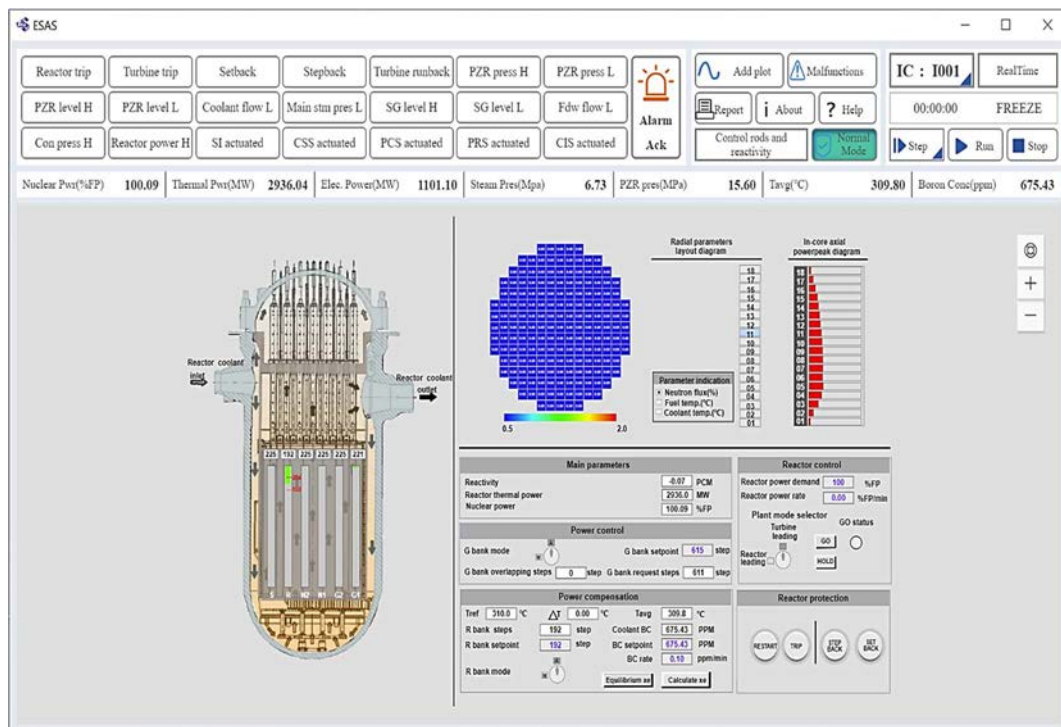


FIG. II-5. Reactor power rise from hot shutdown to 100% FP.

SIMULATOR EXERCISES FOR MALFUNCTION AND TRANSIENT EVENTS

This section contains the exercises for users to practice the operations under malfunction or accident conditions and help them to further understand the principle of reference nuclear power plant (PWR). The following exercises are described:

- 1) Spurious turbine trip and recovery;
- 2) Turbine runback;
- 3) Reactor trip and restart;
- 4) Loss of feed water;
- 5) PZR safety valve groupstuck at open;
- 6) One reactor coolant pump trip;
- 7) Steam line break outside containment (MSLB);
- 8) Steam generator tube rupture (SGTR);
- 9) Primary break (LOCA).

II-6. SPURIOUS TURBINE TRIP AND RECOVERY

The ESAS steps and parameters for spurious turbine trip and recovery are shown in Table II-6.

TABLE II-6. DETAILS OF SPURIOUS TURBINE TRIP AND RECOVERY

| No. | Step | GUI sheet | Expected response |
|-------------------------------|---|------------------------|--|
| 1 | Load a 100% FP IC | IC | IC loaded successfully |
| 2 | Put simulator in running | Run/Freeze | Run state shown and simulator time begins |
| 3 | Check the following parameters: | | Each parameter is stable near the following value: |
| | 1) Reactor power (% FP) | Fixed column | 100±2% FP |
| | 2) Turbine generator electric output (MW) | | 1100±5 MW |
| | 3) T _{avg} (°C) | | 310±1°C |
| | 4) PZR pressure (MPa) | | 15.4±0.2 MPa |
| | 5) PZR level (m) | Reactor coolant | 6.6±0.2 m |
| | 6) Feed water flow (kg/s) | system | 571±10 kg/s (for each SG) |
| | 7) Steam pressure (MPa) | Secondary system | 6.7±0.5 MPa |
| | 8) Steam flow (kg/s) | | 571±10 kg/s (for each SG) |
| | 9) SG level (m) | | 12.65±0.2 m (for each SG) |
| | 10) Turbine speed (rpm) | | 1500±5 rpm |
| | 11) Turbine bypass valve opening (%) | | 0±1% |
| | 12) R bank position (steps) | Control rods | 192±10 steps |
| | 13) G bank overlapping position (steps) | | 615±7 steps |
| 14) Boron concentration (ppm) | 675±20 ppm | | |
| 4 | Check the following control state: | | |
| | 1) Change to “turbine leading” mode; | Control rods | — Switch to “turbine leading” mode; |
| | 2) G bank in auto control mode; | | — G bank mode selector in AUTO; |
| | 3) R bank in auto control mode; | | — R bank mode switch to AUTO; |
| | 4) Feed water flow valve in auto control; | Secondary system | — Feed water valve in auto state; |
| | 5) Turbine bypass valve in auto control; | Reactor coolant system | — Bypass valve in auto state; |
| | 6) PZR pressure control in auto mode; | | — PZR spray valve and heaters in AUTO; |
| | 7) PZR level control in auto mode. | | — PZR level control mode switch to AUTO. |

TABLE II–6. DETAILS OF SPURIOUS TURBINE TRIP AND RECOVERY (cont.)

| No. | Step | GUI sheet | Expected response |
|---|---|---------------------------------|---|
| 5 | Push turbine trip button or insert “turbine trip” malfunction | Secondary system Malfunction | — Turbine generator load drops to 0 MW; |
| | | | — Generator outgoing breaker opened; |
| | | | — Turbine trip alarm appears; |
| | | | — Turbine speed starts to decrease. |
| 6 | Verify steam flow and turbine bypass system: | Secondary system | — Steam flow rises fast after dropping, then starts to decrease smoothly; |
| | | | — Turbine bypass valve quickly opened and then closing slowly. |
| 7 | Verify reactor power reduction: 1) G bank request position drops to 366 steps (programmed at 30% FP); 2) Reactor power is decreasing to 30% FP. | Control rods | — G bank starts to insert and stop at approximately 366 steps finally; |
| | | | — Nuclear power indication starts to decrease and stable at approximately 30% FP. |
| | | | |
| 8 | Verify T _{avg} and PZR during reactor power decreasing: | Control rods | — T _{avg} start to decrease tracing T _{ref} ; |
| | | | — PZR level starts to decrease tracing the reference programmed on T _{avg} ; |
| | | | — PZR pressure is stabilized at 15.4 MPa. |
| When all parameters become stable, then check the following parameters: | | | Each parameter is stable near the following value: |
| 9 | 1) Reactor power (% FP) | Fixed column | 30±5% FP |
| | 2) Turbine generator electric output (MW) | | 0 MW |
| | 3) T _{avg} (°C) | | 297°C |
| | 4) PZR pressure (MPa) | | 15.4 MPa |
| | 5) PZR level (m) | Reactor coolant | 3.22~4.5 m |
| | 6) Feed water flow (kg/s) | system | 160~171 kg/s (for each SG) |
| | 7) Steam pressure (MPa) | | 7.23 MPa |
| | 8) Steam flow (kg/s) | | 160~171 kg/s (for each SG) |
| | 9) SG level (m) | Secondary system | 12.65±0.2 m (for each SG) |
| | 10) Turbine speed (rpm) | | 0 rpm |
| | 11) Turbine bypass valve opening (%) | | 15~20% |
| | 12) R bank position (steps) | | 192 steps |
| | 13) G bank overlapping position (steps) | Control rods | 615 steps |
| | 14) Boron concentration (ppm) | | 675±50 ppm |
| 10 | Start-up the turbine: 1) Reset turbine trip signal: Push trip reset button. 2) Start turbine speed-up: Push Run-up button. | Secondary system | — Turbine trip alarm disappears; |
| | | | — Turbine inlet valve has a little opening; |
| | | | — Turbine speed starts to rise and stable at 1500 rpm finally; |
| | | | — Lamp of ready for synchronization lights. |
| 11 | Synchronization: 1) Check synchronization indicator; 2) Push sync. Button. | Secondary system | — Generator outgoing break closed automatically; |
| | | | — Generator have a minimum load (approximately 50 MW); |
| | | | — Turbine bypass valve opening decreases automatically. |

TABLE II–6. DETAILS OF SPURIOUS TURBINE TRIP AND RECOVERY (cont.)

| No. | Step | GUI sheet | Expected response |
|-----|--|---|--|
| 12 | Continue increase turbine load to 100% FP: | — | Turbine load starts to rise; |
| | 1) Increase turbine generator load; | — | G bank position rises automatically; |
| | 2) Set turbine load demand at Secondary system 1100 MW ; | — | T _{ref} starts to rise and T _{avg} is controlled near T _{ref} ; |
| | 3) Set load rate at 30 MW/min ; | Control rods | Turbine bypass valve opening decreases to 0% slowly. |
| 13 | 4) Release, push GO button. | — | PZR level rises and maintained near reference value programmed based on T _{avg} ; |
| | Check the following auto control: | Reactor coolant system | — |
| | 1) PZR level control; | Secondary system | — |
| | 2) Feed water flow control; | — | Feed water flow rises along with turbine load; |
| 14 | 3) PZR pressure control. | — | — |
| | When turbine load reach 1100 MW, check the following parameters: | Each parameter is stable near the following values: | — |
| | 1) Reactor power (% FP) | — | 100% FP |
| | 2) Turbine generator electric output (MW) | Fixed column | 1100 MW |
| 14 | 3) T _{avg} (°C) | — | 310°C |
| | 4) PZR pressure (MPa) | — | 15.4 MPa |
| | 5) PZR level (m) | Reactor coolant system | 6.6 m |
| | 6) Feed water flow (kg/s) | — | 571 kg/s (for each SG) |
| 14 | 7) Steam pressure (MPa) | — | 6.7 MPa |
| | 8) Steam flow (kg/s) | Secondary system | 571 kg/s (for each SG) |
| | 9) SG level (m) | — | 12.65 m (for each SG) |
| | 10) R bank position (steps) | — | 180~204 steps |
| 14 | 11) G bank overlapping position (steps) | Control rods | 615 steps |
| | 12) Boron concentration (ppm) | — | 600-900 ppm |

Figure II–6 shows the turbine trip signal/alarm.

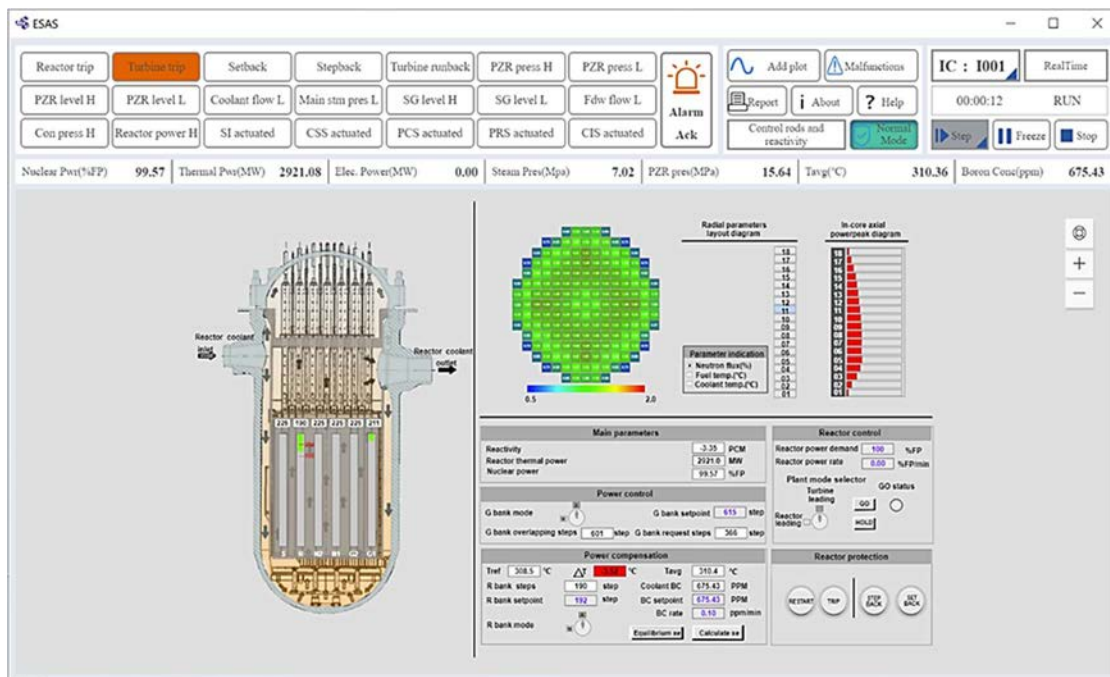


FIG. II–6. Spurious turbine trip recovery.

II-7. TURBINE RUNBACK

The ESAS steps and parameters for turbine runback are shown in Table II-7.

TABLE II-7. DETAILS OF TURBINE RUNBACK

| No. | Step | GUI sheet | Expected response |
|-----|--|--|---|
| 1 | Load a 100% FP IC | IC | IC loaded successfully |
| 2 | Put simulator in running | Run/Freeze | Run state shown and simulator time begins |
| 3 | Check the following parameters: | | Each parameter is stable near the following value: |
| | 1) Reactor power (% FP) | Fixed column | 100±2% FP |
| | 2) Turbine generator electric output (MW) | | 1100±5 MW |
| | 3) T _{avg} (°C) | | 310±1°C |
| | 4) PZR pressure (MPa) | | 15.4±0.2 MPa |
| | 5) PZR level (m) | Reactor coolant | 6.6±0.2 m |
| | 6) Feed water flow (kg/s) | system | 571±10 kg/s (for each SG) |
| | 7) Steam pressure (MPa) | Secondary system | 6.7±0.5 MPa |
| | 8) Steam flow (kg/s) | | 571±10 kg/s (for each SG) |
| | 9) SG level (m) | | 12.65±0.2 m (for each SG) |
| | 10) Turbine speed (rpm) | | 1500±5 rpm |
| | 11) Turbine bypass valve opening (%) | | 0±1% |
| | 12) R bank position (steps) | Control rods | 192±10 steps |
| | 13) G bank overlapping position (steps) | | 615±7 steps |
| | 14) Boron concentration (ppm) | | 675±20 ppm |
| 4 | Check the following control state: | | |
| | 1) Change to “turbine leading” mode; | Control rods Secondary system Reactor coolant system | — Switch to “turbine leading” mode; |
| | 2) G bank in auto control mode; | | — G bank mode selector in AUTO; |
| | 3) R bank in auto control mode; | | — R bank mode selector in AUTO; |
| | 4) Feed water flow valve in auto control; | | — Feed water valve in auto state; |
| | 5) Turbine bypass valve in auto control; | | — Bypass valve in auto state; |
| | 6) PZR pressure control in auto mode; | | — PZR spray valve and heaters in AUTO; |
| | 7) PZR level control in auto mode. | | — PZR level control mode switch to AUTO. |
| 5 | Insert “Spurious turbine runback” malfunction | Secondary system Malfunction | — Turbine generator load drops rapidly; — Turbine runback alarm appears. |
| 6 | Verify steam flow and turbine bypass system: | Secondary system | — Turbine load stable near 550 MW; — Steam flow rises fast after dropping, then starts to decrease smoothly; — Turbine bypass valve quickly opened and then closing slowly. |
| 7 | Verify reactor power reduction: | | |
| | 1) G bank request position drops to 412 steps (programmed at 50% FP); 2) Reactor power is decreasing to 50% FP. | Control rods | — G bank starts to insert and stop at approximately 412 steps finally; — Nuclear power indication starts to decrease and stable at approximately 50% FP. |
| 8 | Verify T _{avg} and PZR: | Reactor coolant system | — T _{avg} start to decrease tracing T _{ref} ; — PZR level starts to decrease tracing the reference programmed on T _{avg} ; — PZR pressure is stabilized at 15.4 MPa.g. |

TABLE II–7. DETAILS OF TURBINE RUNBACK (cont.)

| No. | Step | GUI sheet | Expected response |
|-----|---|------------------------|--|
| | When all parameters become stable, then check the following parameters: | | Each parameter is stable near the following value: |
| | 1) Reactor power (% FP) | | 50% FP |
| | 2) Turbine generator electric output (MW) | Fixed column | 550 MW |
| | 3) T_{avg} ($^{\circ}C$) | | 300.7 $^{\circ}C$ |
| | 4) PZR pressure (MPa) | | 15.4 MPa |
| 9 | 5) PZR level (m) | Reactor coolant system | 4.01~4.7 m |
| | 6) Feed water flow (kg/s) | | 270~285 kg/s (for each SG) |
| | 7) Steam pressure (MPa) | | 7.05 MPa |
| | 8) Steam flow (kg/s) | Secondary system | 270~285 kg/s (for each SG) |
| | 9) SG level (m) | | 12.65 m (for each SG) |
| | 10) Turbine bypass valve opening (%) | | 0% |
| | 11) R bank position (steps) | | 180~204 steps |
| | 12) G bank overlapping position (steps) | Control rods | 412 steps |
| | 13) Boron concentration (ppm) | | 675 ppm |

Figure II–7 shows the turbine runback signal/alarm.

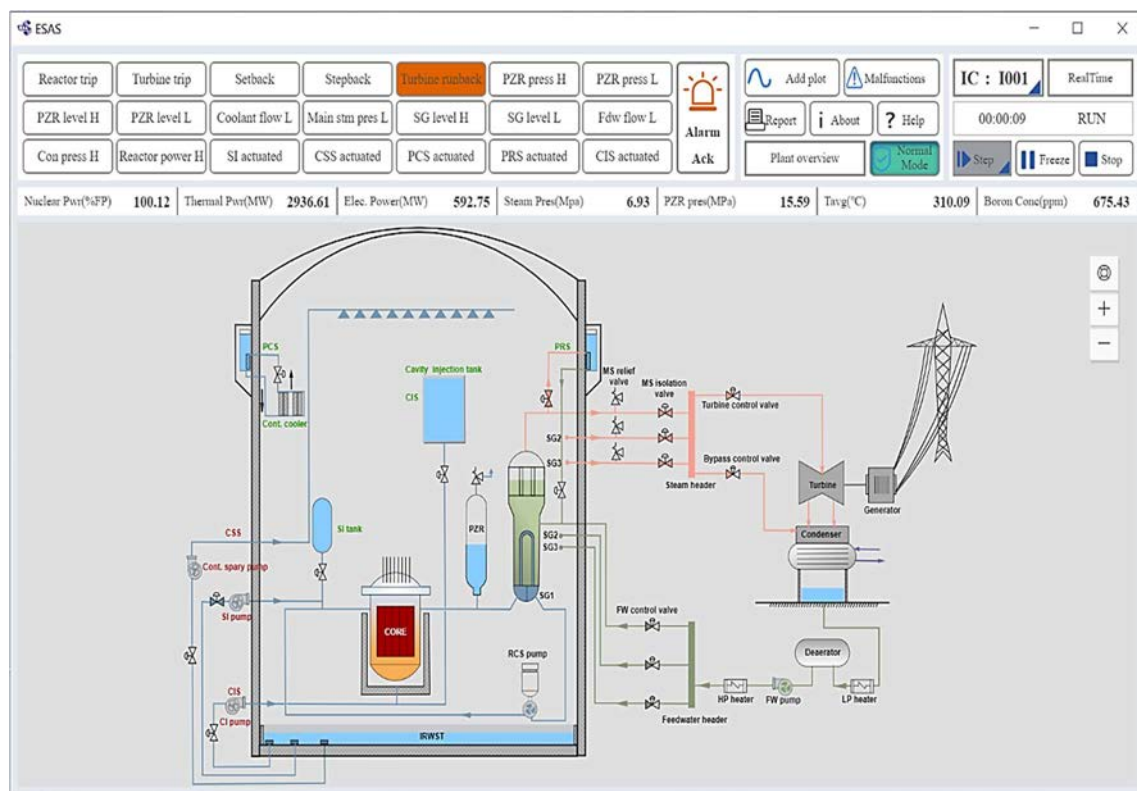


FIG. II–7. Turbine runback.

II-8. RESTART

The ESAS steps and parameters for simulating the reactor trip and restarting the reactor are shown in Table II-8.

TABLE II-8. DETAILS OF REACTOR TRIP AND RESTART

| No. | Step | GUI sheet | Expected response |
|-----|--|------------------------|--|
| 1 | Load a 100% FP IC | IC | IC loaded successfully |
| 2 | Put simulator in running | Run/Freeze | Run state shown and simulator time begins |
| 3 | Check the following parameters: | | Each parameter is stable near the following value: |
| | 1) Reactor power (% FP) | Fixed column | 100±2% FP |
| | 2) Turbine generator electric output (MW) | | 1100±5 MW |
| | 3) T _{avg} (°C) | | 310±1°C |
| | 4) PZR pressure (MPa) | | 15.4±0.2 MPa |
| | 5) PZR level (m) | Reactor coolant | 6.6±0.2 m |
| | 6) Feed water flow (kg/s) | system | 571±10 kg/s (for each SG) |
| | 7) Steam pressure (MPa) | Secondary system | 6.7±0.5 MPa |
| | 8) Steam flow (kg/s) | | 571±10 kg/s (for each SG) |
| | 9) SG level (m) | | 12.65±0.2 m (for each SG) |
| | 10) Turbine speed (rpm) | | 1500±5 rpm |
| | 11) Turbine bypass valve opening (%) | | 0±1% |
| | 12) R bank position (steps) | Control rods | 192±10 steps |
| | 13) G bank overlapping position (steps) | | 615±7 steps |
| | 14) Boron concentration (ppm) | | 675±20 ppm |
| 4 | Check the following control state: | | — switch to “turbine leading” mode; |
| | 1) Change to “turbine leading” mode: | Control rods | — G bank mode selector in AUTO; |
| | 2) G bank in auto control mode; | Secondary system | — R bank mode selector in AUTO; |
| | 3) R bank in auto control mode; | | — Feed water valve in auto state; |
| | 4) Feed water flow valve in auto control; | Reactor coolant system | — Bypass valve in auto state; |
| | 5) Turbine bypass valve in auto control; | | — PZR spray valve and heaters in AUTO; |
| | 6) PZR pressure control in auto mode; | | — PZR level control mode switch to AUTO. |
| 5 | Push “trip” button under reactor protection | Control rods | — All control rods dropped to the bottom; |
| | | | — Reactor power dropped below 2% FP quickly; |
| | | | — Reactor trip alarm appears. |
| 6 | Verify turbine state: | Secondary system | — Turbine generator load drops to 0 MW; |
| | | | — Generator outgoing breaker opened; |
| | | | — Turbine trip alarm appears; |
| 7 | Verify steam flow and turbine bypass system: | Secondary system | — Turbine speed starts to decrease. |
| | | | — Steam flow decreases rapidly; |
| 8 | Verify SG level and feed water flow: | Secondary system | — Turbine bypass valve starts to open then close slowly when steam pressure below 7.5 MPa. |
| | | | — SG level rises slowly after a rapid dropping; |
| | | | — Feed water flow decreases rapidly. |

TABLE II–8. DETAILS OF REACTOR TRIP AND RESTART (cont.)

| No. | Step | GUI sheet | Expected response | |
|------------------------------------|---|---|--|--|
| 9 | Verify T _{avg} and PZR: | Reactor coolant | <ul style="list-style-type: none">— T_{ref} dropped to programmed value on zero power (approximately 291.4°C);— PZR level starts to decrease tracing the reference (approximately 2.3 m) programmed on T_{avg};— PZR pressure decreases quickly, but would be stabilized at 15.4 MPa finally. | |
| 10 | When all parameters become stable, then check the following parameters: | | Each parameter is stable near the following value: | |
| | 1) Reactor power (% FP) | Fixed column | 0% FP | |
| | 2) Turbine generator electric output (MW) | | 0 MW | |
| | 3) T _{avg} (°C) | | 291.4±1°C | |
| | 4) PZR pressure (MPa) | | 15.4±0.2 MPa | |
| | 5) PZR level (m) | Reactor coolant system | 1.97~4 m | |
| | 6) Feed water flow (kg/s) | | 0~43 kg/s (for each SG) | |
| | 7) Steam pressure (MPa) | Secondary system | 7.5±0.2 MPa | |
| | 8) Steam flow (kg/s) | | 0~43 kg/s (for each SG) | |
| | 9) SG level (m) | | 12±0.2 m (for each SG) | |
| | 10) Turbine bypass valve opening (%) | Control rods | 0~5% | |
| | 11) R bank position (steps) | | 0 steps | |
| | 12) G bank overlapping position (steps) | | 0 steps | |
| 11 | Check the control systems state: | | | |
| | 1) Change to “Turbine leading” mode; | Control rods | — Switch to “turbine leading” mode; | |
| | 2) Set G bank in manual control mode; | Secondary system | — G bank mode selector in MANUAL; | |
| | 3) Set R bank in manual control mode; | | — R bank mode selector in MANUAL; | |
| | 4) Feed water flow valve in auto control; | | — Feed water valve in auto state | |
| | 5) Turbine bypass valve in auto control; | Reactor coolant system | — Bypass valve in auto state; | |
| | 6) PZR pressure control in auto mode; | | — PZR spray valve and heaters in AUTO; | |
| 7) PZR level control in auto mode. | — PZR level control mode switch to AUTO. | | | |
| 12 | Reactor start-up to critical state: Push reactor RESTART button | | <ul style="list-style-type: none">— S bank position initiated to 225 steps;— G bank overlapping position initiated to 315 steps;— R bank position initiated to 190 steps;— Reactivity rises (still negative);— About 40 s later, boron concentration initiated to critical value (upon the xenon state);— Reactivity rises to critical value (positive and about 0-10 pcm). | |
| | Start to increase reactor power. | | — G bank position starts to rise; | |
| | 13 | Withdraw G bank: Adjust G bank set point (add 3 steps and wait several minutes for each time) | Control rods | — Reactivity rises to a positive value and stable (at 45 pcm recommended). |
| | | | | |

TABLE II–8. DETAILS OF REACTOR TRIP AND RESTART (cont.)

| No. | Step | GUI sheet | Expected response |
|-----|--|--|--|
| 14 | Wait for 5-10 minutes, check the reactor power level by nuclear power | Fixed column | <ul style="list-style-type: none"> — Nuclear power indication starts to rise from 0; — T_{avg} starts to rise; — Reactivity starts to decrease and become stable; — Turbine bypass valve further opens. |
| 15 | Bring reactor to hot standby state (2% FP): When reactor power rises to 2% FP, stop withdrawing G bank (if exceeding 2% FP, insert G bank by several steps) | Control rods Reactor coolant system | <ul style="list-style-type: none"> — Reactor power stable at approximately 2% FP; — Reactivity near 0pcm(± 5 pcm); — T_{avg} stable at approximately 292.5°C. |
| 16 | Continue to increase reactor power to 8% FP: Withdraw G bank: Adjust G bank set point (add 3 steps and wait several minutes for each time) | Control rods Reactor coolant system | <ul style="list-style-type: none"> — G bank overlapping position rises; — Reactivity rises to a positive value, then decreases slowly; — Nuclear power indication continues to rise; — T_{avg} continue to rise; — Turbine bypass valve further opens. |
| 17 | When reactor power rises to 8% FP, stop withdrawing G bank (if exceeding 8% FP too much, insert G bank by several steps) | Fixed column | <ul style="list-style-type: none"> — Reactor power stable at approximately 8% FP; — Reactivity near 0 pcm (± 5 pcm); — T_{avg} stable at approximately 295°C. |
| 18 | Start-up the turbine: 1) Reset turbine trip signal: Push trip reset button. 2) Start turbine speed-up: Push Run-up button. | Secondary system | <ul style="list-style-type: none"> — Turbine trip alarm disappears; — Turbine inlet valve has a little opening; — Turbine speed starts to rise and stable at 1500 rpm finally; — Lamp of ready for synchronization lights. |
| 19 | Continue to increase reactor power to 15% FP: Check G bank overlapping step and request steps: 1) If overlapping step is higher than request value, decrease BC: Adjust BC set point (reduce set point by 3 ppm and wait several minutes for each time); 2) Otherwise, withdraw G bank: Adjust G bank set point (add 3 steps and wait several minutes for each time). | Control rods | <ul style="list-style-type: none"> — G bank overlapping position rises or BC decreases; — Reactivity rises to a positive value, then decreases slowly; — Nuclear power indication continues to rise; — T_{avg} continue to rise; — Turbine bypass valve further opens. |
| 20 | When reactor power rises to 15% FP, stop withdrawing G bank (if exceeding 15% FP too much, insert G bank by several steps) or adjusting BC set point (if exceeding 15% FP too much, increase BC set point by several ppm) | Control rods | <ul style="list-style-type: none"> — Reactor power stable at approximately 15% FP; — Reactivity near 0 pcm (± 5 pcm); — T_{avg} stable at approximately 296.3°C. |
| 21 | Synchronization: 1) Check synchronization indicator; 2) Push sync. Button. | Secondary | <ul style="list-style-type: none"> — Generator outgoing break closed automatically; — Generator have a minimum load (approximately 50 MW); — Turbine bypass valve opening decreases automatically. |

TABLE II–8. DETAILS OF REACTOR TRIP AND RESTART (cont.)

| No. | Step | GUI sheet | Expected response |
|-----|---|-----------------|---|
| 22 | Increase turbine load, and ready to changeover G bank and R bank to auto mode: | | — Turbine load starts to rise; |
| | 1) Increase turbine generator load: | Secondary | — G bank request step starts to rise; |
| | 2) Set turbine load demand at 150 MW ; | system | — T_{ref} value starts to rise; |
| | 3) Set load rate at 30 MW/min ; | Control rods | — Turbine bypass valve opening further decreases automatically. |
| | 4) Release : push GO button. | | |
| 23 | When G bank request step become near the overlapping step and T_{ref} become near T_{avg} : | | — G bank request step near overlapping step (deviation <3 steps); |
| | 1) Changeover G bank to auto mode; | Control rods | — T_{ref} near T_{avg} (deviation < 0.9°C); |
| | 2) Changeover R bank to auto mode. | | — G bank in auto mode; |
| 24 | | | — R bank in auto mode. |
| | Continue increase turbine load to 100% FP: | | — Turbine load starts to rise; |
| | 1) Increase turbine generator load: | | — G bank position rises automatically; |
| | 2) Set turbine load demand at 1100 MW ; | Control rods | — T_{ref} starts to rise and T_{avg} is controlled near T_{ref} ; |
| | 3) Set load rate at 30 MW/min ; | | — Turbine bypass valve become closed. |
| 25 | 4) Release : push GO button. | | |
| | Check the following auto control: | | — PZR level rises and maintained near reference value programmed based on T_{avg} ; |
| | 1) PZR level control; | Reactor coolant | |
| | 2) Feed water flow control; | Secondary | — Feed water flow rises along with turbine load; |
| 26 | 3) PZR pressure control. | system | — PZR pressure always controlled 15.4 MPa. |
| | When turbine load reach 1100 MW, check the following parameters: | | Each parameter is stable near the following values: |
| | 1) Reactor power (% FP) | | 100% FP |
| | 2) Turbine generator electric output (MW) | | 1100 MW |
| | 3) T_{avg} (°C) | Fixed column | 310°C |
| | 4) PZR pressure (MPa) | | 15.4 MPa |
| | 5) PZR level (m) | Reactor coolant | 6.6 m |
| | 6) Feed water flow (kg/s) | system | 571 kg/s (for each SG) |
| | 7) Steam pressure (MPa) | | 6.7 MPa |
| | 8) Steam flow (kg/s) | | 571 kg/s (for each SG) |
| | 9) SG level (m) | Secondary | 12.65 m (for each SG) |
| | 10) Turbine speed (rpm) | system | 1500 rpm |
| | 11) Turbine bypass valve opening (%) | | 0% |
| | 12) R bank position (steps) | | 192 steps |
| | 13) G bank overlapping position (steps) | Control rods | 615 steps |
| | 14) Boron concentration (ppm) | | 675 ppm |

Figure II–8 shows the reactor trip signal/alarm.

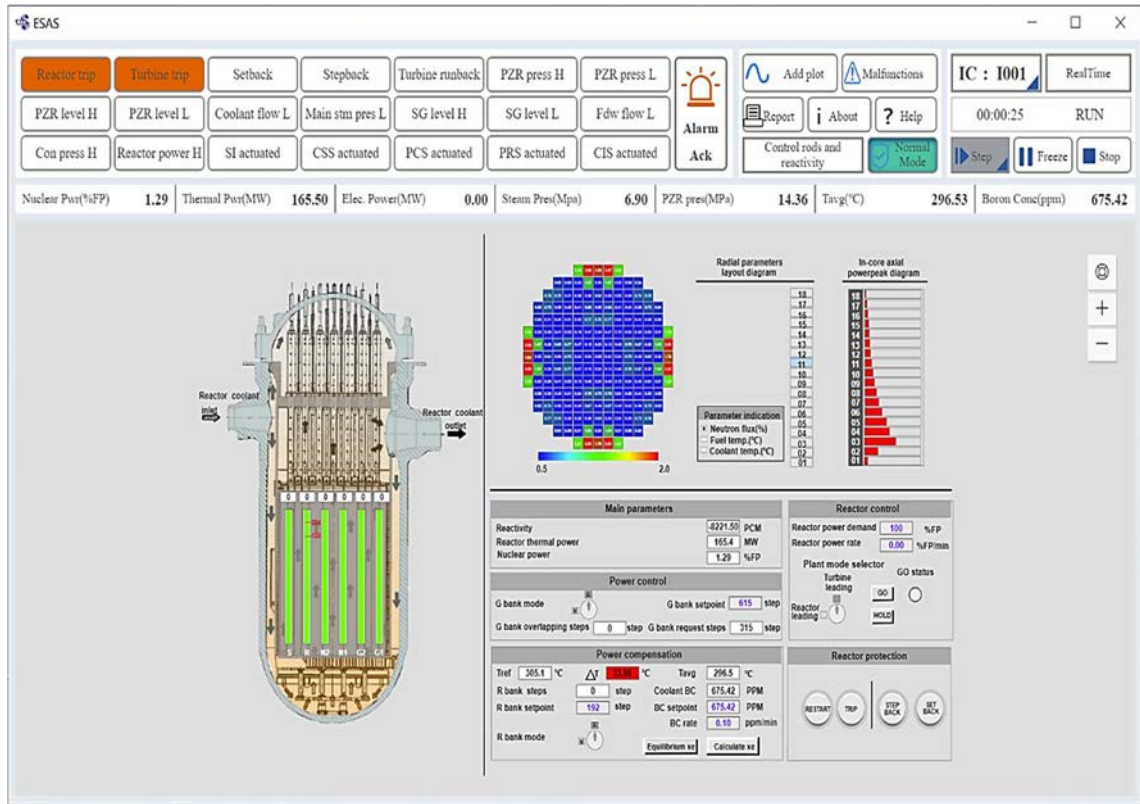


FIG. II–8. Reactor trip and restart.

II-9. LOSS OF FEED WATER

The ESAS steps and parameters for simulating the loss of feed water are shown in Table II-9.

TABLE II-9. DETAILS OF LOSS OF FEED WATER

| No. | Step | GUI sheet | Expected response |
|-----|---|---------------------------------|---|
| 1 | Load a 100% FP IC | IC | IC loaded successfully |
| 2 | Put simulator in running | Run/Freeze | Run state shown and simulator time begins |
| 3 | Check the following parameters: | | Each parameter is stable near the following value: |
| | 1) Reactor power (% FP) | Fixed column | 100±2% FP |
| | 2) Turbine generator electric output (MW) | | 1100±5 MW |
| | 3) T _{avg} (°C) | | 310±1°C |
| | 4) PZR pressure (MPa) | | 15.4±0.2 MPa |
| | 5) PZR level (m) | Reactor coolant | 6.6±0.2 m |
| | 6) Feed water flow (kg/s) | system | 571±10 kg/s (for each SG) |
| | 7) Steam pressure (MPa) | Secondary system | 6.7±0.5 MPa |
| | 8) Steam flow (kg/s) | | 571±10 kg/s (for each SG) |
| | 9) SG level (m) | | 12.65±0.2 m (for each SG) |
| | 10) Turbine speed (rpm) | | 1500±5 rpm |
| | 11) Turbine bypass valve opening (%) | | 0±1% |
| | 12) R bank position (steps) | Control rods | 192±10 steps |
| | 13) G bank overlapping position (steps) | | 615±7 steps |
| | 14) Boron concentration (ppm) | | 675±20 ppm |
| 4 | Check the following control state: | | — Switch to “turbine leading” mode; — G bank mode selector in AUTO; — R bank mode selector in AUTO; — Feed water valve in auto state; — Bypass valve in auto state; — PZR spray valve and heaters in AUTO; — PZR level control mode switch to AUTO. |
| | 1) Change to “turbine leading” mode; | Control rods | |
| | 2) G bank in auto control mode; | Secondary system | |
| | 3) R bank in auto control mode; | | |
| | 4) Feed water flow valve in auto control; | | |
| | 5) Turbine bypass valve in auto control; | | |
| | 6) PZR pressure control in auto mode; | | |
| | 7) PZR level control in auto mode. | | |
| 5 | Insert “Loss of normal feed water (feed water pump trip)” malfunction | Secondary system Malfunction | — Feed water pump trip; |
| | | | — Feed water flow drops near 0 kg/s rapidly; |
| | | | — Feed water flow valves fully opened. |
| 6 | Verify reactor trip: | Control rods Trip parameter | — All control rods drop to the bottom; |
| | | | — Reactor power drops to 0 quickly; |
| | | | — ATWT as first-out trip signal can be confirmed on trip sheet. |
| 7 | Verify Turbine trip: | Secondary system | — Turbine load drops to 0 MW; |
| | | | — Steam flow drops rapidly; |
| | | | — Turbine bypass valve starts to open then close slowly when steam pressure below 7.5 MPa. |
| 8 | Verify SG level: | Secondary system | — SG level decreases continuously due to loss of feed water supply |

TABLE II-9. DETAILS OF LOSS OF FEED WATER (cont.)

| No. | Step | GUI sheet | Expected response |
|-----|---|---|--|
| 9 | Verify T_{avg} and PZR: | Control rods | <ul style="list-style-type: none"> — T_{avg} decreases and stable at the programmed value on zero power (approximately 291.4°C); — PZR level decreases and stable due to T_{avg}; — PZR pressure decreases and up to stable at set point. |
| 10 | When SG level below 11.03 m, check PRS actuated automatically | Secondary system Alarm Safety system | <ul style="list-style-type: none"> — SG level below 11.03 m; — SG level L alarm appears; — PRS start-up alarm appears; — PRS valves opened; — PRS flow established (approximately 15-18 kg/s in total for 3 SGs). |
| 11 | Check the final state: 1) SG level stabilized by PRS; 2) Reactor residual heat is removed by PRS; 3) T_{avg} and PZR pressure is stabilized at hot shutdown state. | Secondary system Reactor coolant system | <ul style="list-style-type: none"> — SG level increase slowly by PRS injection; — T_{avg} decrease slowly by PRS cooling; — PZR pressure decrease and become stable (approximately at 14.5 MPa). |

The signal/alarm in Figure II-9 shows low feedwater flow.

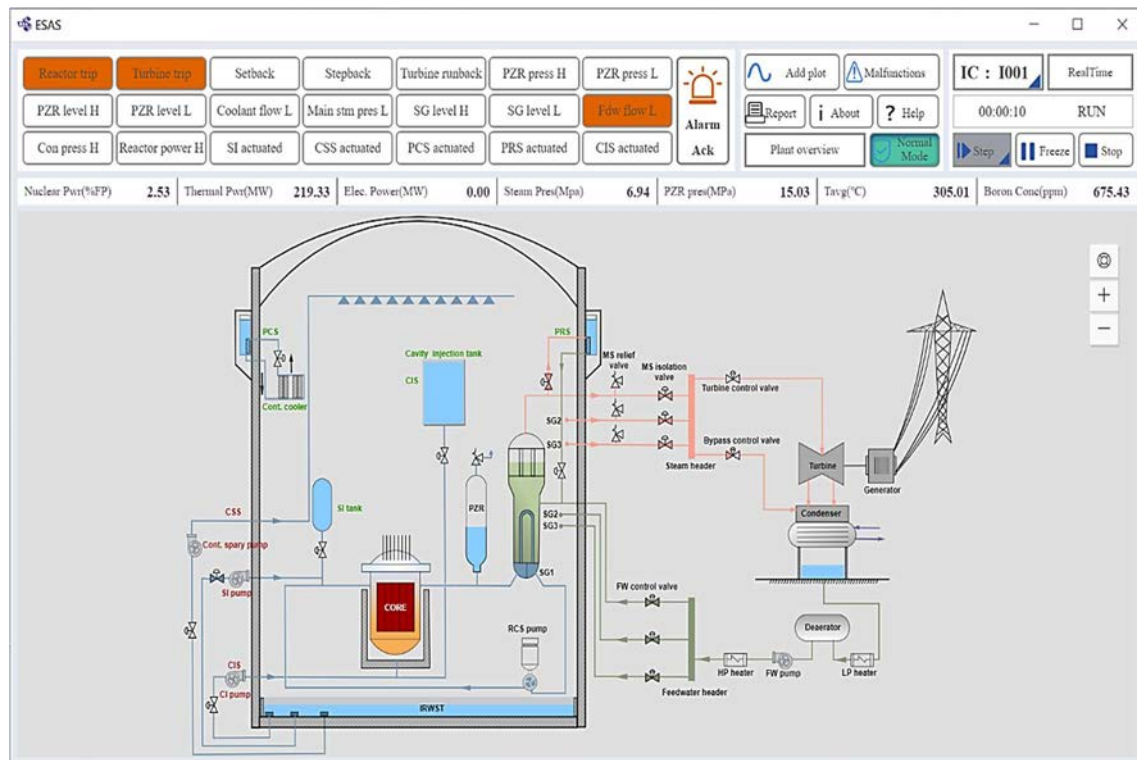


FIG. II-9. Loss of feed water.

II-10. PZR SAFETY VALVE GROUP STUCK AT OPEN

The ESAS steps and parameters for simulating the PZR safety valve group stuck at open are shown in Table II-10.

TABLE II-10. DETAILS OF PZR SAFETY VALVE GROUP STUCK AT OPEN

| No. | Step | GUI sheet | Expected response |
|-----|---|------------------------------------|---|
| 1 | Load a 100% FP IC | IC | IC loaded successfully |
| 2 | Put simulator in running | Run/Freeze | Run state shown and simulator time begins |
| 3 | Check the following parameters: | | Each parameter is stable near the following value: |
| | 1) Reactor power (% FP) | Fixed column | 100±2% FP |
| | 2) Turbine generator electric output (MW) | | 1100±5 MW |
| | 3) T _{avg} (°C) | | 310±1°C |
| | 4) PZR pressure (MPa) | | 15.4±0.2 MPa |
| | 5) PZR level (m) | Reactor coolant | 6.6±0.2 m |
| | 6) Feed water flow (kg/s) | system | 571±10 kg/s (for each SG) |
| | 7) Steam pressure (MPa) | Secondary system | 6.7±0.5 MPa |
| | 8) Steam flow (kg/s) | | 571±10 kg/s (for each SG) |
| | 9) SG level (m) | | 12.65±0.2 m (for each SG) |
| | 10) Turbine bypass valve opening (%) | | 0±1% |
| | 11) R bank position (steps) | Control rods | 192±10 steps |
| | 12) G bank overlapping position (steps) | | 615±7 steps |
| | 13) Boron concentration (ppm) | | 675±20 ppm |
| 4 | Check the following control state: | | |
| | 1) Change to “turbine leading” mode; | Control rods | — Switch to “turbine leading” mode; |
| | 2) G bank in auto control mode; | | — G bank mode selector in AUTO; |
| | 3) R bank in auto control mode; | | — R bank mode selector in AUTO; |
| | 4) Feed water flow valve in auto control; | | — Feed water valve in auto state; |
| | 5) Turbine bypass valve in auto control; | Secondary system | — Bypass valve in auto state; |
| | 6) PZR pressure control in auto mode; | | — PZR spray valve and heaters in AUTO; |
| 5 | Insert “Inadvertent opening of a pressure relief valve” malfunction | Reactor coolant system Malfunction | — PZR level control mode switch to AUTO. |
| | | | — RCS03V shows open; |
| | | | — PZR pressure decreases quickly; |
| | | | — PZR heater full power running; |
| | | | — PZR spray valves RCS01V/02V closed; |
| 6 | When PZR pressure decreases below 13.1 MPa, verify reactor trip: | Control rods Trip parameter | — PZR level starts to rise then decreases quickly. |
| | | | — All control rods drop to the bottom; |
| | | | — Reactor power drops to 0 quickly; |
| | | | — ‘Low PZR pressure’ as first-out trip signal can be confirmed on trip sheet; |
| | | | — PZR level starts to decrease rapidly; |
| 7 | Verify Turbine trip: | Secondary system | — T _{avg} decreases rapidly. |
| | | | — Turbine load drops to 0 MW; |
| | | | — Steam flow drops rapidly; |
| | | | — Turbine bypass valve starts to open then close when steam pressure decreases below 7.5 MPa. |

| No. | Step | GUI sheet | Expected response |
|-----|--|---|---|
| 8 | When PZR pressure decreases below 11.89 MPa, verify safety injection (SI) system actuated: | Reactor coolant system Safety system | <ul style="list-style-type: none"> — Safety injection pump starts; — Safety injection valves open; — 'Low PZR pressure's first-out SI signal can be confirmed on trip sheet. |
| 9 | Verify PZR and SI state: | Reactor coolant system Safety system | <ul style="list-style-type: none"> — PZR pressure decreases continuously; — SI pump flow established only after PZR pressure below approximately 10 MPa.a; — PZR level start to rise due to SI flow; — PZR pressure stop decreasing and stable (approximately at 7.4 MPa) for a while due to SI flow. |
| 10 | Verify reactor state: | Control rods | <ul style="list-style-type: none"> — Reactivity is negative; — Boron concentration is rising; — Thermal power is decreasing; — Nuclear power show 0%. |
| 11 | Check the final state: | Reactor coolant system Safety system | <ul style="list-style-type: none"> — PZR would be fully filled by SI; — Primary pressure would start to rise after PZR full; — T_{avg} would become stable or rise; — SG level would be stabilized automatically. |

ESAS

Reactor trip | Turbine trip | Setback | Stepback | Turbine runback | PZR press H | PZR press L | Alarm | Add plot | Malfunctions | IC : 1001 | RealTime

PZR level H | PZR level L | Coolant flow L | Main stm pres L | SG level H | SG level L | Fdw flow L | Report | About | Help | 00:01:10 | RUN

Con press H | Reactor power H | SI actuated | CSS actuated | PCS actuated | PRS actuated | CIS actuated | Reactor coolant system | Normal Mode | Step | Freeze | Stop

Nuclear Pwr(%FP) 0.95 | Thermal Pwr(MW) 148.59 | Elec. Power(MW) 0.00 | Steam Pres(Mpa) 7.14 | PZR pres(MPa) 10.56 | Tavg(°C) 293.51 | Boron Conc(ppm) 677.37

Charging valve control | **PZR heater control** | **PZR pressure control** | **PZR level control**

Control mode | Valve opening setpoint | Control mode | Heater power setpoint | Pressure setpoint | Control mode | Level setpoint

W | 12 % | W | 99 % | 15.50 MPA | W | 26.5 %

Loop 2

RC S02SG

Steam F 71.8 kg/s

SG P 7.14 MPA

PW F 134.6 kg/s

RC S02P

Charging F 3.56 kg/s

Boron and chemical control unit

Letdown F 3.00 kg/s

Coolant F 5055.3 kg/s

Loop 3

RC S03SG

Steam F 72.0 kg/s

SG P 7.14 MPA

PW F 134.6 kg/s

RC S03P

Coolant F 5055.2 kg/s

Loop 1

RC S01SG

Steam F 85.2 kg/s

SG P 7.14 MPA

PW F 195.4 kg/s

RC S01P

Coolant F 5018.4 kg/s

PZR heater power 100.0 %

Coolant flow to and from PZR 120.2 kg/s

To PZR relief tank

RC S01V

RC S02V

RC S03V

Pressure setpoint 15.50 MPA

Level setpoint 26.5 %

Charging valve control

PZR heater control

PZR pressure control

PZR level control

170

II-11. ONE REACTOR COOLANT PUMP TRIP

The ESAS steps and parameters for simulating the trip of one reactor coolant pump are shown in Table II-11.

TABLE II-11. DETAILS OF ONE REACTOR COOLANT PUMP TRIP

| No. | Step | GUI sheet | Expected response |
|------------------------------------|--|--|--|
| 1 | Load a 100% FP IC | IC | IC loaded successfully |
| 2 | Put simulator in running | Run/Freeze | Run state shown and simulator time begins |
| 3 | Check the following parameters: | | Each parameter is stable near the following value: |
| | 1) Reactor power (% FP) | Fixed column | 100±2% FP |
| | 2) Turbine generator electric output (MW) | | 1100±5 MW |
| | 3) T _{avg} (°C) | | 310±1°C |
| | 4) PZR pressure (MPa) | | 15.4±0.2 MPa |
| | 5) PZR level (m) | Reactor coolant | 6.6±0.2 m |
| | 6) Feed water flow (kg/s) | system | 571±10 kg/s (for each SG) |
| | 7) Steam pressure (MPa) | Secondary system | 6.7±0.5 MPa |
| | 8) Steam flow (kg/s) | | 571±10 kg/s (for each SG) |
| | 9) SG level (m) | | 12.65±0.2 m (for each SG) |
| | 10) Turbine bypass valve opening (%) | | 0±1% |
| | 11) R bank position (steps) | Control rods | 192±10 steps |
| | 12) G bank overlapping position (steps) | | 615±7 steps |
| | 13) Boron concentration (ppm) | | 675±20 ppm |
| 4 | Check the following control state: | | |
| | 1) Change to “turbine leading” mode; | Control rods | — Switch to “turbine leading” mode; |
| | 2) G bank in auto control mode; | Secondary system | — G bank mode selector in AUTO; |
| | 3) R bank in auto control mode; | | — R bank mode selector in AUTO; |
| | 4) Feed water flow valve in auto control; | | — Feed water valve in auto state; |
| | 5) Turbine bypass valve in auto control; | | — Bypass valve in auto state; |
| | 6) PZR pressure control in auto mode; | Reactor coolant | — PZR spray valve and heaters in AUTO; |
| 7) PZR level control in auto mode. | system | — PZR level control mode switch to AUTO. | |
| 5 | Insert “No.1 reactor coolant pump trip)” malfunction | Reactor coolant | — RCS01P shows trip state; |
| | | system Malfunction | — Loop 1 reactor coolant flow drops. |
| 6 | Verify reactor trip: | Control rods Trip parameter | — All control rods drop to the bottom; |
| | | | — Reactor power drops to 0 quickly; |
| | | | — “Reactor pump trip” as first-out trip signal can be confirmed on trip sheet; |
| | | | — “Reactor trip” and “coolant flow L” alarm appears. |
| 7 | Verify Turbine trip: | Secondary system | — Turbine load drops to 0 MW; |
| | | | — Steam flow drops rapidly; |
| | | | — Turbine bypass valve starts to open. |

TABLE II–11. DETAILS OF ONE REACTOR COOLANT PUMP TRIP (cont.)

| No. | Step | GUI sheet | Expected response |
|-----|------------------------|-------------------------------------|---|
| 8 | Verify PZR state: | Reactor coolant system | <ul style="list-style-type: none"> — PZR pressure decreases (minimum to 14.01 MPa), then starts to rise; — PZR level decreases and become stable slowly; — T_{avg} decreases and become stable slowly. |
| 9 | Verify SG state: | Secondary system | <ul style="list-style-type: none"> — Steam flow decreases and become stable slowly by turbine bypass system; — SG level decreases, then starts to recover. |
| 10 | Check the final state: | Reactor coolant system Secondary | <ul style="list-style-type: none"> — Primary pressure would be stabilized at set point finally; — T_{avg} would be stabilized at the programmed value on zero power (approximately 291.4°C); — Reactor coolant flow of loop 1 would stabilize at a negative value by another two loops (approximately -700~840 kg/s); — SG level would be stabilized at programmed value on zero power (approximately 11~12.07 m). |

Figure II–11 shows low coolant flow signal/alarm.

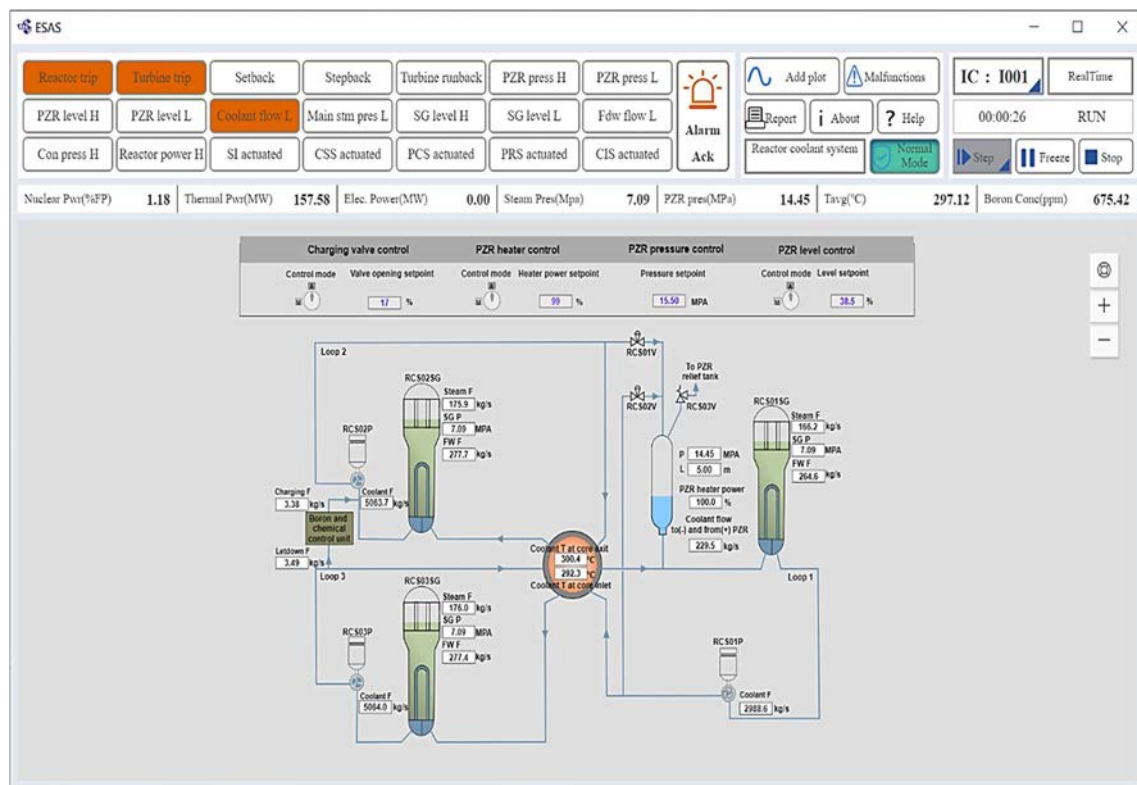


FIG. II–11. One reactor coolant pump trip.

II-12. STEAM LINE BREAK OUTSIDE CONTAINMENT

The ESAS steps and parameters for simulating the main steam line break are shown in Table II-12.

TABLE II-12. DETAILS OF STEAM LINE BREAK OUTSIDE CONTAINMENT

| No. | Step | GUI sheet | Expected response |
|------------------------------------|--|--|---|
| 1 | Load a 100% FP IC | IC | IC loaded successfully |
| 2 | Put simulator in running | Run/Freeze | Run state shown and simulator time begins |
| 3 | Check the following parameters: | | Each parameter is stable near the following value: |
| | 1) Reactor power (% FP) | Fixed column | 100±2% FP |
| | 2) Turbine generator electric output (MW) | | 1100±5 MW |
| | 3) T _{avg} (°C) | | 310±1 (°C) |
| | 4) PZR pressure (MPa) | | 15.4±0.2 MPa |
| | 5) PZR level (m) | Reactor coolant | 6.6±0.2 m |
| | 6) Feed water flow (kg/s) | system | 571±10 kg/s (for each SG) |
| | 7) Steam pressure (MPa) | Secondary system | 6.7±0.5 MPa |
| | 8) Steam flow (kg/s) | | 571±10 kg/s (for each SG) |
| | 9) SG level (m) | | 12.65±0.2 m (for each SG) |
| | 10) Turbine bypass valve opening (%) | | 0±1% |
| | 11) R bank position (steps) | Control rods | 192±10 steps |
| | 12) G bank overlapping position (steps) | | 615±7 steps |
| | 13) Boron concentration (ppm) | | 675±20 ppm |
| 4 | Check the following control state: | | |
| | 1) Change to “turbine leading” mode; | Control rods | — Switch to “turbine leading” mode; |
| | 2) G bank in auto control mode; | Secondary system | — G bank mode selector in AUTO; |
| | 3) R bank in auto control mode; | | — R bank mode selector in AUTO; |
| | 4) Feed water flow valve in auto control; | | — Feed water valve in auto state; |
| | 5) Turbine bypass valve in auto control; | — Bypass valve in auto state; | |
| | 6) PZR pressure control in auto mode; | Reactor coolant | — PZR spray valve and heaters in AUTO; |
| 7) PZR level control in auto mode. | system | — PZR level control mode switch to AUTO. | |
| 5 | Insert “Main steam pipeline break outside containment” malfunction | Reactor coolant system Malfunction | — Steam flow of three SGs rises rapidly; |
| | | | — Steam pressure of steam head drops; |
| | | | — T _{avg} starts to decrease; |
| | | | — PZR pressure starts to decrease; |
| | | | — PZR level starts to decrease; |
| 6 | When reactor power rises above 109% FP, Verify reactor trip: | Control rods Trip parameter | — Reactor power starts to rise. |
| | | | — All control rods drops to the bottom; |
| | | | — Reactor power drops to 0 quickly; |
| | | | — “Reactor power high” as first-out trip signal can be confirmed on trip sheet; |
| 7 | Verify Turbine trip: | Secondary system | — “Reactor trip” and “turbine trip” alarm appears. |
| | | | — Turbine load drops to 0 MW; |
| | | | — Steam flow drops rapidly; |
| | | | — Turbine bypass valve starts to open then close when steam pressure decreases below 7.5 MPa. |

TABLE II-12. DETAILS OF STEAM LINE BREAK OUTSIDE CONTAINMENT (cont.)

| No. | Step | GUI sheet | Expected response |
|-----|--|---|--|
| 8 | When PZR pressure decreases below 11.89 MPa, verify safety injection (SI) system actuated: | Reactor coolant system Safety system | <ul style="list-style-type: none"> — Safety injection pump starts; — Safety injection valves open; — “Low PZR pressure” as first-out SI signal can be confirmed on trip sheet; — SI pump flow established only after PZR pressure below approximately 10 MPa. |
| 9 | Verify primary state: | Reactor coolant system | <ul style="list-style-type: none"> — PZR pressure decreases continuously; — PZR level decreases continuously; — T_{avg} decreases continuously. |
| 10 | Verify SG state: | Secondary system | <ul style="list-style-type: none"> — Steam flow decreases after reactor trip and stable at a certain value; — SG level decreases, then starts to recover slowly; — SG pressure decreases continuously. |
| 11 | Check the final state: | Reactor coolant system Secondary | <ul style="list-style-type: none"> — PZR pressure would recover due to SI; — T_{avg} would decrease continuously; — PZR level would start recover due to SI; — SG pressure would be stable at approximately 3.2 MPa or decrease; — SG level would be stabilized automatically. |

Figure II–12 shows low PZR pressure signal/alarm.

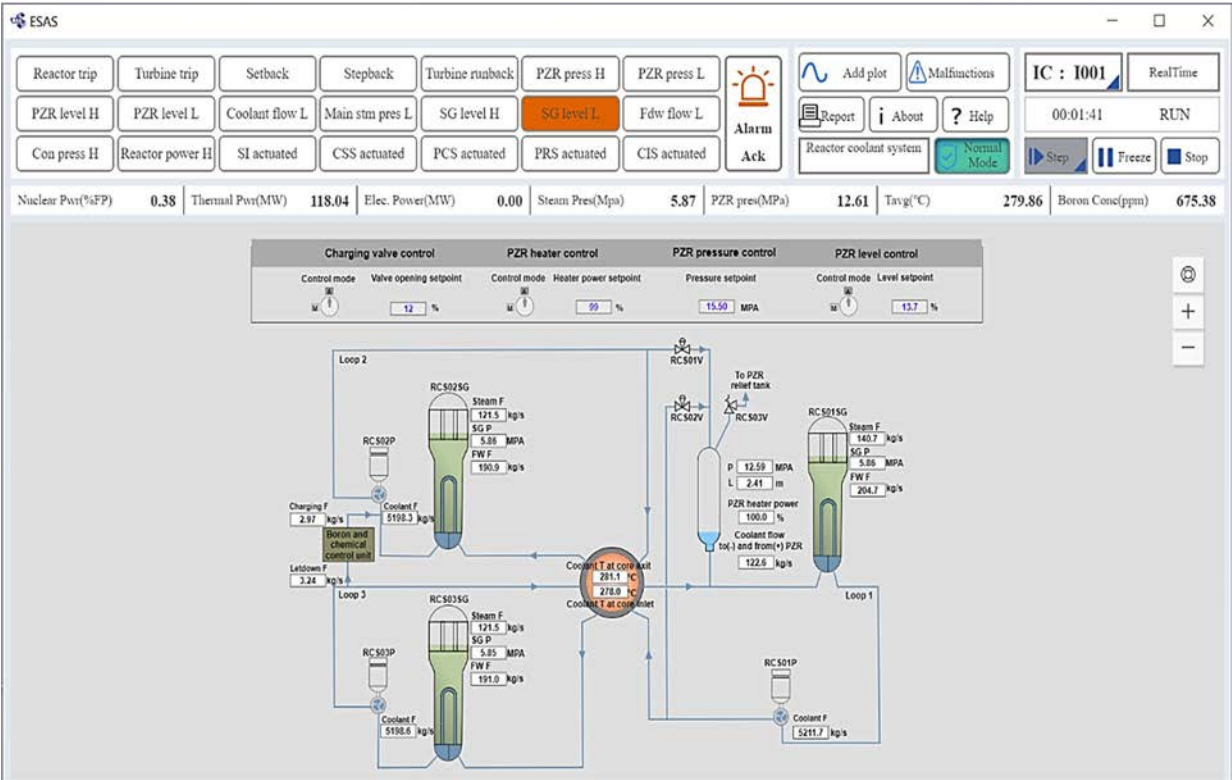


FIG. II–12. Steam line break outside containment.

II-13. STEAM GENERATOR TUBE RAPTURE

The ESAS steps and parameters for simulating the steam generator tube rupture are shown in Table II-13.

TABLE II-13. DETAILS OF STEAM GENERATOR TUBE RAPTURE

| No. | Step | GUI sheet | Expected response |
|-----|--|------------------------|--|
| 1 | Load a 100% FP IC | IC | IC loaded successfully |
| 2 | Put simulator in running | Run/Freeze | Run state shown and simulator time begins |
| 3 | Check the following parameters: | | Each parameter is stable near the following value: |
| | 1) Reactor power (% FP) | Fixed column | 100±2% FP |
| | 2) Turbine generator electric output (MW) | | 1100±5 MW |
| | 3) T _{avg} (°C) | | 310±1°C |
| | 4) PZR pressure (MPa) | | 15.4±0.2 MPa |
| | 5) PZR level (m) | Reactor coolant | 6.6±0.2 m |
| | 6) Feed water flow (kg/s) | system | 571±10 kg/s (for each SG) |
| | 7) Steam pressure (MPa) | Secondary system | 6.7±0.5 MPa |
| | 8) Steam flow (kg/s) | | 571±10 kg/s (for each SG) |
| | 9) SG level (m) | | 12.65±0.2 m (for each SG) |
| | 10) Turbine bypass valve opening (%) | | 0±1% |
| | 11) R bank position (steps) | Control rods | 192±10 steps |
| | 12) G bank overlapping position (steps) | | 615±7 steps |
| | 13) Boron concentration (ppm) | | 675±20 ppm |
| 4 | Check the following control state: | | |
| | 1) Change to “turbine leading” mode; | Control rods | — Switch to “turbine leading” mode; |
| | 2) G bank in auto control mode; | | — G bank mode selector in AUTO; |
| | 3) R bank in auto control mode; | | — R bank mode selector in AUTO; |
| | 4) Feed water flow valve in auto control; | Secondary system | — Feed water valve in auto state; |
| | 5) Turbine bypass valve in auto control; | | — Bypass valve in auto state; |
| | 6) PZR pressure control in auto mode; | Reactor coolant | — PZR spray valve and heaters in AUTO; |
| 5 | Insert “No.1 steam generator tube rupture (Sa1)” malfunction | system | — PZR level control mode switch to AUTO. |
| | | Malfunction | — PZR level starts to decrease; |
| | | | — PZR pressure starts to decrease; |
| | | | — PZR heater power rises automatically; |
| | | | — PZR spray valves RCS01V/02V closed; |
| 6 | Check the PZR state: | Reactor coolant system | — Charging flow rises automatically. |
| | | | — PZR heater full power running (100%); |
| | | | — Charging full flow running (7.3 kg/s); |
| | | | — PZR level decreases continuously; |
| 7 | Check SG state: | Secondary system | — PZR pressure decreases continuously. |
| | | | — SG1 steam flow rises; |
| | | | — SG1 feed water flow decreases (FW01V); |
| | | | — SG1 level rises continuously for a while (max to 13.0 m), then controlled to decrease automatically. |

TABLE II-13. DETAILS OF STEAM GENERATOR TUBE RAPTURE (cont.)

| No. | Step | GUI sheet | Expected response |
|-----|--|---|---|
| 8 | When PZR pressure decreases below 13.1 MPa, verify reactor trip: | Control rods Trip parameter | <ul style="list-style-type: none"> — All control rods drop to the bottom; — Reactor power drops to 0 quickly; — “Low PZR pressure” as first-out trip signal can be confirmed on trip sheet; — PZR level decreases rapidly to empty; — T_{avg} decreases rapidly to approximately 291°C. |
| 9 | Verify Turbine trip: | Secondary system | <ul style="list-style-type: none"> — Turbine load drops to 0MW; — Steam flow drops rapidly; — Turbine bypass valve starts to open then close when steam pressure decreases below 7.5 MPa; |
| 10 | When PZR pressure decreases below 11.89 MPa, verify safety injection (SI) system actuated: | Reactor coolant system Safety system | <ul style="list-style-type: none"> — Safety injection pump starts; — Safety injection valves open; — “Low PZR pressure” as first-out SI signal can be confirmed on trip sheet. |
| 11 | Verify PZR and SI state: | Reactor coolant Safety system | <ul style="list-style-type: none"> — PZR pressure decreases continuously; — SI pump flow established only after PZR pressure below approximately 10 MPa; — PZR pressure stop; decreasing (minimum approximately at 9.4 MPa), then start to recover due to SI flow. |
| 12 | Verify reactor state: | Control rod | <ul style="list-style-type: none"> — Reactivity is negative; — Boron concentration is rising; — Thermal power is decreasing; — Nuclear power decrease to 0% slowly. |
| 13 | Check the final state: | Reactor coolant Safety system | <ul style="list-style-type: none"> — PZR level start to rise and become stable; — Primary pressure rises and become stable; — SI flow decreases to 0 after PZR pressure above 10 MPa; — T_{avg} would become stable or rise slowly; — SG level would be stabilized automatically. |

Figure II–13 shows the drop-down box for SGTR malfunction and other malfunctions.

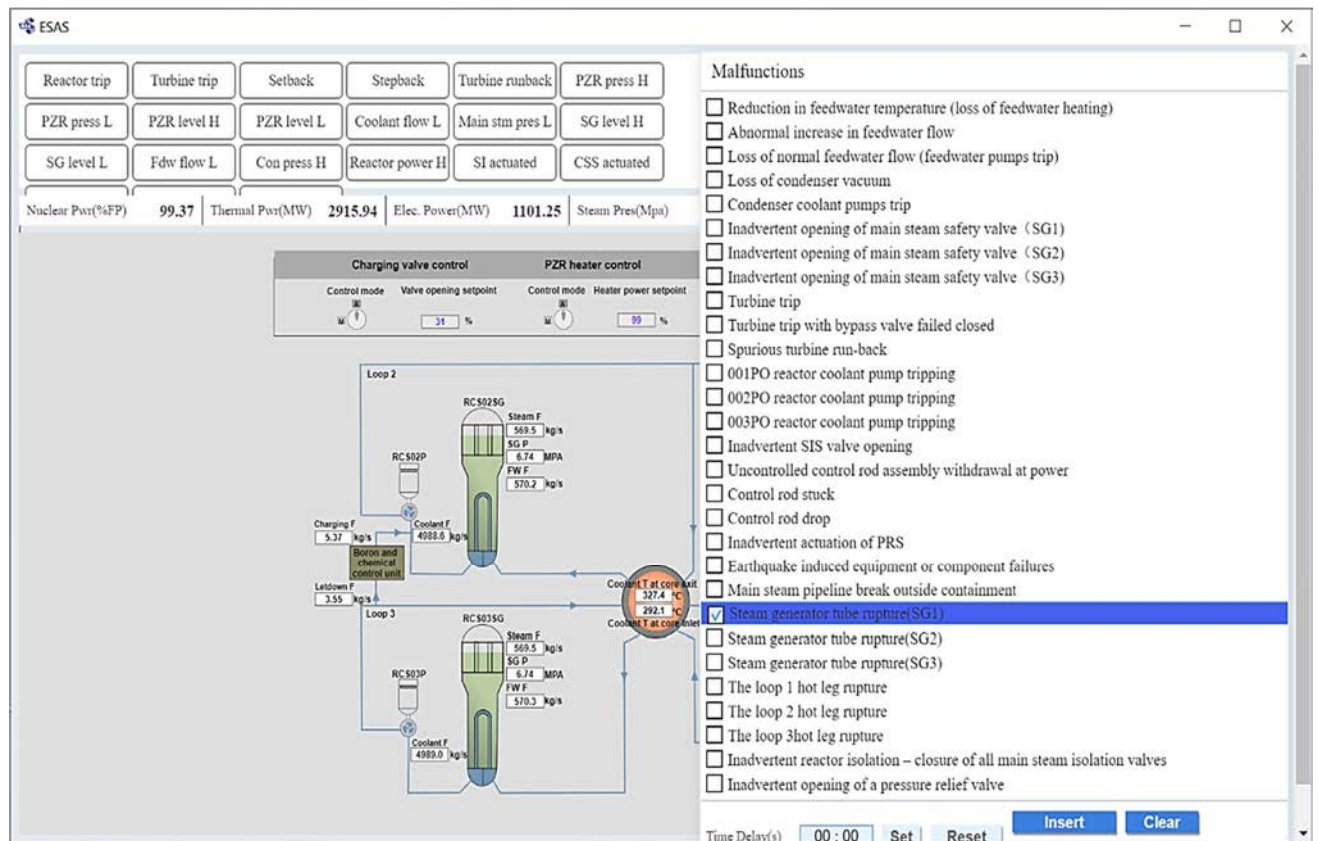


FIG. II–13. Steam generator tube rupture.

II-14. PRIMARY BREAK (LOCA)

The ESAS steps and parameters for simulating the primary break are shown in Table II-14.

TABLE II-14. DETAILS OF PRIMARY BREAK (LOCA)

| No. | Step | GUI sheet | Expected response |
|------------------------------------|---|--|---|
| 1 | Load a 100% FP IC | IC | IC loaded successfully |
| 2 | Put simulator in running | Run/Freeze | Run state shown and simulator time begins |
| 3 | Check the following parameters: | | Each parameter is stable near the following value: |
| | 1) Reactor power (% FP) | Fixed column | 100±2% FP |
| | 2) Turbine generator electric output (MW) | | 1100±5 MW |
| | 3) T _{avg} (°C) | | 310±1°C |
| | 4) PZR pressure (MPa) | | 15.4±0.2 MPa |
| | 5) PZR level (m) | Reactor coolant | 6.6±0.2 m |
| | 6) Feed water flow (kg/s) | system | 571±10 kg/s (for each SG) |
| | 7) Steam pressure (MPa) | Secondary system | 6.7±0.5 MPa |
| | 8) Steam flow (kg/s) | | 571±10 kg/s (for each SG) |
| | 9) SG level (m) | | 12.65±0.2 m (for each SG) |
| | 10) Turbine bypass valve opening (%) | | 0±1% |
| | 11) R bank position (steps) | Control rods | 192±10 steps |
| | 12) G bank overlapping position (steps) | | 615±7 steps |
| | 13) Boron concentration (ppm) | | 675±20 ppm |
| 4 | Check the following control state: | | — Switch to “turbine leading” mode; |
| | 1) Change to “turbine leading” mode; | Control rods | — G bank mode selector in AUTO; |
| | 2) G bank in auto control mode; | | — R bank mode selector in AUTO; |
| | 3) R bank in auto control mode; | Secondary system | — Feed water valve in auto state; |
| | 4) Feed water flow valve in auto control; | | — Bypass valve in auto state; |
| | 5) Turbine bypass valve in auto control; | | — PZR spray valve and heaters in AUTO; |
| | 6) PZR pressure control in auto mode; | Reactor coolant | — PZR level control mode witch to AUTO. |
| 7) PZR level control in auto mode. | system | | |
| 5 | Insert “The loop 1 hot leg rupture” malfunction | Reactor coolant system Malfunction | — PZR level decreases rapidly to empty; — PZR pressure decreases rapidly. |
| 6 | Check reactor trip after PZR pressure or reactor coolant flow rate dropped below set point: | Reactor coolant system | — All control rods drop to the bottom; — Reactor power drops to 0 quickly; — “Low PZR pressure” or “Low reactor coolant flow rate” as first-out trip signal can be confirmed on trip sheet. |
| 7 | Verify Turbine trip: | Secondary system | — Turbine load drops to 0 MW; — Steam flow drops rapidly; — Turbine bypass valve starts to open. |
| 8 | Verify safety injection (SI) system actuated after PZR pressure dropped below 11.89 MPa.a | Reactor coolant system Safety system | — Safety injection pump starts; — Safety injection valves open; — “Low PZR pressure” as first-out SI signal can be confirmed on trip sheet. |

TABLE II–14. DETAILS OF PRIMARY BREAK (LOCA) (cont.)

| No. | Step | GUI sheet | Expected response |
|-----|--|---|--|
| 9 | Verify PZR and SI state: | Reactor coolant system Safety system | <ul style="list-style-type: none"> — SI pump flow established only after PZR pressure below approximately 10 MPa; — SI accumulator flow established after PZR pressure below approximately 4.5 MPa; — PZR pressure stop decreasing finally then become stable due to SI flow. |
| 10 | Verify containment state: | Safety system | <ul style="list-style-type: none"> — Containment pressure rises quickly; — Containment temperature rises quickly; — Containment radioactivity rises. |
| 11 | Verify containment spray system (CSS) start-up after containment pressure rises above 240 KPa.a: | Reactor coolant system Safety system | <ul style="list-style-type: none"> — Spray pump start up; — Spray valve open; — Spray flow established (>390 kg/s); — Containment pressure and temperature starts to decrease after spray flow lasts for a while. |
| 12 | Verify PCS start-up if containment temperature rises above 115°C: | Safety system | <ul style="list-style-type: none"> — PCS valve open; — PCS flow established. |
| 13 | Check refuelling water tank (IRWST) state: | Safety system | <ul style="list-style-type: none"> — IRWST level starts to decrease; — IRWST temperature starts to rise slowly; |
| 14 | Check the final state: | Reactor coolant system Safety system | <ul style="list-style-type: none"> — PZR pressure decreases continuously or stable; — PZR become empty; — T_{avg} decrease continuously; — Containment state is stabilized by CSS or PCS. |

Figure II–14 shows low PZR pressure signal/alarm.

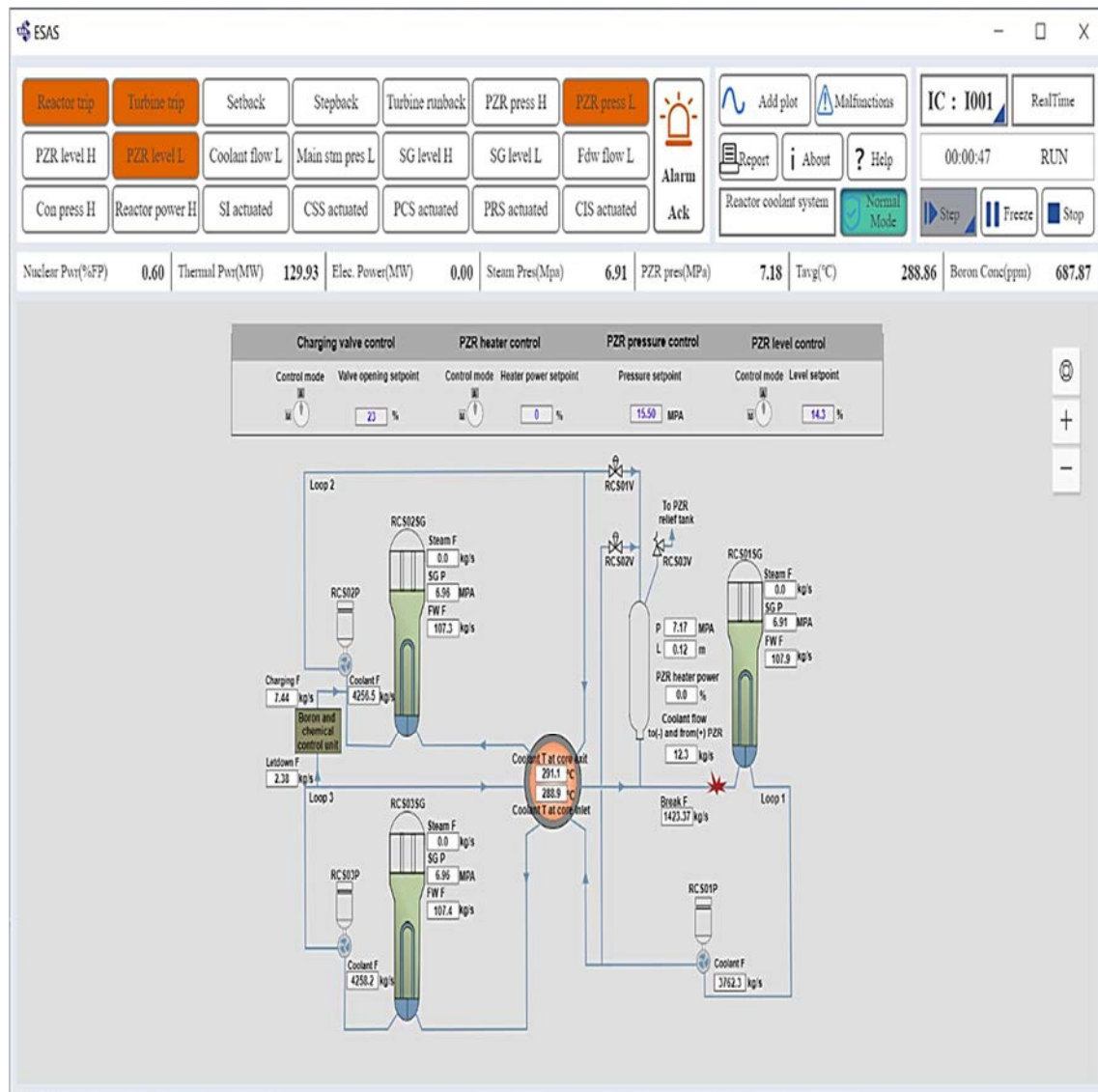


FIG. II–14. Primary break (LOCA).

SIMULATOR EXERCISES FOR SEVERE ACCIDENT SCENARIOS

This section contains the exercises for users to observe visually the phenomena during severe accident progress and help them to further understand the principle of severe accident evolution. The following exercises are described:

- 1) Initial condition verification;
- 2) Large break of cold leg with SI failure;
- 3) SBO with loss of normal feed water and PRS;
- 4) MSLLB with SI failure and loss of normal feed water and PRS;
- 5) SGTR with SI failure;
- 6) PZR safety valve open with SI failure.

II-15. INITIAL CONDITION VERIFICATION

This section is used to check the initial state of main parameters, especially related with severe accidents (Table II-15).

TABLE II-15. DATA FOR INITIAL CONDITION VERIFICATION

| No. | Description | Unit | Reference value | Real value (t=5s) | Real value (t=1h) | Deviation |
|-----|---|------|-----------------|----------------------|----------------------|-----------|
| 1 | Thermal power | MW | 2900 | | | ±30 |
| 2 | Nuclear power | %FP | 100 | | | ±1 |
| 3 | Electric power | MW | 1100 | | | ±12 |
| 4 | PZR pressure | MPa | 15.4 | | | ±0.2 |
| 5 | PZR level | M | 6.6 | | | ±0.4 |
| 6 | Coolant flow rate 1 | Kg/s | 4700 | | | ±200 |
| 7 | Coolant flowrate 2 | Kg/s | 4700 | | | ±200 |
| 8 | Coolant flowrate 3 | Kg/s | 4700 | | | ±200 |
| 9 | Charging flow | Kg/s | 4.05 | | | ±0.2 |
| 10 | Letdown flow | Kg/s | 3.6 | | | ±0.2 |
| 11 | Primary average temperature (T_{avg}) | °C | 310 | | | ±2 |
| 12 | Boron concentration | Ppm | 675 | | | ±10 |
| 13 | RPV water level | M | 12 | | | ±0.5 |
| 14 | Core exit temperature | °C | 345 | | | ±5 |
| 15 | Containment pressure | MPa | 0.1 | | | ±0.02 |
| 16 | Containment temperature | °C | 40 | | | ±5 |

TABLE II–15. DATA FOR INITIAL CONDITION VERIFICATION (cont.)

| No. | Description | Unit | Reference value | Real value (t=5s) | Real value (t=1h) | Deviation |
|-----|---------------------------|------|-----------------|----------------------|----------------------|-----------|
| 17 | Hydrogen concentration | % | 0 | | | n.a. |
| 18 | Containment radioactivity | Gy/h | 0 | | | n.a. |
| 19 | IRWST level | M | 2.5 | | | ±0.1 |
| 20 | SG1 pressure | MPa | 6.75 | | | ±0.2 |
| 21 | SG2 pressure | MPa | 6.75 | | | ±0.2 |
| 22 | SG3 pressure | MPa | 6.75 | | | ±0.2 |
| 23 | SG1 level | M | 12.66 | | | ±0.03 |
| 24 | SG2 level | M | 12.66 | | | ±0.03 |
| 25 | SG3 level | m | 12.66 | | | ±0.03 |
| 26 | SG1 flow | Kg/s | 571 | | | ±6 |
| 27 | SG2 flow | Kg/s | 571 | | | ±6 |
| 28 | SG3 flow | Kg/s | 571 | | | ±6 |
| 29 | SG1 feedwater flow | Kg/s | 570 | | | ±6 |
| 30 | SG2 feedwater flow | Kg/s | 570 | | | ±6 |
| 31 | SG3 feedwater flow | Kg/s | 570 | | | ±6 |
| 32 | Condenser pressure | KPa | 4.25 | | | ±0.3 |

Figure II–15 shows the plant main display of ESAS which appears when the simulator is launched in severe accident mode.

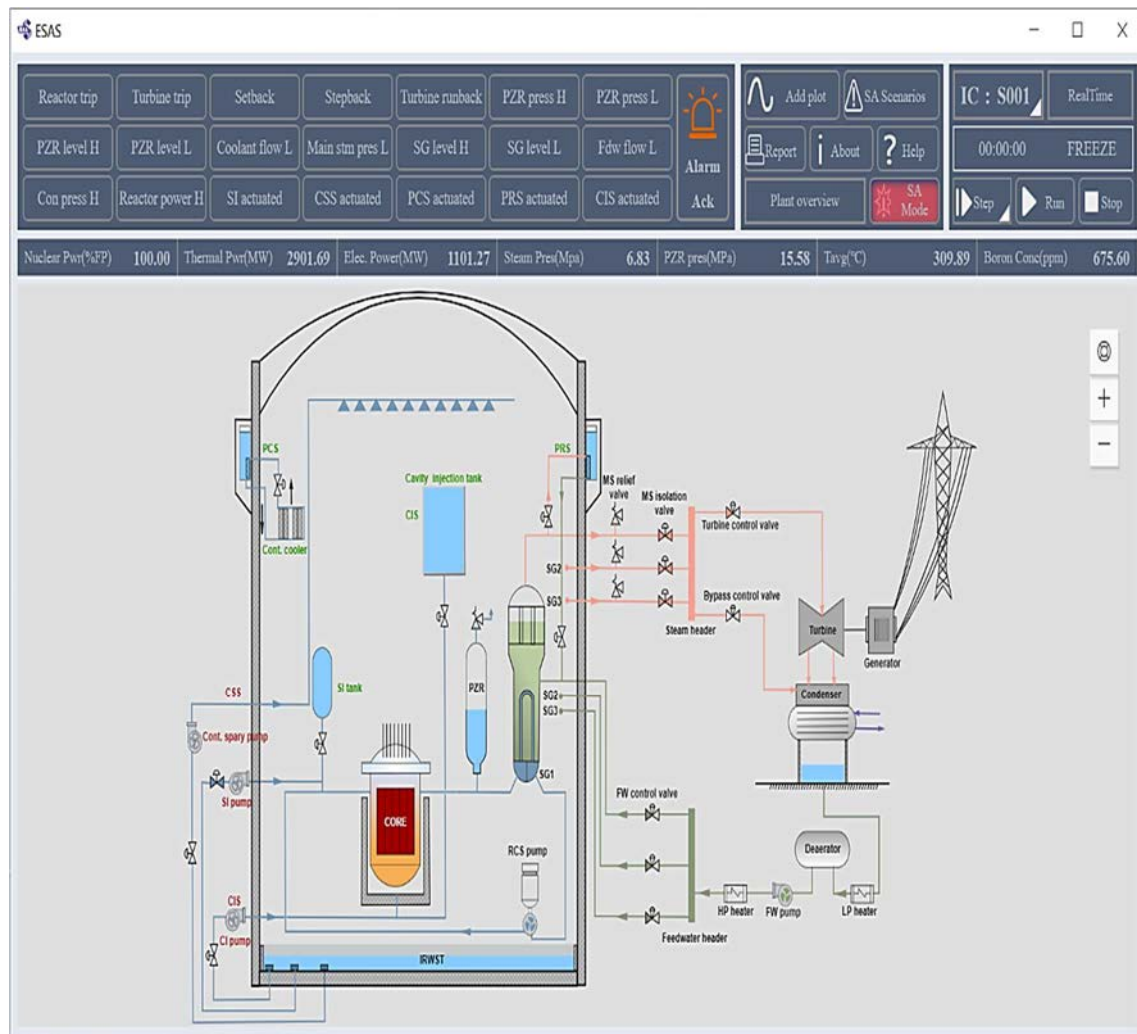


FIG. II–15. Initial conditions of severe accident.

II-16. LARGE BREAK OF COLD LEG WITH SI FAILURE

The ESAS steps and parameters for simulating the large break of cold leg with SI failure are shown in Table II-16.

TABLE II-16. DETAILS OF LARGE BREAK OF COLD LEG WITH SI FAILURE

| No. | Step | GUI sheet | Expected response |
|-----|---|--|--|
| 1 | Load a 100% FP IC | IC | IC loaded successfully |
| 2 | Put simulator in running | Run/Freeze 3D display | Run state shown and simulator time begins |
| 3 | Check the following parameters: | | Each parameter is stable near the following value: |
| | 1) Reactor power (% FP) | Fixed column | 100±2% FP |
| | 2) Turbine generator electric output (MW) | | 1100±5 MW |
| | 3) T _{avg} (°C) | | 310±1°C |
| | 4) PZR pressure (MPa) | | 15.4±0.2 MPa |
| | 5) PZR level (m) | Reactor coolant | 6.6±0.2 m |
| | 6) Feed water flow (kg/s) | system | 571±10 kg/s (for each SG) |
| | 7) Steam pressure (MPa) | Secondary system | 6.7±0.2 MPa |
| | 8) Steam flow (kg/s) | | 571±10 kg/s (for each SG) |
| | 9) SG level (m) | | 12.65±0.2 m (for each SG) |
| | 10) Turbine bypass valve opening (%) | | 0±1% |
| | 11) Boron concentration (ppm) | Control rods | 675±20 ppm |
| 4 | Insert SA scenario: “Double end break at cold leg and SI failure” | Reactor coolant | — Break shows on 3D display of primary system; |
| | | SA scenarios | — PZR level drops quickly to empty; |
| | | 3D display | — PZR pressure drops quickly. |
| 5 | Check reactor trip after PZR pressure dropped below set point (13.1 MPa): | Reactor coolant system | — Reactor power drops to 0 quickly; — “Low PZR pressure” as first-out trip signal can be confirmed on trip sheet. |
| 6 | Verify Turbine trip: | Secondary system | — Turbine load drops to 0 MW; — Steam flow drops rapidly; — Turbine bypass valve starts to open. |
| 7 | Verify safety injection (SI) system actuated after PZR pressure dropped below 11.89 MPa | Reactor coolant system Safety system | — Safety injection pump fail to start; — Safety injection valves fail to open; — “Low PZR pressure” as first-out SI signal can be confirmed on trip sheet. |
| 8 | Verify PZR and SI state: | Reactor coolant system Safety system | — There is no SI pump flow and accumulator flow established; — PZR pressure decreases continuously. |
| 9 | Verify containment state: | Safety system | — Containment pressure rises quickly which can be visually observed on 3D display of containment 3D-Pressure; — Containment temperature rises quickly which can be visually observed on 3D display of containment 3D-temperature; — Containment radioactivity rises. |

TABLE II–16. DETAILS OF LARGE BREAK OF COLD LEG WITH SI FAILURE (cont.)

| No. | Step | GUI sheet | Expected response |
|-----|---|---|---|
| 10 | Verify containment spray system (CSS) start-up after containment pressure rises above 240 KPa | Reactor coolant system Safety system | <ul style="list-style-type: none"> — Spray pump start up; — Spray valve open; — Spray flow established (approximately 600 kg/s) and visually observed on 3D display of containment 3D; — Containment pressure/temperature starts to decrease after spray flow established. |
| 11 | Check refuelling water tank (IRWST) state: | Safety system | <ul style="list-style-type: none"> — IRWST level first rises, then decreases; — IRWST temperature starts to rise slowly. |
| 12 | Check the RPV state: | Reactor coolant system Safety system 3D display | <ul style="list-style-type: none"> — RPV level starts to decrease and visually observed on 3D display of primary system; — The “Core uncovered” state would changeover to Yes after RPV level decreases below reactor core; — Core temperature starts to rise quickly after reactor core uncovered, which can be visually observed on 3D display of Core. |
| 13 | When core temperature rises above 650°C, check cavity injection system (CIS) start-up | Safety system | <ul style="list-style-type: none"> — CIS pump starts up; — CIS valves open; — CIS pump flow and passive injection flow established. |
| 14 | Check reactor core: | 3D display | <ul style="list-style-type: none"> — H₂ concentration, which can be verified at fixed column on 3D display, starts to rise after core temperature rises above 840°C, due to Zr-H₂O reaction; — H₂ depletion rate and depletion mass, which can be verified at fixed column on 3D display, starts to rise due to the work of H₂ recombiner; — Reactor core starts to melt (approximately after 40 minutes) along with RPV level decreasing, which can be visually observed on 3D display of Primary system by zooming in RPV component. |

Figure II–16 shows the 3D display of the containment during large break of cold leg with SI failure.



FIG. II–16. Large break of cold leg with SI failure.

II-17. SBO WITH LOSS OF NORMAL FEED WATER AND PRS

The ESAS steps and parameters for simulating the SBO with loss of normal feed water and PRS are shown in Table II-17.

TABLE II-17. DETAILS OF SBO WITH LOSS OF NORMAL FEED WATER AND PRS

| No. | Step | GUI sheet | Expected response |
|-----|---|--|--|
| 1 | Load a 100% FP IC | IC | IC loaded successfully |
| 2 | Put simulator in running | Run/Freeze 3D display | Run state shown and simulator time begins |
| 3 | Check the following parameters: | | Each parameter is stable near the following value: |
| | 1) Reactor power (% FP) | Fixed column | 100±2% FP |
| | 2) Turbine generator electric output (MW) | | 1100±5 MW |
| | 3) T _{avg} (°C) | | 310±1°C |
| | 4) PZR pressure (MPa) | | 15.4±0.2 MPa |
| | 5) PZR level (m) | Reactor coolant | 6.6±0.2 m |
| | 6) Feed water flow (kg/s) | system | 571±10 kg/s (for each SG) |
| | 7) Steam pressure (MPa) | Secondary system | 6.7±0.2 MPa |
| | 8) Steam flow (kg/s) | | 571±10 kg/s (for each SG) |
| | 9) SG level (m) | | 12.65±0.2 m (for each SG) |
| | 10) Turbine bypass valve opening (%) | | 0±1% |
| | 11) Boron concentration (ppm) | Control rods | 675±20 ppm |
| 4 | Insert SA scenario: “SBO with loss of normal feed water and PRS” | SA scenarios Reactor coolant Secondary | — Reactor coolant pump and feed water pump trip; — Reactor coolant flow drops quickly; — Feed water flow drops quickly; |
| 5 | Check reactor trip: | Reactor coolant | — Reactor power drops to 0 quickly; — “Reactor coolant pump trip” as first-out trip signal can be confirmed on trip sheet. |
| 6 | Verify Turbine trip: | Secondary | — Turbine load drops to 0 MW; — Steam flow drops rapidly; — Turbine bypass valve starts to open. |
| 7 | Verify primary state: | Reactor coolant | — PZR level decreases quickly to empty; — PZR pressure decreases; — T _{avg} decreases quickly; — Reactor coolant flow stable at natural circulation state (approximately 220 kg/s for each loop); — SG level decreases quickly due to loss of feed water. |
| 8 | Verify safety injection (SI) system actuated after PZR pressure dropped below 11.89 MPa | Reactor coolant system Safety system | — Safety injection pump fail to start; — Safety injection valves open; — “Low PZR pressure” as first-out SI signal can be confirmed on trip sheet. |

TABLE II-17. DETAILS OF SBO WITH LOSS OF NORMAL FEED WATER AND PRS (cont.)

| No. | Step | GUI sheet | Expected response |
|-----|--|--|---|
| 9 | Verify PZR and SI state: | Reactor coolant system Safety system | — There is no SI pump flow and accumulator flow established; — PZR pressure decreases continuously. |
| 10 | Check PRS start-up after SG level below 11.03 m: | Trip parameter Safety system Secondary | — PRS actuation signal can be confirmed on trip sheet or by alarm; — PRS valve fail to open due to SBO; — There is no PRS flow established; — SG level decreases continuously. |
| 11 | After approximately 10 minutes, Verify primary state: | Reactor coolant system 3D display | — PZR pressure starts to rise after decreasing to the minimum (approximately 4.3~5 MPa); — T_{avg} starts to rise after decreasing to the minimum (approximately 260~270°C); — Reactor core temperature starts to rise as well on 3D display of core; — PZR level starts to recover, which can be visually observed on 3D display of primary system; — SG level starts to rise as well. |
| 12 | Check reactor coolant state along with T_{avg} rising continuously: | 3D display | — Reactor coolant within reactor vessel, PZR and pipes starts boiling, along with T_{avg} rising, which can be visually observed on 3D display of primary system. |
| 13 | Check SG state: | Secondary system | — SG level starts to decrease continuously after rising for 30 min, and almost empty about 2 h 35 min later. |
| 14 | After PZR pressure rises above the set point of safety valve (happens about 2h40min later), check PZR state: | Reactor coolant system 3D display | — PZR safety valve opens for a while, then closed rapidly due to pressure drops below set point for closing; — PZR safety valve would keep this open-close operation mode, which can be visually observed on 3D display of primary system by zooming in PZR component. |
| 15 | After the relief tank blow up (about 3 h later) due to several times of PZR safety valve open-close, Verify containment state: | Safety system 3D display | — Containment pressure rises slowly, which can be visually observed on 3D display of containment 3D-Pressure; — Containment temperature rises slowly, which can be visually observed on 3D display of containment 3D-temperature; — Containment radioactivity rises slowly. |

TABLE II–17. DETAILS OF SBO WITH LOSS OF NORMAL FEED WATER AND PRS (cont.)

| No. | Step | GUI sheet | Expected response |
|-----|---|---|--|
| 16 | When containment pressure rises above 240 KPa (about 3~5 h), Verify containment spray system state: | Safety system | <ul style="list-style-type: none"> — Containment spray actuation signal can be confirmed on trip sheet or by alarm; — Containment spray pump fail to start due to SBO; — Containment valve fail to open — There is no spray flow established; — Containment pressure and temperature rises continuously. |
| 17 | When containment pressure rises above design value: 520 KPa (after 6h30min), check containment state: | 3D display | <ul style="list-style-type: none"> — “Containment failure” state become Yes; — Containment pressure starts to decrease after failure. |
| 18 | After many times of PZR safety valve open-close action, check the RPV state: | Reactor coolant system Safety system 3D display | <ul style="list-style-type: none"> — RPV level starts to decrease and visually observed on 3D display of primary system; — The “Core uncovered” state would changeover to Yes after RPV level decreases below reactor core (about 6h30min later); — Core temperature starts to rise quickly after reactor core uncovered, which can be visually observed on 3D display of Core. |
| 19 | When core temperature rises above 650°C check cavity injection system (CIS) start-up | Safety system | <ul style="list-style-type: none"> — CIS pump fails to start up; — CIS valves fail to open; — There are no CIS pump flow and passive injection flow established. |
| 20 | Check reactor core: | 3D display | <ul style="list-style-type: none"> — H₂ concentration, which can be verified at fixed column on 3D display, starts to rise after core temperature rises above 840°C, due to Zr-H₂O reaction; — H₂ depletion rate and depletion mass, which can be verified at fixed column on 3D display, starts to rise due to the work of H₂ recombiner; — Reactor core starts to melt along with RPV level decreasing, which can be visually observed on 3D display of Primary system by zooming in RPV component. |

Figure II–17 shows SBO with loss of normal feed water and PRS signal/alarm.

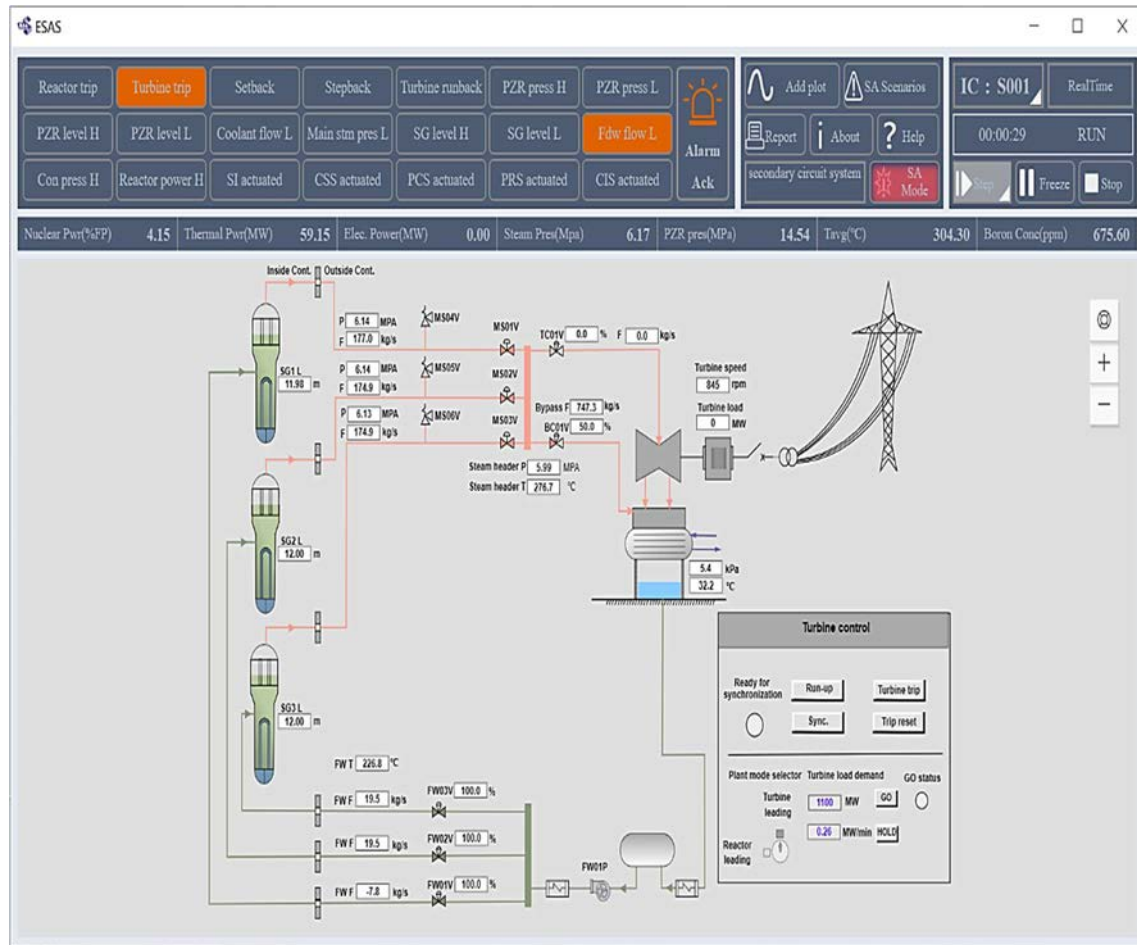


FIG. II–17. SBO with loss of normal feed water and PRS.

II-18. MSLB WITH SI FAILURE AND LOSS OF NORMAL FEED WATER AND PRS

The ESAS steps and parameters for simulating the MSLB with SI failure and loss of normal feed water and PRS are shown in Table II-18.

TABLE II-18. DETAILS OF MSLB WITH SI FAILURE AND LOSS OF NORMAL FEED WATER AND PRS

| No. | Step | GUI sheet | Expected response |
|-----|---|---|---|
| 1 | Load a 100% FP IC | IC | IC loaded successfully |
| 2 | Put simulator in running | Run/Freeze | Run state shown and simulator time begins |
| 3 | Check the following parameters: | | Each parameter is stable near the following value: |
| | 1) Reactor power (% FP) | Fixed column | 100±2% FP |
| | 2) Turbine generator electric output (MW) | | 1100±5 MW |
| | 3) T _{avg} (°C) | | 310±1°C |
| | 4) PZR pressure (MPa) | | 15.4±0.2 MPa |
| | 5) PZR level (m) | Reactor coolant | 6.6±0.2 m |
| | 6) Feed water flow (kg/s) | system | 571±10 kg/s (for each SG) |
| | 7) Steam pressure (MPa) | Secondary system | 6.7±0.2 MPa |
| | 8) Steam flow (kg/s) | | 571±10 kg/s (for each SG) |
| | 9) SG level (m) | | 12.65±0.2 m (for each SG) |
| | 10) Turbine bypass valve opening (%) | | 0±1% |
| | 11) Boron concentration (ppm) | Control rods | 675±20 ppm |
| 4 | Insert SA scenario: “MSLB with SI failure and loss of normal feed water and PRS” | SA scenarios | — Steam flow of three SGs rises rapidly; |
| | | Reactor coolant system | — Steam pressure of steam head drops; |
| | | Secondary system | — Feed water pump trip; |
| | | | — Feed water flow drops to 0 quickly. |
| 5 | Verify reactor trip: | Control rods Trip parameter | — Reactor power drops to 0 quickly; |
| | | | — “ATWT” as first-out trip signal can be confirmed on trip sheet; |
| | | | — “Reactor trip” and “turbine trip” alarm appears; |
| | | | — PZR pressure, T _{avg} , PZR level and SG level start to decrease quickly after reactor trip. |
| 6 | Verify Turbine trip: | Secondary system | — Turbine load drops to 0 MW; |
| | | | — Steam flow drops rapidly; |
| | | | — Turbine bypass valve starts to open. |
| 7 | When PZR pressure decreases below 11.89 MPa, verify safety injection (SI) system: | Reactor coolant system Safety system | — Safety injection pump fail to start; |
| | | | — Safety injection valves fail to open; |
| | | | — “Low PZR pressure” as first-out SI signal can be confirmed on trip sheet; |
| 8 | Check PRS start-up after SG level below 11.03 m: | Trip parameter Safety system Secondary system | — There is no SI pump flow established after PZR pressure below approximately 10 MPa. |
| | | | — PRS actuation signal can be confirmed on trip sheet or by alarm; |
| | | | — PRS valve fail to open due to malfunction; |
| | | | — There is no PRS flow established. |

TABLE II–18. DETAILS OF MSLB WITH SI FAILURE AND LOSS OF NORMAL FEED WATER AND PRS (cont.)

| No. | Step | GUI sheet | Expected response |
|-----|--|--------------------------------------|--|
| 9 | Verify SG state: | Secondary system | <ul style="list-style-type: none"> — Steam isolation valve closed automatically after steam pressure decreases below 3.45 MPa; — SG level decreases for a while, then become stable due to steam isolation. |
| 10 | Verify primary state: | Reactor coolant system | <ul style="list-style-type: none"> — T_{avg} decreases for a while, then starts to rise due to steam isolation; — PZR level decreases for a while, then starts to rise due to T_{avg} rising; — PZR pressure decreases for a while, then starts to rise due to T_{avg} rising; |
| 11 | Check reactor coolant state along with T_{avg} rising continuously: | 3D display | <ul style="list-style-type: none"> — Reactor coolant within reactor vessel, PZR and pipes starts boiling, along with T_{avg} rising, which can be visually observed on 3D display of primary system. |
| 12 | Check SG pressure: | 3D display | <ul style="list-style-type: none"> — SG pressure starts to rise due to T_{avg} rising. |
| 13 | When SG pressure rises above 8.7 MPa (about 35 min later), check steam safety valve action: | Secondary system | <ul style="list-style-type: none"> — Steam relief valve opens; — Steam flow rises; — Steam pressure is stabilized at 8.7 MPa; — SG level starts to decrease continuously due to stable steam flow established. |
| 14 | Check primary state after steam flow established by safety valves: | Primary system | <ul style="list-style-type: none"> — T_{avg} become stable (at approximately 308°C) and rise slowly; — PZR level become stable and rise slowly along with T_{avg} change; — PZR pressure become stable and rise slowly along with T_{avg} change. |
| 15 | After SG level decrease to 0 (SG is empty) (about 1h40min later), check primary state: | Primary system Secondary system | <ul style="list-style-type: none"> — T_{avg} continue to rise quickly; — PZR level start to rise quickly be fully filled (about 1.5 h later) due to T_{avg} rising; — PZR pressure start to rise due to T_{avg} rising, and would rise quickly after PZR fully filled. |
| 16 | After PZR pressure rises above the set point of safety valve (happens about 1h50min later), check PZR state: | Reactor coolant system 3D display | <ul style="list-style-type: none"> — PZR safety valve opens for a while, then closed rapidly due to pressure drops below set point for closing; — PZR safety valve would keep this open-close operation mode, which can be visually observed on 3D display of primary system by zooming in PZR component. |

TABLE II–18. DETAILS OF MSLB WITH SI FAILURE AND LOSS OF NORMAL FEED WATER AND PRS (cont.)

| No. | Step | GUI sheet | Expected response |
|-----|--|---|--|
| 17 | After the relief tank blow up (about 2 h later) due to several times of PZR safety valve open-close, Verify containment state: | Safety system 3D display | <ul style="list-style-type: none"> — Containment pressure rises slowly, which can be visually observed on 3D display of containment 3D-Pressure; — Containment temperature rises slowly, which can be visually observed on 3D display of containment 3D-temperature; — Containment radioactivity rises slowly. |
| 18 | After many times of PZR safety valve open-close action, check the RPV state: | Reactor coolant system Safety system 3D display | <ul style="list-style-type: none"> — RPV level starts to decrease (about 2h20mins later) and visually observed on 3D display of primary system; — The “Core uncovered” state would changeover to Yes after RPV level decreases below reactor core (approximately 6.3 m) (about 2h46min later); — Core temperature starts to rise quickly after reactor core uncovered, which can be visually observed on 3D display of Core. |
| 19 | When containment pressure rises above 240 KPa (about 2 h50 min later), Verify containment spray system state: | Safety system | <ul style="list-style-type: none"> — Containment spray actuation signal can be confirmed on trip sheet or by alarm; — Containment spray pump starts up and spray valve opens; — Containment spray flow established (approximately 400~610 kg/s); — Containment pressure and temperature starts to decrease after spray flow established. |
| 20 | When core temperature rises above 650°C, check cavity injection system (CIS) start-up | Safety system | <ul style="list-style-type: none"> — CIS pump starts up; — CIS valves opens; — CIS pump flow and passive injection flow established. |
| 21 | Check reactor core: | 3D display | <ul style="list-style-type: none"> — H₂ concentration, which can be verified at fixed column on 3D display, starts to rise after core temperature rises above 840°C, due to Zr-H₂O reaction; — H₂ depletion rate and depletion mass, which can be verified at fixed column on 3D display, starts to rise due to the work of H₂ recombiner; — Reactor core starts to melt along with RPV level decreasing, which can be visually observed on 3D display of Primary system by zooming in RPV component. |

Figure II-18 shows the trip parameters for MSLB with failure and loss of normal feed water and PRS.

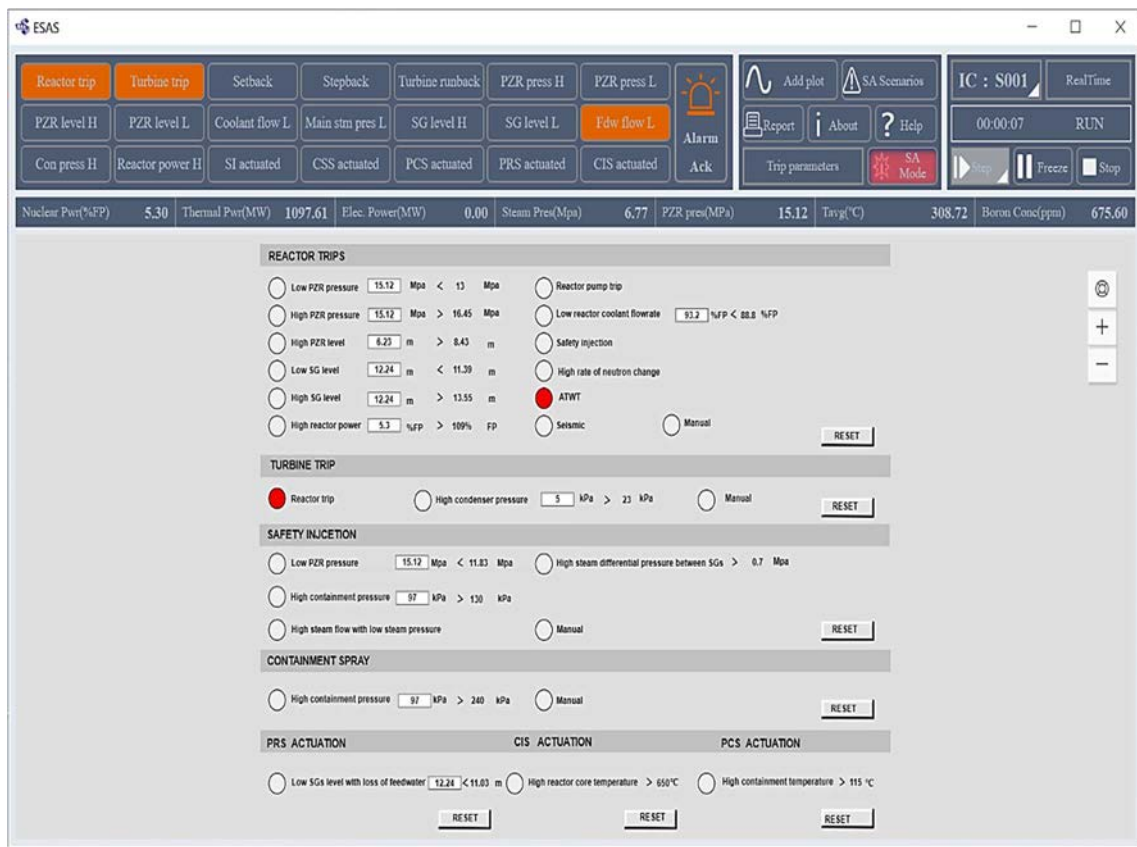


FIG. II-18. MSLB with failure and loss of normal feed water and PRS.

II-19. SGTR WITH SI FAILURE

The ESAS steps and parameters for simulating the SGTR with SI failure are shown in Table II-19.

TABLE II-19. REPRESENT DETAILS OF SGTR WITH SI FAILURE

| No. | Step | GUI sheet | Expected response |
|-----|---|--|---|
| 1 | Load a 100% FP IC | IC | IC loaded successfully |
| 2 | Put simulator in running | Run/Freeze 3D display | Run state shown and simulator time begins |
| 3 | Check the following parameters: | | Each parameter is stable near the following value: |
| | 1) Reactor power (% FP) | Fixed column | 100±2% FP |
| | 2) Turbine generator electric output (MW) | | 1100±5 MW |
| | 3) T _{avg} (°C) | | 310±1°C |
| | 4) PZR pressure (MPa) | | 15.4±0.2 MPa |
| | 5) PZR level (m) | Reactor coolant system | 6.6±0.2 m |
| | 6) Feed water flow (kg/s) | Secondary system | 571±10 kg/s (for each SG) |
| | 7) Steam pressure (MPa) | | 6.7±0.2 MPa |
| | 8) Steam flow (kg/s) | | 571±10 kg/s (for each SG) |
| | 9) SG level (m) | | 12.65±0.2 m (for each SG) |
| | 10) Turbine bypass valve opening (%) | | 0±1% |
| | 11) Boron concentration (ppm) | Control rods | 675±20 ppm |
| 4 | Insert SA scenario: “SGTR and SI failure” | Reactor coolant system SA scenarios 3D display | <ul style="list-style-type: none"> — SG1 break shows on 3D display of primary system; — PZR level drops quickly to empty; — PZR pressure drops quickly; — SG1 level rises quickly. |
| 5 | Check reactor trip after SG1 level rises above set point (13.55 m): | Reactor coolant system | <ul style="list-style-type: none"> — Reactor power drops to 0 quickly; — “High SG level” as first-out trip signal can be confirmed on trip sheet; — T_{avg} decreases quickly. |
| 6 | Verify Turbine trip: | Secondary system | <ul style="list-style-type: none"> — Turbine load drops to 0 MW; — Steam flow drops rapidly; — Turbine bypass valve starts to open. |
| 7 | Verify safety injection (SI) system actuated after PZR pressure dropped below 11.89 MPa.a | Reactor coolant system Safety system | <ul style="list-style-type: none"> — Safety injection pump fail to start; — Safety injection valves open; — “Low PZR pressure” as first-out SI signal can be confirmed on trip sheet. |
| 8 | Verify PZR and SI state: | Reactor coolant system Safety system | <ul style="list-style-type: none"> — There is no SI pump flow and accumulator flow established; — PZR pressure decreases continuously. |
| 9 | Verify SG state: | Safety system | <ul style="list-style-type: none"> — SG1 level rises continuously until to be fully filled at 14.45 m (after 6 min); — SG2 and SG3 levels are stabilized by automatic control system; — Steam isolation valve closed automatically after steam pressure decreases below 3 MPa (after 6.5 min); — Steam flow drops to 0 after steam isolation. |

TABLE II–19. REPRESENT DETAILS OF SGTR WITH SI FAILURE (cont.)

| No. | Step | GUI sheet | Expected response |
|-----|--|------------------------|---|
| 10 | Verify primary state after steam isolation: | Reactor coolant system | <ul style="list-style-type: none"> — T_{avg} starts to rise due to steam isolation; — PZR level starts to rise due to T_{avg} rising; — PZR pressure starts to rise due to T_{avg} rising. |
| 11 | Check reactor coolant state along with T_{avg} rising continuously: | 3D display | <ul style="list-style-type: none"> — Reactor coolant within reactor vessel, PZR and pipes starts boiling, along with T_{avg} rising, which can be visually observed on 3D display of primary system. |
| 12 | Check SG pressure: | 3D display | <ul style="list-style-type: none"> — SG1(rupture) pressure rises quickly same with primary pressure after steam isolation; — SG2 and SG3 pressure starts to rise due to T_{avg} rising as well. |
| 13 | When SG1 pressure first rises above 8.7 MPa (about 37 min later), check steam safety valve action: | Secondary system | <ul style="list-style-type: none"> — SG1 steam safety relief valve opens for a short time; — SG1 Steam flow rises, then drops to 0; — SG1 pressure is stabilized near 8.3 MPa. |
| 14 | Check primary state after steam flow established by safety valves: | Reactor coolant system | <ul style="list-style-type: none"> — T_{avg} drops a little (at approximately 270°C) and rise slowly; — PZR level become stable and rise slowly along with T_{avg} change; — PZR pressure become stable (at approximately 8.2 MPa), then rise slowly along with T_{avg} change. |
| 15 | When SG2 and SG3 pressure rises above 8.7 MPa. (About 1 h 15 mins later), verify their safety valves action: | Secondary system | <ul style="list-style-type: none"> — SG2 and SG3 steam safety valves open; — Stable SG2 and SG3 steam flow established. |
| 16 | When primary pressure rises above 8.7 MPa. (About 1 h 17 min later), check SG1 state: | Secondary system | <ul style="list-style-type: none"> — SG1 pressure rises above 8.7 MPa at the same time; — SG1 safety valve opens; — Stable SG1 steam flow established. |
| 17 | Check SG state: | Secondary system | <ul style="list-style-type: none"> — Three SGs pressure are stabilized at 8.7 MPa; — Stable steam flow established for three SGs. |

TABLE II–19. REPRESENT DETAILS OF SGTR WITH SI FAILURE (cont.)

| No. | Step | GUI sheet | Expected response |
|-----|--|------------------------|---|
| 18 | Check SG level: | Secondary system | <ul style="list-style-type: none"> — SG1(rapture) level stable or decreases very slowly; — SG2 and SG3 level starts to decrease due to steam flow established but would be maintained at programmed set point (approximately 12.07 m) by feed water system. |
| 19 | Check primary state after steam flow established by safety valves: | Reactor coolant system | <ul style="list-style-type: none"> — T_{avg} become stable (at approximately 308°C); — PZR level become stable (at approximately 8.5 m) along with T_{avg} change; — PZR pressure become stable (at approximately 8.8 MPa) along with T_{avg} change. |
| 20 | Check reactor core state: | 3D display | <ul style="list-style-type: none"> — RPV level is stable and visually observed on 3D display of primary system; — The reactor core covered by coolant, which can be visually observed on 3D display of primary system; — Core temperature stable at approximately 308°C, which can be visually observed on 3D display of Core. |

Figure II–19 shows the 3D display of the primary system during SGTR with SI failure.

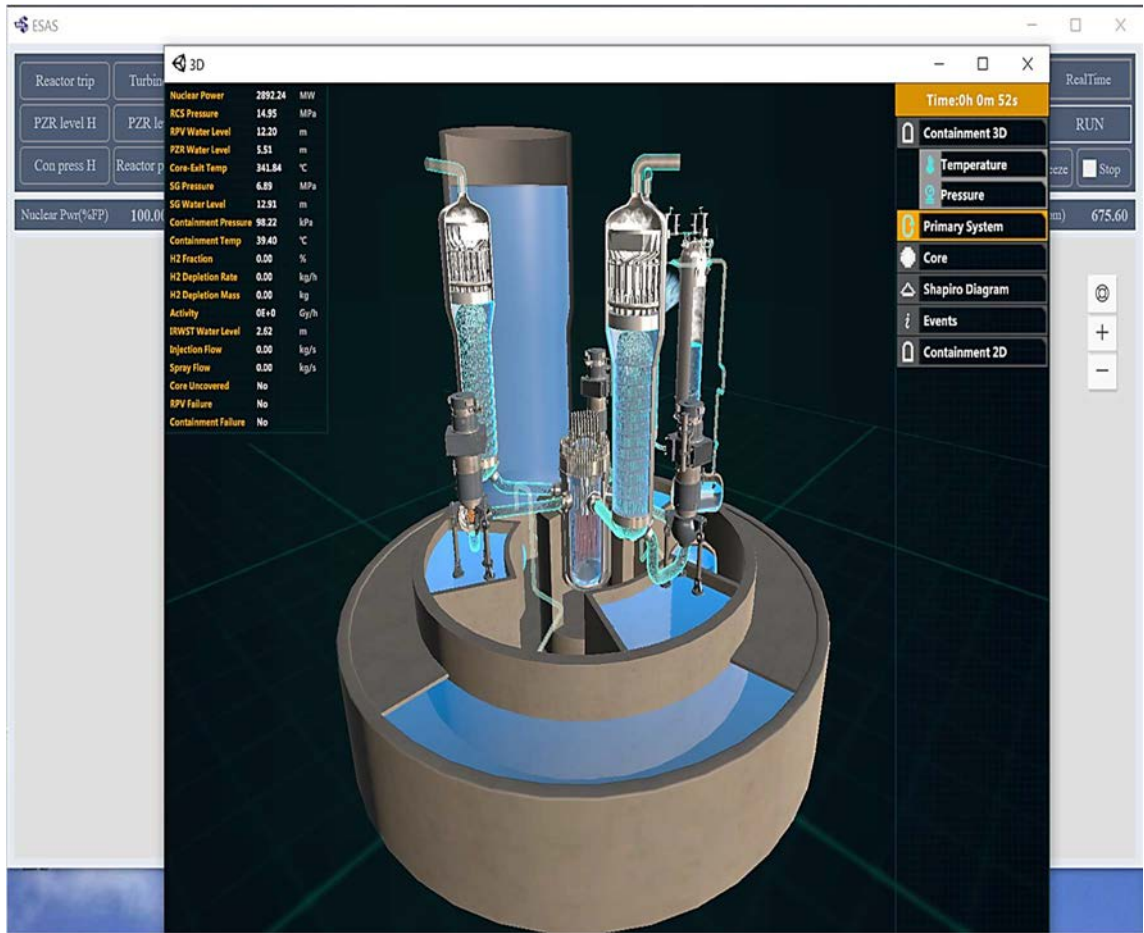


FIG. II–19. SGTR with SI failure.

II-20. PZR SAFETY VALVE OPEN WITH SI FAILURE.

The ESAS steps and parameters for simulating the PZR safety valve open with SI failure are shown in Table II-20.

TABLE II-20. REPRESENT DETAILS OF PZR SAFETY VALVE OPEN WITH SI FAILURE

| No. | Step | GUI sheet | Expected response |
|-----|---|---|---|
| 1 | Load a 100% FP IC | IC | IC loaded successfully |
| 2 | Put simulator in running | Run/Freeze 3D display | Run state shown and simulator time begins |
| 3 | Check the following parameters: | | Each parameter is stable near the following value |
| | 1) Reactor power (% FP) | Fixed column | 100±2% FP |
| | 2) Turbine generator electric output (MW) | | 1100±5 MW |
| | 3) T _{avg} (°C) | | 310±1°C |
| | 4) PZR pressure (MPa) | | 15.4±0.2 Mpa |
| | 5) PZR level (m) | Reactor coolant | 6.6±0.2 m |
| | 6) Feed water flow (kg/s) | system | 571±10 kg/s (for each SG) |
| | 7) Steam pressure (Mpa) | Secondary system | 6.7±0.2 Mpa |
| | 8) Steam flow (kg/s) | | 571±10 kg/s (for each SG) |
| | 9) SG level (m) | | 12.65±0.2 m (for each SG) |
| | 10) Turbine bypass valve opening (%) | | 0±2% |
| | 11) Boron concentration (ppm) | Control rods | 675±20 ppm |
| 4 | Insert SA scenario: "PZR safety valve open and SI failure" | Reactor coolant system SA scenarios 3D display | <ul style="list-style-type: none"> — PZR safety valve shows open on 3D display of primary system; — Relief flow to relief tank can be visually observed by 3D display of primary system; — PZR pressure drops quickly. |
| 5 | Check reactor trip after PZR pressure dropped below set point (13.1 Mpa): | Reactor coolant system | <ul style="list-style-type: none"> — Reactor power drops to 0 quickly; — "Low PZR pressure" as first-out trip signal can be confirmed on trip sheet; — PZR pressure and T_{avg} decreases quickly after reactor trip. |
| 6 | Verify Turbine trip: | Secondary system | <ul style="list-style-type: none"> — Turbine load drops to 0 MW; — Steam flow drops rapidly; — Turbine bypass valve starts to open. |
| 7 | Verify safety injection (SI) system actuated after PZR pressure dropped below 11.89 Mpa | Reactor coolant system Safety system | <ul style="list-style-type: none"> — Safety injection pump fail to start; — Safety injection valves fail to open; — "Low PZR pressure" as first-out SI signal can be confirmed on trip sheet. |
| 8 | Verify PZR and SI state: | Reactor coolant system Safety system | <ul style="list-style-type: none"> — There is no SI pump flow and accumulator flow established; — SI accumulator flow established after PZR pressure below 4.5 Mpa; — PZR pressure continue to decrease; — PZR level starts to rise quickly until to be fully filled after decreasing for a short time, due to safety valve open. |

TABLE II–20. REPRESENT DETAILS OF PZR SAFETY VALVE OPEN WITH SI FAILURE (cont.)

| No. | Step | GUI sheet | Expected response |
|-----|--|--|---|
| 9 | After relief tank blows up (about 1min later), verify containment state: | Safety system 3D display | <ul style="list-style-type: none"> — Containment pressure rises quickly which can be visually observed on 3D display of containment 3D-Pressure; — Containment temperature rises quickly which can be visually observed on 3D display of containment 3D-temperature; — Containment radioactivity rises slowly. |
| 10 | Check SG state: | Reactor coolant system Secondary system | <ul style="list-style-type: none"> — SG pressure decreases quickly along with T_{avg} decreasing; — Steam isolation valve closed automatically after steam pressure decreases below 3.45 Mpa (about 6.5 min later). |
| 11 | Check reactor coolant state along with T_{avg} rising continuously: | 3D display | <ul style="list-style-type: none"> — Reactor coolant within reactor vessel, PZR and pipes starts boiling, along with T_{avg} rising, which can be visually observed on 3D display of primary system |
| 12 | Check the RPV state: | Reactor coolant system Safety system 3D display | <ul style="list-style-type: none"> — RPV level starts to decrease (about 18mins later) and visually observed on 3D display of primary system; — The “Core uncovered” state would changeover to Yes (about 33 min later) after RPV level decreases below reactor core (6.6 m); — Core temperature starts to rise quickly after reactor core uncovered, which can be visually observed on 3D display of Core; — RCP Stop occurs in the event record window. |
| 13 | When core temperature rises above 650°C, check cavity injection system (CIS) start-up (about 43 min later) | Safety system | <ul style="list-style-type: none"> — CIS pump starts up; — CIS valves open; — CIS pump flow and passive injection flow established: 280 kg/s for active part and 14 kg/s for passive part. |
| 14 | Check primary state after RPV level decreasing: | | <ul style="list-style-type: none"> — PZR level starts to decrease quickly; — PZR pressure start to decrease quickly. |
| 15 | Verify containment spray system (CSS) start- up after containment pressure rises above 240 KPa.a (about 57 min later): | Reactor coolant system Safety system 3D display | <ul style="list-style-type: none"> — Spray pump start up; — Spray valve open; — Spray flow established (approximately 600 kg/s) and visually observed on 3D display of containment 3D; — Containment starts to decrease after spray flow established. |
| 16 | Check refuelling water tank (IRWST) state: | Safety system | <ul style="list-style-type: none"> — IRWST level decreases due to the extraction of CSS and CIS pump; — IRWST temperature starts to rise slowly. |

TABLE II–20. REPRESENT DETAILS OF PZR SAFETY VALVE OPEN WITH SI FAILURE (cont.)

| No. | Step | GUI sheet | Expected response |
|-----|---|------------|---|
| 17 | Check reactor core after it is uncovered: | 3D display | — H ₂ concentration, which can be verified at fixed column on 3D display, starts to rise after core temperature rises above 840°C, due to Zr-H ₂ O reaction; |
| | | | — H ₂ depletion rate and depletion mass, which can be verified at fixed column on 3D display, starts to rise due to the work of H ₂ recombiner; |
| | | | — Reactor cores start to melt (approximately after 40 minutes) along with RPV level decreasing, which can be visually observed on 3D display of Primary system by zooming in RPV component. |
| | | | |

Figure II–20 shows SI actuated PRS signal/alarm.

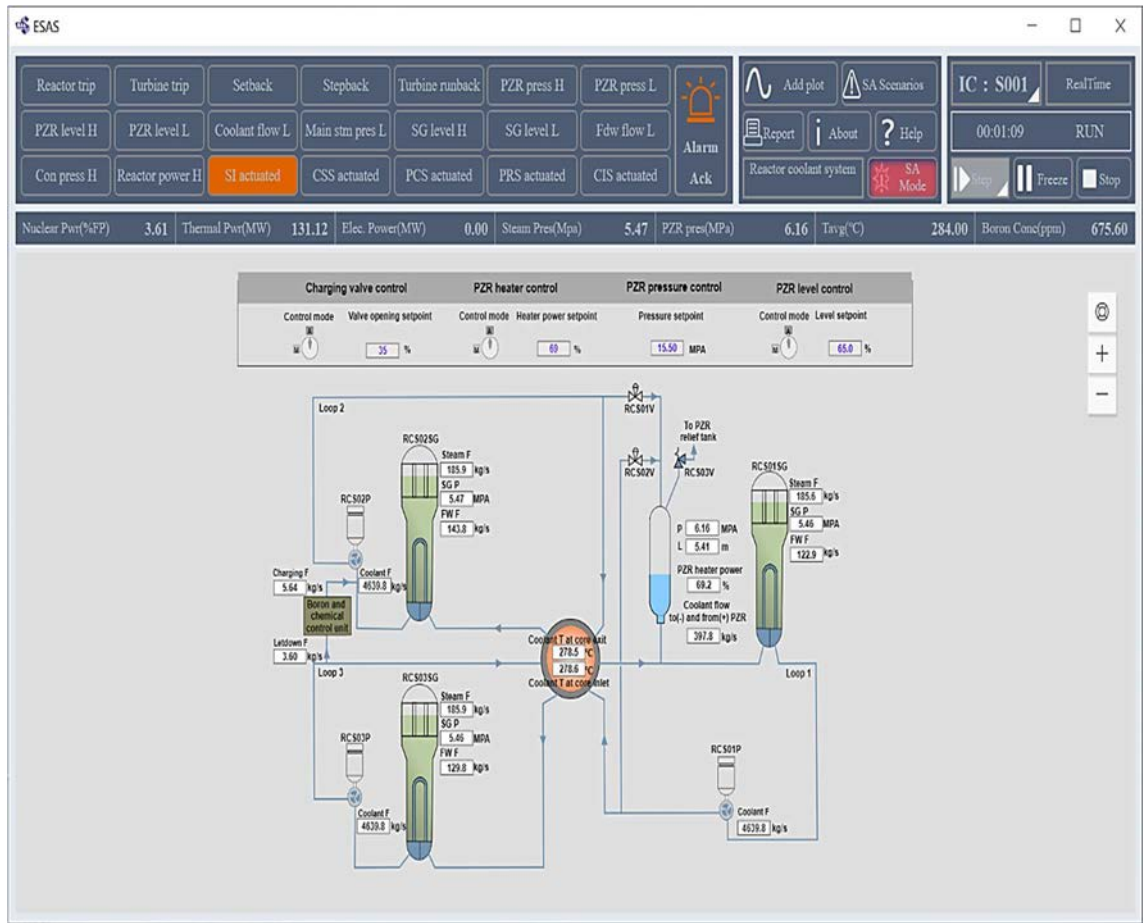


FIG. II–20. PZR safety valve open with SI failure.

ABBREVIATIONS

| | |
|-------|--|
| ATWT | Anticipated transients without trip |
| BC | Boron concentration |
| CNPO | China Nuclear Power Operation Technology Corporation, Ltd. |
| CIS | Cavity injection and cooling system |
| CSS | Containment spray system |
| 3D | Three dimensional |
| ESAS | Educational hypothetical severe accident simulator |
| FP | Full power |
| GUI | Graphical user interface |
| IAEA | International Atomic Energy Agency |
| IC | Initial condition |
| IRWST | Internal refuelling water storage tank |
| LOCA | Loss of coolant accident |
| MSLB | Main steam line break |
| NPP | Nuclear power plant |
| PCS | Passive containment heat removal system |
| PRS | Passive residual heat removal system on secondary side |
| PWR | Pressurized water reactor |
| PZR | Pressurizer |
| RCS | Reactor coolant system |
| RPV | Reactor pressure vessel |
| SBO | Station blackout |
| SG | Steam generator |
| SGTR | Steam generator tube rupture |
| SI | Safety injection |
| SIS | Safety injection system |

NOMENCLATURE FOR SEVERE ACCIDENT MODEL

| | |
|------------|---------------------------------------|
| A | heat transfer area |
| b | width |
| cp | specific heat |
| D | tube diameter |
| f | fraction of covered surface |
| g | gravity constant |
| h | heat transfer coefficient or enthalpy |
| k | thermal conductivity |
| L | length |
| m | mass |
| Nu | Nusselt number |
| P | tube-to-tube pitch |
| Q | heat transfer rate |
| q'' | heat flux |
| q | heat rate |
| R | radius |
| Ra | Rayleigh number |
| T | temperature |
| U | total energy |
| v | specific volume |
| W | mass flow rate |
| z | height |
| Δx | node radial increment |
| Δz | node axial increment |

Subscripts

| | |
|-----|----------------------------------|
| abl | ablation |
| b | boundary |
| cnd | conduction heat |
| cnv | convection heat |
| crd | control rod drive |
| d | downward |
| dec | decay heat |
| dis | discharge |
| frz | freezing |
| gap | crust-to-steel gap |
| j | crust node index |
| jcm | uppermost node covered by debris |
| lim | limiting |
| liq | liquidus or liquid |
| lp | lower plenum |
| mlt | melting |

| | |
|---------------|----------------------------------|
| mp | melting point |
| pl | debris central region |
| px | molten or frozen debris |
| qnc | quench by water ingress |
| rad | radiation |
| rlc | relocation |
| s | sideward |
| sat | saturation |
| sol | solidus or solid |
| ss | metallic debris |
| st | steam |
| u | upward |
| v | volumetric |
| x | crust or radial |
| xe | embedded crust |
| xl | lower crust |
| xu | upper crust |
| z | axial |
| 2Φ | two-phase mixture |
| | |
| α | thermal diffusivity |
| β | volumetric expansion coefficient |
| δ | thickness |
| Δ | increment |
| ε | emissivity |
| Φ | fraction |
| λ | latent heat of fusion |
| ν | kinematic viscosity |
| ρ | density |
| σ | Stefan-Boltzmann constant |

NOTE: The naming method in the table is for reference only. The meaning of the letters in the equation is subject to the description in the body.

CONTRIBUTORS TO DRAFTING AND REVIEW

| | |
|------------------|---|
| Batra, C. | International Atomic Energy Agency |
| Guzman Rios, B. | International Atomic Energy Agency |
| Kaleem, A. | International Atomic Energy Agency |
| Khuwaileh, B. | University of Sharjah, United Arab Emirates |
| Krause, M. | International Atomic Energy Agency |
| Liang, D. | International Atomic Energy Agency |
| Massoudi, A. | International Atomic Energy Agency |
| Ozoani, O.J. | International Atomic Energy Agency |
| Rehman, H. ur | International Atomic Energy Agency |
| Riaz, W. | International Atomic Energy Agency |
| Seyffert, C. | International Atomic Energy Agency |
| Suarez Ortiz, F. | Tecnatom, Spain |
| Sun, H. | China Nuclear Power Operation Technology Corporation, Ltd |
| Sungur, N. | International Atomic Energy Agency |
| Uwom, I. | International Atomic Energy Agency |
| Wei, W. | China Nuclear Power Operation Technology Corporation, Ltd |



IAEA

International Atomic Energy Agency

CONTACT IAEA PUBLISHING

Feedback on IAEA publications may be given via the on-line form available at:
www.iaea.org/publications/feedback

This form may also be used to report safety issues or environmental queries concerning IAEA publications.

Alternatively, contact IAEA Publishing:

Publishing Section
International Atomic Energy Agency
Vienna International Centre, PO Box 100, 1400 Vienna, Austria
Telephone: +43 1 2600 22529 or 22530
Email: sales.publications@iaea.org
www.iaea.org/publications

Priced and unpriced IAEA publications may be ordered directly from the IAEA.

ORDERING LOCALLY

Priced IAEA publications may be purchased from regional distributors and from major local booksellers.

